THE MECHANISM OF ACTION OF PEROXYGEN BIOCIDES.

BY

NATALIE DIANE JACKSON

SUBMITTED FOR THE DEGREE OF DOCTOR OF PHILOSOPHY

AT THE UNIVERSITY OF YORK

DEPARTMENT OF CHEMISTRY

NOVEMBER 1999

CONTENTS

ACKNOWLEDGEMENTS.

I would like to thank my supervisor, Professor Bruce Gilbert for his constant support and enthusiasm (and sustained efforts to teach me the basic principles of punctuation) over the past three years. Mention must also be made of Drs. Graham Timmins and David Roper whose advice has been invaluable. Thanks are also due to Dr Adrian Whitwood, not only for his technical assistance and advice, but for reminding me that 'When you average it out it all comes to nothing anyway.' In addition, I would also like to thank Professor Horia Caldararu for useful and enlightening discussions.

I would like to thank my sponsors, Solvay, and in particular Drs Tom Candy and Madeline French for their support. In addition, Thank You to the many others at Solvay who have made me welcome during my visits.

To members of the BCG group, both past and present, many thanks and sorry about the smell, it wasn't me, I promise! In particular, mention must be made of Sarah, who is unfortunate enough to share my taste in music and lack of talent for vocal accompaniment; no-one else would have tolerated my renditions of 'Pasta Manana.' Thanks are also due to Professor John Lindsay-Smith and his research group for tolerating the invasion of their lab and making us feel welcome. It would take too long to name all the others who have made my time at York enjoyable, but to many of those in the BJK group and in 'C' block: Thank You. To all those in the Chemistry Girls Football teams, Thank You and I hope the bruises are fading, if it is any consolation it wasn't malice just lack of co-ordination.

I would also like to thank the people who I have lived with, who have tolerated my strange sock collection and ruthless tidying up. In particular, I would like to thank Alison for always knowing when a cup of tea and a chat was needed

Mention must be made of Bel who graciously allowed me to be part of her life for ten years and who had such an impact on mine. I would also like to thank my Mum and Dad, for ensuring that I received the opportunities that some believed I was not entitled to and encouraging me to take every one of them, and Simon for always being there.

ABSTRACT

The aim of the work described in this Thesis was to elucidate the mechanism of action of peroxygen biocides. In this context, Chapter One reviews the reactions of peroxides, with particular emphasis on radical reactions; the relevance of these reactions in systems of biological interest is then described with reference to specific biomolecules. An introduction to the techniques to be utilised throughout the Thesis is then provided.

Chapter Two describes evidence for radical generation from peroxyacids upon reaction with low-valent transition-metal ions, using the techniques of EPR spin-trapping and rapid flow to study rates of reaction and radical products. The reaction proceeds to produce acyloxyl radicals when either Ti^{3+}-EDTA or Fe^{2+}-EDTA is employed, but is much more complex when Cu^{+} is employed, being highly dependent upon the reducing species and the ligand. It was also found that the rate of reaction was considerably higher with Fe^{2+}-EDTA than with Ti^{3+}-EDTA.

Chapter Three describes investigations into the reactions of peroxyacetic acid with a model protein (BSA), utilising both EPR spin-trapping techniques and biochemical methods. It was found that formulations containing low concentrations of peroxyacetic acid and high concentrations of hydrogen peroxide lead to the generation of a higher concentration of radicals from BSA, greater susceptibility to protease digestion and greater fragmentation, whereas 40% PAA leads to the formation of a higher concentration of side-chain carbonyl groups after oxidation. The reactions of a metalloprotein, namely cytochrome c, with PAA have also been investigated to examine the reactions of endogenous iron with peroxyacids, and have been shown to lead to the production of a highly oxidsing species.

Chapter Four describes a study of the effects of peroxyacetic acid on lipids. Both lipid peroxidation and lipid epoxidation were analysed using standard synthetic procedures, NMR spectroscopy, EPR spin-probe techniques and the TBA test. It has been established that the generation of epoxides from fatty acids and phospholipids is facile and that vesicles comprising epoxidised phospholipids are much less fluid than those

consisting of unmodified phospholipids. In addition it was found that peroxidation of lipid vesicles becomes significant in the presence of added low-valent transition-metal ions

The role of the reactions described thus far in the action of peroxygen biocides was investigated in studies outlined in Chapter Five. These experiments involved the use of *Escherichia coli* in an attempt to relate cell death to generation of radical species and damage to specific cellular components. The techniques employed include EPR studies in addition to quantitative carbonyl determination on protein side-chains and lipid peroxidation. It is concluded from these investigations that a variety of mechanisms contribute to the bactericidal action of peroxygens.

ABBREVIATIONS

5% PAA	Peroxyacetic acid formulation containing 5% (w/w) peroxyacetic acid
40% PAA	Peroxyacetic acid formulation containing 5% (w/w) peroxyacetic acid
MMPP	Magnesium monoperoxyphthalate
total AvOx	The total peroxygen concentration in a formulation of PAA
EDTA	Ethylene diamine tetra acetic acid
DMSO	Dimethyl sulfoxide
GSH	Reduced glutathione
GSSG	Oxidised glutathione
DMPO	5,5-dimethyl-1-pyrroline-*N*-oxide
PBN	*N*-t-butyl-α-phenylnitrone
POBN	*N*-t-butyl-α-(4-pyridyl-*N*-oxide)-nitrone
DBNBS	3,5-dibromo-4-nitrosobenzenesulfonic acid
MNP	2-methyl-2-nitrosopropane
DEPMPO	5-diethoxyphosphoryl-5-methyl-1-pyrroline-*N*-oxide
OPMPO	5-diphenoxyphosphoryl-5-methyl-1-pyrroline-*N*-oxide
BSA	Bovine serum albumin
2,4-DNPH	2,4-dinitrophenylhydrazine
DTNB	5,5'-dithio-bis(2-nitrobenzoic acid)
BCA	Bicinchoninic acid
TCA	Trichloroacetic acid
m-CPBA	*m*-chloroperoxybenzoic acid
MDA	Malondialdehyde
TBA	2-thiobarbituric acid

NEM	*N*-ethylmalemide
NMR spectroscopy	Nuclear magnetic resonance spectroscopy
UV-vis spectrophotometry	Ultraviolet-visible spectrophotometry
MALDI-TOF mass spectrometry	Matrix assisted laser desorption ionisation mass spectrometry
EPR spectroscopy	Electron paramagnetic resonance spectroscopy

CHAPTER 1.

INTRODUCTION.

1.1 INTRODUCTION.

The chemistry of peroxide compounds is broad ranging in character and hence peroxides have found a variety of uses in industrial processes, domestic situations and as synthetic reagents. Industrially, peroxide compounds are employed as disinfection agents[1] and radical initiators for polymerisation processes.[2,3] They are used for disinfection in a variety of contexts including the washing out of kidney dialysis machines in hospitals and the reduction of microbial contamination in paper pulp.[1] Domestically, peroxide compounds are used for the bleaching of stains on laundry.[4] The reactions of peroxides are also of great biological significance since they and the radicals which derive from them are believed to be involved in detrimental processes such as lipid peroxidation,[5] protein damage[6,7,8] and DNA damage;[9,10] all of which have been implicated in diseased states such as carcinogeneisis,[11,12] rheumatoid arthritis[13,14] and ischemia reperfusion injury.[15,16] In contrast, radical processes can be beneficial, or indeed necessary; examples of such being prostaglandin synthesis[17] and immune response.[18]

This introduction aims first to review the reactions of peroxide compounds, both free-radical and non free-radical in nature, then to examine the reactions of free radicals in biological systems. Finally the methods and objectives of the study will be introduced. The remainder of the thesis is concerned with the reactions of peracetic acid with model biomolecules and bacteria in order to probe the mechanism of action of peroxygen biocides.

1.2. CHEMISTRY OF PEROXIDES.

Peroxide compounds owe their reactivity to the weak O-O bond; the bond strength typically being 126 kJ mol^{-1}.[19] The low bond energy is largely attributable to lone pair - lone pair repulsions. Peroxides undergo a diverse range of chemical reactions; these include nucleophilic substitution, reactions with electrophiles and radical reactions which are a result of the homolytic cleavage of the O-O bond. These reactions will be discussed in the following sections.

1.2.1. Reaction of peroxides with nucleophiles.

The oxygen atoms in peroxide compounds are susceptible to nucleophilic attack.[20-23] They are thought to undergo this type of attack via an S_N2 mechanism [reaction 1.1].

$$Nu^- + R^1-O-O-R^2 \longrightarrow Nu-O-R^1 + R^2O^- \qquad \textbf{(1.1)}$$

As would be expected, the reaction is promoted by increasing the nucleophilicity of the reactant and increasing the leaving group ability of the peroxide. Synthetically, the most significant reaction of a peroxide with a nucleophile is the epoxidation of alkenes.[20-28] This reaction illustrates the general trends observed for reactions of peroxides with nucleophiles; the reaction rate is increased as the π-electron density of the alkene is increased (the rate being approximately 6000 times higher for $CR_2=CR_2$ as opposed to $CH_2=CH_2$) and as the leaving group ability increases on the peroxide, peroxyacids being much better epoxidising agents than hydroperoxides (a reflection of the much lower pK_a's of the departing carboxylic acid as opposed to the alcohol). The reaction is slowed down by the use of coordinating solvents which are able to form intermolecular hydrogen bonds with the peroxide.[20]

Other examples of this type of reaction include the oxidation of tertiary amines to amine oxides, oxidation of secondary amines to dialkyl hydroxylamines, oxidation of aromatic compounds to phenols, the oxidation of phosphines to phosphine oxides, sulfhydryls to disulfides and, with excess peroxide, sulfinic and sulfonic acids and sulfides to sulfoxides and ultimately sulfones [reactions (1.2) to (1.7)].[20]

$$R_3N \longrightarrow R_3\overset{+}{N}-O^- \qquad \textbf{(1.2)}$$

$$R_2N-H \longrightarrow R_2N-OH \qquad \textbf{(1.3)}$$

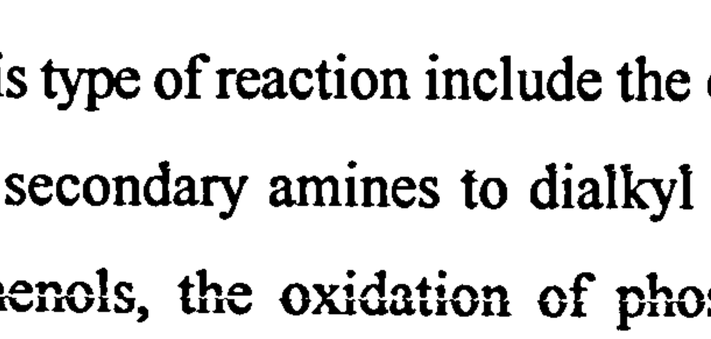

(1.4)

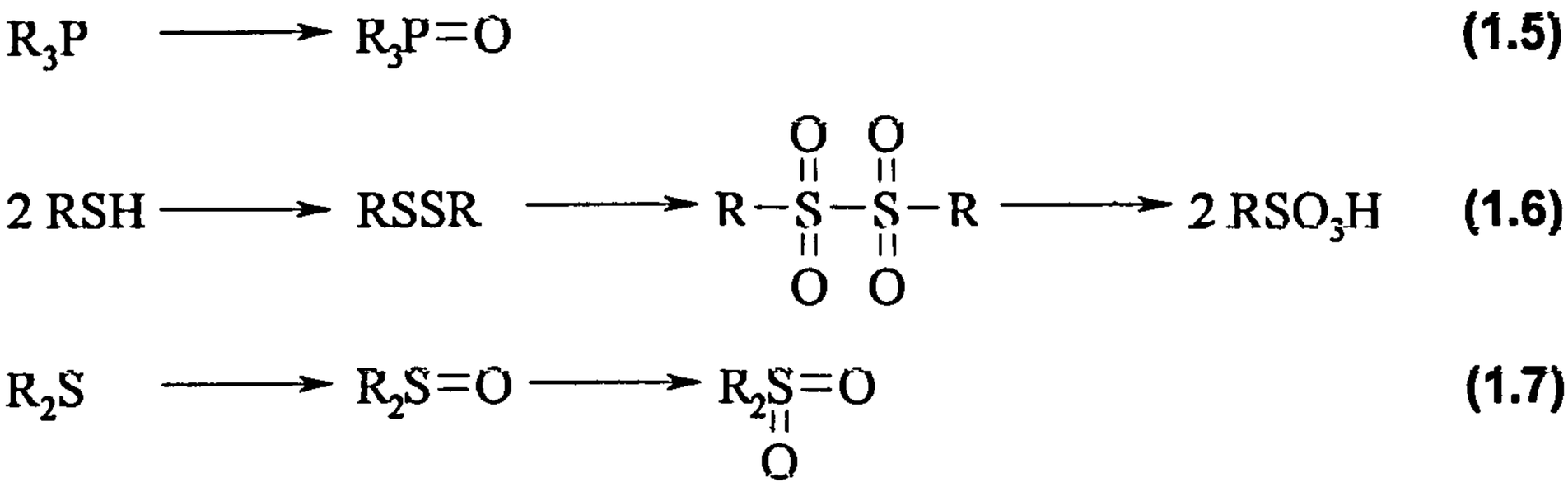

$$R_3P \longrightarrow R_3P{=}O \qquad (1.5)$$

$$2\,RSH \longrightarrow RSSR \longrightarrow R{-}\overset{\overset{O}{\|}}{\underset{\underset{O}{\|}}{S}}{-}\overset{\overset{O}{\|}}{\underset{\underset{O}{\|}}{S}}{-}R \longrightarrow 2\,RSO_3H \qquad (1.6)$$

$$R_2S \longrightarrow R_2S{=}O \longrightarrow R_2\overset{\overset{O}{\|}}{S}{=}O \qquad (1.7)$$

1.2.2. Reactions of peroxides with electrophiles.

As a result of the lone pairs of electrons on the oxygen atoms, peroxide compounds also have the ability to act as nucleophiles.[20,21,23,28,29] The reactions in which peroxides behave as nucleophiles can be divided into two major groups namely, substitution of a group and addition to a double bond [reactions (1.8) and (1.9)].

$$ROO^- + -\overset{|}{\underset{|}{C}}\text{-}X \longrightarrow ROO\text{-}\overset{|}{\underset{|}{C}}- + X^- \qquad (1.8)$$

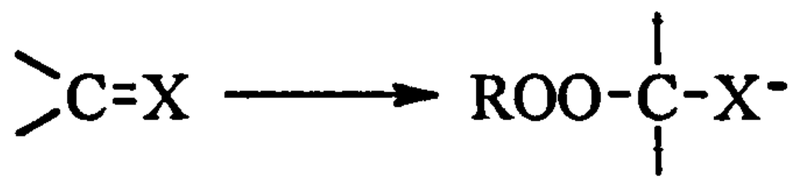

$$ROO^- + \rangle C{=}X \longrightarrow ROO\text{-}\overset{|}{\underset{|}{C}}\text{-}X^- \qquad (1.9)$$

The most prominent reaction in this group, which has been used extensively in organic synthesis, is the Baeyer-Villiger reaction [reaction (1.10)][20,21,23,24,28,29] in which the nucleophilic peroxide oxygen attacks the carbonyl carbon of an aldehyde or ketone to produce a peroxidic intermediate which then undergoes rearrangement via migration of R^3 to the peroxide oxygen to furnish an ester.

The reaction is accelerated by acid or base, acid catalysis promoting the protonation of the aldehyde / ketone oxygen and promoting the rearrangement step through hydrogen bonding through the peroxide oxygen. Base catalysis increases the nucleophilicity of the attacking peroxide and leads to an oxyanion intermediate which promotes the rearrangement step by exerting an electron-donating effect.[20] Other reactions in this category include alkaline epoxidation of α,β unsaturated ketones and self reaction leading

to decomposition [reactions (1.11) and (1.12)].

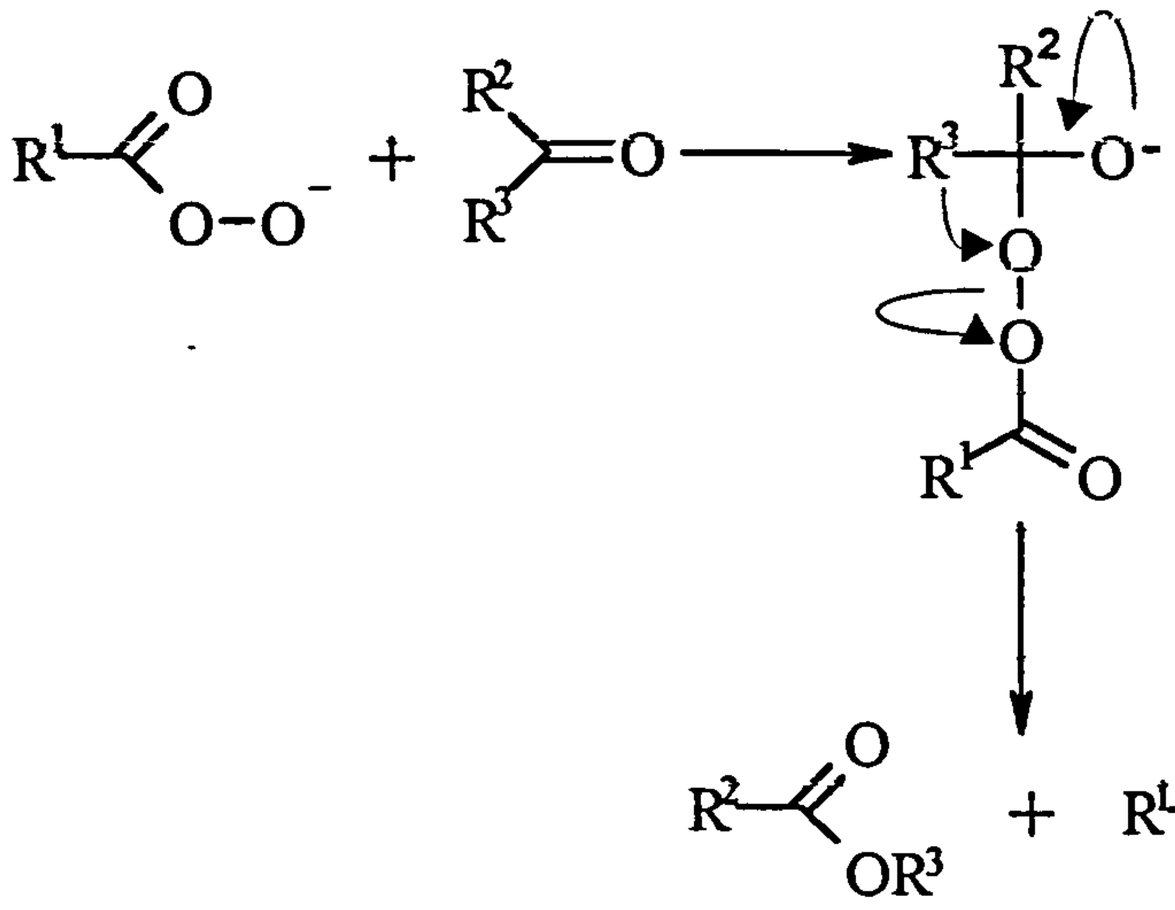

(1.10)

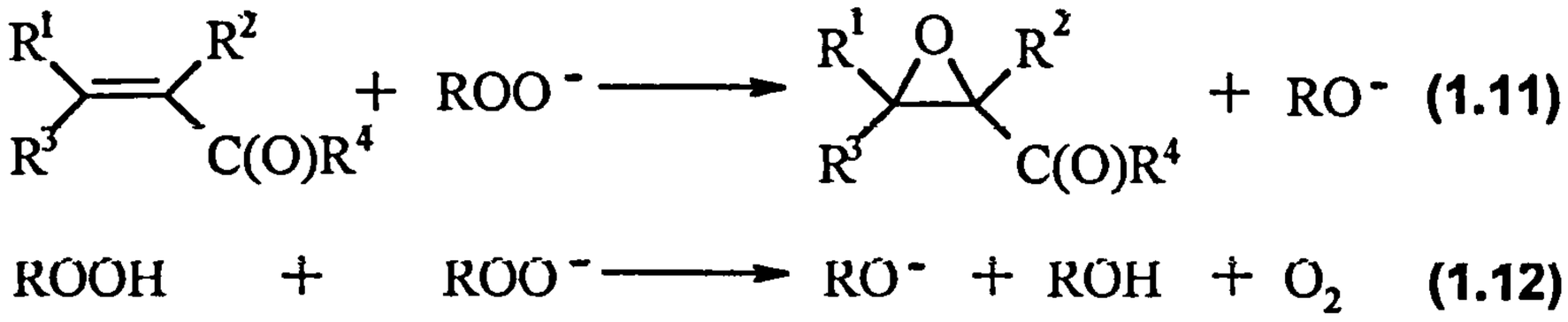

(1.11)

(1.12)

1.2.3 Radical reactions of peroxides.

Peroxides decompose by thermolysis, photolysis, or electron transfer, producing radicals. The reactions of radicals generated from peroxide decomposition will be discussed in the following sections.

i) Hydrogen peroxide.

Hydrogen peroxide can be homolytically cleaved by UV light or heat to form hydroxyl radicals [Reaction (1.13)]. Radiolysis or electron transfer from a low-valent metal ion, for example Fe^{2+}, leads to the formation of $\cdot OH$ and ^{-}OH [reactions (1.14) and (1.15)].

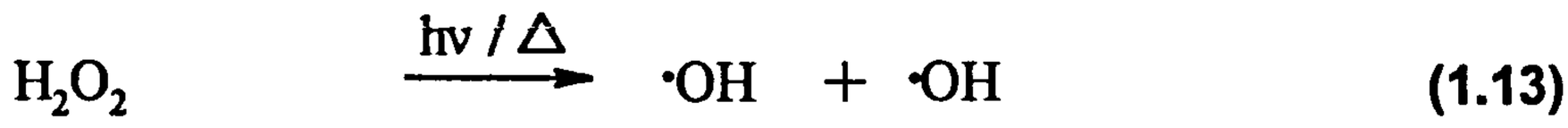

(1.13)

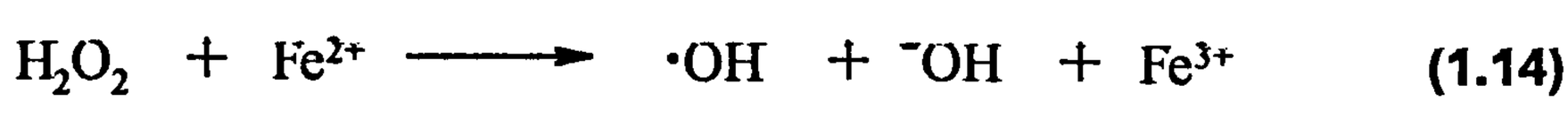

(1.14)

$$H_2O_2 + e^-_{(aq)} \longrightarrow \cdot OH + {}^-OH \qquad \textbf{(1.15)}$$

The reaction of Fe^{2+} with H_2O_2 was discovered in 1894 by Fenton.[30,31] The reaction was found to lead to the rapid decomposition of the peroxide, but the mechanism of the reaction, involving the formation of hydroxyl radicals, was not clarified until 1934 by Haber and Weiss [reactions (1.16) - (1.20)].[32] This mechanism is widely accepted although alternative mechanisms have been proposed involving the formation of high-valent iron species such as FeO^{2+} species[33-35] and $Fe^{2+}(H_2O_2)$ complexes.[36]

$$Fe^{2+} + H_2O_2 \longrightarrow Fe^{3+} + \cdot OH + {}^-OH \qquad \textbf{(1.16)}$$

$$Fe^{3+} + H_2O_2 \longrightarrow Fe^{2+} + HO_2\cdot + H^+ \qquad \textbf{(1.17)}$$

$$\cdot OH + H_2O_2 \longrightarrow HO_2\cdot + H_2O \qquad \textbf{(1.18)}$$

$$Fe^{3+} + HO_2\cdot \longrightarrow Fe^{2+} + O_2 + H^+ \qquad \textbf{(1.19)}$$

$$Fe^{2+} + \cdot OH \longrightarrow Fe^{3+} + {}^-OH \qquad \textbf{(1.20)}$$

The hydroxyl radical is a powerful oxidant and in the presence of an organic substrate will typically undergo either addition to a multiple bond or hydrogen-atom abstraction. The radicals which result can then proceed to react by one or more of a myriad of pathways. The products of these reactions are often dependent on the way in which the hydroxyl radical has been generated. Thus, radicals such as *t*-alkyl radicals, hydroxyalkyl radicals and aminoalkyl radicals are often subject to oxidation by the Fe^{3+} in the Fenton system while some radicals [37] may be susceptible to reduction by Fe^{2+}.In contrast, when the hydroxyl radical is generated photolytically the reactions of the first-formed substrate-derived radicals are dominated by dimerisation, and further radical reactions.[38]

An example is the oxidation of propan-2-ol by ·OH. When the hydroxyl radical is generated photolytically the first formed radical, the 2-hydroxypropyl radical, either

undergoes dimerisation, forming pinacol, or disproportionates to produce propanone and water.[37] In contrast when propan-2-ol is oxidised by ·OH formed in the Fenton system the first formed radical undergoes oxidation by Fe^{3+} to form the corresponding cation which then adds ^{-}OH and eliminates water to produce propanone. No pinacol is formed.[38]

Other metal ions have been used instead of Fe^{2+} in oxidising systems with hydrogen peroxide. These include Ti^{3+}, Cu^{+} and Cr^{2+} all of which are believed to form ·OH as the oxidising species,[39-42] although there is some debate as to whether the oxidising species in the copper system is ·OH, Cu^{3+} or a copper-peroxy complex.[42,43]

ii) Inorganic peroxides

Although the range of inorganic peroxides is not as wide as the range of organic peroxides, several are commercially available [(1.1) to (1.4)] and have found use in a variety of reactions.

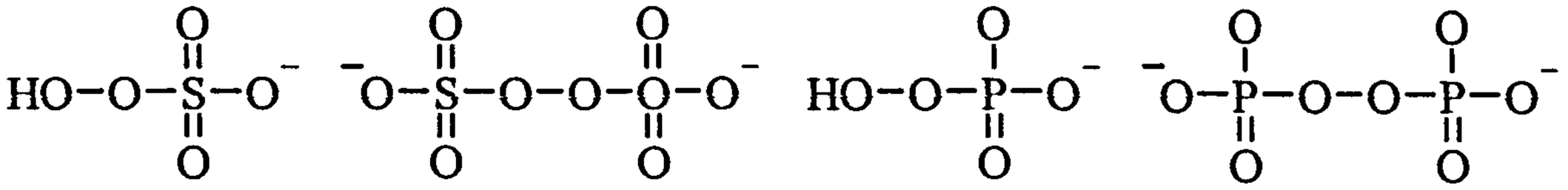

(1.1) **(1.2)** **(1.3)** **(1.4)**

The homolytic or thermal fission of the peroxymonosulfate anion by UV light or thermolysis yields a mixture of the hydroxyl radical and the sulfate radical anion ($SO_4^{\cdot-}$). When peroxymonosulfate is decomposed by electron transfer from a low-valent transition metal ion, the direction of the reaction is determined by the metal ion. In the presence of Co^{2+}, Fe^{2+} or Ti^{3+} peroxymonosulfate decomposes to form $SO_4^{\cdot-}$ and ^{-}OH [reaction (1.21)] whereas in the presence of Cu^{+} peroxymonosulfate decomposes to produce SO_4^{2-} and ·OH [reaction (1.22)].[44,45] In contrast, pulse radiolysis studies have shown that in the presence of $e^{-}_{(aq)}$ peroxymonosulfate decomposes to give a 4:1 mixture of ·OH : $SO_4^{\cdot-}$.[46] A further route of decomposition for peroxymonosulfate is observed in the presence of Ce^{4+} which

undergoes one electron *reduction* to Ce^{3+} concomitantly producing $SO_5^{\cdot-}$ and H^+ [reaction (1.23)].[47,48]

$$HOOSO_3^- + M^{n+} \longrightarrow SO_4^{\cdot-} + {}^-OH + M^{(n+1)+} \quad \textbf{(1.21)}$$

$M^{n+} = Ti^{3+}, Fe^{2+}, Co^{2+}$

$$HOOSO_3^- + Cu^+ \longrightarrow SO_4^{2-} + {}^{\cdot}OH + Cu^{2+} \quad \textbf{(1.22)}$$

$$HOOSO_3^- + Ce^{4+} \longrightarrow SO_5^{\cdot-} + H^+ + Ce^{3+} \quad \textbf{(1.23)}$$

$SO_4^{\cdot-}$ can facilitate three types of reactions, hydrogen atom abstraction, addition to a double bond and electron transfer, rendering it a powerful oxidant which has the ability to oxidise organic molecules with low ionisation potentials. Electron transfer is thought to occur through an addition-elimination sequence which can lead to the direct formation of a radical-cation, [reaction (1.24)] which may be observed in some cases.[49] However, it is more common for the first-formed sulfate radical-anion adduct or the radical-cation to hydrate rapidly [reaction (1.25)] to form the corresponding hydroxyl radical adduct.[50]

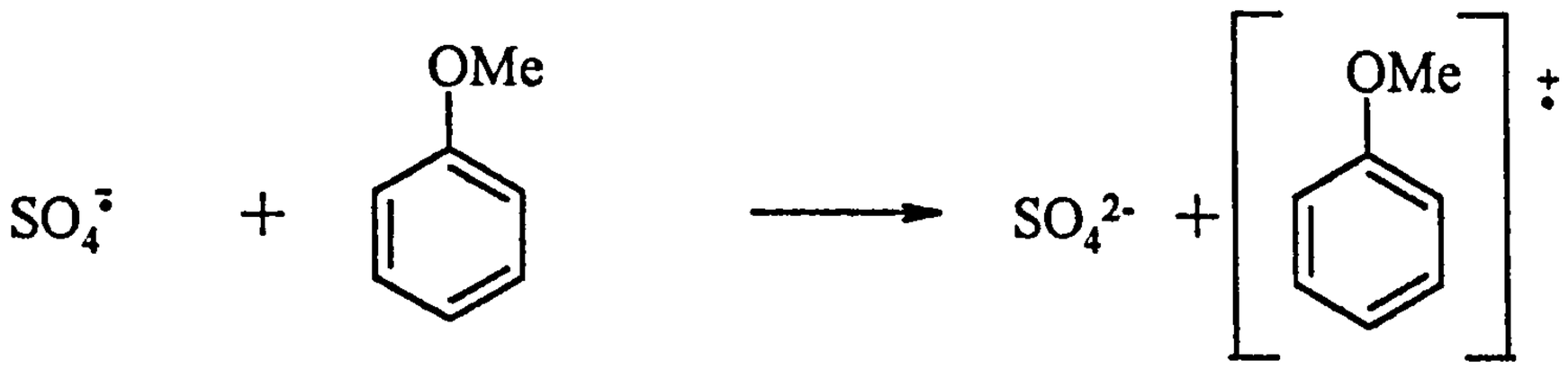

(1.24)

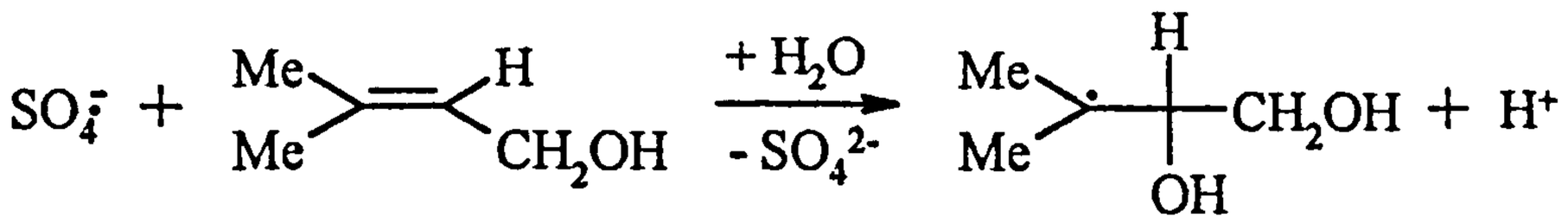

(1.25)

Although not used widely in synthesis, the metal-induced decomposition of peroxymonosulfate has been used to initiate radical polymerisation[51] and oxidise alcohols.[44, 52]

Photolysis or thermolysis of peroxydisulfate leads to the formation of the sulfate radical anion ($SO_4^{\cdot-}$).[53] Peroxydisulfate can also be cleaved on reaction with $e^-_{(aq)}$ (formed on radiolysis of an aqueous solution),[54] or from low-valent transition-metal ions[55-58] or from

a nucleophilic radical such as α-hydroxyalkyl or α-aminoalkyl radicals.[58] The decomposition of peroxydisulfate by either photolysis or electron transfer has been utilised for the oxidation of organic substrates in a similar way to the Fenton system; for example methylbenzene can be oxidised to a mixture of benzyl alcohol, benzaldehyde and benzoic acid.[59]

The radical reactions of peroxydiphosphate and peroxymonophosphate [(1.3) and (1.4)] are not as well characterised as those for the corresponding sulfur compounds. Peroxymonophoshate has been reported to decompose during radiolysis to produce largely ·OH and $HPO_4^{\cdot-}$.[60] Peroxydiphosphate displays greater thermal stability than peroxydisulfate[61] but has been shown to decompose under thermolysis and photolysis to produce $PO_4^{2\cdot-}$.[38,62] Peroxydiphosphate has also been reported to undergo one-electron reduction in the presence of low-valent transition-metal ions such as silver, copper, vanadium[61] and certain iron complexes[63] to form $PO_4^{2\cdot-}$. The radical decomposition of peroxydiphosphate has found limited use synthetically, a notable example being the oxidation of propan-2-ol to propanone by peroxydiphosphate, either under photolytic conditions[64] or in the presence of Fe^{2+}.[52]

iii) Organic Peroxides.

There are several groups of compounds which can be defined under the broad heading of organic peroxides. These include, alkyl hydroperoxides, dialkyl peroxides, peroxyacids, peroxyesters and dicarbonyl peroxides. The radical reactions of these compounds will be discussed in further detail below.

a) Alkyl hydroperoxides.

Alkyl hydroperoxides are important intermediates in many oxidation reactions including lipid peroxidation[64] and metal-catalysed protein oxidation.[65] The decomposition of these compounds is therefore of significance in biological damage processes.

Alkyl hydroperoxides decompose by a variety of routes. Under thermolysis or

photolysis conditions they undergo unimolecular homolysis to form RO· and ·OH [reaction (1.26)] where as in the presence of low-valent transition-metal ions such as Fe^{2+}, Cu^{+} and Ti^{3+} they decompose to form RO· and $^{-}$OH [reaction (1.27)].[66,67] In contrast, in the presence of high-valent transition-metal ions such as cupric, cobaltic or manganic ions, alkyl hydroperoxides decompose to produce, the corresponding alkylperoxyl radical, ROO· [reaction (1.28)].[21,67] Alkoxyl radicals can abstract the peroxidic hydrogen from hydroperoxides producing peroxyl radicals [reaction (1.29)]. A radical may also displace one of the peroxidic oxygen atoms [reaction (1.30)].[66]

$$ROOH \xrightarrow{h\nu\ /\ \Delta} RO\cdot + \cdot OH \qquad \textbf{(1.26)}$$

$$ROOH + M^{n+} \longrightarrow ROO\cdot + H^{+} + M^{(n+1)+} \qquad \textbf{(1.27)}$$

$$ROOH + M^{n+} \longrightarrow RO\cdot + {}^{-}OH + M^{(n-1)+} \qquad \textbf{(1.28)}$$

$$ROOH + R^{1}O\cdot \longrightarrow ROO\cdot + R^{1}OH \qquad \textbf{(1.29)}$$

$$ROOH + R^{1}\cdot \longrightarrow \begin{cases} ROR^{1} + \cdot OH \\ R^{1}OH + RO\cdot \end{cases} \qquad \textbf{(1.30)}$$

Alkoxyl radicals react by a number of routes. They may abstract a hydrogen atom to furnish an alcohol, [reaction (1.31)] or undergo β-scission, forming a ketone or aldehyde and an alkyl radical, [reaction (1.32)]. The speed of this reaction depends largely on the stabilities of the alkyl radical and the ketone produced during β-scission and also exhibits a strong solvent dependence.[68] If β-scission is the favoured route of decomposition, the resulting alkyl radical can itself react in a number of ways: it may dimerise, abstract a hydrogen atom or react with molecular oxygen. Alternatively alkoxyl radicals may add to alkenes [reaction (1.33)] or they may disproportionate [reaction (1.34)].

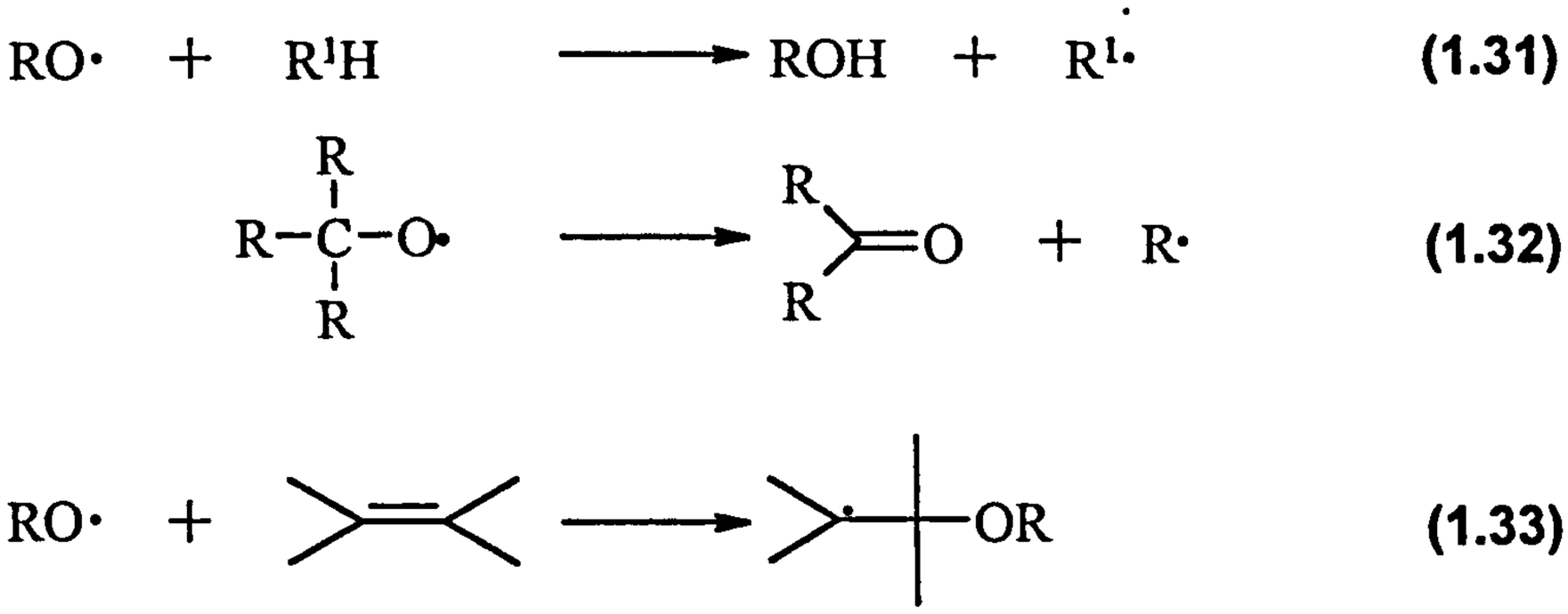

(1.31)

(1.32)

(1.33)

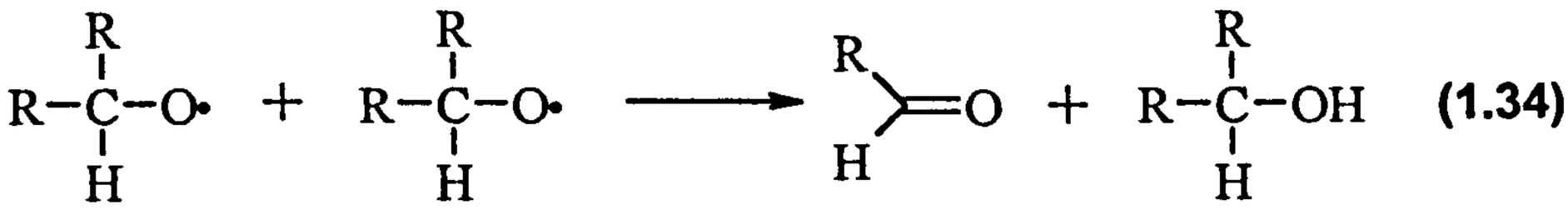

(1.34)

It is of note, however that the method of radical generation can significantly affect the final product distribution. If the peroxide bond is decomposed by electron transfer from a low-valent transition metal ion, the oxidised metal is able to react with the alkyl radical (formed by β-scission) to produce mixtures of alcohols, alkanes and alkenes.[69] However if the alkoxyl radical is generated by photolytic or thermolytic decomposition alkenes and alcohols are not observed.

Peroxyl radicals produced by hydrogen-atom abstraction from the hydroperoxide or reaction of the hydroperoxide with a high-valent transition-metal ion exhibit a range of reactions. They can abstract a hydrogen atom, [reaction (1.35)] dimerise then lose oxygen to produce two alkoxyl radicals [reaction (1.36)] or add to alkenes, leading to the ultimate formation of epoxides [reaction (1.37)].

(1.35)

(1.36)

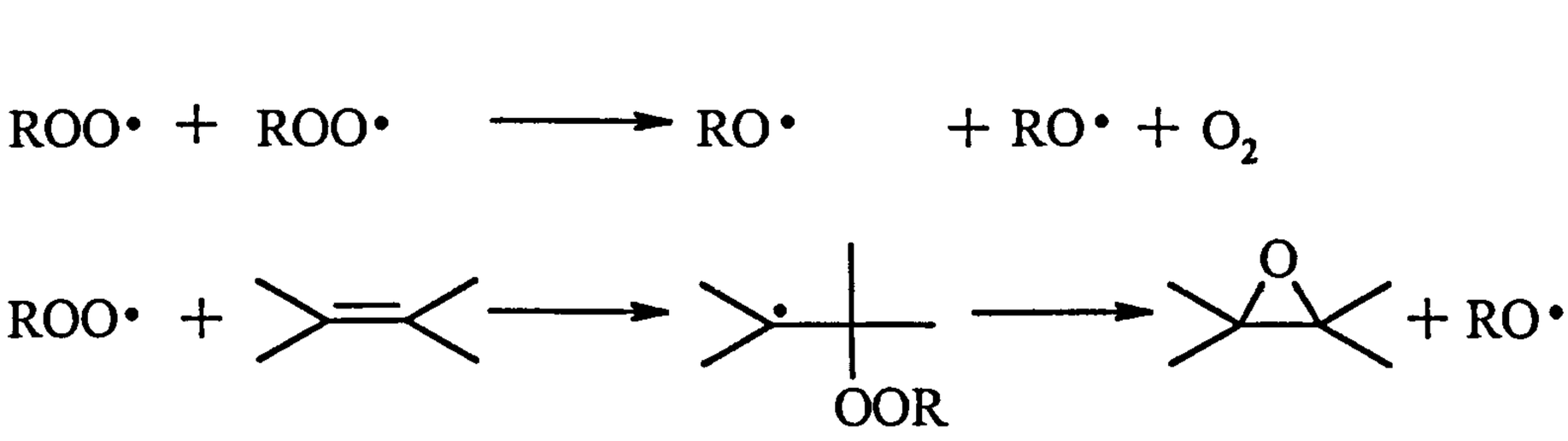

(1.37)

b) Dialkyl peroxides.

Dialkyl peroxides produce alkoxyl radicals on thermolysis or photolysis (for reactions of these species see above). As would be expected the bond strength of dialkyl peroxides is strongly influenced by the alkyl groups [Table 1.1]. It has been demonstrated that replacement of alkyl groups with electron withdrawing halogenated alkyl groups strengthens the O-O bond whereas replacement with electron donating acetyl groups, to form a diacyl peroxide, reduces the bond strength.[68]

Peroxide	D^0_{298} / kJ mol^{-1}
MeC(O)O-O(O)CMe	125.8
$(CF_3)_3CO$-$OC(CF_3)_3$	149.0
t-BuO-OBu-*t*	152.0
MeO-OMe	155.0
CF_3O-OCF_3	193.0

Table 1.1. The bond strengths of some dialkyl peroxides.[70]

The low-valent transition-metal catalysed decomposition of dialkyl peroxides proceeds as for the metal catalysed decomposition of alkyl hydroperoxides, to produce alkoxyl radicals and alkoxide anions.[71-74] The reactions of alkoxyl radicals are reviewed above.

c) Peroxyacids

The typical bond strength of the O-O bond in a peroxyacid is 138 kJ mol^{-1},[76] making it susceptible to homolytic decomposition under thermolysis or photolysis to produce the corresponding acyloxyl radical and the hydroxyl radical [reaction (1.38)]. On reaction of peroxyacids with low-valent transition-metal ions such as Co^{2+}, Mn^{2+}, Fe^{2+} and Ti^{3+} the acyloxyl radical and ^{-}OH are produced [reaction (1.39)].[76-79] However, it has been shown that in the presence of Cu^{+} some peroxyacids undergo decomposition to produce ·OH and

the corresponding anion [reaction (1.40)].[77,80] It has also been established the under radiolysis some peracids, for example nitroperbenzoic acids,[81] undergo decay to form mostly hydroxyl radicals and the alkanoate anion [reaction 1.41)]. Reaction of peracids with high-valent transition-metal ions affords $RCO_3\cdot$ and H^+ [reaction (1.42)].

$$RCO_3H \xrightarrow{h\nu\,/\,\Delta} RCO_2\cdot + \cdot OH \qquad \textbf{(1.38)}$$

$$RCO_3H + M^{n+} \longrightarrow RCO_2\cdot + M^{(n+1)+} + {}^{-}OH \qquad \textbf{(1.39)}$$

$M^{n+} = Ti^{3+}, Fe^{2+}$

$$RCO_3H + Cu^{+} \longrightarrow RCO_2^{-} + Cu^{2+} + \cdot OH \qquad \textbf{(1.40)}$$

$$RCO_3H + e^{-}_{(aq)} \longrightarrow RCO_2^{-} + \cdot OH \qquad \textbf{(1.41)}$$

$$RCO_3H + Ce^{4+} \longrightarrow RCO_3\cdot + Ce^{3+} + H^{+} \qquad \textbf{(1.42)}$$

Acyloxyl radicals are generally unstable and decarboxylate rapidly to produce the corresponding alkyl radical and CO_2. The rate of decarboxylation is governed by the stability of the alkyl radical formed on decarboxylation, the rate of fragmentation of $CH_3CO_2\cdot$ being appreciably faster than the rate of decarboxylation of $PhCO_2\cdot$.[78]

The acyloxyl radical may also add to double bonds or abstract a hydrogen atom if the concentration of substrate is large enough and the stability of the acyloxyl radical such that these reactions may compete with decarboxylation. If this is not the case, the free-radical reactions of peracids are dominated by the reactions of the resulting alkyl radical.

d) Peroxyesters

Peroxyesters provide another source of acyloxyl radicals when subjected to thermolysis or photolysis. Thermolytic decomposition of peroxyesters can proceed by one of two routes, one-bond homolysis [reaction (1.43)] or concerted two-bond homolysis [reaction (1.44)].[20] The mechanism of thermolysis depends upon the stability of the

peroxyester, the more stable peroxyesters generally decomposing via one-bond homolysis and the less stable peroxyesters decomposing via two-bond concerted homolysis.[82] However it is thought that photolysis of any peroxyester results in one-bond homolysis only [reaction (1.43)].

One electron reduction by low-valent transition metal ions proceeds to produce the alkoxyl radical and the carboxylate anion only [reaction (1.45)]. The copper-catalysed decomposition of peroxyesters has been used extensively in organic synthesis to bring about acyloxy substitution.[20,83]

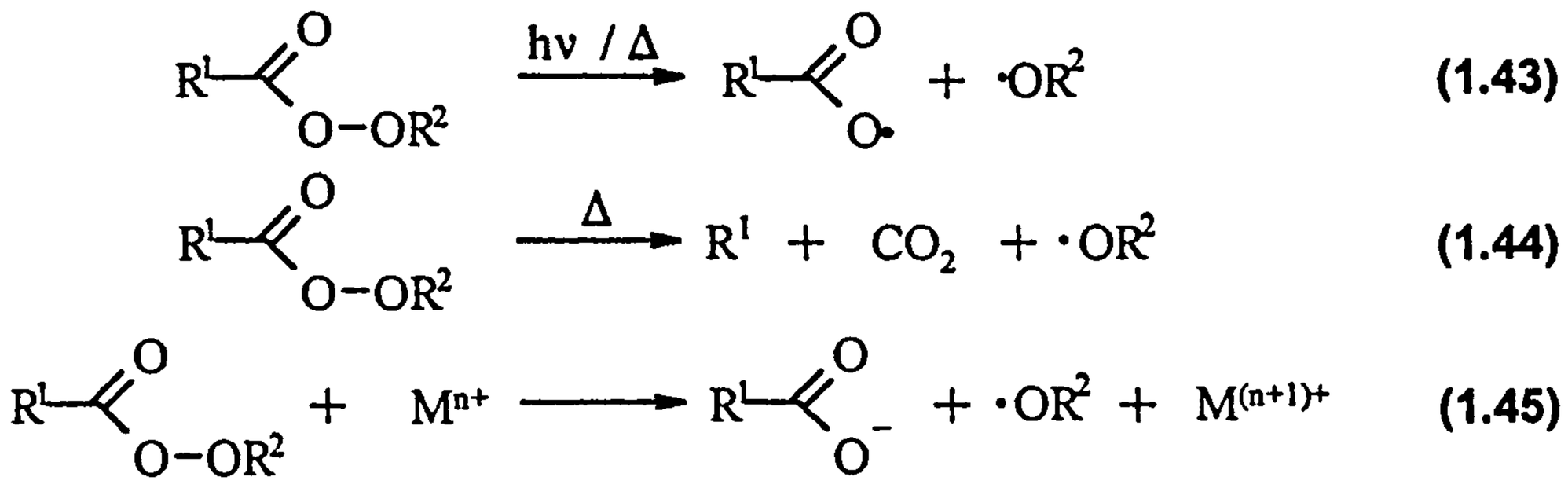

(1.43)

(1.44)

(1.45)

e) Diacyl Peroxides

Under thermolytic or photolytic conditions fission of the peroxide bond in dicarbonyl peroxides occurs to form two acyloxyl radicals, the reactions of which have been discussed previously. Reaction with low-valent transition-metal ions including Fe^{2+}, Cu^{+} and Cr^{2+} proceeds, as expected, to produce the acyloxyl radical and the carboxylate anion.[73,84,85]

1.3. FREE RADICALS IN BIOLOGICAL SYSTEMS.

Free-radical chemistry is now believed to be of great significance in biological systems, both mammalian and bacterial. The reactions of free-radicals in biological systems will be reviewed below as will the consequences of these reactions and defence mechanisms which these systems have in place to minimise free-radical damage.

1.3.1. Radical Production in Biological Systems.

Radical reactions in biological systems can be broadly classified into those that are beneficial to the system and those which are detrimental.

In mammalian systems there are several beneficial radical processes. These include prostaglandin synthesis,[17] the action of ribonucleotide reductase[18] and immune response.[15,16] However, these are outweighed by deleterious radical-producing reactions including those resulting from a leaky electron-transport chain,[86] escape of $O_2^{\cdot-}$ from cytochrome P_{450},[87] ischemia reperfusion injury,[15,16] the actions of some toxins, for example, halocarbons[88] and some anti-tumour drugs.[89]

Many of these processes are shared by bacterial systems. The action of ribonucleotide reductase is obviously of critical importance to the functioning of bacterial cell metabolism, but a leaky electron transport chain, immune response, the action of some toxins and bactericides are all highly harmful to bacteria.

i) Ribonucleotide reductase

Ribonucleotide reductase catalyses the formation of deoxyribonucleotides, the building blocks for DNA synthesis, from ribonucleotides. It is known to contain a tyrosyl free radical, which has been demonstrated to be vital for enzyme action. The radical participates in the removal of the C(2) - OH group and its substitution by a hydrogen atom.[90,91]

ii) Electron-transport chain

The electron transport chain is comprised of a series of enzymes which are responsible for the reduction of molecular oxygen to water in cells. This transfer of electrons from NADH or $FADH_2$ to molecular oxygen is coupled to ATP formation in a process known as *oxidative phosphorylation*. In eukaryotic cells the respiratory assembly is located within the mitochondrial membrane, whereas in prokaryotic cells this assembly

is found in the cytoplasmic membrane. Irrespective of the location of the respiratory assemblies, the step-wise reduction of oxygen occurs at the active site of the enzyme cytochrome oxidase. Until recently the mechanism was believed to be that illustrated in Scheme 1.1, but recent advances in the clarification of the three dimensional structure have lead to the suggestion of an alternative mechanism.[92] This enzyme contains two heme groups and two copper ions at the active site which are responsible for keeping the oxygen tightly bound until complete reduction to two molecules of water is achieved. However the enzyme is not always totally efficient and the release of partially reduced oxygen species, particularly the superoxide anion ($O_2^{\cdot-}$) occurs as a result. If $O_2^{\cdot-}$ escapes from the active site of cytochrome oxidase it can cause extensive damage to surrounding biomolecules.[86]

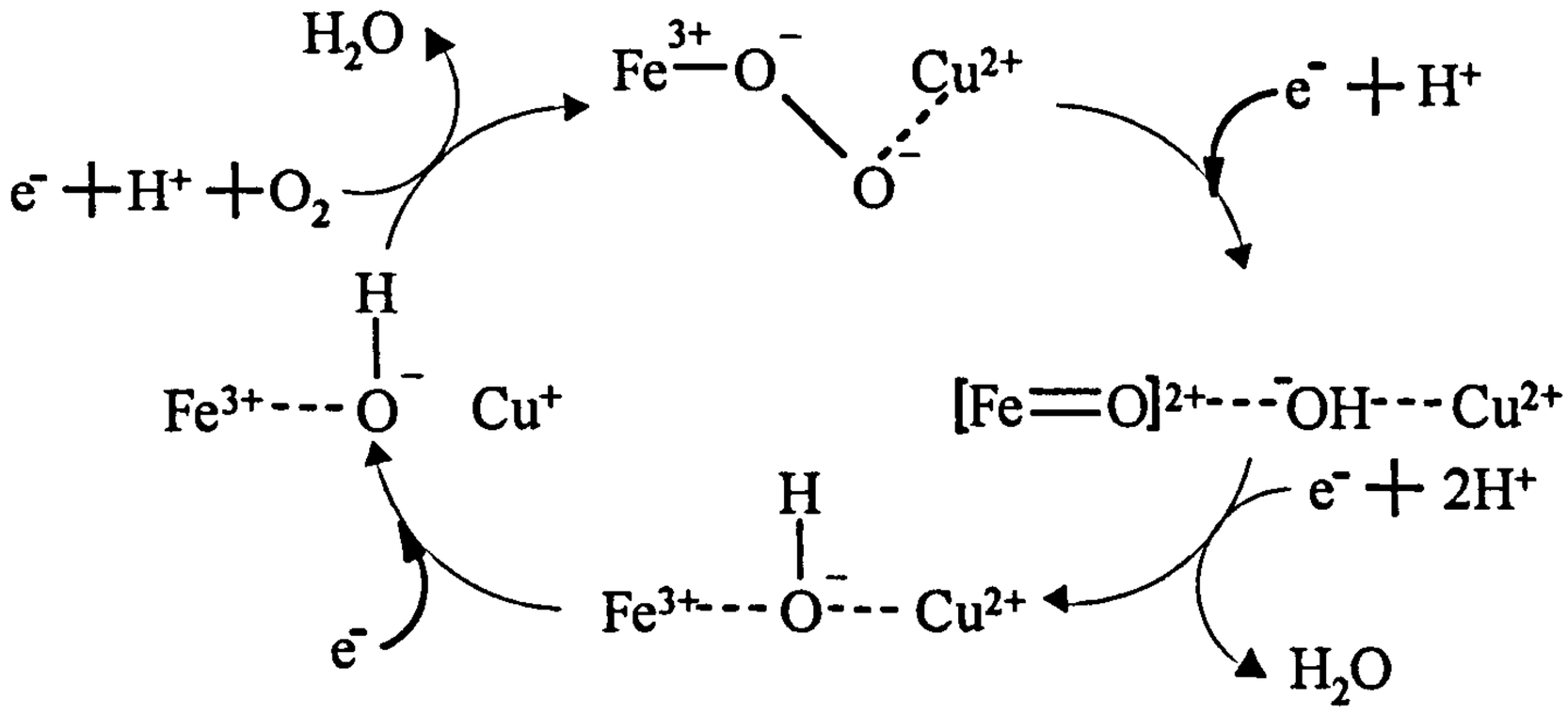

Scheme 1.1. Proposed mechanism for the four electron reduction of O_2 by cytochrome oxidase.[86]

iii) Immune Response

Phagocytic cells, such as neutrophils, monocytes, macrophages and eosinophils, are all involved with the destruction of pathogenic species; these cells migrate to the site of infection or injury and are stimulated to undergo a series of biochemical changes which results in a metabolic burst.[91-95] Metabolic burst is associated by a substantial increase in oxygen consumption, and subsequent generation of $O_2^{\cdot-}$ which is produced by the reactions of NADPH and NADPH oxidase with oxygen [reaction (1.46)] and H_2O_2 which is generated by the subsequent dismutation of $O_2^{\cdot-}$ by the enzyme superoxide dismutase [reaction

(1.47)]. H_2O_2 can undergo subsequent reactions to produce hydroxyl radicals or alternatively undergo reaction with chloride ions [reaction (1.48)], in a reaction catalysed by myeloperoxidase, which is generated by phagocytic cells.[96-98] It has been established that $O_2^{\cdot-}$ and HOCl are very effective at killing bacteria.

$$2O_2 + NADPH \longrightarrow 2O_2^{\cdot-} + NADP^+ + H^+ \quad \textbf{(1.46)}$$

$$2O_2^{\cdot-} + 2H^+ \longrightarrow H_2O_2 + O_2 \quad \textbf{(1.47)}$$

$$H_2O_2 + Cl^- \longrightarrow HOCl + {}^{\cdot}OH \quad \textbf{(1.48)}$$

iv) Bactericidal Action

It is known that ·OH is highly toxic to bacteria, as studies involving the generation of hydroxyl radicals by radiolysis in the presence of bacterial suspensions have demonstrated.[99] In the absence of such a guaranteed source of hydroxyl radicals, definitive evidence of its involvement in bactericidal activity is scarce and widely debated. It has been suggested that hydrogen peroxide reacts with intracellular iron to produce ·OH which then attacks intracellular targets.[100-102] This has been established by examining the effect of hydroxyl-radical scavengers and iron chelators on the antimicrobial activity of hydrogen peroxide.[100,101] However it has been argued that for hydrogen peroxide two modes of damage exist, one at low concentrations of H_2O_2 for which the oxidising species has not been identified and one at higher concentrations of hydrogen peroxide which is thought to be hydroxyl radical mediated.[101,103-105] Mode-one killing results from mutagenesis, but during mode-two killing damage to other cellular components is suggested.

Alkyl hydroperoxides have also proved to be highly bactericidal, both against actively metabolising cells and spores.[106,107] The activity of these compounds has been attributed to the alkylperoxyl radicals derived from them, as metal ion chelators such as *o*-phenanthroline have been shown to be protective.[107] However, it has also been demonstrated that the spin-trap 5,5-dimethyl-1-pyrroline-*N*-oxide (DMPO) and

antioxidants including α-tocopherol and ascorbate are not effective at protecting cells from alkyl hydroperoxide-mediated damage.[107] Nevertheless, there is little doubt that should alkylperoxyl radicals be produced they will be highly bactericidal.[108]

Peracids, in particular peroxyacetic acid, have been found to be extremely effective biocides. Peroxyacetic acid has been shown to be several times more effective than hydrogen peroxide against a range of bacterial strains in both actively metabolising cells and spores.[1,109-111] Evidence has been presented for the involvement of free radicals in damaging processes:[102,110] it has been shown that while spores are *resistant to* damage by low-valent transition-metal ions and transition-metal chelators,[110] the level of damage in vegetative cells is significantly *increased.*[102,110] It has also been shown that α-tocopherol and ascorbate are protective towards damage to spores and bacterial cells, but specific hydroxyl radical scavengers are not particularly effective, indicating that the damaging species is not ·OH.[111]

1.3.2. Defences Against Free-radicals in Biological Systems.

Cells have evolved so that they can tolerate limited levels of reactive oxygen species. Cells have two defence strategies against free-radical attack, enzymes and antioxidant molecules; if these defence mechanisms should fail they also have repair enzymes which will repair damage to biomolecules.

i) Enzymatic defences against free-radicals.

Cells contain a variety of enzymes capable of removing partially-reduced oxygen species. One of these is the heme-containing enzyme catalase which reacts with hydrogen peroxide to produce water and oxygen [reaction (1.49)]. In systems which can exist either in aerobic or anaerobic conditions, such as *Escherichia coli* it has been found that there are two forms of catalase, one which is constitutive and one which is inducible.[112]

$$2\,H_2O_2 \longrightarrow 2\,H_2O + O_2 \qquad \textbf{(1.48)}$$

There are other enzymes which, like catalase will destroy hydrogen peroxide, but unlike catalase will catalyse the safe decomposition of other peroxides. This family of enzymes includes glutathione peroxidase, glutathione-S-transferase and related glutathione-dependent enzymes. Glutathione peroxidase is found in two forms, one which is selenium dependent and can catalyse the breakdown of hydrogen peroxide and organic hydroperoxides, and one which is not reliant on selenium and only catalyses the breakdown of organic hydroperoxides.[113] Both forms are dependent on the presence of glutathione. The general reactions are illustrated in Scheme 1.2.

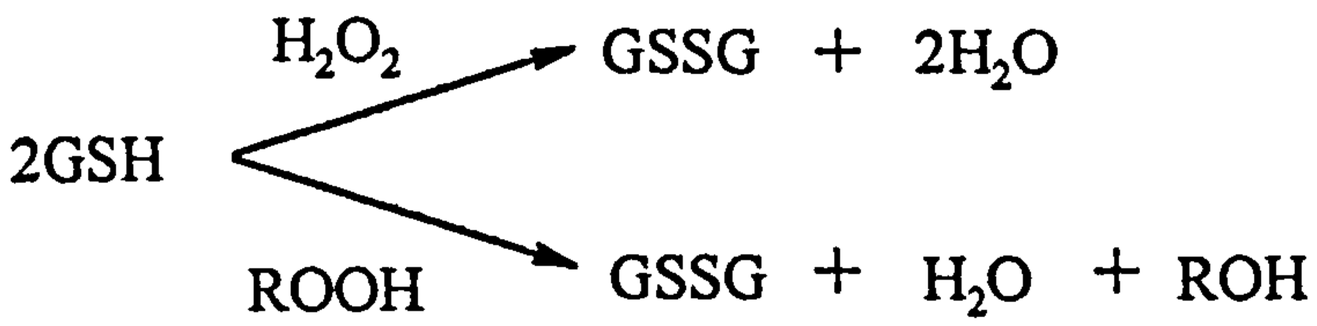

Scheme 1.2. The reactions of gluthathione with hydrogen peroxide and organic hydroperoxides as catalysed by glutathione peroxidase.

The other major enzyme which has the ability to scavenge partially-reduced oxygen species is superoxide dismutase which catalyses the conversion of $O_2^{\cdot-}$ to hydrogen peroxide and water. In mammalian systems, there are two types of superoxide dismutase, one with manganese at the active site and one with copper and zinc at the active site.[112,114] In bacterial systems such as *Escherichia coli*, which can grow in the presence or absence of oxygen, there are also two types of superoxide dismutase, one based upon iron which is constitutive and another based upon manganese which is inducible by the presence of oxygen.[112,115]

The action of these enzymes, under normal conditions, will ensure that hydroxyl radicals are not formed since superoxide dismutase will convert any $O_2^{\cdot-}$ to hydrogen peroxide which may then be safely decomposed by catalase. This is fortuitous since the specific enzymatic scavenging of a molecule as reactive as the hydroxyl radical would be impossible.

ii) Non-enzymatic defences against free-radicals

Mammals share some aspects of their molecular antioxidant defences with bacteria. Both bacterial and mammalian systems have intracellular antioxidant defences against free-radical damage, but mammalian systems have their intracellular defences augmented by extracellular support. Many of the antioxidant molecules are common to both systems.

Both bacteria and mammals have intracellular pools of thiols which are oxidised to the corresponding disulfides during periods of oxidative stress and are therefore primarily responsible for maintaining the reduced cell environment. The most significant of these is glutathione (1.5) which is found in cells at millimolar concentrations.[17]

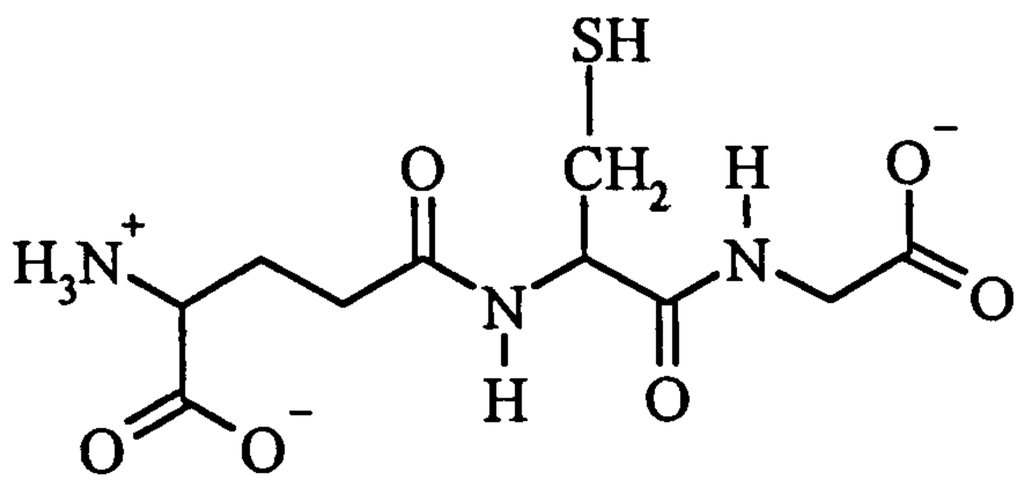

(1.5)

It maintains the reduced cell environment in two ways. It may react directly with free-radical species[116] [reactions (1.49) and (1.50)] and is also a vital cofactor in the action of some antioxidant enzymes such as glutathione peroxidase (see above).[113]

$$GSH + {}^{\cdot}OH \longrightarrow GS^{\cdot} + H_2O \qquad \textbf{(1.49)}$$

$$GSH + Biomolecule^{\cdot} \longrightarrow GS^{\cdot} + Biomolecule \qquad \textbf{(1.50)}$$

Other important antioxidants common to both mammals and bacteria include ascorbate. In mammals it is found both intra-cellularly and extra-cellularly.[117,118] It reacts with a variety of oxidising species including $O_2^{\cdot-}$, ·OH, $^1O_2$ and HOCl and various lipid peroxyl radicals and hydroperoxides, producing the resonance-stabilised ascorbyl radical. Further reduction leads to the formation of dehydroascorbate [Scheme (1.3)].

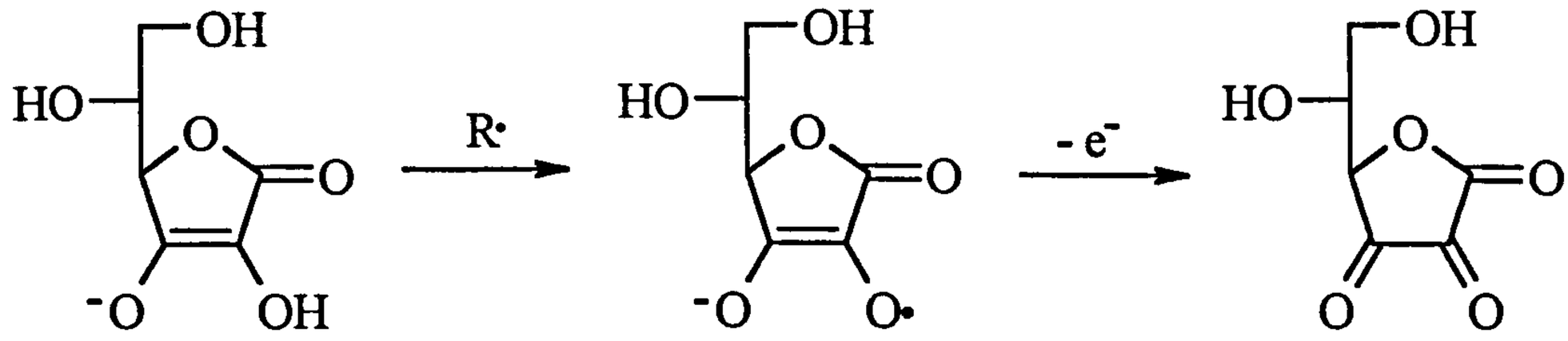

Scheme 1.3. The antioxidant reactions of L-ascorbic acid.

The most important membrane-soluble antioxidant is α-tocopherol which can react with a variety of oxidising species to produce a resonance-stabilised phenoxyl radical.[119] This radical can then meet with a variety of fates. It may react further with peroxyl radicals to produce non-radical products or it may react with the water-soluble antioxidant, ascorbate at the membrane interface.[120] β-Carotene is another lipid soluble antioxidant. It scavenges peroxyl radicals to produce a highly stabilised carbon-centred radical. Due to the stability of this radical, further reaction is disfavoured, especially in a membrane environment where the concentration of oxygen is not substantial under normal conditions.

In addition to the compounds described above, bacteria contain bacterioferritin, which sequesters and stores iron, thus rendering it redox inactive.[121-123] Mammals also have iron-binding proteins which afford similar protection, some of which are intracellular and some of which are found in the extracellular fluid (see below).[117,118]

Mammalian systems have another line of defence against reactive oxygen species in that they also contain extracellular antioxidants including ascorbate.[117,118] Other extracellular antioxidants include the iron-transport proteins lactoferrin and transferrin which keep iron safely sequestered and redox inactive.[117,118] Similarly, haptoglobin and hemopexin complex to hemoglobin and render its iron centre redox inactive. The protein ceruloplasmin complexes and stores copper and therefore ensures that copper is unavailable to initiate free-radical damage. Serum albumin complexes copper in a similar manner and, if necessary, acts as a sacrificial substrate for oxidation as it can be rapidly removed from circulation and degraded. Further protection from radical-induced damage is provided by uric acid which exhibits two modes of action. It binds copper and iron very strongly, therefore inhibiting their redox activity, and it is also a potent scavenger of

hydroxyl radicals, alkoxyl radicals, peroxyl radicals, singlet oxygen and hypochlorite. Bilirubin has also been reported to possess antioxidant activity: it is a product of heme catabolism which is transported bound to serum albumin. It is thought that it may protect albumin-bound fatty acids from free-radical attack. It has been suggested that glucose is an effective extracellular antioxidant based upon its speed of reaction with hydroxyl radicals although it has not been demonstrated whether or not it is physiologically important.[117,118]

It is also important to remember that under certain circumstances most antioxidants can act as prooxidants; for example, ascorbic acid is an effective promoter of lipid peroxidation in the presence of iron, as it enables Fe^{3+} to be reduced to Fe^{2+} and hence generate radicals. Also the oxidation of ascorbate itself by O_2 leads to the production of $O_2^{\cdot-}$ [reaction (1.51)]. Iron-storage and transport proteins have been shown to be effective promoters of free-radical damage when exposed to acidic conditions which mobilise the iron from their binding sites.[118]

$$AH^- + O_2 \longrightarrow A^{\cdot} + O_2^{\cdot-} + H^+ \qquad (1.51)$$

iii) Repair enzymes

When cellular antioxidant defences fail, there is a further mechanism by which cellular damage can be limited: repair enzymes can remove damaged molecules therefore preventing an accumulation of damage. Damaged lipids can be removed by phospholipases, which have been shown to be more effective at removing peroxidised lipids than undamaged lipids.[124] Proteolytic enzymes have been shown to degrade oxidatively modified proteins more effectively than the corresponding native protein;[6,65,125] oxidatively damaged DNA may also be repaired. The damaged section is removed by a DNA endonuclease; the missing section of DNA is then copied by DNA polymerase and replaced by DNA ligase.[86]

1.3.3. Consequences of free-radicals in Biological Systems.

i) Lipid damage

Lipid peroxidation is a chain process initiated by any species capable of abstracting an allylic hydrogen [Scheme (1.4)];[5,17,64] commonly these species are hydroxyl, alkoxyl or peroxyl radicals. The initial reaction involved in propagating this chain is addition of molecular oxygen to the first-formed radical producing a lipid peroxyl radical. This radical can meet with one of a number of fates. It may dimerise leading to the formation of two alkoxyl radicals and oxygen, attack surrounding membrane proteins or abstract a hydrogen from another fatty acid leading to the formation of a lipid hydroperoxide. Lipid hydroperoxides are subject to decomposition by transition metal ions or heme proteins,[126] producing alkoxyl radicals and peroxyl radicals and thus ensuring that the chain reaction is sustained. The peroxidation of lipids leads to changes in membrane structure and function. The degree of saturation in the fatty acids of biological membranes is, at least in part, responsible for the fluidity of the membrane; increasing levels of saturation leading to a loss in membrane fluidity.[86] Vital membrane-transport processes such as calcium-shuttling and membrane-bound-receptor function are also known to be disrupted by lipid peroxidation.[5,64] In addition to the intrinsic membrane damage caused by lipid peroxidation, the end products of the process are often toxic. These include aldehydes,[5,64] the most noxious of which is the unsaturated aldehyde, 4-hydroxy-2-*trans*-nonenal, which may lead to the cross-linking of proteins[127] among other detrimental reactions.

ii) Damage to Proteins

The generation of reactive oxygen species is believed to lead to extensive protein oxidation:[8,128] the nature of the damage is dependent on the method of radical generation. Exposure of proteins to ionising radiation has been shown to cause immense and mainly random protein damage.[129] Under anaerobic conditions, reactions involving the addition of molecular oxygen to first-formed protein-radicals are precluded as are those of $HO_2^{\bullet}$

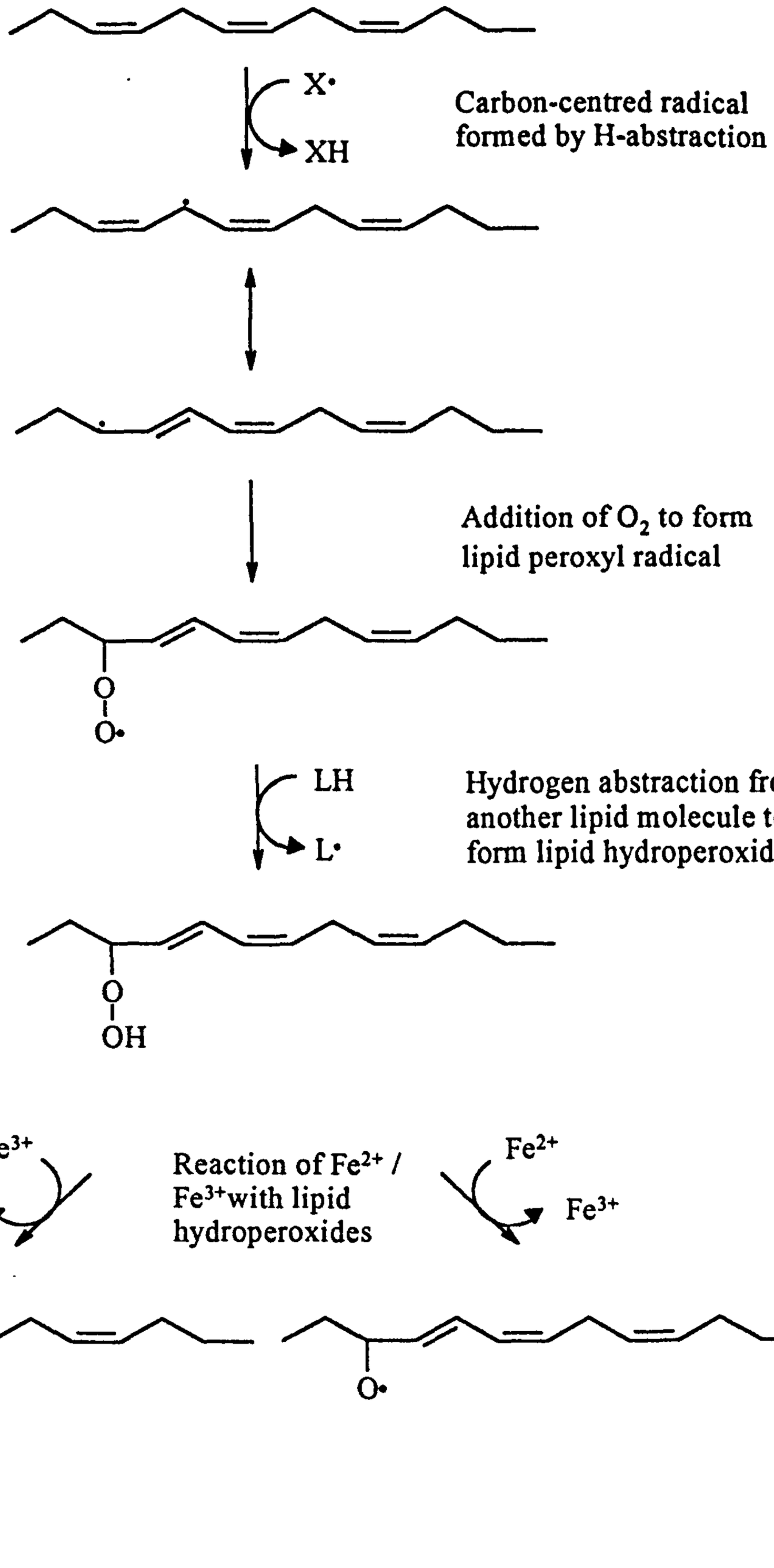

Scheme 1.4. The mechanism of lipid peroxidation.

and $O_2^{\bullet-}$. The main reaction of the first-formed protein-radicals is dimerisation, leading to the formation of high molecular-weight protein aggregates. Dimerisation occurs between carbon-centred radicals and also between cysteine and tyrosine residues, the formation of bityrosyl often being used as a marker for oxidative protein modification. [8,128,130] Irradiation of proteins under aerobic conditions has different implications, fragmentation of the protein occurring in preference to aggregation, due to the presence of oxygen-centred radicals.[129] This is assumed to occur via the α-amidation pathway [Scheme (1.5)]. Oxidation of amino-acid side-chains to carbonyl derivatives is another consequence of aerobic protein irradiation. Long-lived protein hydroperoxides, structural perturbations including changes in hydrophobicity, changes in viscosity, increase in susceptibility to proteolytic degradation and in the case of enzymes, loss of catalytic activity are all associated with oxidative protein damage induced by irradiation.[129]

In contrast metal-catalysed oxidation of proteins has been shown to be somewhat more specific in nature.[129] The amino-acid residues which have been shown to be most susceptible to attack are histidine, arginine, lysine, proline, methionine and cysteine. In general, attack is localised in metal-catalysed systems as the metal will often be located in a binding site; for this reason, free-radical scavengers are not particularly good at reducing levels of damage caused by metal-catalysed protein oxidation as the reaction often takes place in a protein "cage". Attack has also been shown to be less extensive in proteins that have been treated with metal-catalysed oxidation systems than with radiation; commonly only a few amino acids are oxidised in a metal-catalysed oxidation system in contrast to an irradiated system in which a large number of amino acids are attacked.. This is again believed to be a reflection of the caged nature of the oxidation process. The physical and chemical consequences of metal-catalysed protein oxidation are similar to those caused by aerobic irradiation.[129]

iii) Damage to DNA

Radical attack on DNA and its components has been studied extensively because of its possible role in carcinogenesis.[12] The effect of radicals generated in both Fenton-type

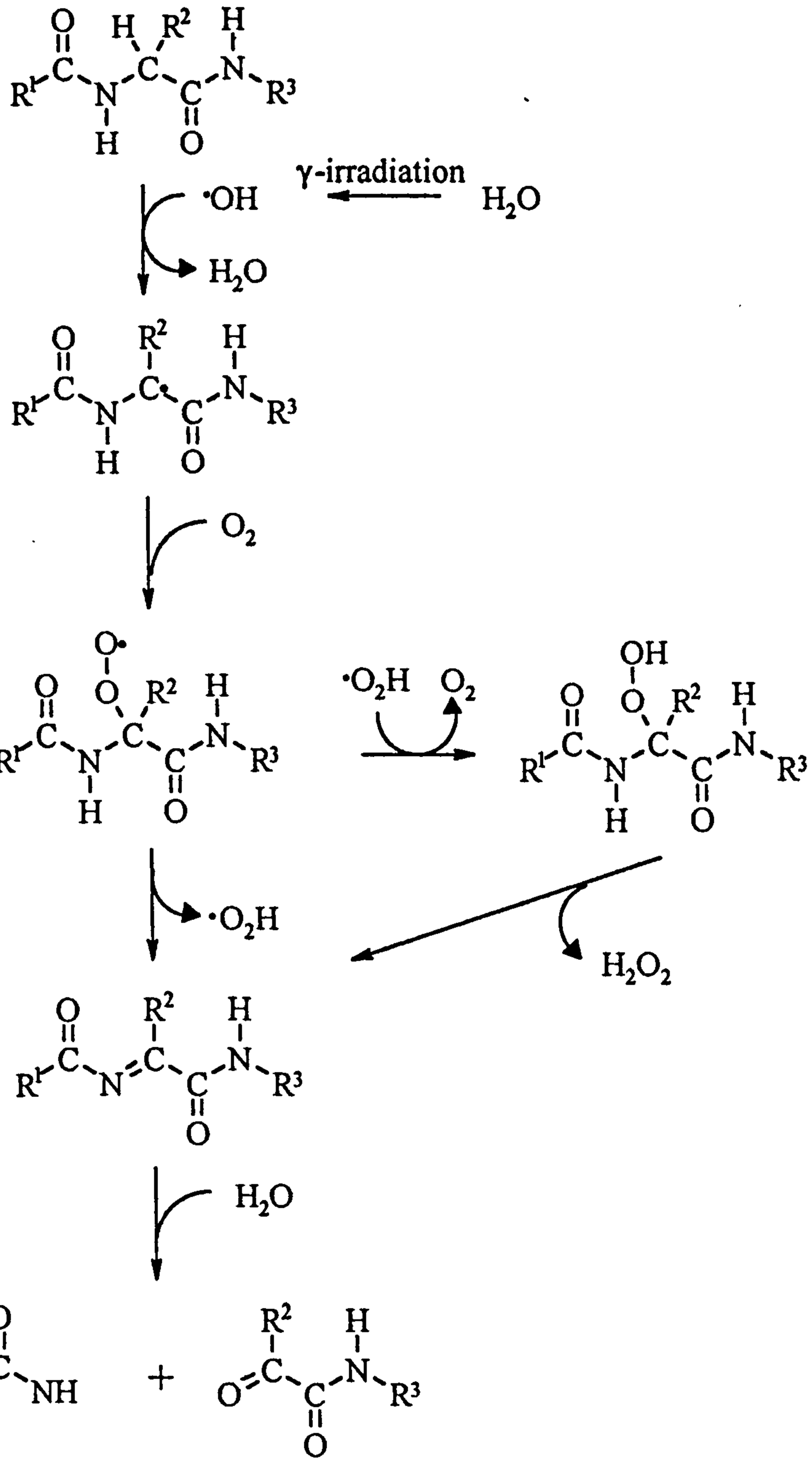

Scheme 1.5. γ-radiolytic cleavage of peptide bonds by the α-amidation pathway.[130]

systems and by ionising radiation have been studied. Two modes of attack have been identified; the addition of ·OH to the double bonds of purine and pyrimidine bases and hydrogen abstraction from the 2-deoxyribose sugar units.[10-12] It has also been demonstrated that base-derived radicals can abstract a hydrogen atom from a neighbouring sugar, transferring damage from the bases to the sugar backbone (Scheme 1.6).[131] If unrepaired, attack on the sugar backbone leads to single-strand breaks. If two of these are incurred in the same region double-strand breaks occur which are usually irreparable. Base lesions are similarly damaging.[12]

In a manner similar to protein oxidation the nature of radiolytic damage depends upon the presence or absence of oxygen. Under normoxic conditions, DNA peroxyl radicals can be formed leading to many possible reactions. When metal-catalysed oxidation is utilised to produce damaging radicals, damage is dependent upon the chelation of the metal. For example Fe^{2+}-EDTA causes random damage to DNA as electrostatic repulsion precludes it from binding at a specific site.[10] However, some complexes have been shown to have affinity for binding to DNA, leading to site specific damage.[10]

1.4. AIMS AND METHODS OF STUDY.

1.4.1. Aims of Study.

The general aim of this study was to probe the mechanism of action of peroxygen biocides, in particular peroxyacetic acid. It is believed that one-electron reduction of the peroxyacid by intracellular transition-metal ions, to produce free radicals, may be responsible for this biocidal action.[100-102] It was therefore decided to investigate the one-electron reduction of peroxyacids in order to probe the nature of radical generation and to examine the reactions of these radicals with model biomolecules. The reactions of peroxyacids with bacteria were also to be investigated to examine the significance of the reactions studied in whole cells.

The initial objectives of this study were to investigate the low-valent transition-metal catalysed cleavage of peracids, in particular peroxyacetic acid, to examine the effect

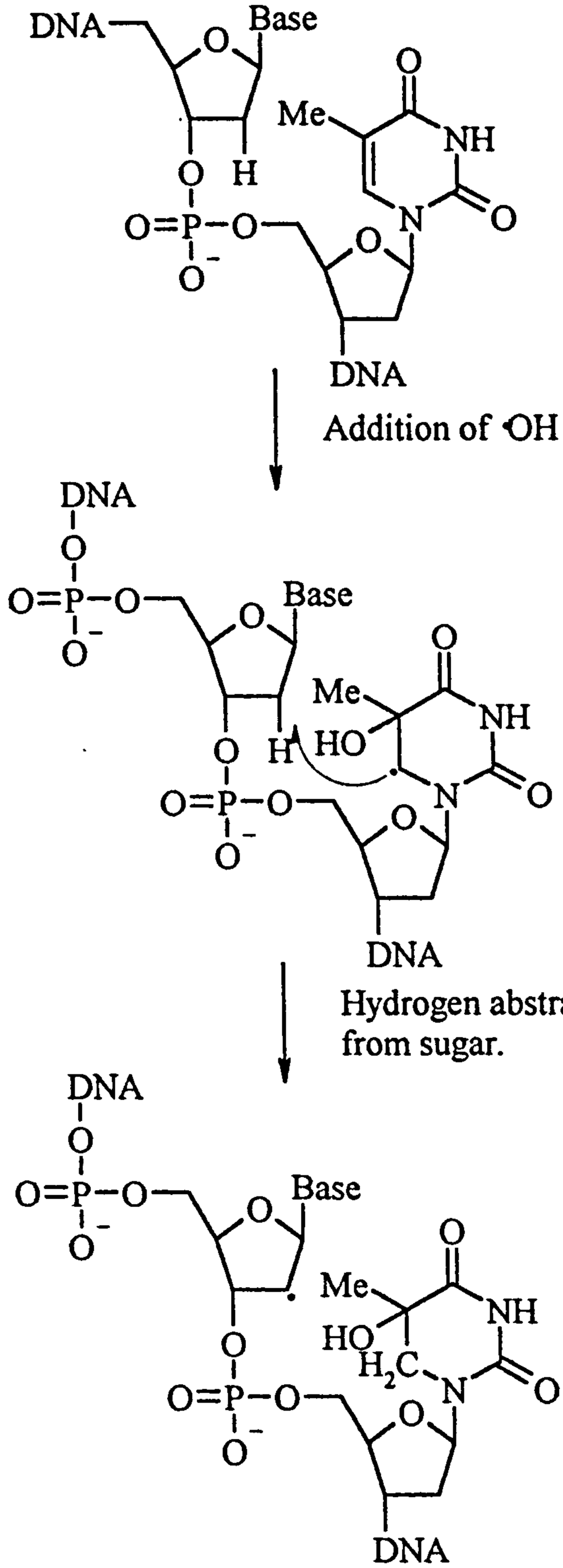

Scheme 1.6. Addition of ·OH to the 5 position of thymine and abstraction of a hydrogen atom from the neighbouring sugar.

of metal and peroxyacetic acid formulation on the direction of O-O bond cleavage. The reactions of Fe^{2+}, Ti^{3+} and Cu^{+} will be contrasted as will the reactions with different peroxyacetic acid formulations. The techniques utilised will include spin-trapping and continuous-flow monitored by EPR spectroscopy. The information gained should allow an insight into the possible metal-catalysed reactions of peroxyacetic acid in bacterial cells.

The reactions of low-valent transition-metal ion / peroxyacetic acid oxidising couples with systems of biological relevance were then to be examined in order to probe the sites and degree of attack by the oxidising species formed. These systems were designed to include a model protein, BSA. Damage was to be assessed in a number of ways. These include EPR spin-trapping, determination of protein carbonyls, assessment of susceptibility of oxidised protein to proteolytic degradation, and assessment of fragmentation of the oxidised protein.

It was also intended to investigate two modes of lipid damage with the aim of assessing transition-metal dependent peroxidation of liposomes and bacterial cell membranes and transition-metal independent epoxidation of fatty acids, phospholipid and liposomes. The techniques employed were to include UV-visible detection of thiobarbituric acid-reactive species for the assessment of peroxidation, NMR spectroscopy for the detection of phospholipid epoxides and EPR spin-probe techniques for the assessment of the effect of lipid epoxidation on physical properties of liposomal membranes.

1.4.2. Methods of Study.

i) EPR Spectroscopy

EPR spectroscopy is a sensitive technique for the detection and characterisation of species with unpaired electrons.[132,133] These include free radicals including biradicals and triplet states and some transition metal ions. EPR is not only very sensitive (radical concentrations of 10^{-7} - 10^{-8} mol dm^{-3} can be detected in aqueous solution) but provides a wealth of information about the structure of the radicals, their environment and the kinetics of their formation and decay. The technique relies upon the absorption of microwave

radiation by an unpaired electron as it undergoes transitions between different energy states induced by the application of an electromagnetic field.

An electron possesses a spin of ½ so it has a magnetic moment. When it is placed in a magnetic field it has two non-degenerate spin-states which have spin quantum numbers [m_s] of -½ and +½ depending on whether the spin is aligned parallel or anti-parallel to the external magnetic field. If a species has all its electrons paired there will be no resultant magnetic moment and hence no overall spin, in which case the species will be EPR silent. However, if all the electrons are not paired there will be an overall spin and the species will be EPR active. Irradiation of such a species with energy of the appropriate frequency leads to transitions, both upward and downward, between the two spin states which are separated by an energy equal to $g\beta B$ [equation (1.1)]. Since, initially, there will be more spins in the lower energy state, according to the Boltzmann distribution, the net effect of irradiation at the appropriate frequency will be absorption. The maintenance of the excess of spins in the lower energy state is ensured by non-radiative relaxation processes.

$$\Delta E = h\nu = g\beta B \qquad \textbf{Eqn 1.1.}$$

g = g-value for the free electron

β = Bohr magneton

H = applied magnetic field

ν = frequency of incident microwave radiation

h = Planck's constant

Conventional X-band EPR spectrometers typically employ a fixed frequency of about 9.5 GHz provided by a microwave source, which may be either a klystron oscillator or a Gunn diode, and a variable magnetic field produced by an electromagnet [Figure (1.1)]. The other feature worthy of mention is that EPR spectra are usually recorded as first derivative plots, a consequence of the detection method employed.

The EPR spectrum of a species can be characterised by three parameters, the g-value, the hyperfine splitting(s) and the linewidth, all of which give important information about the radical concerned.

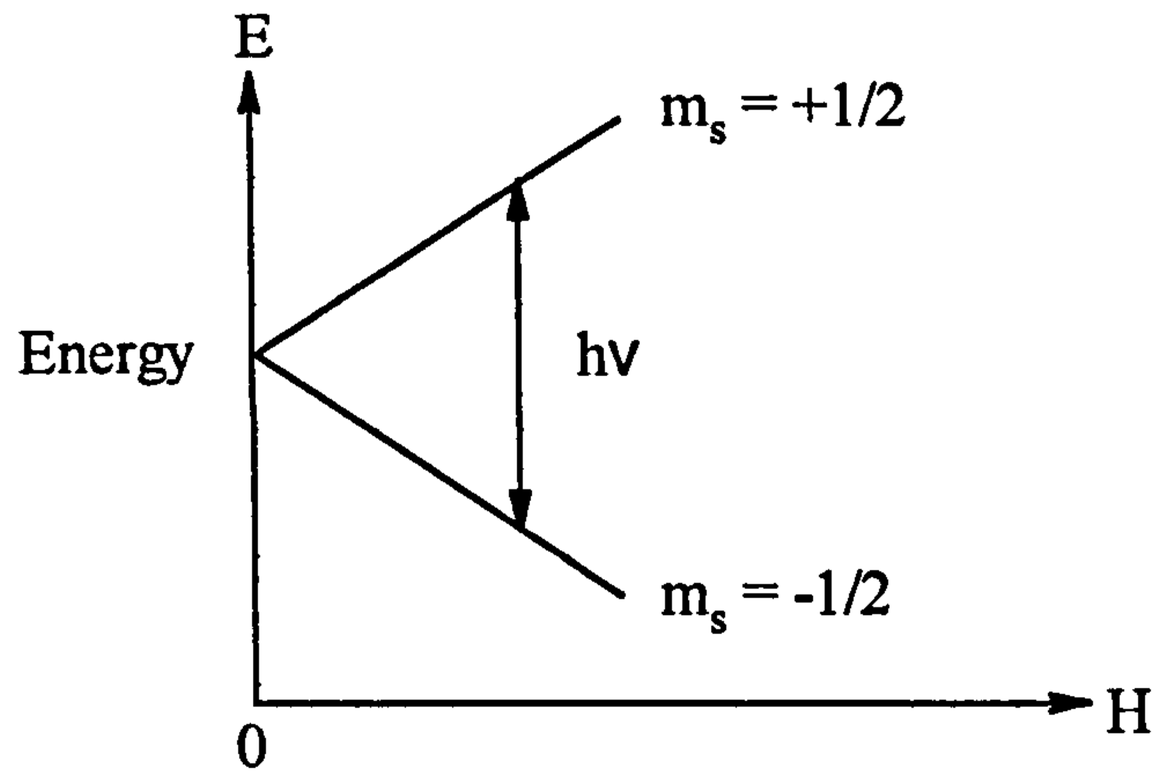

Figure 1.1. The energy levels and EPR transition for an electron as a function of magnetic field.

a) *g*-value

The *g*-value of a radical is analogous to the chemical shift for a proton in a ^{1}H NMR experiment in that it is dependent upon the chemical environment of the radical centre. The *g*-value for most radicals lies close to that for the free electron (2.00232). However, the g-value is dependent on the atom on which the unpaired electron is centred, heteroatoms producing particularly marked deviations from the value for the free electron. The magnitude of the g-value is also affected by the extent of delocalisation of the unpaired electron over neighbouring heteroatoms and spin-orbit coupling. The *g*-value may be measured by reference to an internal standard or by accurate determination of the magnetic field and frequency.

b) Hyperfine splittings

Hyperfine splittings, usually expressed as a_x for an atom x and measured in mT, in EPR spectra arise from the interaction of the unpaired electron with the nuclear spins of neighbouring nuclei, in the same way that hyperfine splittings in NMR spectroscopy arise

from the interaction of the nuclear spin of the atom in resonance with that of neighbouring magnetic nuclei. The interaction between the unpaired electron and neighbouring nuclear spins, which may augment or diminish the resultant magnetic field felt by the unpaired electron leading to several values of the applied magnetic field for which the electron will be in resonance (note the overall change in spin must be 1 for a transition to be allowed) and results in more than one line appearing in the spectrum. In general, for an electron interacting with n equivalent nuclei of spin I there will be 2nI + 1 lines evident in the EPR spectrum, for example an electron interacting with two equivalent protons will give a 1:2:1 splitting pattern and an electron interacting with three equivalent protons will produce a spectrum with a 1:3:3:1 splitting pattern, (see Figure 1.2) the relative intensities of the lines corresponding to the coefficients of the binomial distribution for the number of equivalent protons, n. Non-equivalent nuclei obviously lead to more complex splitting patterns as would be expected by analogy with NMR. The spin-density associated with a nucleus may be calculated from the hyperfine coupling constants using either equation 1.2 or equation 1.3 for nuclei α and β to the radical centre respectively for planar radicals. It should also be noted that nuclei γ and δ to the radical centre may also give small splittings

$$a_{(\alpha\text{-}H)} = Q_h\rho \qquad \textbf{Eqn 1.2.}$$

Q_h = constant

ρ = spin density on α

$$a_{(\beta\text{-}H)} = \rho_\alpha B\cos^2\theta \qquad \textbf{Eqn 1.3.}$$

ρ_α = spin density associated with α

B = constant

θ = dihedral angle formed between the orbital containing the unpaired electron and β-H

c) Line broadening

Several factors contribute to line-broadening observed in EPR spectra including, rotational correlation time and the presence of other paramagnetic species. The rotational

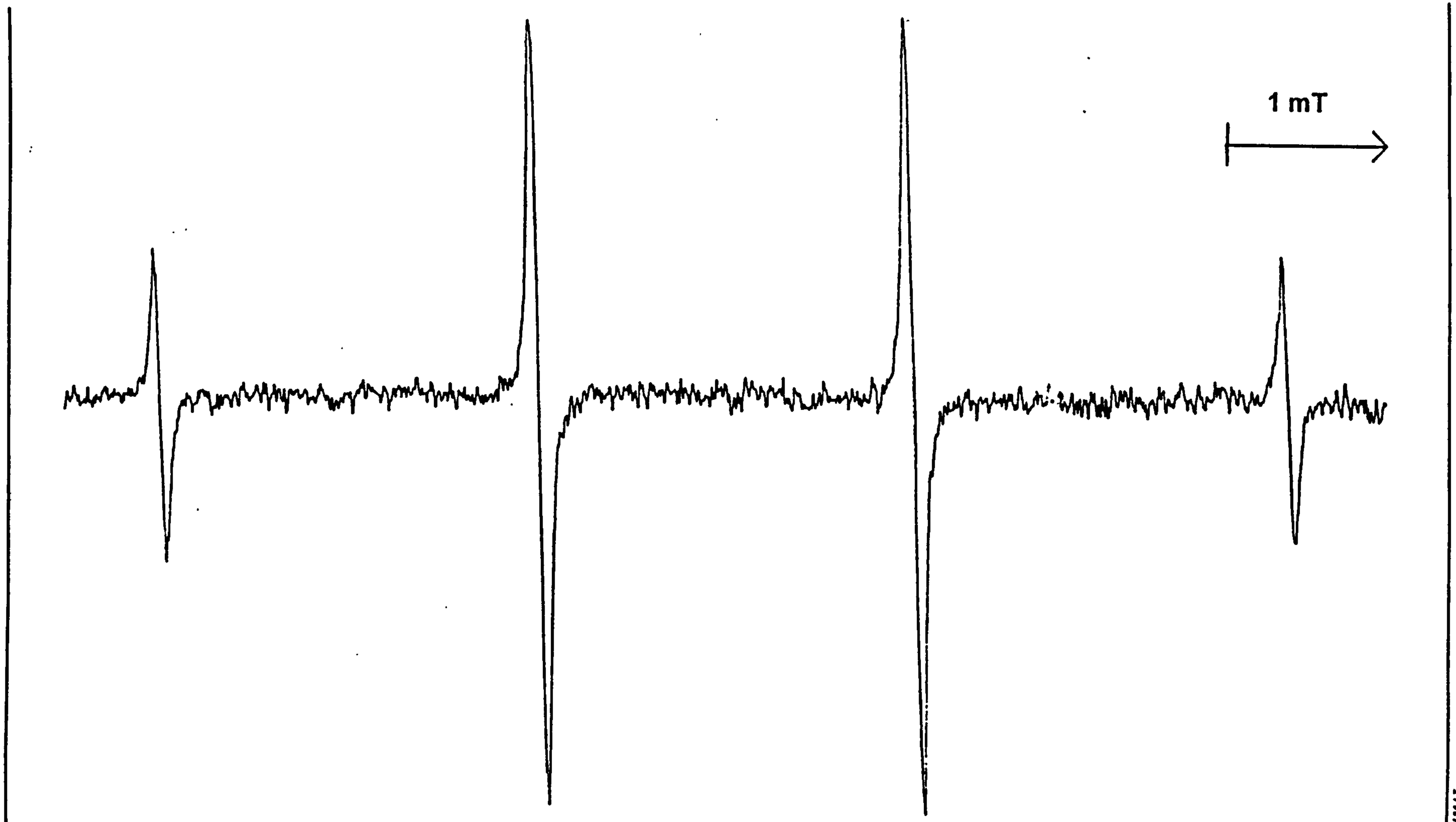

Figure 1.2. The EPR spectrum of the methyl radical generated in a flow system by the reaction of Ti^{3+} with hydrogen peroxide and DMSO.

correlation time (τ_c) is the time taken for the molecule to complete one rotation. This is usually in the order of 10^{-11}s for a rapidly-tumbling radical. Factors which affect $\tau_c$include the molecular weight of the radical species, low molecular weight species being able to tumble freely and therefore giving rise to spectra with sharp well-resolved lines known as isotropic spectra and large molecular weight species, which are unable to tumble freely, giving rise to poorly-resolved anisotropic spectra. Factors which lead to changes in τ_c are the viscosity of the surrounding medium, low viscosity media enabling the free radical to tumble freely, and the temperature of the sample, low temperatures restricting the motion of the radical.

The EPR spectrum observed for a rapidly tumbling nitroxide (with no β-hydrogens) consists of a sharp, well resolved triplet resulting from the nitrogen. However when the same species is in a viscous medium or at a low temperature, the anisotropic spectrum which results is superimposition of the spectra from all of the molecules at slightly different orientations in the magnetic field.[134] Figure 1.3 shows the change in appearance of the EPR spectrum of a 2,2,6,6-tetramethyl-1-piperidinyl-1-oxyl (TEMPO) derivative as the temperature is varied from 100 K to 333 K.

Line-broadening can also be observed in the presence of paramagnetic species other than the one of interest or a high concentration of those being studied, common examples being oxygen and Fe^{3+}. These species reduce the relaxation time and therefore create an uncertainty in the energy differences between the two spin-states leading to line-broadening. Line-broadening can be a useful tool for the examination of the environment of a free radical species, for example in the spin-probe and spin-labelling techniques.[134] The spin-probe technique involves the introduction of a nitroxide species into the system of interest. Close examination of the resulting EPR spectra allows τ_c to be calculated and hence deductions about the physical properties of the solution, such as temperature, polarity, relative viscosity and relative dissolved oxygen concentration, to be determined. Similar deductions can be made from spin-labelling data. Spin-labelling differs from the spin-probe technique in that the spin-label is actually chemically bound to the molecule of interest, usually through a carbonyl or NCO moiety.

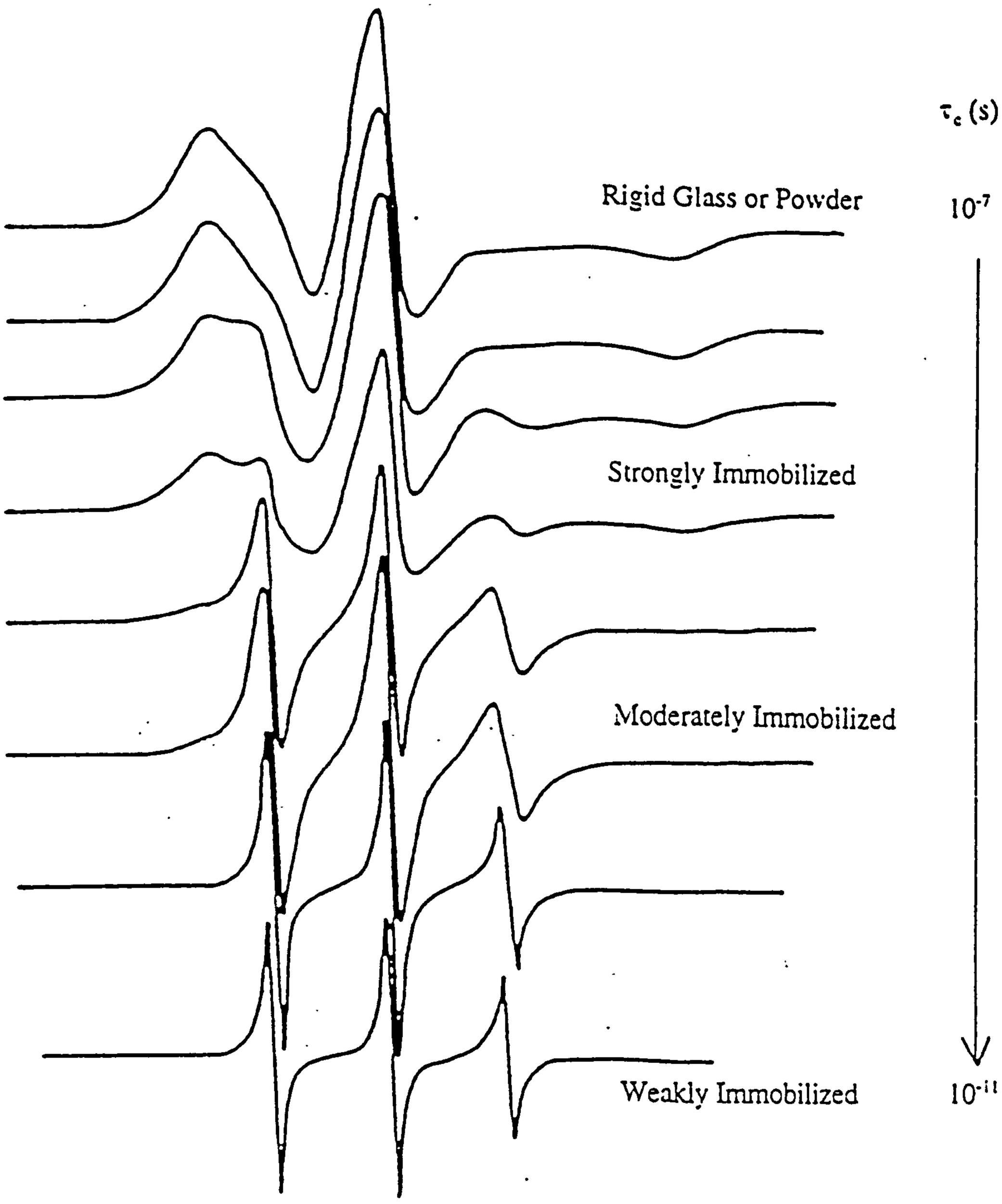

Figure 1.3. Typical variation with temperature of the EPR spectrum of a 2,2,6,6-tetramethyl-1-piperidinyl-1-oxyl (TEMPO) derivative and appropriate values of rotational correlation time (τ_c) from 100 K to 300 K. Reproduced from reference 134.

d) Methods of radical generation / detection

Most free radicals are short-lived necessitating the rapid generation of radicals or the prevention of rapid radical decay processes to enable detection. Commonly used methods include rapid-flow, spin-trapping (for brief review see Chapter 2), continuous photolysis and matrix isolation.

The rapid-flow technique generates a steady state concentration of radicals in the cavity of the spectrometer by employing a peristaltic pump which pumps three streams of reactants into a mixing chamber situated just prior to the entrance of the cavity. Typically, Ti^{3+} and H_2O_2 will be present in two of the reactant streams to generate ·OH, the reactions of which with a substrate in the third stream can then be examined. This technique is extremely useful as it allows the direct detection and characterisation of radicals and kinetic data can be derived. However, the large volumes of reactants required precludes its use to examine the reactions of expensive materials or those which are not readily available.

Continuous *in-situ* photolysis employing a high-intensity UV lamp is another technique for the generation of a high steady-state concentration of radicals in the spectrometer cavity. Typically a peroxide will be photolysed and the reactions of the radicals derived from it with a substrate will be examined. The advantages of this technique are that only small amounts of substrate are required and it allows direct radical detection However, direct photolysis of the substrate may sometimes occur producing misleading results.

Matrix isolation of radicals at low temperatures allows direct radical detection but can be problematic. For example, sample manipulation and the freezing process itself might lead to perturbations in the structure of the radical and even the cleavage of chemical bonds and structural characterisation may be difficult due to the anisotropic nature of the signal obtained.

ii) Other methods used in this study

In addition, where appropriate, spectroscopic techniques such as NMR spectroscopy and UV-visible spectrophotometry have been used in conjunction with chemical derivatisation procedures to analyse products. For example, the analysis of protein carbonyls by derivatisation with 2,4-dinitrophenylhydrazine (DNPH) followed by spectrophotometric analysis of the resulting protein hydrazones is to be of primary importance in analysing oxidative protein modification. Analogously, the formation of malondialdehyde during the course of lipid peroxidation is to be assessed by derivatisation with 2-thiobarbituric acid and spectrophotometric analysis of the resulting TBA_2-MDA adduct. ^{1}H and ^{13}C NMR spectroscopies will be employed to analyse the products of non-free-radical induced damage in lipid systems.

CHAPTER 2.

EPR INVESTIGATIONS OF THE REACTIONS OF SOME TRANSITION-METAL IONS WITH PEROXYACIDS.

2.1. INTRODUCTION

The use of EPR spectroscopy in conjunction with ancillary techniques such as *in-situ* photolysis, rapid-flow and spin-trapping provides a sensitive method for the characterisation of a wide variety of short-lived free radical species. However, whilst rapid-flow and *in-situ* photolysis provide *direct* methods for radical detection and characterisation, not all radicals are detectable under these conditions, the classic example being the hydroxyl radical which is too short lived (and too anisotropic) to be detected even on the rapid-flow timescale. It is in cases such as this that *indirect* methods of radical characterisation such as spin-trapping become useful (see section 2.2).

It is known that reaction of Fe^{2+} or Ti^{3+} with hydrogen peroxide, either in the presence (at pH ≥2) or absence of a chelator such as EDTA, produces the hydroxyl radical and the hydroxide ion.[135] In the case of non-symmetrical peroxides electron-transfer can occur in one of two directions. It has already been established that, for peroxyacids, electron-transfer can occur to produce the hydroxide ion and the corresponding carbonyloxyl radical [reaction (2.1)][76-79] or to produce the hydroxyl radical and the carboxylate anion [reaction (2.2)][77,80] or even in some cases a mixture of both reaction pathways is observed.[81]

$$RCO_3H + M^{n+} \longrightarrow RCO_2\cdot + {}^{-}OH + M^{(n+1)+} \qquad \textbf{(2.1)}$$

$$RCO_3H + M^{n+} \longrightarrow RCO_2^{-} + \cdot OH + M^{(n+1)+} \qquad \textbf{(2.2)}$$

. Peroxyacetic acid formulations are an equilibrium mixture containing peroxyacetic acid, hydrogen peroxide and acetic acid. The synthesis is facile, equilibrium usually being reached after twenty four hours at room temperature in the presence of a strong acid catalyst [reaction (2.3)].[20] The concentration of peroxyacetic acid at equilibrium is obviously controlled by the amount of hydrogen peroxide and acetic acid in the reaction mixture, making it possible to obtain various formulations containing different amounts of peroxyacetic acid. The formulations to be compared in this thesis are 40% (w/w) PAA,

which contains approximately 5.3 mol dm^{-3} peroxyacetic acid and 1.5 mol dm^{-3} hydrogen peroxide and an undefined amount of acetic acid and 5% (w/w) PAA which contains approximately 0.65 mol dm^{-3} peroxyacetic acid, 5.9 mol dm^{-3} hydrogen peroxide and an undefined concentration of acetic acid.

$$CH_3CO_2H + H_2O_2 \overset{H^+}{\rightleftharpoons} CH_3CO_3H + H_2O \qquad \textbf{(2.3)}$$

This chapter describes the technique of EPR spin-trapping and investigations into the one-electron reduction of peroxyacetic acid and magnesium monoperoxyphthalate (2.1) using both EPR spin-trapping and EPR rapid-flow techniques to examine the effect of the low-valent transition-metal catalyst and also the peroxyacid on the direction and speed of the reaction in order that their relevance in biological systems may be assessed.

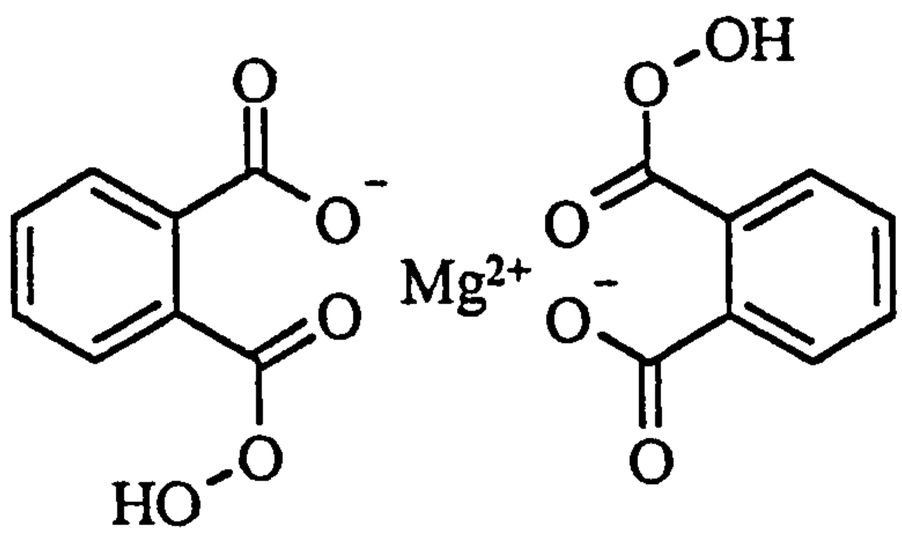

(2.1)

2.2. EPR SPIN-TRAPPING - AN OVERVIEW

EPR spin-trapping was developed during the early 1970's[136,137] to augment the range of ancillary EPR techniques then available. It offers the advantages over direct radical detection that radicals not usually detectable by EPR methods may be characterised, and that extremely low radical concentrations generated over prolonged periods of time may be detected because the nitroxide radical products *(spin-adducts)* are relatively long-lived, having lifetimes of up to about thirty minutes or longer.[136,137]

The most commonly used spin-traps fall into two categories, nitrone and nitroso compounds [(2.2) - (2.8)] and these react with radicals *(addends)* to produce nitroxide

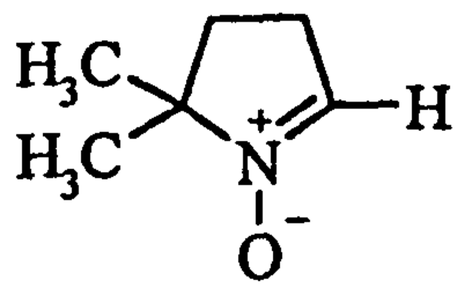

5,5-dimethyl-1-pyrroline-*N*-oxide

(DMPO)

(2.2)

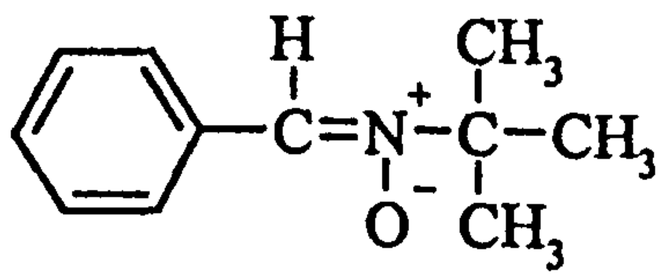

N-t-butyl-α-phenylnitrone

(PBN)

(2.3)

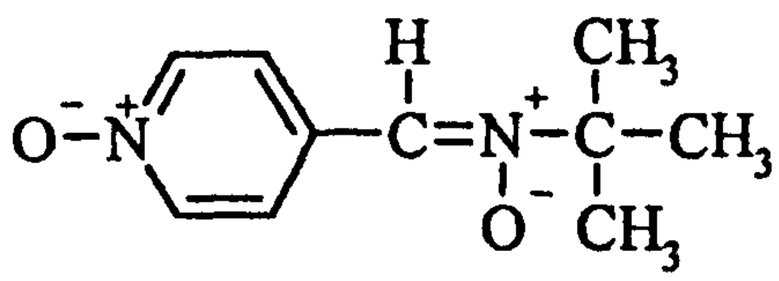

N-t-butyl-α-(4-pyridyl -N-oxide)-nitrone

(POBN)

(2.4)

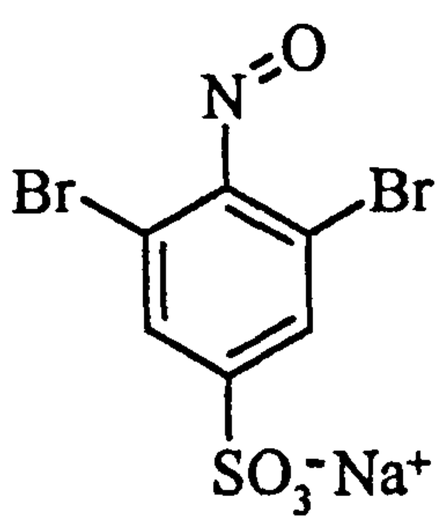

3,5-dibromo-4-nitrosobenzenesulfonic acid

(DBNBS)

(2.5)

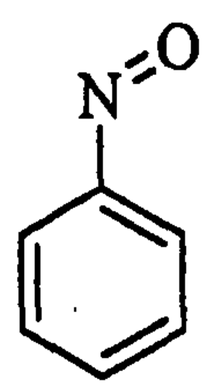

nitrosobenzene

(NB)

(2.6)

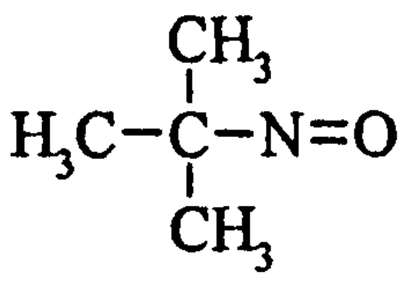

2-methyl-2-nitrosopropane

(MNP)

(2.7)

spin-adducts [reactions (2.4) and (2.5)]

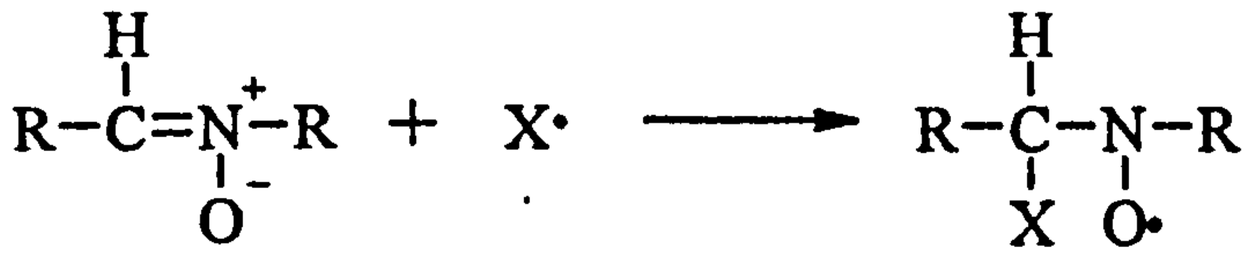

(2.4)

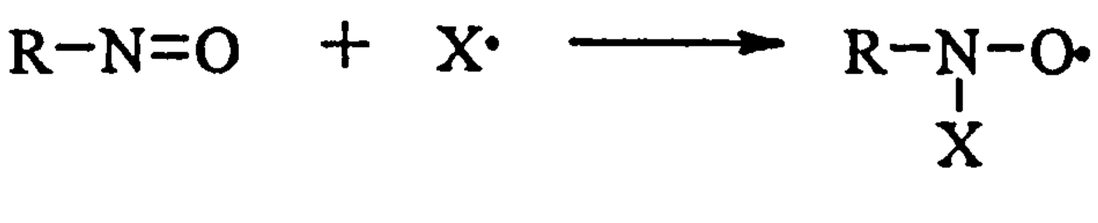

(2.5)

Nitrone and nitroso compounds share characteristics which are essential for their use as spin-traps. Both react with a variety of free radicals at rapid rates to form long-lived spin-adducts; examples can be designed that are soluble in a variety of solvents, both are relatively inert to alternative chemical modification [although this is not universal (see later)] and both produce spin-adducts which display hyperfine coupling constants which are definitive enough, in some cases, to allow characterisation of the addend.[136,137]

Several considerations need to be borne in mind when choosing a spin-trap and also when assigning mechanisms on the basis of EPR spin-trapping data.

i. Nitrone spin-traps effectively trap both carbon-centred and heteroatom-centred radicals. In contrast, nitroso spin-traps usually only form persistent spin-adducts with carbon-centred radicals.[138-140]

ii. Spin-adducts derived from the reactions of nitroso spin-traps usually give EPR spectra which provide more structural information than those produced from the corresponding reactions of nitrone spin-traps. This is a consequence of the addend adding directly to the nitrogen atom of nitroso spin-traps, whereas the addend adds to the carbon α to the nitrogen in nitrone spin-traps.[137]

iii. Both nitrone and nitroso spin-traps are susceptible to non radical chemical modification which leads to EPR-detectable species being formed, necessitating careful background experiments to be performed. For example, it has been found that nitroso spin-traps are susceptible to photolytic degradation which may preclude their use under photolytic conditions, although the use of filters, the presence of molecules with higher extinction coefficients or the use of aromatic

nitroso compounds with less photolabile C-N bonds may reduce the impact of this problem. For example, under photolysis 2-methyl-2-nitrosopropane [MNP] decomposes to form NO and $(CH_3)_3C\cdot$, which may then add to MNP to produce the well known DTBN spin-adduct [reactions (2.5) and (2.6)].[136,141]

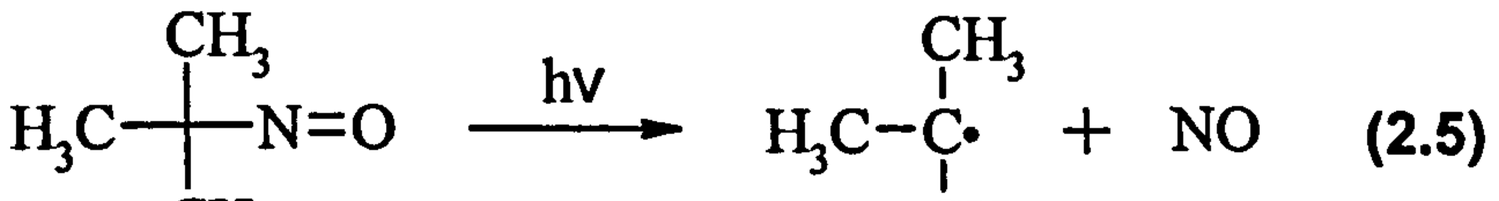

(2.5)

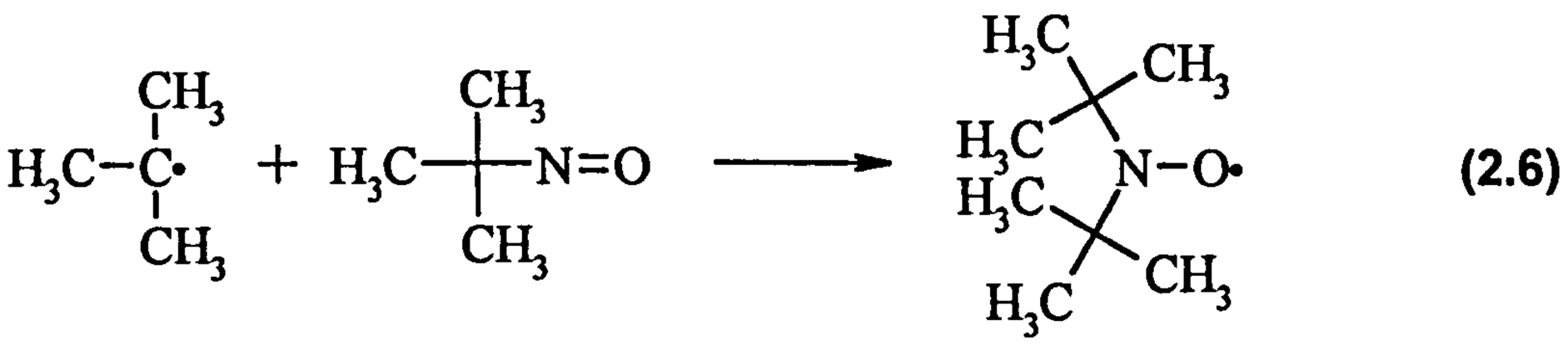

(2.6)

iv. Some nitroso spin-traps also undergo a rapid non free-radical reaction with double bonds known as the 'ene' reaction [reactions (2.7) and (2.8)] which leads to the formation of hydroxylamines which may be readily oxidised to nitroxides. These nitroxides are indistinguishable from those formed by a radical process and therefore great care must be exercised when using nitroso compounds in double-bond rich environments such as cell membranes.[141-144]

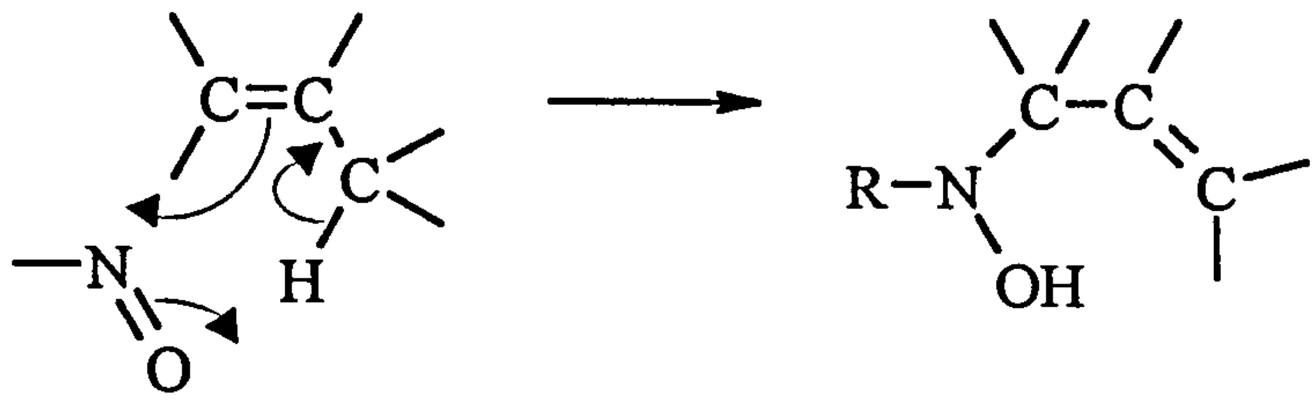

(2.7)

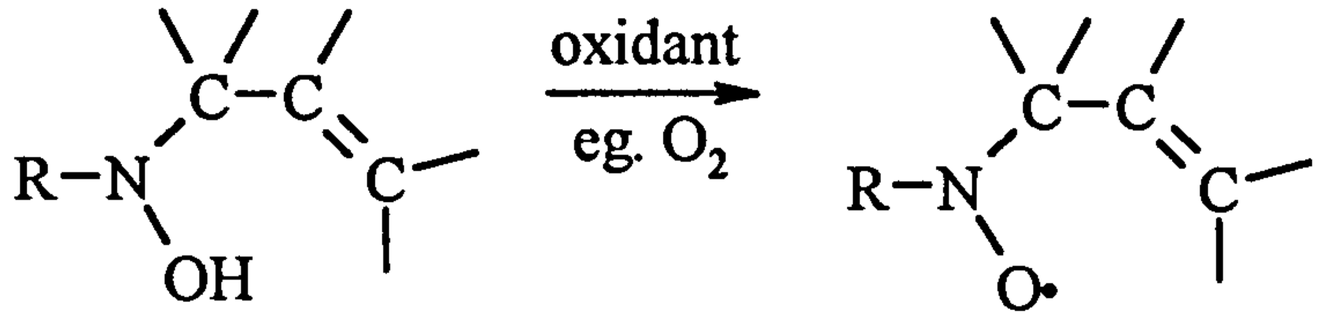

(2.8)

v. Nitrone spin-traps have been shown to undergo many reactions to form nitroxide spin-adducts which have not necessarily involved the direct reaction of radical species with the nitrone. For example, nucleophilic addition to a nitrone followed

by oxidation, a mechanism known as the Forrester-Hepburn mechanism,[145] leads to the formation of nitroxides [reactions (2.9) and (2.10)]. Nucleophiles which have reported as being capable of facilitating this type of reaction include $CF_3CO_2^-$ and F^-.[146,147] It is noteworthy that the generation of DMPO-OH in systems containing unchelated Fe^{3+} or Ti^{4+} has been observed and has been tentatively attributed to metal-ion catalysed Forrester-Hepburn nucleophilic addition of water to the spin-trap, although inverse spin-trapping has not been ruled out.[148-150]

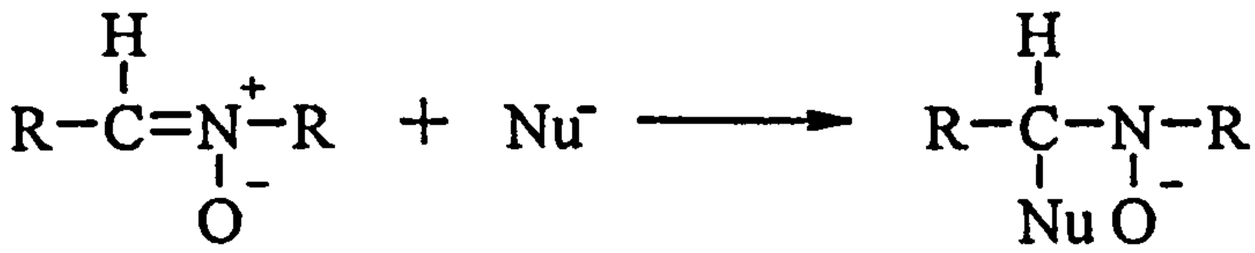

(2.9)

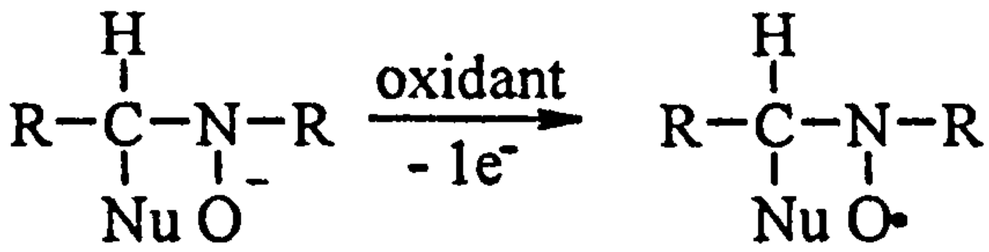

(2.10)

vi. Similarly, oxidation of nitrones to their corresponding radical-cations followed by addition of a nucleophile, a reaction commonly known as inverse spin-trapping, leads to the formation of nitroxides [reactions (2.11) and (2.12)].[151,152]

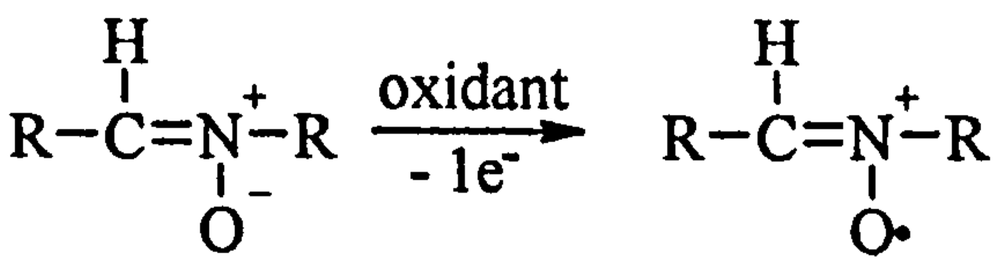

(2.11)

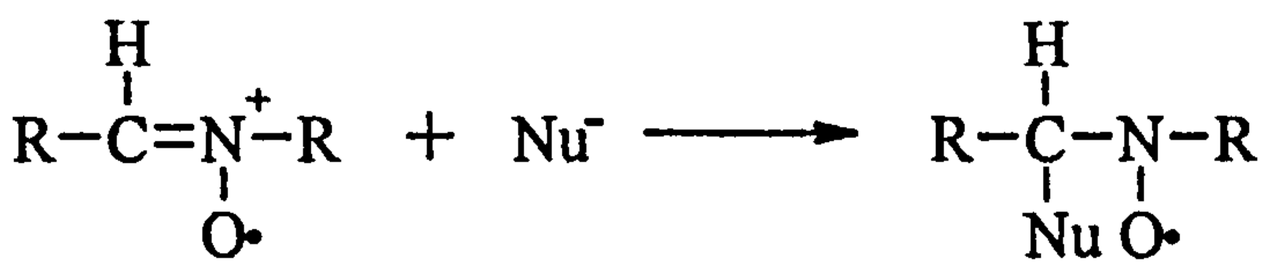

(2.12)

vii. Nucleophilic substitution of the addend in nitrone spin-adducts by water in aqueous systems can occur, leading to the formation of the hydroxyl-radical adduct. This is a particular problem when the initial radical is also a good leaving group. This is illustrated for example by the series of phosphate spin-adducts, PBN-PO_4^{2-}, PBN-HPO_4^- and PBN-H_2PO_4 for which only the corresponding

phosphate adduct is observed when the attacking species is $PO_4^{2-\cdot}$. However, when the attacking species is $HPO_4^{-\cdot}$ a mixture of hydroxyl and $HPO_4^{-\cdot}$ spin-adducts is observed where as if the attacking species is $H_2PO_4^{\cdot}$ only the hydroxyl-radical adduct is observed.[153]

viii. Another common modification of a spin-adduct which can lead to the incorrect assignment of the presence of hydroxyl radicals is the rapid decomposition of DMPO-OOH leading to the production of DMPO-OH.[154,155]

2.3. REACTIONS OF Ti^{3+} AND Fe^{2+} WITH 5% (W/W) PAA, 40% (W/W) PAA AND MMPP AS STUDIED BY EPR SPIN-TRAPPING.

2.3.1. One-electron reduction of peroxyacids by Ti^{3+}.

Initial experiments involved the use of Ti^{3+} and 5% PAA with DMPO. Titanium was employed because, unlike the biologically abundant Fe^{2+}, upon oxidation to Ti^{4+} it is not believed to react with the peroxyacetic acid or hydrogen peroxide at an appreciable rate and therefore does not complicate the observations. DMPO was employed in these experiments because it can trap both carbon and oxygen-centred radicals effectively. The conditions and composition of the reaction mixture were as follows: 0.048 M (total AvOx) 5% PAA, which contains 0.0048 M peroxyacetic acid and 0.0432 M hydrogen peroxide, 0.0048 M Ti^{3+}-EDTA at pH *ca.* 6 in the presence of 0.048 M DMPO. All reactants were thoroughly purged with a stream of oxygen-free nitrogen before use and were at room temperature.

It was thought that some evidence of methyl-radical formation or hydroxyl-radical formation from the reaction of the peroxyacid with the low-valent transition metal ion might be observed as would hydroxyl-radical formation from the reaction of hydrogen peroxide with Ti^{3+} if electron-transfer occurs. It was also thought that formation of $\cdot CH_2CO_2H$ or $\cdot CH_2CO_3H$ may be observed from the reaction of hydroxyl radicals with the acetic acid in the reaction mixture and the parent peroxyacid, respectively. It was not anticipated that the acetoxyl radical spin-adduct would be observed as the acetoxyl radical

decarboxylates rapidly (k is greater than 2×10^7 s^{-1} and estimated to be approximately 1.3 $\times 10^9$ s^{-1} at room temperature)[78,156] which is much faster than the rate of trapping for this type of radical for which the rate constant is estimated to be 4×10^5 mol^{-1} dm^3 s^{-1} at room temperature by analogy to the rate of trapping of the benzoyloxyl radical.[157]

The EPR spectrum of this reaction mixture displayed a triplet splitting from the nitroxide nitrogen with $a_N = 0.71 \pm 0.01$ mT and a further splitting by the two equivalent γ- protons of 0.41 ± 0.01 mT. No β-proton splitting was observed. This signal is assigned to DMPOX (2.8), an oxidative degradation product of DMPO.[158]

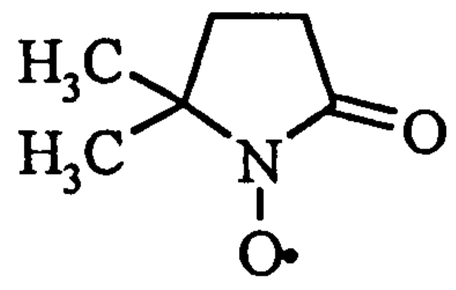

(2.8)

Further experiments used a lower final concentration of 5% PAA, typically 0.0048 M (total AvOx) which is comprised of 0.00048 M peroxyacetic acid and 0.00432 M hydrogen peroxide. The EPR spectrum of this mixture comprises of a four-line signal with relative peak heights of 1:2:2:1 [Figure 2.1.a]. This is indicative of DMPO-OH for which the β-proton splitting is equal to the nitrogen splitting of 1.49 ± 0.01 mT.[158] No carbon-centred radical-adduct was observed. When the concentration of DMPO was increased to 0.096 M the EPR spectrum of the reaction mixture remained essentially unchanged and there was still no evidence for carbon-centred radical formation. This could be the result of one of two possibilities; firstly, the peroxyacetic acid in the reaction mixture could be cleaving to produce the hydroxyl radical and the acetate anion [reaction (2.2)] as opposed to the acetoxyl radical and hydroxide [reaction (2.1)], or the methyl radical may not be being formed in sufficient concentration for its trapping to compete with the trapping of the hydroxyl radical. This seems likely as the hydrogen peroxide is in approximately nine-fold molar excess over the peroxyacetic acid and is thought to react faster with the low-valent transition metal with a rate constant of 2.08×10^3 mol^{-1} dm^3 s^{-1} compared to the estimated rate constant for the reaction of peroxyacetic acid with Ti^{3+} which is 6.57×10^2

mol^{-1} dm^3 s^{-1} (see later).[159] The rate of trapping of the methyl radical by DMPO is also estimated to be somewhat slower than the corresponding rate for the hydroxyl radical. [137,141]

When 40% PAA was employed at equivalent total AvOx, (with the concentration of peroxyacetic acid 0.00378 M and the concentration of hydrogen peroxide 0.00102 M) and was mixed with a solution containing 0.0048 M Ti^{3+}-EDTA and 0.048 M DMPO at pH *ca.* 6 the resulting EPR spectrum displayed a mixture of two signals (Figure 2.1.b). The major signal consists of a nitrogen splitting of 1.64 ± 0.01 mT and a β-hydrogen splitting of 2.34 ± 0.01 mT; this is attributed to a carbon-centred radical spin-adduct.[158] This may be the methyl radical [reaction (2.13)] or a carbon-centred radical formed as a result of hydrogen atom abstraction on the peroxyacid or acetic acid [reactions (2.14) and (2.15)]. A minor signal ($a_N = a_{\beta\text{-}H}$ = 1.49 ± 0.01 mT) was also evident which is assigned to the hydroxyl radical spin-adduct of DMPO.[158] When a higher concentration of DMPO was utilised (0.096 M) the spectrum remained essentially unchanged.

$$CH_3CO_2\cdot \longrightarrow \cdot CH_3 + CO_2 \qquad \textbf{(2.13)}$$

$$CH_3CO_3H + \cdot OH \longrightarrow \cdot CH_2CO_3H + H_2O \qquad \textbf{(2.14)}$$

$$CH_3CO_2H + \cdot OH \longrightarrow \cdot CH_2CO_2H + H_2O \qquad \textbf{(2.15)}$$

These reactions of the peroxyacetic acid were then compared to the reactions of magnesium monoperoxyphthalate (2.1). Magnesium monoperoxyphthalate is obtained as an essentially pure, white solid. Upon dissolution in aqueous solution under ambient conditions it decomposes relatively rapidly to produce phthalic acid and hydrogen peroxide,[160] but as long as fresh solutions are prepared frequently it may be considered to be free of hydrogen peroxide. Reaction mixtures containing 0.0048 M of MMPP, 0.0048 M Ti^{3+}-EDTA and 0.048 M DMPO at pH *ca.* 6 produced an EPR spectrum with a mixture of three spin-adducts (Figure 2.2). The major radical has a nitrogen splitting of 1.58 ± 0.01 mT and a β-hydrogen splitting of 2.40 ± 0.01 mT. This is attributed to trapping of the carbon-centred radical (2.9). The remaining two radical adducts were observed to be in

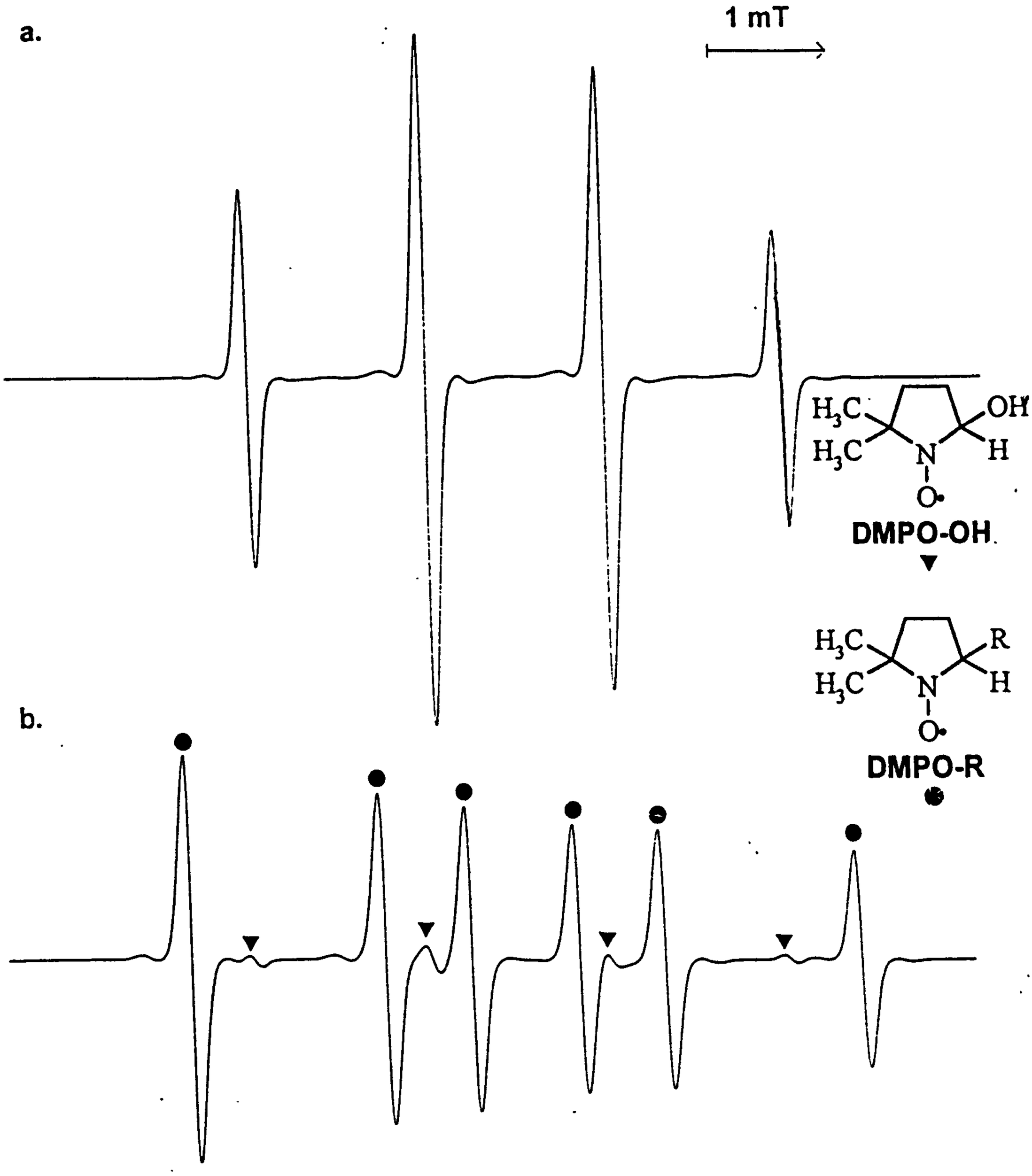

Figure 2.1.a. EPR spectrum showing a signal due to DMPO-OH generated by the reaction between Ti^{3+}-EDTA, 5% PAA and DMPO.

Figure 2.1.b. EPR spectrum showing signals due to DMPO-OH and DMPO-R generated by the reaction between Ti^{3+}-EDTA, 40% PAA and DMPO. Concentrations employed:- Ti^{3+}-EDTA, 0.0048 M, PAA, 0.0048 M (total AvOx), DMPO, 0.048 M

much lower concentration. The first had $a_N = a_{\beta\text{-}H} = 1.49 \pm 0.01$ mT and is assigned to the hydroxyl radical spin-adduct of DMPO. The intensity of this signal was dependent upon the length of time the MMPP solution had been standing. Freshly prepared solutions of MMPP resulted in EPR spectra in which the intensity of the DMPO-OH signal was relatively weak, but when the MMPP solution had been prepared even only ten minutes previously it was possible to observe a marked increase in the intensity of the DMPO-OH signal relative to the signals of both of the other adducts. This is attributable to the rapid decay of MMPP in solution to form phthalic acid and hydrogen peroxide, the hydroxyl radicals being a product of the reaction of the hydrogen peroxide with Ti^{3+}-EDTA.

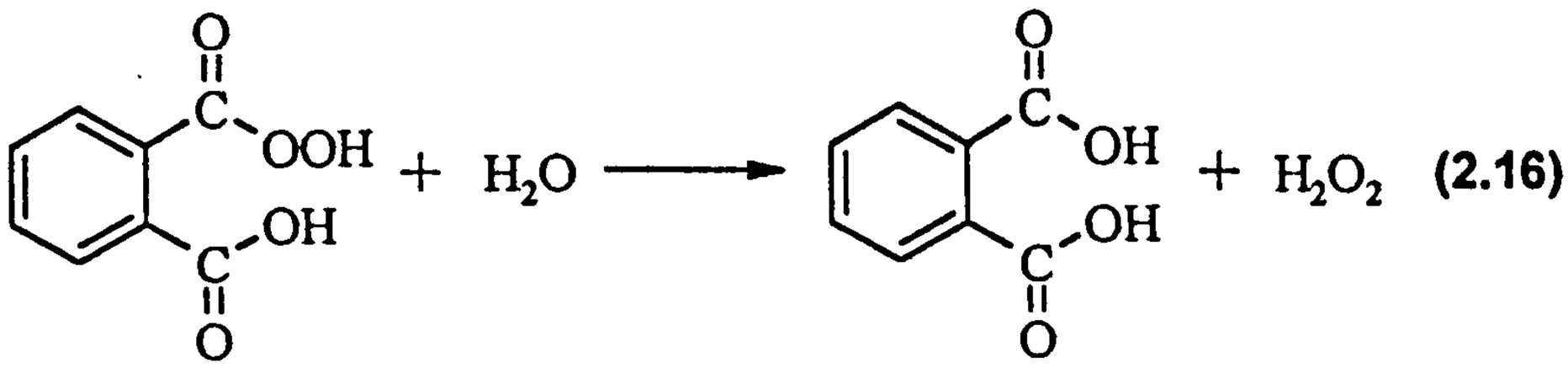

(2.16)

The least prominent signal comprised of a nitrogen splitting of 1.38 ± 0.01 mT, a β-hydrogen splitting of 1.03 ± 0.01 mT and a further very small γ-hydrogen splitting. The β-hydrogen splitting is in the region observed for the trapping of carbonyloxyl radicals[77,157,161] and as a result of this the signal is assigned to the spin-adduct of the arylcarbonyloxyl radical (2.10). Arylcarbonyloxyl radicals ($ArCO_2\cdot$) are in general more stable than their alkyl counterparts ($RCO_2\cdot$) as a result of the Ar-C bond strength being appreciably higher than the R-C bond strength and the stability of alkyl radicals being appreciably greater than that of aryl radicals. Therefore, arylcarbonyloxyl radicals decarboxylate much less rapidly, with rate constants estimated to be in the region of 10^5-10^6 s^{-1}, depending upon the nature of the ring substituents.[162] Hence, it is possible to observe the spin-adducts of these species as their reaction with a spin-trap may successfully compete with their decarboxylation.

On increasing the concentration of DMPO to 0.096 M the relative concentration of the carbon-centred radical spin-adduct was observed to decrease and the relative intensity of the arylcarbonyloxyl radical was seen to decrease which is consistent with the

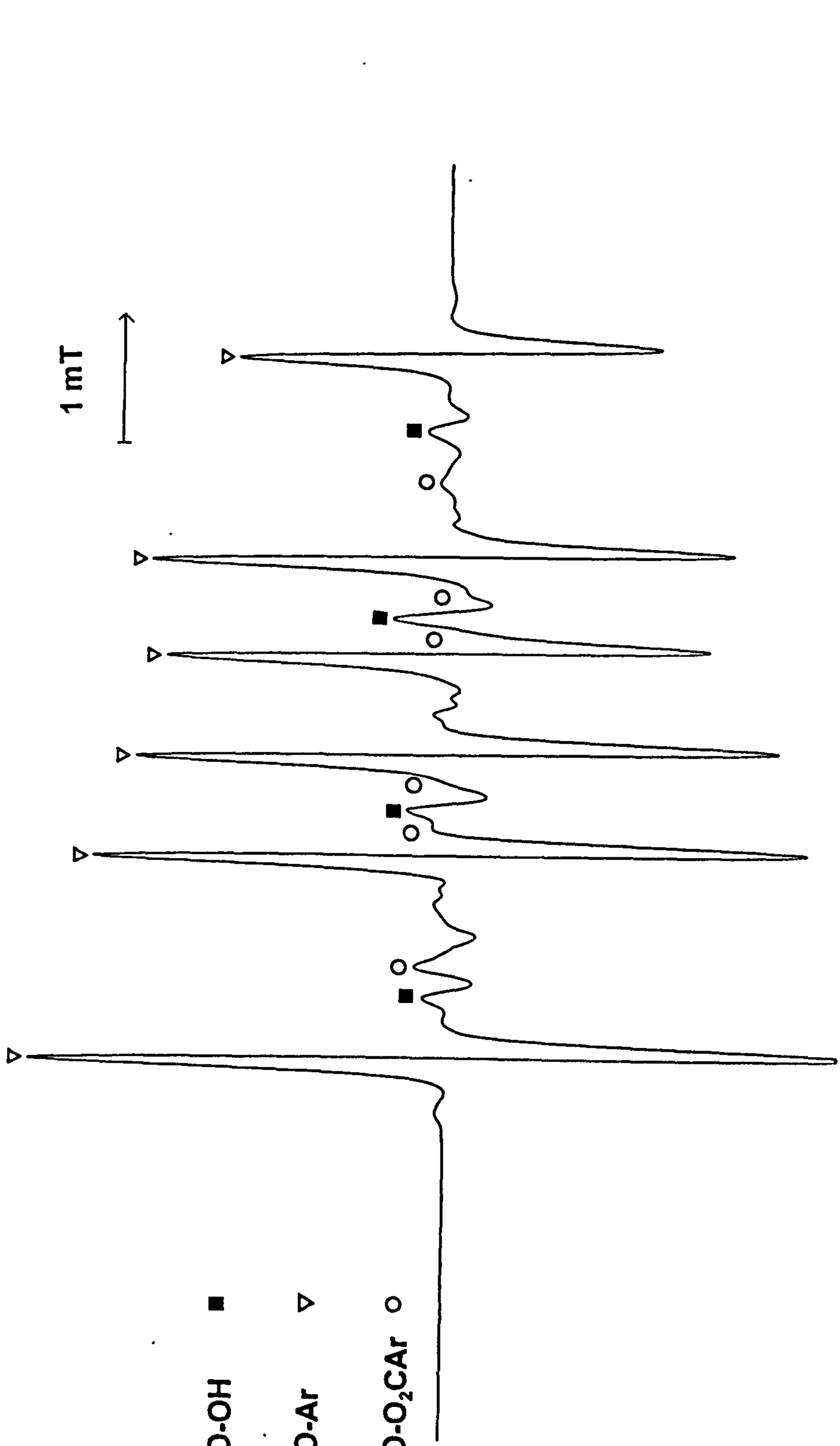

Figure 2.2. EPR spectrum displaying signals indicative of DMPO-Ar, DMPO-O$_2$CAr and DMPO-OH resulting from the reaction between Ti^{3+}-EDTA, MMPP and DMPO.
Concentrations employed:- Ti^{3+}-EDTA, 0.0048 M, MMPP, 0.0048 M, DMPO, 0.048 M

carbon-centred radical being a product of the decarboxylation of the arylcarbonyloxyl radical (see Scheme 2.1).

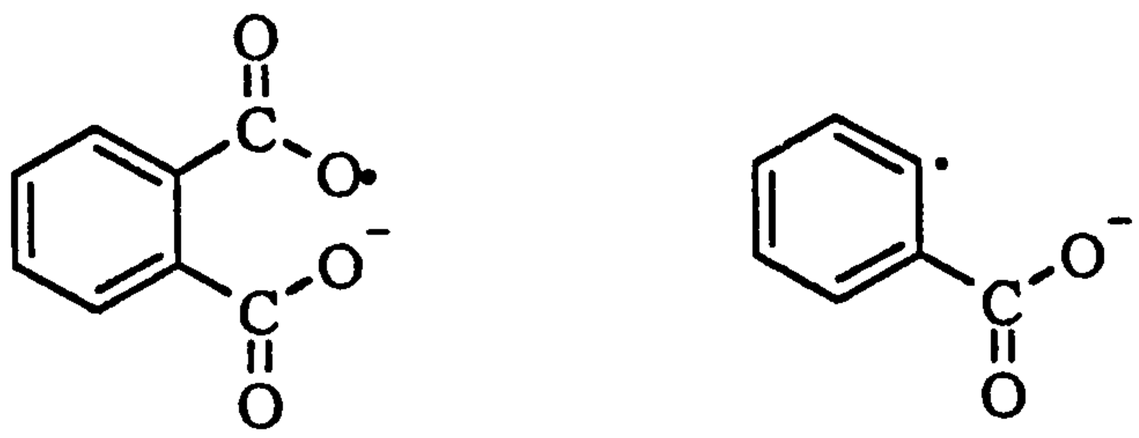

(2.9) **(2.10)**

In conclusion, the reactions of Ti^{3+}-EDTA with peroxyacids proceeds entirely in one direction to produce the acyloxyl radical and hydroxide. In the case of MMPP the acyloxyl radicals may be observed as their spin-adducts whereas in the case of PAA the methyl radical spin-adduct is observed. Hydroxyl radical adducts are also observed in the EPR spectra. Table 1.1 provides a summary of the splitting constants observed in the spectra recorded for the reactions of MMPP and peroxyacetic acid formulations with Ti^{3+}-EDTA in the presence of DMPO.

System	Radicals	a_N / mT[a]	$a_{\beta-H}$ / mT[a]
Ti^{3+}-EDTA / 5% PAA / DMPO	DMPO-OH	1.49	1.49
Ti^{3+}-EDTA / 40% PAA / DMPO	DMPO-R	1.64	2.34
	DMPO-OH	1.49	1.49
Ti^{3+}-EDTA / MMPP / DMPO	DMPO-Ar	1.58	2.40
	DMPO-O_2CAr	1.38	1.03
	DMPO-OH	1.49	1.49

a. hyperfine coupling constants have a typical error of ± 0.01 mT.

Table 2.1. Summary of EPR data obtained in spin-trapping experiments employing 5% PAA, 40% PAA and MMPP with Ti^{3+}-EDTA.

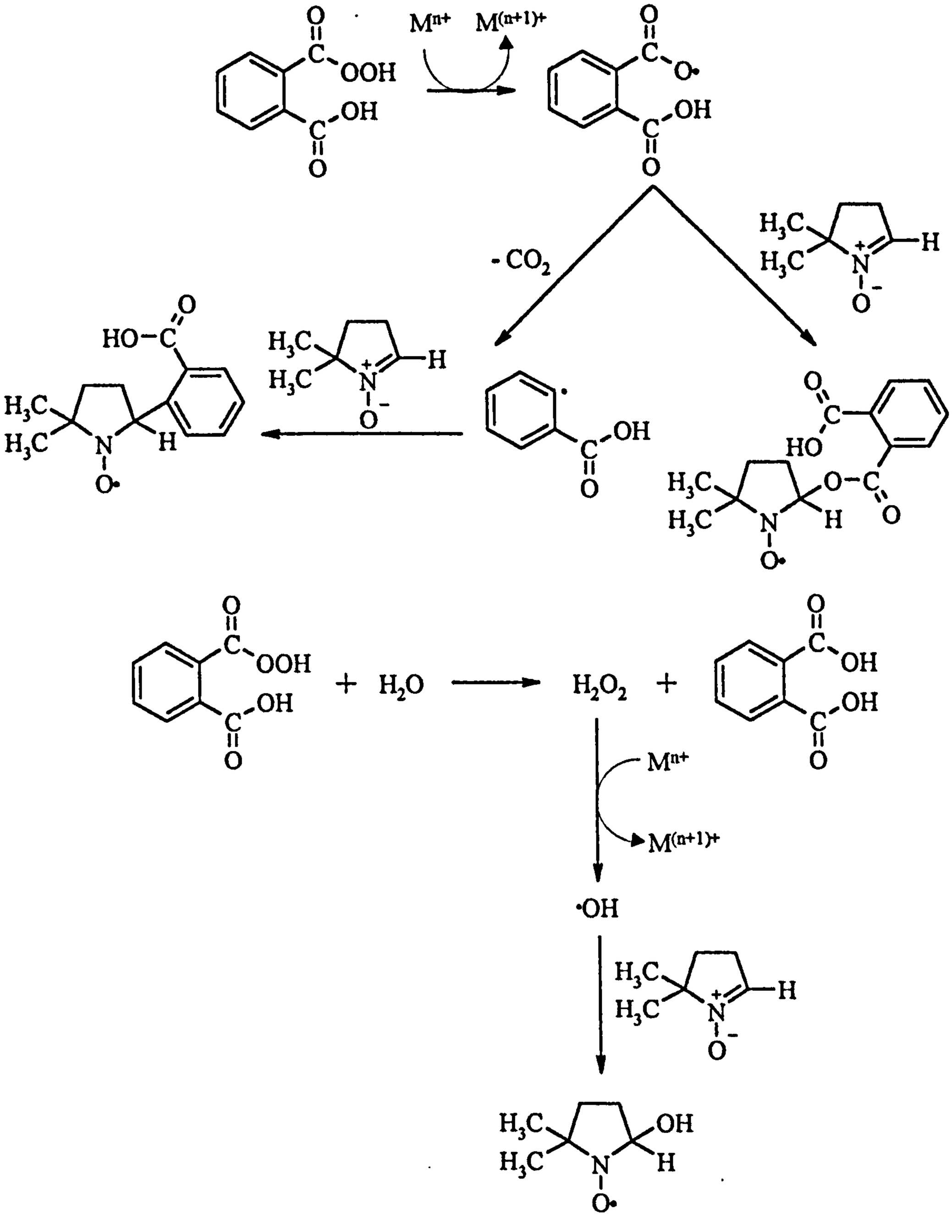

Scheme 2.1. The generation of radicals from MMPP by one electron reduction by Ti^{3+}-EDTA or Fe^{2+}-EDTA.

2.3.2. One electron reduction of peroxyacids by Fe^{2+}.

The reactions of Fe^{2+}-EDTA with peroxyacetic acid and magnesium monoperoxyphthalate were next examined as these reactions are thought to be of more relevance in the biocidal action of peroxygen compounds. Initial experiments employed reaction mixtures containing 0.0048 M Fe^{2+}-EDTA, 0.048 M (total AvOx) 5% PAA and 0.048 M DMPO. All solutions were thoroughly degassed and at room temperature. The EPR spectrum of this reaction mixture displayed the characteristic splitting pattern of DMPOX, an oxidative degradation product of DMPO, possibly formed via oxidation of DMPO-OH.[158] Further experiments were performed in which the concentration of PAA was 0.0048 M (total AvOx). The EPR spectrum of this reaction mixture consisted of a four-line splitting pattern with relative intensities of 1:2:2:1 indicative of DMPO-OH ($a_N = a_{\beta\text{-}H} = 1.49 \pm 0.01$ mT).[158] On changing the peroxyacetic acid composition to 40% PAA the EPR spectrum consisted of two signals, the major one being indicative of the trapping of a carbon-centred radical ($a_N = 1.64 \pm 0.01$ mT, $a_{\beta\text{-}H} = 2.34 \pm 0.01$ mT)[158] and the other one being assigned to DMPO-OH ($a_N = a_{\beta\text{-}H} = 1.49 \pm 0.01$ mT).[158] The ratio of carbon-centred adduct to hydroxyl- radical adduct was observed to be approximately 10:1.

In the corresponding experiments with magnesium monoperoxyphthalate a mixture of three species was observed in the EPR spectrum. The major spin-adduct was assigned to a carbon-centred radical, probably the aryl radical derived from MMPP.[77] The two minor species are assigned as DMPO-OH[158] and the arylcarbonyloxyl radical.[77,157,161] When the concentration of the spin-trap in the reaction mixture was raised to 0.096 M the intensity of the signal from the carbon-centred radical adduct decreased relative to that from the signal assigned to the arylcarbonyloxyl radical-adduct, providing evidence that the carbon-centred radical is indeed the aryl radical derived from MMPP. The intensity of the hydroxyl radical adduct was dependent upon the age of the MMPP solution, solutions that had been left to stand for more than ten minutes producing spectra with progressively more hydroxyl radical adduct present indicating the rapid decay of MMPP to phthalic acid and hydrogen peroxide.

2.3.3. The use of scavengers to confirm the presence of the hydroxyl radical.

Carbon-centred radical adducts and hydroxyl-radical adducts are clearly formed upon the reactions of 5% PAA, 40% PAA and MMPP with Ti^{3+}-EDTA. However, hydroxyl radical spin-adducts have been observed in many systems where hydroxyl radicals have not been produced.[148-155] It was therefore considered prudent to confirm the presence of hydroxyl radicals by using compounds that are known to react specifically with ·OH to produce radical species which may then be trapped by DMPO. Dimethyl sulfoxide (DMSO) is known to react specifically with ·OH [reaction (2.17)] to produce $\cdot CH_3$ with a rate constant of $5 \times 10^9\ mol^{-1}dm^3s^{-1}$ so if it is used in excess over the reactants it may be considered to scavenge all of the hydroxyl radicals in the system.[163] Similarly, formate (HCO_2^-) reacts specifically with ·OH with a rate constant estimated to be $2.9 \times 10^9\ mol^{-1}\ dm^3\ s^{-1}$ to produce $CO_2^{\cdot-}$.[reaction (2.18)].[164]

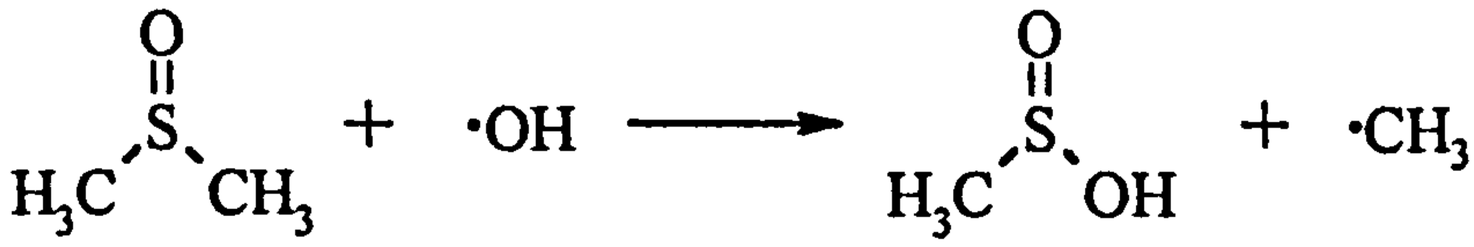

(2.17)

(2.18)

When DMSO (final concentration = 1.1 M) was included in the reaction mixture containing 0.0048 M Ti^{3+}-EDTA, 0.0048 M (total AvOx) 5% PAA and 0.048 M DMPO the four-line spectrum, indicative of DMPO-OH was reduced to a trace, to be largely replaced by a six-line spectrum with $a_N = 1.64 \pm 0.01$ mT and $a_{\beta\text{-}H} = 2.34 \pm 0.01$ mT, indicating that hydroxyl radicals are formed and react with the DMSO to produce methyl radicals which had then been trapped by DMPO.[158] The origin of the low level of the DMPO-OH signal which was not eliminated by the addition of DMSO will be discussed later. Similarly, on addition of sodium formate at a final concentration of 1.1 M to the reaction mixture the signal due to DMPO-OH was virtually eliminated, to be replaced by a signal of the $CO_2^{\cdot-}$ radical-adduct which was characterised by a nitrogen splitting of 1.56

± 0.01 mT and a β-hydrogen splitting of 1.87 ± 0.01 mT (Figure 2.3.a).[158]

When DMSO was included in the reaction mixture containing Ti^{3+}-EDTA, 40% PAA and DMPO the four-line signal characteristic of DMPO-OH virtually disappeared, corresponding with an increase in the intensity of the DMPO-carbon centred adduct, indicating that hydroxyl radicals had been produced in the reaction. This was confirmed by the replacement of DMSO by sodium formate which led to almost complete loss of the signal corresponding to DMPO-OH and the concomitant appearance of DMPO-CO_2^- (Figure 2.3.b).[158] It is noteworthy that a small signal consistent with the formation of DMPO-OH was still evident in these experiments.

The effect of hydroxyl-radical scavengers on the EPR spectra of reaction mixtures containing MMPP was found to be largely dependent upon the age of the MMPP solution. When Ti^{3+}-EDTA was mixed with MMPP and DMSO in the presence of DMPO there was no apparent effect of the scavenger on the spectrum which remained dominated by a carbon-centred radical adduct with minor contributions being made by the arylcarbonyloxyl radical-adduct[77,157,161] and the hydroxyl radical adduct.[158] Analogously, when 1.1 M sodium formate was added to the reaction mixture no CO_2^- adduct became apparent. However, if the solution of MMPP was not freshly prepared the scavengers were found to have an effect on the spectra, the corresponding scavenger-derived spin-adduct becoming visible, although the DMPO-OH signal was not eliminated completely in either of these cases.

When Ti^{3+}-EDTA was replaced by Fe^{2+}-EDTA, the same observations were made. Evidence of hydroxyl-radical formation was obtained by the use of the scavengers DMSO and formate for the reactions between 5% PAA and Fe^{2+}-EDTA and 40% PAA and Fe^{2+}-EDTA. In contrast, it was found that freshly prepared solutions of MMPP did not give rise to hydroxyl radical formation although a minor signal attributable to DMPO-OH was seen in the EPR spectrum. If the MMPP solution was left to stand, an appreciable increase in the amplitude of the DMPO-OH signal was apparent and presence of hydroxyl radicals was confirmed by the addition of hydroxyl-radical scavengers. This is attributed to the rapid decay of magnesium monoperoxyphthalate in aqueous solution to produce phthalic acid and hydrogen peroxide, the hydrogen peroxide reacting with the Fe^{2+}-EDTA to

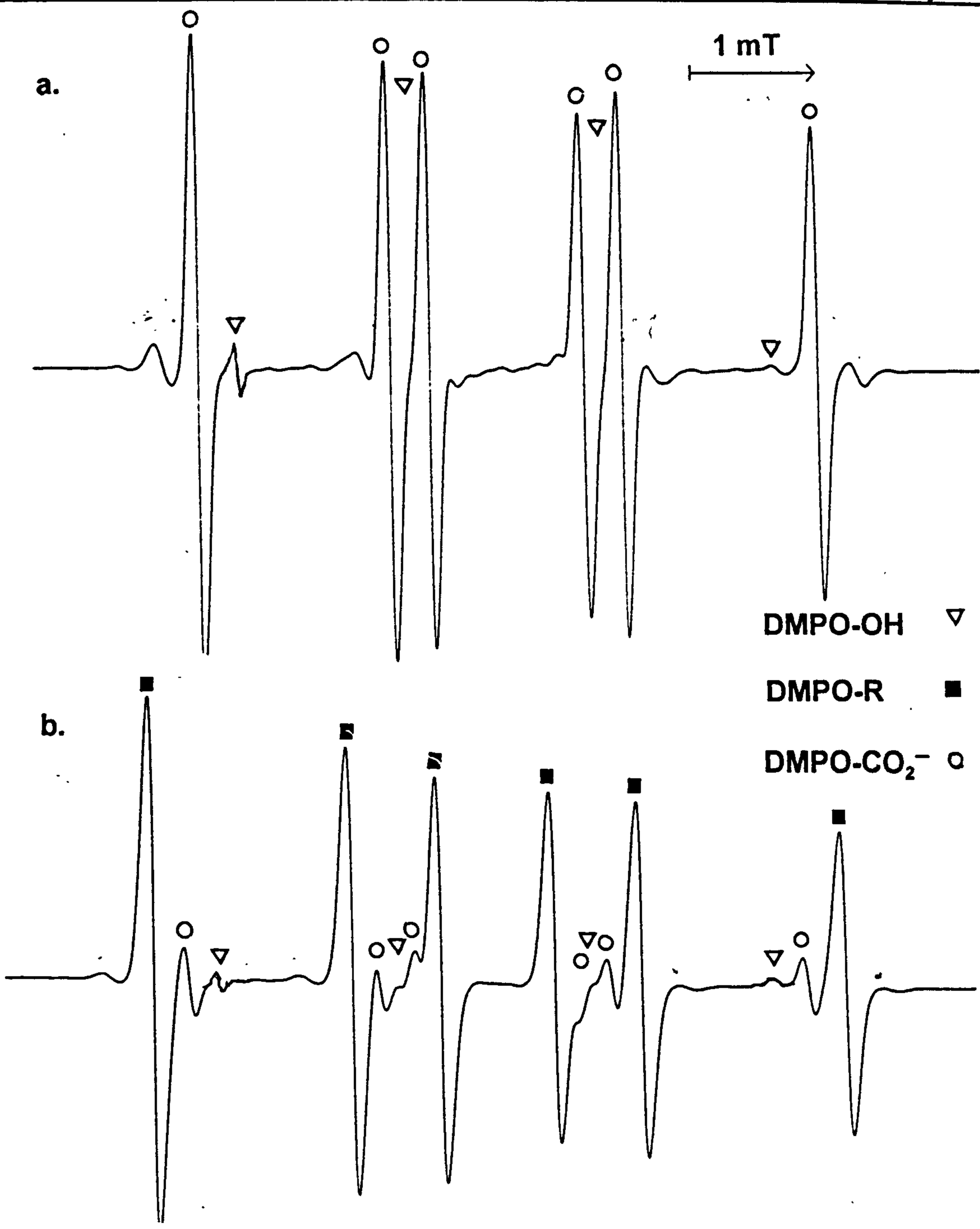

Figure 2.3.a. EPR spectrum showing a mixture of DMPO-CO_2^- and DMPO-OH generated by the reaction of Ti^{3+}-EDTA, 5% PAA, sodium formate and DMPO.

Figure 2.3.b. EPR spectrum showing a mixture of DMPO-CO_2^-, DMPO-R and DMPO-OH generated by the reaction of Ti^{3+}-EDTA,40% PAA, sodium formate and DMPO.

Concentrations employed:- Ti^{3+}-EDTA, 0.0048 M, PAA, 0.0048 M (total AvOx), DMPO, 0.048 M, sodium formate, 1.1 M.

produce hydroxyl radicals.

It has therefore been shown that hydroxyl radicals are formed upon reaction between 5% PAA and 40% PAA with Ti^{3+}-EDTA or Fe^{2+} -EDTA. It has also been demonstrated that magnesium monoperoxyphthate does not produce hydroxyl radicals unless the solution is allowed to stand, in which case it is thought that the formation of hydrogen peroxide is responsible for the formation of hydroxyl radicals. In all cases it was found that the hydroxyl radical-adduct signal was not completely eliminated by the presence of scavenging compounds, indicating a small but significant contribution to the formation of DMPO-OH by a non-classical free-radical mechanism which will be investigated further.

2.3.4. The use of catalase to ascertain the origin of the hydroxyl radical.

Although the presence of the hydroxyl radical has been confirmed by the use of scavengers in conjunction with spin-trapping, the origin of the hydroxyl radical remains unknown. For the peroxyacetic acid samples it is not known whether the hydroxyl radical is purely formed via the reactions of the hydrogen peroxide in the formulations with the low-valent transition metal ions or if there is a contribution from the reactions of the peroxyacetic acid itself with Ti^{3+}-EDTA and Fe^{2+}-EDTA . It is believed that formation of hydroxyl radicals from the reactions of MMPP with low-valent transition-metal ions is a result of the decomposition of magnesium monoperoxyphthalate to phthalic acid and hydrogen peroxide; however this has not been confirmed.

In order to find the origin of the hydroxyl radical catalase was employed. Catalase is an enzyme that specifically catalyses the conversion of hydrogen peroxide into water and oxygen [reaction (2.19)]. Although it is reported to form compound 1, (the enzyme-substrate complex) with peroxyacetic acid this has been found to be very slow compared to the formation of compound 1 with hydrogen peroxide, especially if the peroxyacetic acid is ionised to any great degree, and it has also been shown that products are not released from the active site.[165]

$$2\,H_2O_2 \xrightarrow{\text{catalase}} 2\,H_2O + O_2 \qquad (2.19)$$

It was therefore decided to treat peroxyacetic acid samples with an excess of catalase prior to their addition to the reaction mixture to remove the hydrogen peroxide. Typically a 1 ml aliquot of PAA would be removed from a freshly prepared 0.02 M (total AvOx) solution in 0.1 M phosphate buffer and approximately 0.005 g of catalase was added. The sample was observed until the visible effervescence ceased and was then left for five minutes at room temperature before use to ensure complete removal of hydrogen peroxide To confirm this, all catalase treated samples were then tested for hydrogen peroxide content then used immediately. It has previously been demonstrated that treatment of peroxyacetic acid formulations in this manner is effective at removing the hydrogen peroxide without significant loss of peroxyacetic acid either through reaction with catalase, or shifting of the equilibrium in an effort to maintain the hydrogen peroxide concentration, as the attainment of equilibrium is slow on the experimental timescale.[165]

A reaction mixture containing 0.0048 M (total AvOx prior to catalase treatment) 5% PAA, 0.0048 M Ti^{3+}-EDTA and 0.048 M DMPO at pH *ca.* 6 gave an EPR spectrum which displayed only a trace of a signal attributable to DMPO-OH.[158] Inclusion of hydroxyl-radical scavengers (to a final concentration of 1.1 M) in the reaction mixture prior to the addition of catalase treated 5% PAA, led to a trace of DMPO-OH still being evident. This demonstrated that the spin-adduct was not formed through a classical free-radical mechanism indicating that no cleavage of the peroxyacetic acid in the mixture had occurred to produce the hydroxyl radical. However, the majority of the signal (*ca.* 95%) is attributed to hydroxyl radical formation from the hydrogen peroxide in the reaction mixture.

On mixing catalase-treated 40% PAA with Ti^{3+}-EDTA in the presence of DMPO the EPR spectrum of the resulting mixture displayed a mixture of two signals. The major signal is attributable to a carbon-centred radical-adduct[157] with $a_N = 1.64 \pm 0.01$ mT and $a_{\beta\text{-}H} = 2.34 \pm 0.01$ mT. The amplitude of the DMPO-OH signal was reduced but was still apparent. Addition of either DMSO or formate to this reaction mixture did not produce any change in the resulting EPR spectrum indicating that the remaining DMPO-OH had

not been formed through a conventional free-radical mechanism as opposed to the trapping of ·OH produced from the reaction of peroxyacetic acid with Ti^{3+}-EDTA.

Unsurprisingly, treatment of fresh solutions of MMPP with catalase as described above had no effect on the EPR spectrum observed for reaction mixtures containing Ti^{3+}-EDTA, MMPP and DMPO, three signals were still evident corresponding to a carbon-centred radical adduct of DMPO,[158] the arylcarbonyloxyl radical adduct of DMPO[77,157,161] and the hydroxyl radical adduct.[158] However treatment of older solutions of MMPP with catalase had a significant effect on the EPR spectrum of the reaction mixture. The signal attributed to DMPO-OH was observed to decrease dramatically, indicating that the majority of the signal that had been observed when MMPP had not been freshly prepared were indeed due to the decay of the MMPP leading to the formation of hydrogen peroxide and it was this that was reacting with the low-valent transition metal ion to form hydroxyl radicals. The use of DMSO or formate in conjunction with catalase illustrates that the low level of DMPO-OH still evident had been formed via an artefactual mechanism.

When Ti^{3+}-EDTA was replaced by Fe^{2+}-EDTA these observations were repeated allowing it to be concluded that peroxyacetic acid reacts with Ti^{3+}-EDTA or Fe^{2+}-EDTA to form acetoxyl radicals and the hydrogen peroxide in the reaction mixtures reacts with the low-valent transition-metal ions to produce hydroxyl radicals. It has also been shown that MMPP decomposes rapidly in aqueous solution producing hydrogen peroxide which may react with low-valent transition metal ions to produce hydroxyl radicals. Furthermore, it has been demonstrated that an alternative route to conventional spin-trapping can lead to the formation of hydroxyl radical spin-adducts in these systems.The results of these experiments are summarised in Table 2.2.

Peroxyacid	Radicals and relative intensities	Relative intensity of OH signal in scavenger treated systems	Relative intensity of OH signal in catalase treated systems
5% PAA	·OH (++++++)	(+)	(+)
40% PAA	C-centred (++++) ·OH (++)	(+)	(+)
MMPP	Ar· (+++)[a] $ArCO_2$· (+)[a] ·OH (++)[b]	(+)[b]	(+)[b]

a. indicating that these are the relative intensities of the signals when [DMPO] = 0.048 M

b. indicating that this is the relative intensity of the DMPO-OH signal when the MMPP solution is freshly made.

Table 2.2. Effect of hydroxyl radical scavengers and catalase on EPR spectra observed in systems comprising of either Ti^{3+}-EDTA or Fe^{2+} -EDTA with peroxygens and DMPO showing the similarities between the systems.

2.3.5. The use of DBNBS to determine the structure of the carbon-centred radicals.

Nitroso spin-traps hold the advantage over nitrone spin-traps that the addend is bonded directly to the nitrogen allowing more detailed structural characterisation of it to be made. A nitroso spin-trap was therefore employed to characterise any carbon-centred radical(s) produced from the reactions between peroxyacids and low-valent transition metal ions. DBNBS was chosen for this purpose because it is highly soluble in water, unlike the majority of other nitroso spin-traps.[166,167]

Initial experiments employed reaction mixtures containing 0.0048 M Ti^{3+}-EDTA, 0.0048 mol dm^{-3} (total AvOx) 5% PAA and 0.0048 mol dm^{-3} DBNBS, which gave rise to distinctive EPR spectra with a weak but discernable signal with $a_N = 1.43 \pm 0.01$ mT, $a_{3\beta\text{-H}}$

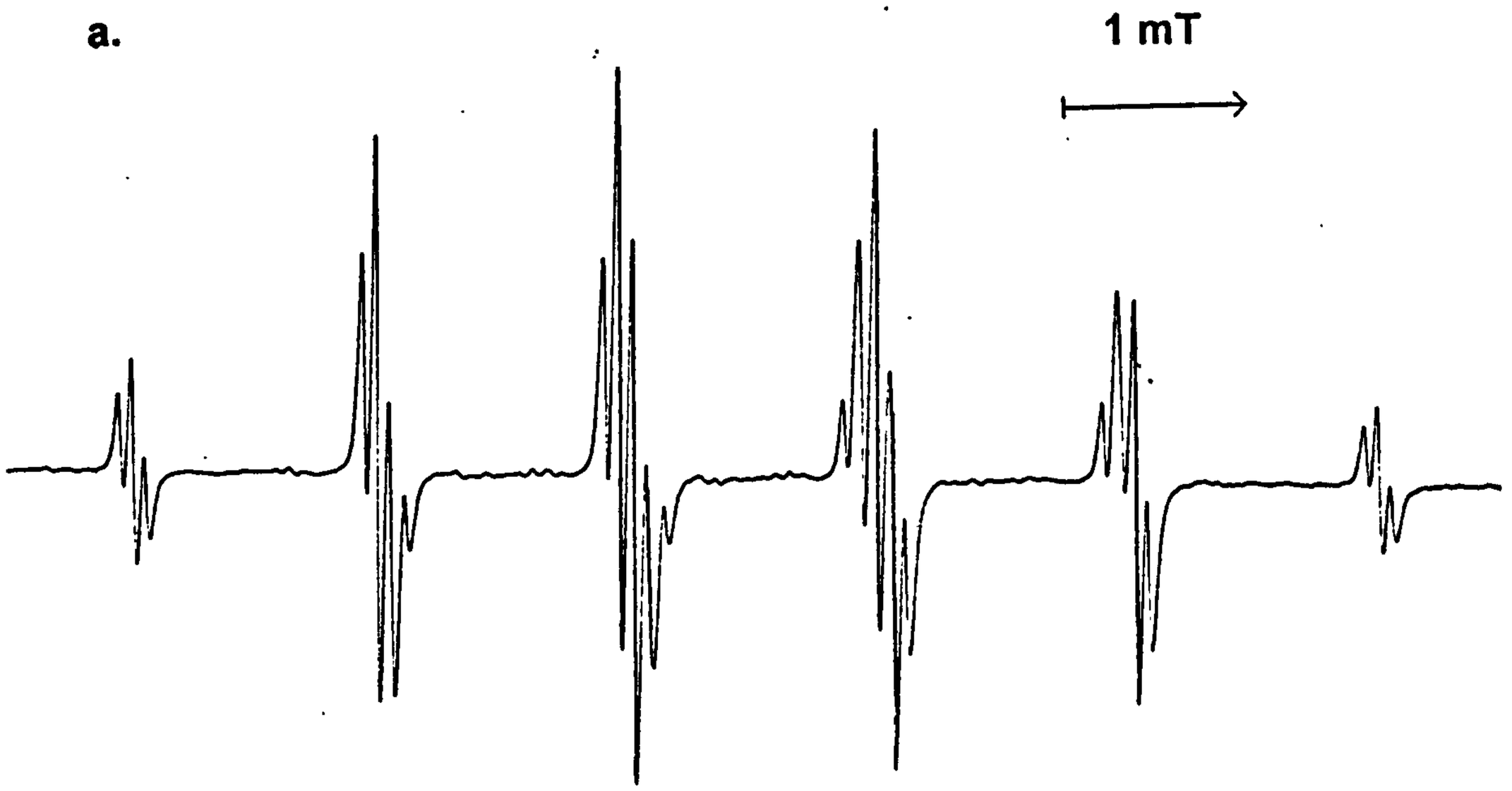

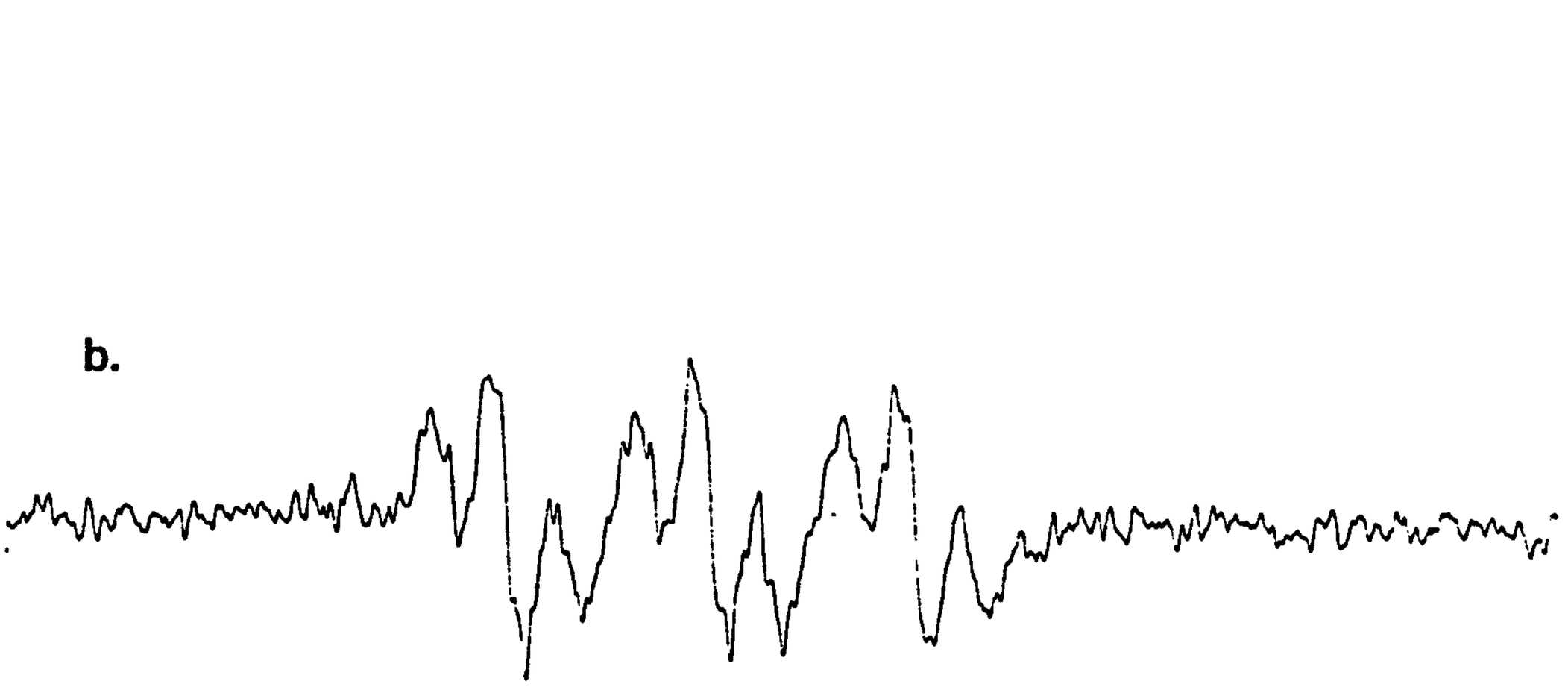

Figure 2.4.a. EPR spectrum showing the DBNBS-CH_3 adduct generated by the reaction of Ti^{3+}-EDTA with 40% PAA in the presence of DBNBS.

Figure 2.4.b. EPR spectrum showing the aryl radical adduct of DBNBS generated by the reaction of Ti^{3+}-EDTA with MMPP in the presence of DBNBS.

Concentrations employed:- Ti^{3+}-EDTA, 0.0048 M, peroxygen, 0.0048 M, DBNBS, 0.0048 M.

0.01 mT and $a_{\gamma\text{-}H} = 0.07 \pm 0.01$ mT, which is assigned to DBNBS-CH_3[158,166-169] indicating that the peroxyacetic acid in the reaction mixture does indeed react with the Ti^{3+}-EDTA to produce acetoxyl radicals and hydroxide ions [see reaction (2.20)]. In the corresponding reactions in which 40% PAA was employed a spectrum consistent with the formation of DBNBS-CH_3 was seen. It is noteworthy that the concentration of the spin-adduct is such that satellites due to ^{15}N may be seen (Figure 2.4).

$$CH_3CO_3H + Ti^{3+} \longrightarrow CH_3CO_2\cdot + {}^{-}OH + Ti^{4+} \qquad \textbf{(2.20)}$$

On mixing MMPP, Ti^{3+}-EDTA and DBNBS a weak EPR spectrum (Figure 2.4) consisting of a nitrogen splitting of 1.04 ± 0.01 mT, a hydrogen splitting of 0.33 ± 0.01 mT (1 H), a further hydrogen splitting of 0.26 ± 0.01 mT (1 H) and small hydrogen splitting due to the *m*-protons in the DBNBS ring of 0.05 ± 0.01 mT (2 H) was observed which is in agreement with the splittings quoted for the MMPP aryl radical-adduct of DBNBS.[169,170]

On replacing Ti^{3+}-EDTA with Fe^{2+}-EDTA largely similar results were observed. The main differences which were common to all the spectra was that the DBNBS ring-proton splittings were not evident, and the addend proton splittings were also not as well resolved. This was probably a result of paramagnetic broadening by Fe^{3+} which makes small splittings indiscernible. A further feature which was observed was that in the EPR spectrum of the reaction mixture containing Fe^{2+}-EDTA, 5% PAA and DBNBS, two species were visible, the methyl radical adduct and an unidentified second adduct with splittings $a_N = 1.30 \pm 0.01$ mT and $a_{2\beta\text{-}H} = 0.92 \pm 0.01$ mT. It was thought that this species may be the spin-adduct of $\cdot CH_2CO_2H$ or $\cdot CH_2CO_3H$ formed by hydrogen atom abstraction by hydroxyl radicals from acetic acid or peroxyacetic acid respectively. These possibilities were investigated by the independent formation of DBNBS-CH_2CO_2H. In order to determine the EPR parameters for the acetic acid adduct, a mixture of 0.05 M H_2O_2, 0.025 M DBNBS and 5 M acetic acid was photolysed in the cavity of the EPR spectrometer. The resulting spectrum had hyperfine coupling constants of $a_N = 1.29 \pm 0.01$ mT, $a_{2\beta\text{-}H} = 0.92 \pm 0.01$ mT and $a_{2\,ring\text{-}H} = 0.07 \pm 0.01$ mT which corresponds (apart from the ring splittings) to the splittings observed in the spectrum of the reaction mixture containing 0.0048 M

Fe^{2+}-EDTA, 0.0048 M (total AvOx) 5% PAA and 0.0048 M DBNBS confirming that the second species is DBNBS-CH_2CO_2H. It was expected that the spin-adduct of $\cdot CH_2CO_3H$ would have different hyperfine coupling constants although this was not investigated. A summary of the results is provided in Table 2.3.

System	Radicals	a_N / mT[a]	$a_{\beta\text{-}H}$ / mT[a,b,c]	$a_{ring\text{-}H}$[a,b,c]
M^{n+}-EDTA / 5% PAA / DBNBS	DBNBS-CH_3	1.43	1.34 (3)	0.07 (2)
	DBNBS-CH_2CO_2H[d]	1.29	0.92 (2)	0.07 (2)
M^{n+}-EDTA / 40% PAA / DBNBS	DBNBS-CH_3	1.43	1.34 (3)	0.07 (2)
M^{n+}-EDTA / MMPP / DBNBS	DBNBS-Ar	1.04	0.33 (1) 0.26 (1)	0.05 (2)

a. hyperfine coupling constants have a typical error of ± 0.01 mT

b. numbers in parentheses indicate number of protons

c. the ring and addend proton splittings were not always resolved

d. this radical was only observed when Fe^{2+}-EDTA was employed

.Table 2.3. Summary of EPR data obtained in spin-trapping experiments employing 5% PAA, 40% PAA and MMPP with Ti^{3+}-EDTA and Fe^{2+}-EDTA in the presence of DBNBS.

2.3.6. The use of DEPMPO.

The design of new spin-traps is a topic of considerable ongoing research, to overcome the limitations of existing compounds. One of the most recent advances in spin-trap design has included the incorporation of a phosphoryl group in the 5-position in DMPO, as for example in DEPMPO (2.11). For example, it has been demonstrated that the incorporation of this group lengthens the lifetime of the superoxide adduct,[172,173] making it easily discernable from the hydroxyl radical adduct, as well as providing information about the stereochemistry of addend addition, since the *cis* and *trans*

diastereoisomers are spectroscopically distinguishable.[172,173]

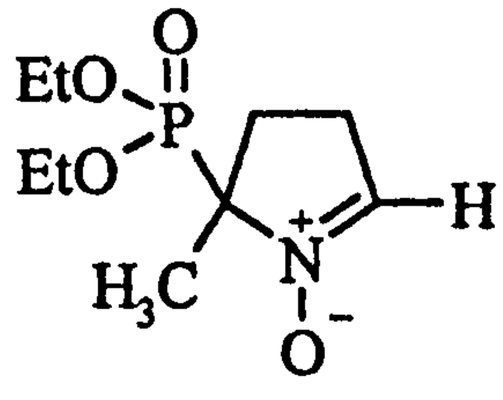

(2.11)

Initial experiments utilised reaction mixtures containing 0.0048 M Ti^{3+}-EDTA, 0.0048 M (total AvOx) 5% PAA and 0.048 M DEPMPO. This resulted in EPR spectra corresponding to DEPMPO-OH with hyperfine coupling constants $a_P = 4.66 \pm 0.01$ mT and $a_N = a_{\beta\text{-}H} = 1.36 \pm 0.01$ mT.[172,173] On replacing 5% PAA with 40% PAA a mixture of two signals was observed, that of DEPMPO-OH[172,173] and that of DEPMPO-CH_3 with splittings $a_P = 4.67 \pm 0.01$ mT, $a_N = 1.52 \pm 0.01$ mT and $a_{\beta\text{-}H} = 2.22 \pm 0.01$ mT.[173] When the peroxygen used was MMPP a mixture of three spin-adducts was observed. These are assigned to the hydroxyl radical adduct ($a_P = 4.66 \pm 0.01$ mT and $a_N = a_{\beta\text{-}H} = 1.36 \pm 0.01$ mT), the aryl radical-adduct of MMPP ($a_P = 4.67 \pm 0.01$ mT, $a_N = 1.48 \pm 0.01$ mT and $a_{\beta\text{-}H} = 2.28$ mT) and the arylcarbonyloxyl spin-adduct of MMPP ($a_P = 4.67 \pm 0.01$ mT, $a_N = 1.28 \pm 0.01$ mT and $a_{\beta\text{-}H} = 0.99 \pm 0.01$ mT). As neither of the latter species had been observed previously the assignment was confirmed by photolysis of a solution containing 0.003 M MMPP and 0.03 M DEPMPO. This produced a spectrum consistent with that observed for MMPP in the presence of Ti^{3+}-EDTA

The use of DEPMPO has therefore confirmed the results described earlier in this Chapter regarding the one-electron reduction of peroxyacids by Ti^{3+}-EDTA to produce acyloxyl radicals and hydroxide whilst providing clear and informative spectra of DEPMPO spin-adducts which will be of use later (see section 2.4 and Chapter 5).

2.3.7. Discussion.

The results described here show that Ti^{3+}-EDTA and Fe^{2+}-EDTA react with

peroxyacetic acid to produce exclusively $CH_3CO_2\cdot$ and ^-OH [reaction (2,1)] although the acetoxyl radical is not observed due to its rapid decarboxylation.[reaction (2.13)] However, hydroxyl radicals are produced, from the reactions of the hydrogen peroxide in the reaction mixtures with the low-valent transition-metal ion and this has been confirmed both by the use of catalase and hydroxyl radical scavengers. Magnesium monoperoxyphthalate reacts in a similar manner to peroxyacetic acid to produce the corresponding arylcarbonyloxyl radical and ^-OH (see Scheme 2.1). However, in contrast to the corresponding reactions with peroxyacetic acid it was possible to observe the spin-adduct of the arylcarbonyloxyl radical since it decarboxylates much less rapidly than the acetoxyl radical. It was also found that due to the rapid decomposition of MMPP in aqueous solutions, older solutions had to be considered to be a mixture of MMPP, phthalic acid and hydrogen peroxide [reaction (2.16)] and the reactions of the hydrogen peroxide were duly considered.

In addition, it was found that in reactions between Fe^{2+}-EDTA and 5% PAA in the presence of DBNBS it was possible to detect a second carbon-centred radical species, this being tentatively assigned to $\cdot CH_2CO_2H$ formed by hydrogen atom abstraction by the hydroxyl radical from acetic acid [reaction (2.15)].

2.4. REACTIONS OF Cu^+ WITH 5% (W/W) PAA, 40% (W/W) PAA AND MMPP AS STUDIED BY EPR SPIN-TRAPPING.

2.4.1. Generation of Cu^+ by the reaction of Cu^{2+} with glutathione.

It has previously been shown that various Cu^+ species (formed by the reduction of Cu^{2+} complexes by reducing agents such as glutathione and L-ascorbic acid) react with hydrogen peroxide and alkyl hydroperoxides to form radicals.[175] It has also been suggested that Cu^+, formed by the reaction of Cu^{2+} with Ti^{3+} in a rapid-flow system, can catalyse the cleavage of peroxyacids to produce the hydroxyl radical and carboxylate anions[77,80] [reaction (2.2)]. Therefore the extent and direction of peroxyacid cleavage in the presence of Cu^+, generated by the reaction of Cu^{2+} with biologically-relevant reducing agents was

investigated. The reaction of an aqueous solution of copper(II) sulfate, in which the copper species is thought to be $Cu(H_2O)_5SO_4$,(2.12) with two molar equivalents of glutathione is known to form a transient copper (II) thiolate complex which undergoes reduction to generate a stable copper (I) thiolate complex [reaction (2.21)].[174]

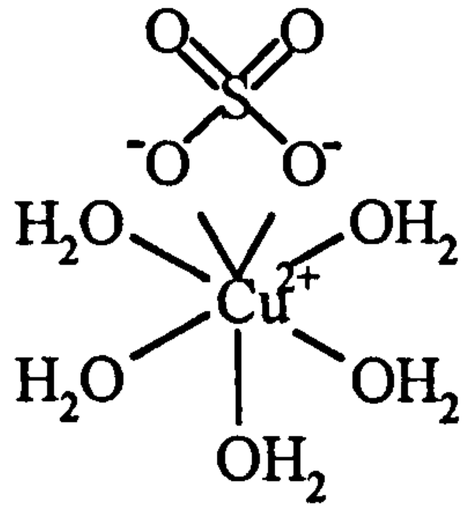

(2.2)

$$Cu^{2+} + 2\ GSH \longrightarrow [Cu^{2+}\text{-}(SG)_2] \longrightarrow Cu^{+}\text{-}SG + \tfrac{1}{2}\ GSSG \quad \textbf{(2.21)}$$

In order to investigate the nature and extent of radical generation from peroxyacetic acid and Cu^{2+} / gluthathione the spin-trapping approach was again employed. Initial experiments employed reaction mixtures containing 0.0048 M $CuSO_4$, 0.0096 M glutathione (pre-mixed), 0.048 M DMPO and 0.0048 M (total AvOx) 5% PAA at pH *ca.* 7.4. All reactants were thoroughly purged with a stream of oxygen-free nitrogen before and during use and were at room temperature. On addition of the glutathione to the copper (II) sulfate it was apparent that reduction had occurred as the pale blue colour faded, leaving a colourless solution. This observation was confirmed by the EPR spectrum of the reaction mixture which revealed no evidence of EPR detectable species. On addition of the peroxyacid it was apparent from the reappearance of the distinctive blue colouration and Cu^{2+} EPR spectrum that Cu^{2+} had been regenerated, but no spin-adducts were evident from the EPR spectrum. This was possibly thought to be a result of nitroxide reduction to EPR silent hydroxylamines by the presence of the reducing agent [reaction (2.22)]

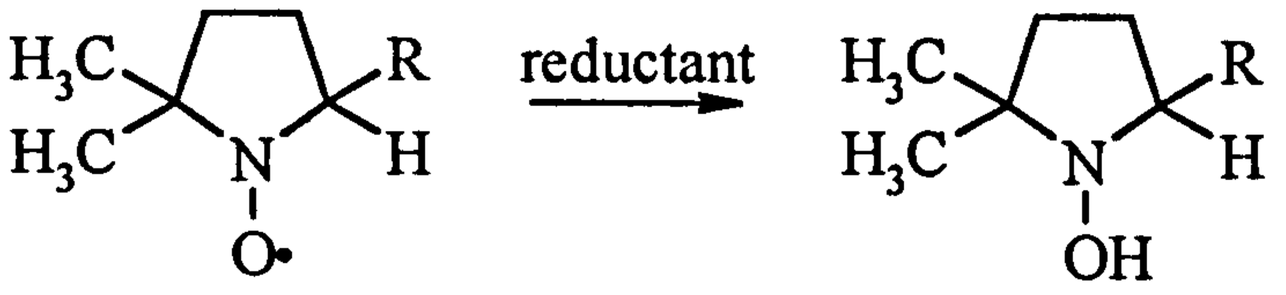

(2.22)

Addition of excess potassium ferricyanide revealed a weak signal attributable to DMPO-OH. It was decided however that further experiments should employ a final concentration of 0.024 M (total AvOx) of peroxyacid compound in an attempt to generate a higher concentration of spin-adducts which would not be subject to complete reduction by glutathione. On repetition of this experiment utilising the higher peroxyacid concentration an EPR spectrum consistent with the formation of a low concentration of DMPO-OH was observed.[158]

On reaction of 0.024 M (total AvOx) 40% PAA with 0.0048 M $CuSO_4$, 0.0096 M glutathione and 0.048 M DMPO, an EPR spectrum consistent with the formation of a low concentration of hydroxyl radicals was observed. No evidence for the formation of carbon-centred radicals was seen, which is in contrast to the spin-trapping results recorded using Fe^{2+}-EDTA and Ti^{3+}-EDTA and may reflect the cleavage of the peroxyacid to produce hydroxyl radicals and acetate anions [reaction (2.2)].

Reaction of 0.0048 M $CuSO_4$ with 0.0096 M glutathione and 0.024 M MMPP in the presence of 0.048 M DMPO produced no signals in the EPR spectrum, even upon addition of potassium ferricyanide. However, oxidation of the copper-thiolate complex was apparent as revealed by the reappearance of the characteristic blue colouration and the reappearance of the copper (II) EPR spectrum for which the *g*-value was found to be 2.10 (Figure 2.5). It can be seen that the EPR spectrum differs significantly from that of $Cu(H_2O)_5SO_4$ indicating that the oxidised copper species is a glutathione disulfide complex.[175] From these results it appears that either the mechanism of oxidation of the copper-thiolate complex by magnesium monoperoxyphthalate does not involve free radicals or that the rate of radical generation is too slow to produce a detectable concentration.

As for the reactions of Ti^{3+}-EDTA and Fe^{2+}-EDTA with peroxyacetic acid it was important to ascertain whether the hydroxyl radical adducts observed in the EPR spectra were formed through spin-trapping of the hydroxyl radical or through an artefactual reaction, possibly involving the nucleophilic addition of ^-OH to DMPO. Experiments involving the use of hydroxyl radical scavengers formate and DMSO were therefore conducted in order to determine this.

On reaction of 0.0048 M Cu^{2+} with 0.0096 M glutathione and 0.024 M (total AvOx) 5% PAA in the presence of 0.048 M DMPO and 1.1 M DMSO an EPR spectrum was seen which was consistent with the formation of a mixture of two spin adducts, a small concentration of DMPO-CH_3[158] and a relatively large concentration of DMPO-OH,[158] indicating that some of the signal attributed to the trapping of hydroxyl radicals had been due to a genuine trapping reaction but that the majority had not been due to a classical spin-trapping mechanism. This was confirmed by replacing DMSO with sodium formate which also produced a slight reduction in the signal assigned as DMPO-OH and the appearance of a signal corresponding to DMPO-CO_2^-.[158]

In the reactions which employed 40% PAA, the addition of hydroxyl radical scavengers produced alterations in the spectra. In both cases, the intensity of the DMPO-OH signal was observed to decrease slightly, to be replaced by the corresponding scavenger-derived radical adduct, indicating the presence of low concentrations of hydroxyl radicals.

The addition of scavengers to the system in which MMPP had been employed as an oxidant provided no evidence for the production of free radicals confirming that reoxidation of the copper-thiolate complex by MMPP occurs via a non-radical mechanism.

Catalase was employed to determine if hydroxyl radicals resulted from the peroxyacid or the hydrogen peroxide in the reaction mixture. The catalase-treated samples of peroxyacetic acid were prepared by the addition of approximately 10 mg of catalase to 1 ml of a freshly prepared 0.04 M (total AvOx) peroxyacetic acid solution in 0.1 M phosphate buffer (pH = 7.4) to ensure that the catalase could function. The solution was observed until effervescence ceased and then left to stand for five minutes to ensure complete removal of hydrogen peroxide. The resulting solution was then tested for hydrogen peroxide content and used immediately.

Reaction of 0.024 M (total AvOx before catalase treatment) 5% PAA with 0.0048 M Cu^+ in the presence of 0.048 M DMPO produced no spin-adducts. This may have been the result of the hydrogen peroxide being responsible for the formation of the low concentration of hydroxyl radicals observed. On combining the catalase treatment with the use of hydroxyl radical scavengers the mixture remained EPR silent. This indicates

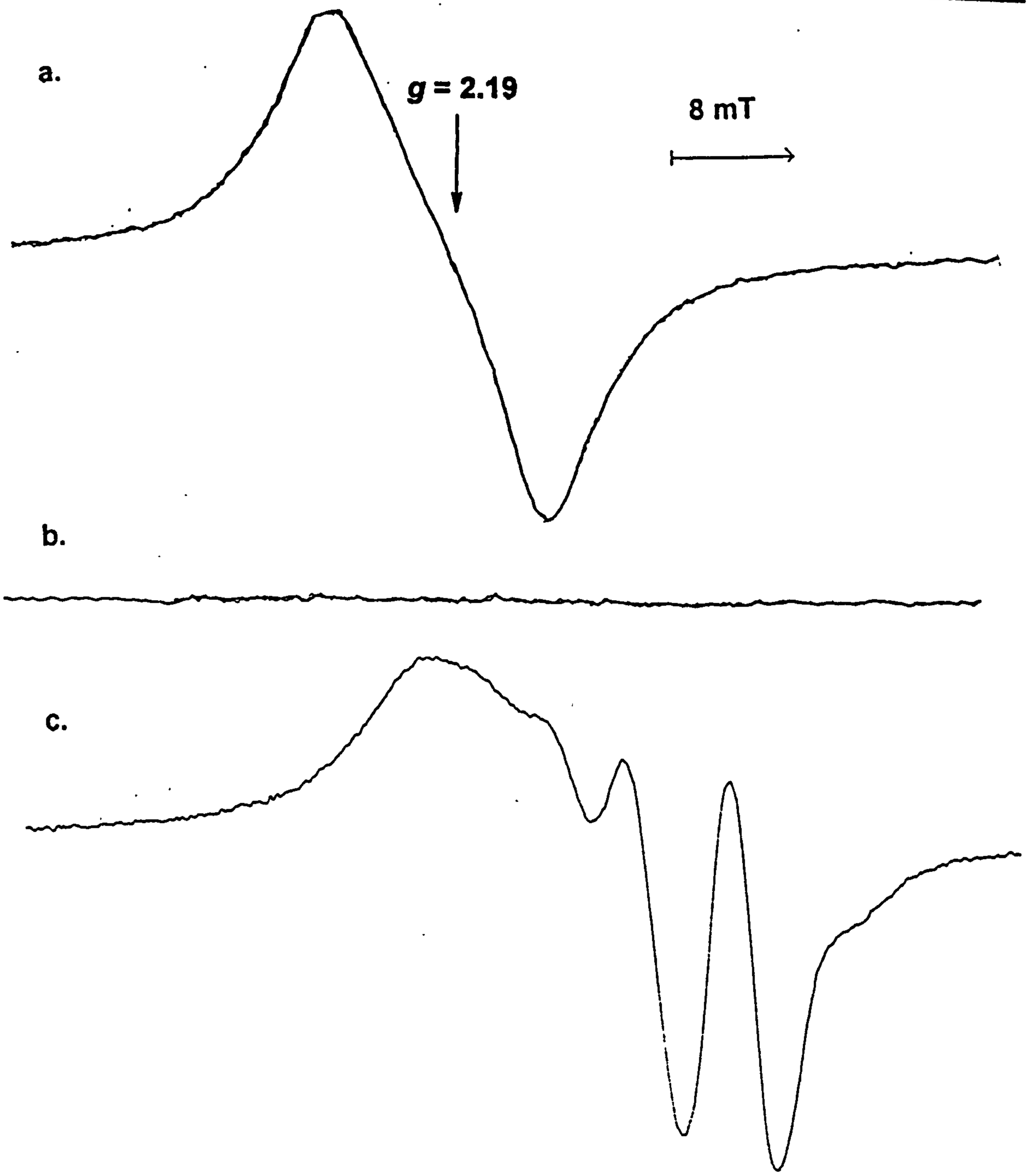

Figure 2.5.a. EPR spectrum showing the signal due to Cu^{2+}(aq).

Figure 2.5.b. EPR spectrum of the reaction mixture containing $CuSO_4$ and glutathione.

Figure 2.5.c. EPR spectrum showing the copper(II) thiolate complex generated by reaction of Cu^{2+}(aq) with glutathione and MMPP.

Concentrations employed:- $CuSO_4$, 0.0048 M, glutathione, 0.0096 M, MMPP, 0.024 M all at pH *ca.* 7.4.

that the low concentrations of hydroxyl radicals observed are produced from the hydrogen peroxide, but that the overall mechanism of oxidation is largely non free-radical. This is in agreement with spin-trapping studies on the oxidation of Cu^{+}-thiolate by hydrogen peroxide which suggests that at the stoichiometry used little evidence of radical production from hydogen peroxide could be discerned.

In reactions where the oxidant employed was 40% PAA, catalase treatment of the peroxyacid produced an EPR spectrum which still consisted of a low concentration of DMPO-OH. When the use of catalase treatment was combined with the use of hydroxyl-radical scavengers DMSO and formate the hydroxyl-radical adduct persisted indicating that it is produced via a non free-radical oxidation mechanism. This suggests that the low concentration of hydroxyl radicals observed are produced from the reaction of hydrogen peroxide with Cu^{+}, but the primary mechanism of oxidation does not involve free radicals.

In conclusion, oxidation of the Cu^{+}-thiolate complex of glutathione with peroxyacids occurs largely through a non free-radical mechanism. However, for the peroxyacetic acid formulations, low concentrations of free radicals are detected and found to be produced from the hydrogen peroxide in the reaction mixture. This is in concordance with previous studies performed on the Cu^{2+}(aq) / glutathione / hydrogen peroxide reaction mixture which found only minimal free radical involvement in the mechanism of Cu^{+} oxidation.[175]

2.4.2. Generation of Cu^{+} by the reaction of Cu^{2+} with L-ascorbic acid.

It is known that L-ascorbic acid, another important biological antioxidant, reacts with Cu^{2+} to produce a copper (I) complex which can be reoxidised by hydrogen peroxide and alkyl hydroperoxides with the concomitant formation of free radicals.[174,175] The nature of the complex is not as well studied as that between copper and glutathione but it is known that the favoured stoichiometry for stable copper (I) complex formation requires the presence of a two-fold molar excess of L-ascorbic acid over Cu^{2+}.[176]

Initial experiments employed reaction mixtures containing 0.0048 M Cu^{2+}, 0.0096 M L-ascorbic acid (pre-mixed), 0.048 M DMPO and 0.024 M 5% (total AvOx) PAA at pH

7. The EPR spectrum of this reaction mixture consisted of the formate radicaladduct [157] and a carbon-centred radical adduct with splittings $a_N = 1.58 \pm 0.01$ mT and $a_{\beta\text{-}H} = 2.56 \pm 0.01$ mT and some evidence of the production of hydroxyl radicals.[158] It is thought that the formate was a degradation product of the L-ascorbic acid although this was not investigated further. A strong doublet indicative of ascorbyl radicals[177] (2.13) was sometimes observed. This radical is resonance stabilised and hence not trapped by DMPO.These observations are in contrast to corresponding experiments in which Ti^{3+}-EDTA, Fe^{2+}-EDTA or Cu^{2+} / glutathione were utilised as the transition metal catalyst in which only DMPO-OH was observed.

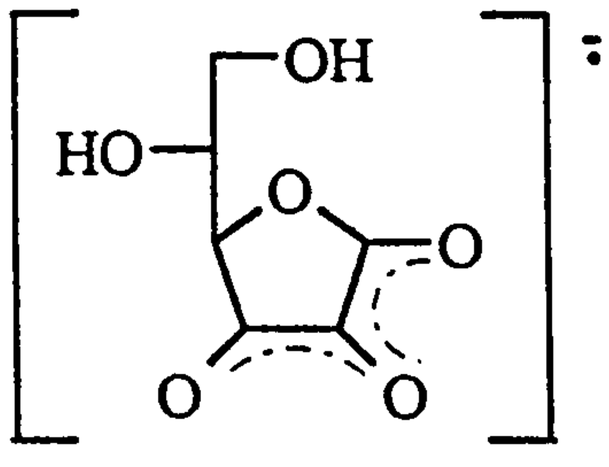

(2.13)

On replacement of 5% PAA with 40% PAA at equivalent total AvOx an EPR spectrum was observed which was consistent with the formation of a low concentration of carbon-centred radicals and a relatively high concentration of hydroxyl radicals. Ascorbyl radical formation was also evident in some cases.

In the corresponding experiments in which MMPP was employed as the oxidant the nature of the spectra is again found to be dependent upon the age of the MMPP solution reflecting the involvement of hydrogen peroxide in the reactions. When Cu^{2+} was mixed with L-ascorbic acid and freshly prepared MMPP in the presence of DMPO a mixture of carbon-centred radical adducts and hydroxyl radical adducts were sometimes observed. Leaving the MMPP solution to stand for any length of time resulted in an increase in the relative intensity of the carbon-centred radical adducts. This is in contrast to the results observed when the reductant used was glutathione where no evidence of radical formation was observed. Table 2.4 provides a summary of the results.

System	Radicals	a_N / mT[a]	$a_{\beta-H}$ / mT[a]	a_{other} / mT[a]
Ascorbate / 5% PAA / DMPO	DMPO-C·	1.64	2.34	-
	DMPO-CO_2^-	1.57	1.89	-
	Ascorbyl	-	-	0.18
Ascorbate / 40% PAA / DMPO	DMPO-C·	1.64	2.34	-
	DMPO-OH	1.49	1.49	-
	Ascorbyl	-	-	0.18
Ascorbate / MMPP / DMPO	DMPO-OH	1.49	1,49	-
	DMPO-C·	1.64	2.34	-

a. hyperfine coupling constants have a typical error of 0.01 mT.

Table 2.4. Summary of EPR data obtained in spin-trapping experiments employing 5% PAA, 40% PAA and MMPP with Cu^{2+} / L-ascorbic acid in the presence of DMPO.

Scavenging experiments were performed in the Cu^{2+} / L-ascorbic acid reaction system to investigate the involvement of hydroxyl radicals in the formation of DMPO-OH. When 0.0048 M Cu^{2+} reacted with 0.0096 M L-ascorbic acid and 0.024 M (total AvOx) 5% PAA in the presence of 0.048 M DMPO and 1.1 M DMSO, the intensity of the hydroxyl radical adduct decreased. This was accompanied by an increase in the intensity of the carbon-centred radical adduct. Similarly, when sodium formate was introduced into the reaction mixture as a hydroxyl radical scavenger the amplitude of the DMPO-OH[157] signal decreased concomitantly with the increase in intensity of the signal attributable to DMPO-CO_2^-. [158]

In analogous experiments performed in the corresponding reaction mixture containing 40% PAA the production of hydroxyl radicals was confirmed by the appearance of scavenger-derived radical adducts in the EPR spectra when DMSO or sodium formate were included in the reaction mixture. However, it is worth noting that not all of the DMPO-OH signal was scavenged by DMSO or formate suggesting the

involvement of a non classical mechanism in the formation of the hydroxyl radical spin-adduct.

When hydroxyl radical scavengers were introduced into the reaction system containing Cu^{2+}, L-ascorbic acid. MMPP and DMPO, the effect of the scavengers was seen to be roughly proportional to the age of the MMPP solution; freshly prepared solutions of MMPP produced EPR spectra in which the hydroxyl radical spin-adduct had predominated over the carbon-centred spin-adduct, where as spectra of reaction mixtures in which the MMPP was older displayed a relative increase in the carbon-centred radical adduct over the hydroxyl radical adduct. Addition of either DMSO or sodium formate to the reaction mixtures containing MMPP produced intense spectra of a mixture of the hydroxyl radical adduct and the appropriate scavenger-derived adduct. The intensity of the scavenger derived adduct was found to increase as the age of the MMPP solution increased, indicating that hydroxyl radical formation was from the hydrogen peroxide derived from degradation of MMPP. Incomplete scavenging of the hydroxyl-radical adduct signal implies the formation of DMPO-OH does not occur via a classical spin-trapping mechanism.

Further experiments, employing catalase-treated peroxyacid samples, were carried out to ascertain the nature and extent of the role of hydrogen peroxide in the formation of the spin-adducts observed in previous experiments. Mixing 0.0048 M Cu^{2+} with 0.0096 M L-ascorbic acid and 0.024 M (total AvOx prior to catalase treatment) 5% PAA in the presence of 0.048 M DMPO produced an EPR-silent mixture. This indicates that the carbon-centred radical, formate radical and hydroxyl radical spin-adducts observed in the original experiments had been formed from the reaction of hydrogen peroxide with Cu^{+} to form hydroxyl radicals, which had then subsequently been trapped by DMPO, or reacted with the L-ascorbic acid to generate the formate radical anion and carbon-centred radical.

Similarly, on addition of catalase to 40% PAA used in the reaction between Cu^{2+}, L-ascorbic acid, 40% PAA and DMPO, the EPR spectrum which had comprised of a mixture of carbon-centred radical adduct(s) and the hydroxyl radical now displayed no signals. This indicated that the spin-adducts observed previously are the result of hydroxyl-radical formation from the hydrogen peroxide in the reaction mixture.

2.4.3. The use of MNP to identify the carbon-centred radicals.

MNP was employed to identify the carbon-centred radicals in the reaction mixtures. In the case of the peroxyacetic acid formulations, it was thought that these would not be methyl radicals from the peroxyacetic acid as catalase treatment had resulted in a loss of these signals. However, it was still not known if these signals were derived from the L-ascorbic acid in the reaction mixtures or from hydrogen-atom abstraction products of acetic acid or peroxyacetic acid. Owing to the poor solubility of MNP in water it was dissolved in a mixture of 30% acetonitrile and 70% water prior to use.

When 0.0048 M Cu^{2+} reacted with 0.0096 M L-ascorbic acid, 0.024 M (total AvOx) 5% PAA and 0.0048 M MNP, a spectrum was seen corresponding to the formation of three radical species. The two major signals were assigned to spin-adducts of the radicals (2.14) and (2.15) derived from hydroxyl radical attack on L-ascorbic acid. The minor spin-adduct was assigned to a degradation product of MNP (see Table 2.5).

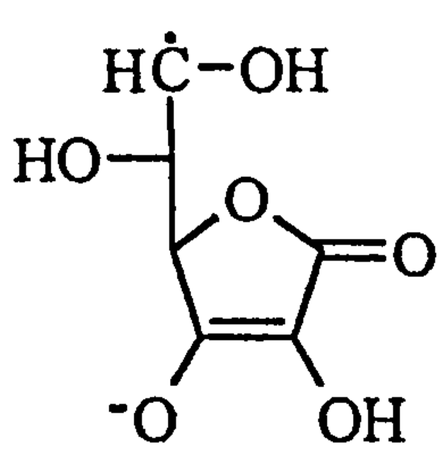

(2.14)

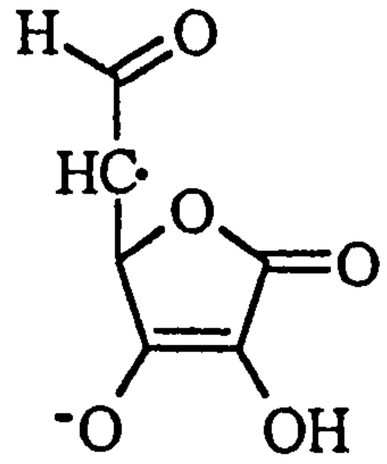

(2.15)

For the corresponding reaction in which 40% PAA was employed as an oxidant a weaker spectrum was seen, but still displaying the same signals as before indicating that the appearance of these signals was indeed dependent upon the hydrogen peroxide in the reaction mixture.

On replacement of DMPO with MNP in reaction systems employing MMPP as the oxidant, no spin-adducts were observed in the spectrum when freshly prepared MMPP was used. However, as the MMPP was allowed to stand weak signals became apparent which could be assigned to spin-adducts of the two L-ascorbic acid derived radicals and the

degradation product of MNP reflecting the increasing concentration of hydrogen peroxide.

To confirm the role of hydrogen peroxide (and hydroxyl radicals) in the production of the L-ascorbic acid derived radicals, a solution of hydrogen peroxide was photolysed in the presence of L-ascorbic acid and MNP. The EPR spectrum of this reaction mixture closely resembled those observed previously thus confirming that the radicals are formed by hydroxyl radical abstraction from L-ascorbic acid. A summary of results is provided in Table 2.5.

System	Radical Addend	a_N / mT[a]	$a_{\beta\text{-}H}$ / mT[a,b]
Ascorbate / 5% PAA / MNP	ascorbate derived	1.51	0.33 (1)
	ascorbate derived	1.51	0.11 (1)
	MNP derived	1.64	1.00 (2)
Ascorbate / 40% PAA / MNP	ascorbate derived	1.51	0.33 (1)
	ascorbate derived	1.51	0.11 (1)
	MNP derived	1.64	1.00 (2)
Ascorbate / MMPP / MNP	[c]	-	-

a. hyperfine coupling constants have a typical error of ± 0.01 mT.

b. numbers in parentheses indicate number of hydrogens.

c. ascorbate derived radicals observed when MMPP is allowed to stand.

Table 2.5. Summary of EPR data obtained in spin-trapping experiments employing 5% PAA, 40% PAA and MMPP with Cu^{2+} / L-ascorbic acid in the presence of MNP.

2.4.4. Discussion.

The spin-trapping studies undertaken here clearly highlight differences in the mechanism of the reaction between copper(I)-thiolate and copper(I)-L-ascorbic acid and peroxyacids. Oxidation of the Cu^{+} in the copper / glutathione system clearly occurs

through a largely non free-radical mechanism whereas there are clearly high concentrations of radical species produced in the ascorbate system. However, even in the ascorbate system the results suggest that the hydrogen peroxide is the predominant source of free radicals, implying that reaction of the copper(I)-ascorbate complex with peroxyacids does not occur via a radical mechanism or is appreciably slower than the reaction with hydrogen peroxide.

2.5. AN INVESTIGATION INTO THE NUCLEOPHILIC ADDITION OF $^{-}$OH TO DMPO.

Earlier in this Chapter it was observed that not all of the hydroxyl radical adducts of DMPO were removed by the addition of formate or DMSO. It was thought that transition-metal assisted nucleophilic addition of water to DMPO may be occurring and this possibility was therefore investigated.

Initial experiments involved the reaction of 0.0048 M Fe^{3+}-EDTA with 0.0048 M DMPO. This mixture produced no EPR visible species. On mixing unchelated Fe^{3+} with DMPO, a persistent EPR spectrum was observed indicative of the formation of DMPO-OH.[158] Further investigation showed that the intensity of the signal increased as the concentration of Fe^{3+} was increased (although paramagnetic broadening at higher concentrations precluded accurate measurements) and as the concentration of DMPO was increased. The mixtures were also observed to turn bright pink / purple and were therefore analysed using UV-visible spectrophotometry. The mixtures were found to have a broad, featureless absorbance with $\lambda_{max} = 525$ nm which on further investigation was found to be dependent upon the concentration of Fe^{3+} and DMPO.

The exact nature of the mechanism is still unknown. The possibility remains that slow reduction of Fe^{3+} was responsible for the generation of hydrogen peroxide and subsequently hydroxyl radicals and superoxide radicals both of which may give rise to hydroxyl radical adducts of DMPO. Therefore reaction of 0.0048 M Fe^{3+}-EDTA with 0.0048 M DMPO in the presence of excess catalase was examined. It was found that the under these conditions the spin-adduct was again generated ruling out the possibility of

the involvement of hydrogen peroxide.

It was thought that the stereochemistry of addition of ^{-}OH might be different to the stereochemistry of addition of ·OH and therefore that DEPMPO would provide a good probe for the stereochemistry of the reaction as, radicals can add either *cis* or *trans* to the spin-trap. Previously, only the *trans*-hydroxyl radical adduct of DEPMPO had been observed but it was thought that the addition of ^{-}OH might occur either *cis* or a mixture of *cis* and *trans* hence providing a probe for the nature of hydroxyl adduct formation. When Fe^{3+} was mixed with DEPMPO a mixture of two signals was observed (see Figure 2.6), one with splittings corresponding to the previously observed *trans* hydroxyl radical adduct and another with $a_P = 4.60 \pm 0.01$ mT, $a_N = 1.45 \pm 0.01$ mT and $a_{\beta\text{-}H} = 2.20 \pm 0.01$ mT which is in the range of hydrogen splittings observed for a *carbon-centred* radical adduct. Other experiments[178,179] in this department involving the use of ^{17}O labelled water show that this second signal is not due to the *cis* hydroxyl radical adduct and a tentative mechanism has been suggested to account for the production of the nitroxide (2.16), a product of sequential reactions following radical cation formation.

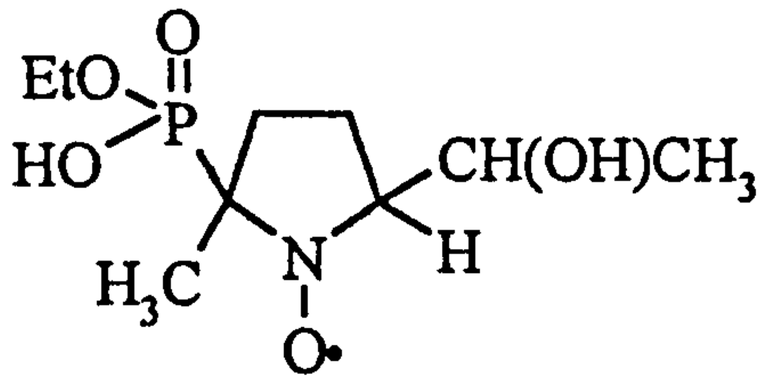

(2.16)

Further support for the structure of this nitroxide was gained from experiments using the related spin-trap OPMPO (2.17), which has two phenyl rings in place of the ethyl groups and therefore would not be able to undergo a molecular rearrangement of the type required to produce the nitroxide (2.16).

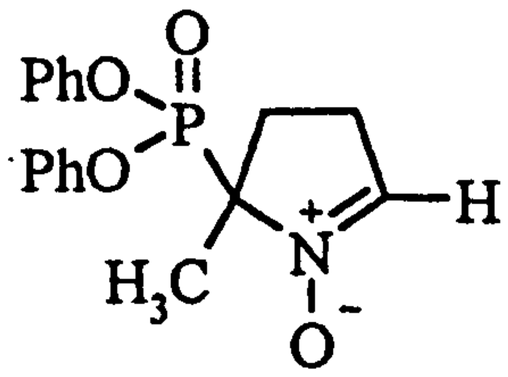

(2.17)

Initial experiments with this spin-trap involved the characterisation of its hydroxyl radical spin-adduct. As OPMPO is only sparingly soluble in water, solutions of OPMPO were made up in 30% acetonitrile and 70% water. Upon photolysis of a solution containing 0.01 M OPMPO and 0.05 M hydrogen peroxide a signal was observed corresponding to OPMPO-OH, which has splittings $a_P = 4.95 \pm 0.01$ mT and $a_N = a_{\beta\text{-}H} = 1.38 \pm 0.01$ mT. For mixtures containing 0.0048 M Fe^{3+} and 0.0048 M OPMPO this signal alone was observed as anticipated by the proposed mechanism for the formation of nitroxide (2.16).

Similar observations in spin-trapping experiments with DEPMPO were made when the high valent metal ion was Cu^{2+} or Mn^{4+}.[179] It may therefore be concluded that the appearance of appreciable concentrations of non-scavengable hydroxyl radical adducts in the experiments in which Cu^{2+}/reductant and peroxyacid were employed was due to the nucleophilic attack of ^{-}OH on $DMPO^{\ddagger}$. However, in the cases of Ti^{4+} or Fe^{3+} this mechanism only operates to any significant degree in the absence of a chelator such as EDTA, in which case from the appearance of a strong colour in mixtures containing Fe^{3+}, would suggest that formation of a DMPO-metal ion complex may be involved. It is therefore believed that this pathway may not be significant in the formation of artefactual spin-adducts in the titanium and iron systems unless for some reason complexation of the EDTA to the metal ion is disrupted.

It may also be concluded that in cases where nucleophilic addition of ^{-}OH to spin-traps is suspected that DEPMPO may prove to be a valuable mechanistic probe for the differentiation of genuine and arefactual spin-adduct formation.

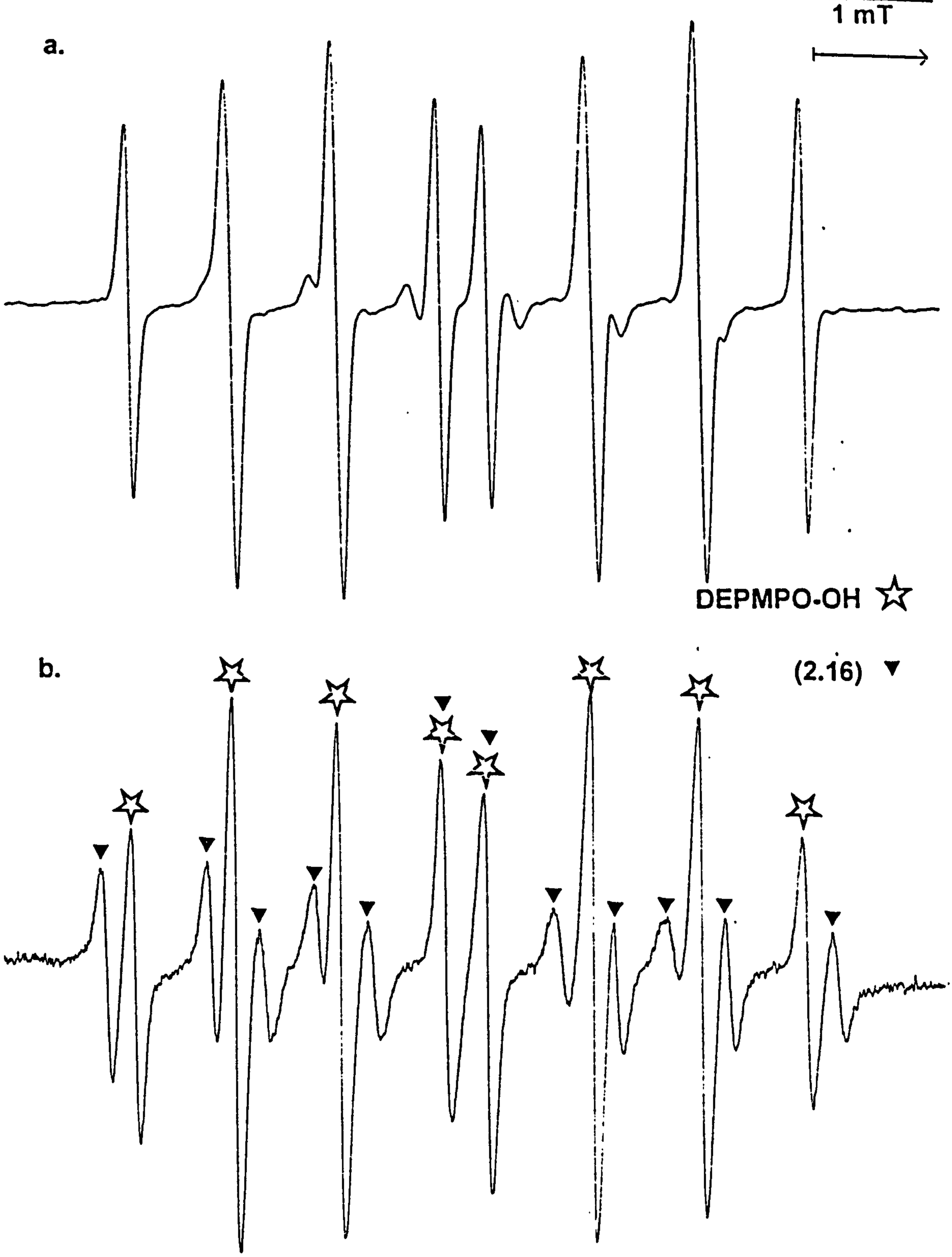

Figure 2.6.a. EPR spectrum showing DEPMPO-OH generated by reaction of 0.001 M Fe^{2+}-EDTA (EDTA in excess) with 0.005 M H_2O_2 and 0.005 M DEPMPO. Figure 2.6.b. EPR spectrum showing DEPMPO-OH and the DEPMPO derived radical (2.16) generated by reaction of 0.0048 M Fe^{3+} with 0.0048 M DEPMPO.

2.6. AN EPR RAPID-FLOW INVESTIGATION INTO THE REACTIONS BETWEEN LOW-VALENT TRANSITION METAL IONS AND PEROXYACETIC ACID.

2.6.1. One-electron reduction of peroxyacetic acid with Ti^{3+}-EDTA.

In order to compliment the spin-trapping results already obtained, it was decided to examine the reactions of low-valent transition metal ions in a continuous flow system in which the complications of spin-trap chemistry would be avoided. Continuous flow EPR experiments were initially performed on the reaction between Ti^{3+} and peroxyacetic acid, using a three way mixer (with water in the third stream) in which solutions were mixed *ca.* 40 ms before entering the cavity of the EPR spectrometer. The pH was adjusted by addition of sulfuric acid or ammonia to the metal ion stream and measured by a pH meter placed in the effluent stream. The flow was maintained by a peristaltic pump and all reactant streams were purged with a stream of oxygen-free nitrogen prior to and during use. All concentrations quoted are those after mixing.

On mixing 0.0017 M Ti^{3+}-EDTA with 0.0083 M (total AvOx) 5% PAA at pH *ca.* 2.5 with an observation time of 0.039s after mixing, a weak signal was evident from the methyl radical which is assigned on the basis of its *g*-value of 2.0025 ± 0.0001 and the 1:3:3:1 splitting pattern with $a_{3\alpha\text{-}H} = 2.27 \pm 0.01$ mT. This supported the spin-trapping data which suggested that the peroxyacetic acid in the formulation underwent reduction on reaction with Ti^{3+}-EDTA to form the acetoxyl radical which then rapidly decarboxylates to form the methyl radical. On adding 10% by volume methanol to the third stream (Figure 2.7.a) a second signal was observed, that of the hydroxymethyl radical, characterised by a *g*-value of 2.0031 ± 0.0001 aswell as the α proton splitting of 1.75 ± 0.01 mT and the β proton splitting of 0.11 ± 0.01 mT, formed by the reaction of methanol with hydroxyl radicals [reaction (2.21)] or possibly methyl radicals [reaction 2.22)].

$$CH_3OH + \cdot OH \longrightarrow \cdot CH_2OH + H_2O \qquad \textbf{(2.21)}$$

$$CH_3OH + \cdot CH_3 \longrightarrow \cdot CH_2OH + CH_4 \qquad \textbf{(2.22)}$$

No evidence for the formation of radicals derived from hydrogen atom abstraction on the parent peroxyacid or the acetic acid in the reaction mixture was seen in contrast to results observed in a similar system previously.[80]

On substituting the peroxyacid formulation with 40% PAA, the EPR spectrum displayed a much more intense spectrum attributable to methyl radicals, reflecting the higher concentration of peroxyacetic acid in the formulation. Addition of 10% by volume of methanol to the third stream led to the production of a low concentration of hydroxymethyl radicals ($g = 2.0031 \pm 0.0001$, $a_{\alpha\text{-H}} = 1.76 \pm 0.01$ mT, $a_{\gamma\text{-H}} = 0.13 \pm 0.01$ mT) in addition to methyl radicals (Figure 2.7.b).

Although the relative concentrations of hydroxymethyl radicals obtained in the experiments employing 5 and 40% PAA and methanol as a substrate strongly suggest that the abstracting species is the hydroxyl radical, subsequent experiments were performed with ethanol as substrate since it has previously been shown that the ratio of α-radicals to β-radicals obtained is indicative of the nature of the attacking species; hydroxyl radicals leading predominantly to the formation of the α-radical and the methyl radical preferably abstracting a hydrogen in the β-position.[181] On addition of 10% by volume of ethanol to the substrate stream in experiments with 5% PAA a mixture of signals was observed indicating the formation of methyl radicals, $\cdot CH_2CH_2OH$ ($g = 2.0026 \pm 0.0001$, $a_{\alpha\text{-H}} = 2.18 \pm 0.01$ mT, $a_{\beta\text{-H}} = 2.78 \pm 0.01$ mT) and $\cdot CH(CH_3)OH$ ($g = 2.0032 \pm 0.0001$, $a_{\alpha\text{-H}} = 1.51 \pm 0.01$ mT, $a_{\beta\text{-H}} = 2.26 \pm 0.01$ mT) with the α-radical predominating over the β-signal indicating that the species responsible for hydrogen atom abstraction is indeed the hydroxyl radical (see Figure 2.8.a). On replacing 5% PAA with 40% PAA little evidence of ethanol-derived radicals was observed, lending support to the theory that the main abstracting species is the hydroxyl radical from hydrogen peroxide (see Figure 2.8.b).

Since the concentration of hydrogen peroxide and therefore hydroxyl radicals was low in 40% PAA reaction mixtures (hydrogen peroxide accounting for approximately one quarter of the total AvOx), it was possible to estimate the rate of reaction between

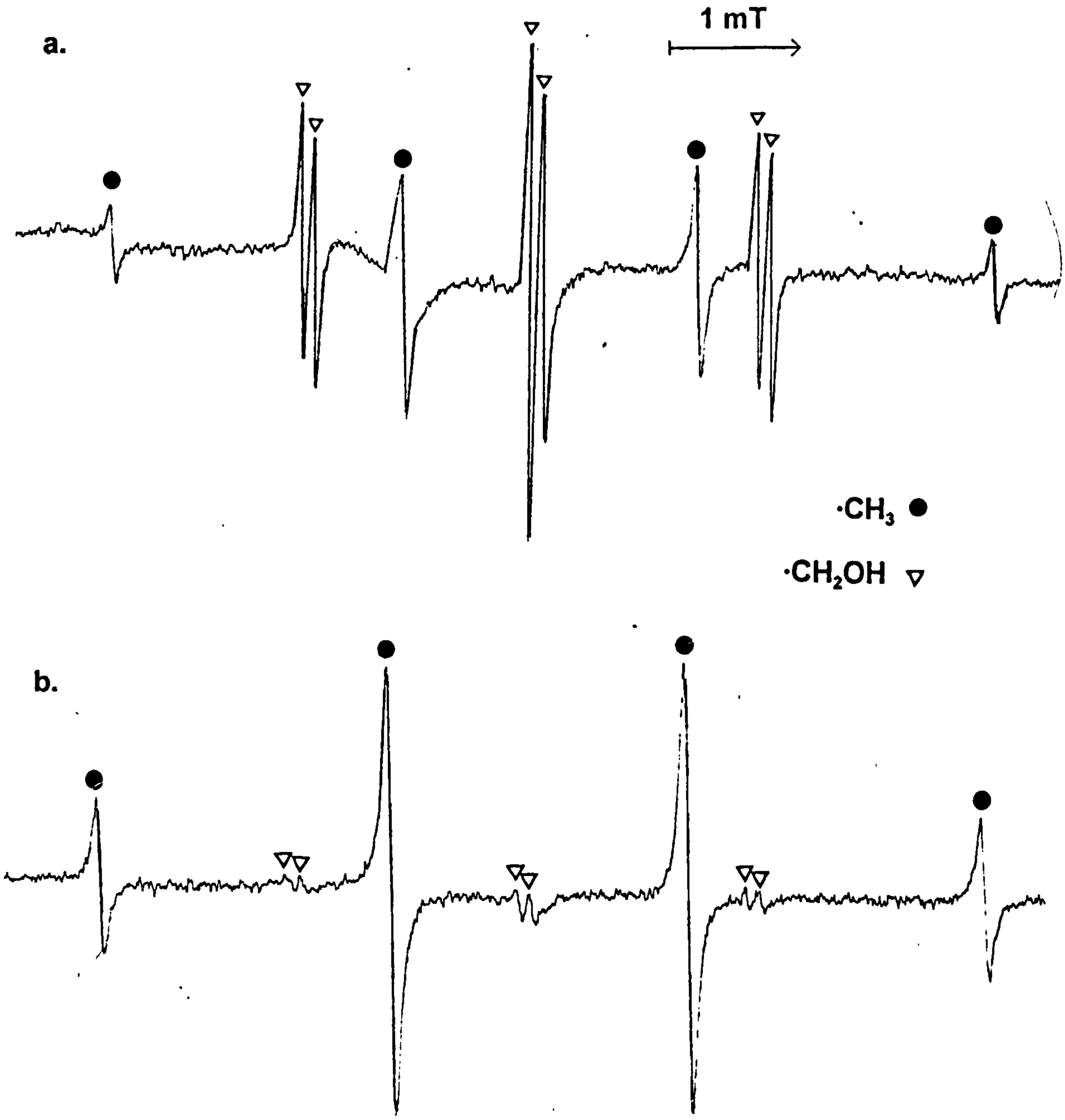

Figure 2.7.a. EPR spectrum showing a low concentration of methyl radicals and a high concentration of hydroxymethyl radicals generated by the reaction of Ti^{3+}-EDTA with 5% PAA and methanol under flow conditions.

Figure 2.7.b. EPR spectrum showing a high concentration of methyl radicals and a low concentration of hydroxymethyl radicals generated by the reaction of Ti^{3+}-EDTA with 40% PAA and methanol under flow conditions. Concentrations employed:- Ti^{3+}-EDTA, 0.0017 M, PAA, 0.0083 M (total AvOx), methanol, 10% v/v.

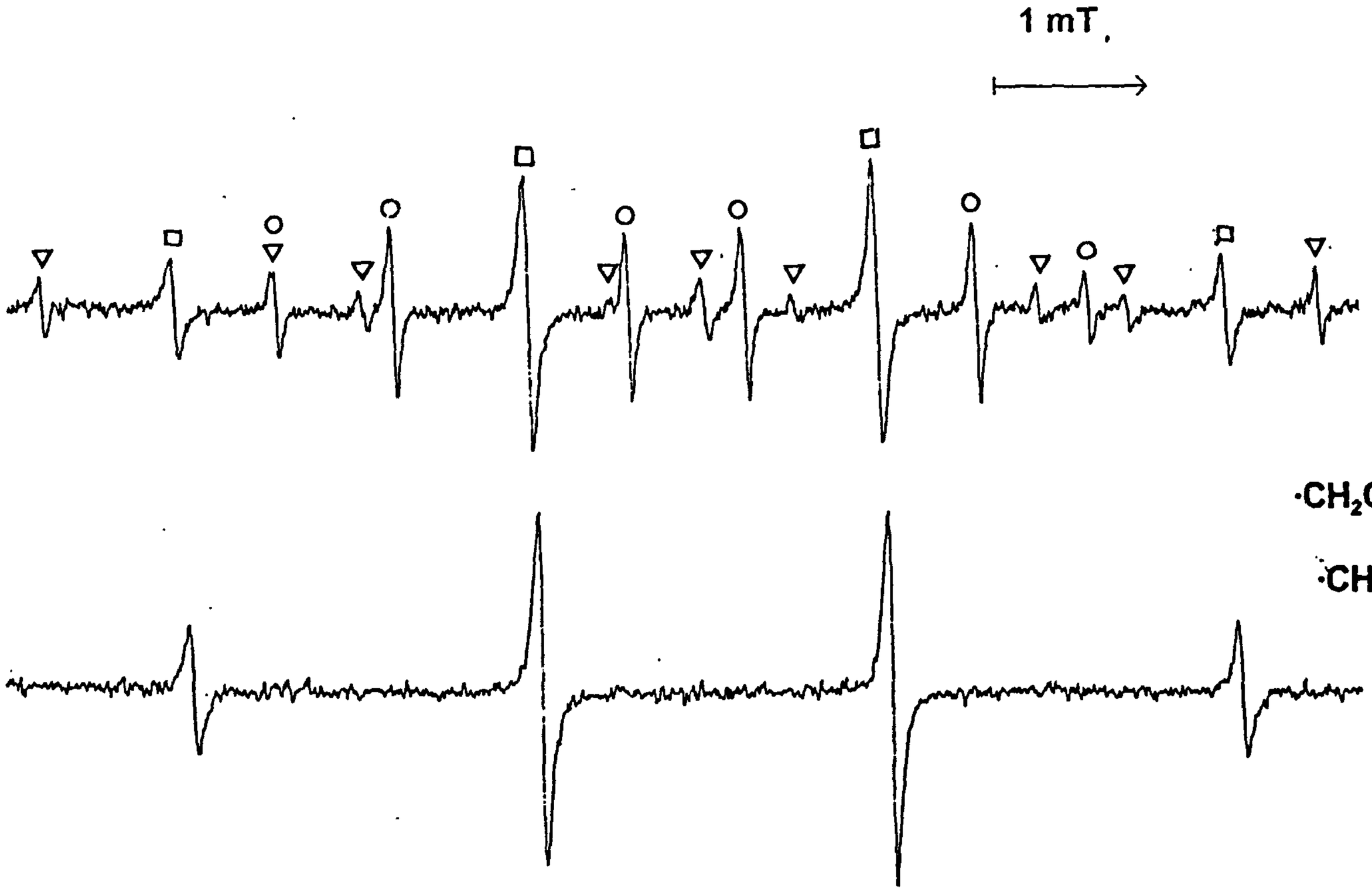

Figure 2.8.a. EPR spectrum showing methyl radicals, α-hydroxyethyl radicals and β-hydroxyethyl radicals generated by the reaction of Ti^{3+}-EDTA, 5% PAA and ethanol under flow conditions.

Figure 2.8.b.EPR spectrum showing methyl radicals generated by the reaction of Ti^{3+}-EDTA, 40% PAA and ethanol under flow conditions.

Concentrations employed:- Ti^{3+}-EDTA, 0.0017 M, PAA, 0.0083 M (total AvOx), ethanol, 10% by volume.

peroxyacetic acid and Ti^{3+}-EDTA. This was achieved by using a kinetic analysis previously described which relies upon the generation of a steady state concentration of radicals in the cavity. Thus, an equation is generated which relates maximum radical concentration to peroxide concentration and mixing time [equation (2.1)].[182,183]

$$[\text{Peroxide}]_{max} = 1 / k_{in}t \qquad \textbf{Eqn 2.1.}$$

$[\text{Peroxide}]_{max}$ = concentration of peroxide at maximum observed radical concentration

k_{in} = rate constant for the reaction in which the radical is first generated

t = time between mixing and observation

When 0.0017 M Ti^{3+}-EDTA was flowed with concentrations of 40% PAA varying from 0.02 - 0.09 M (total AvOx) at pH = 2.5 with a mixing time of 0.039 s, a maximum methyl radical concentration was observed when [PAA (total AvOx)] was 0.05 M (see Figure 2.9) which corresponds to $[CH_3CO_3H] = 0.039$ M and hence using equation 2.1 leads to a value for the rate constant for the reaction of $6.57 \times 10^2 mol^{-1} dm^3 s^{-1}$, which is a little lower than has been found previously for the same reaction at pH = 1.5 in the absence of a chelator.[80]

2.6.2. One-electron reduction of peroxyacetic acid with Fe^{2+}-EDTA.

Next, electron-transfer reactions between peroxyacetic acid formulations and Fe^{2+}-EDTA were investigated. Initial experiments under the same reaction conditions employed to study the analogous reactions with Ti^{3+}-EDTA produced no EPR-detectable species. *Increasing* the concentration of peroxyacid [concentrations up to 0.033 M (total AvOx)] failed to result in the appearance of any signals in the EPR spectrum, but conversely *lowering* the peroxyacid concentration to below 0.005 M resulted in the appearance of weak EPR signals for both 5% PAA and 40% PAA. This is believed to reflect a much *higher* rate of reaction between the peroxyacid and Fe^{2+}-EDTA as opposed to Ti^{3+}-EDTA. Although kinetic analysis as performed above could not be carried out as equation 2.1 only holds when [Peroxide] ➤ [Metal] it may be estimated that $k \geq 2 \times 10^3$ mol^{-1} dm^3 s^{-1} by analogy with kinetic simulation results obtained for the reaction of H_2O_2 with Fe^{2+}-EDTA.[135]

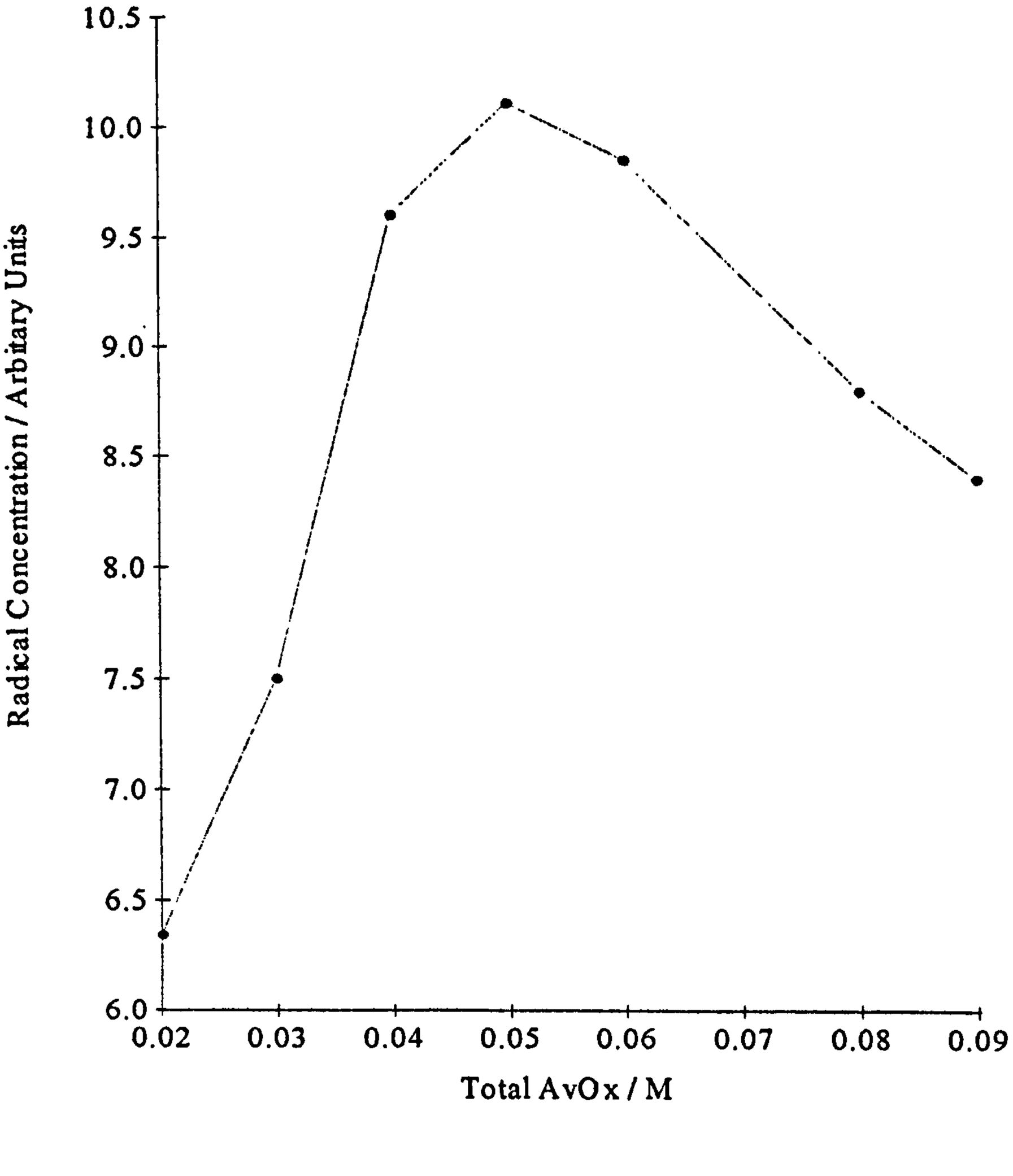

Figure 2.9. The variation in methyl radical concentration observed when 0.0017 M Ti^{3+}-EDTA was mixed with various concentrations of 40% PAA under the conditions described in the text.

The spectra for both 5% PAA and 40% PAA consisted of weak methyl radical signals. On the addition of 10% by volume of methanol to the substrate stream weak spectra consistent with the formation of the hydroxymethyl radical became evident in addition to the methyl radical signals, the relative intensities correlating with the relative concentrations of peroxyacetic acid and hydrogen peroxide in the reaction mixtures. On addition of ethanol to the substrate stream spectra for reaction mixtures in which 5% PAA was employed displayed weak signals attributable to the α and β radicals as well as a signal due to the methyl radical. However, on replacement of 5% PAA with 40% PAA only a methyl radical signal is observed. This is thought to be the result of a combination of the low concentration of hydrogen peroxide present and the weak signals observed in the presence of Fe^{2+}-EDTA.

2.6.3. One-electron reduction of peroxyacetic acid with Cu^{+}.

On changing the metal ion to Cu^{+}, generated by the reaction of Ti^{3+} with Cu^{2+} (1×10^{-5} M) [reaction (2.23)] the spectra of both the system containing 5% PAA and 40 % PAA in the absence of scavengers showed evidence for the formation of methyl radicals, although the concentrations were lower than those observed in the spectra for which the metal ion had been Ti^{3+} possibly reflecting the ability of Cu^{+} to reduce organic radicals, or the ability of Cu^{2+} to oxidise radicals[184] (or possibly the peroxyacetic acid cleaving to produce ·OH and $CH_3CO_2^-$ rather than $CH_3CO_2\cdot$ and ^-OH as was observed for Ti^{3+} and Fe^{2+}).

$$Cu^{2+} + Ti^{3+} \longrightarrow Cu^{+} + Ti^{4+} \qquad \textbf{(2.22)}$$

Again, no evidence for the production of hydrogen-atom abstraction products from the parent peroxyacid or the acetic acid in the reaction mixture was observed. On addition of 10% by volume of methanol to the third stream hydroxymethyl radical signals became apparent, although in lower overall concentration than had been observed previously in the Ti^{3+} system reflecting the ability of Cu^{2+} to act as a reducing agent for organic free

radicals. It appeared though as if the *relative* concentration of hydroxymethyl radical to methyl radical had increased, providing evidence that the peroxyacetic acid cleaves to produce the hydroxyl radical and acetate anions to some extent. On addition of ethanol to the substrate stream reactions in which 5% PAA was employed displayed spectra in which a mixture of $\cdot CH_3$, $\cdot CH_2CH_2OH$ and $\cdot CH(CH_3)OH$ was evident. However, on replacement of 5% PAA with 40% PAA little evidence for either of the ethanol-derived radicals was seen, corresponding to the low concentration of hydrogen peroxide in the reaction mixture

2.7. CONCLUSIONS.

These initial experiments serve to establish the applicability of spin-trapping to investigate the metal-catalysed homolysis of peroxyacetic acid and examine the further reactions of the first-formed radicals as well as to highlight some of the difficulties associated with the use of this technique. It has been demonstrated that although both Ti^{3+}-EDTA and Fe^{2+}-EDTA react with peroxyacetic acid to produce high concentrations of acetoxyl radicals [reaction (2.1)] Cu^+-L-ascorbic acid and Cu^+-glutathione are oxidised largely without the involvement of free radicals, although the hydrogen peroxide in the formulations reacts with Cu^+-L-ascorbic acid (and to a minimal extent the Cu^+ - glutathione) to produce hydroxyl radicals.

Rapid flow EPR techniques have allowed a more quantitative insight into the reactions of peroxyacetic acid with low-valent transition metals to be gained. It has been shown that the rate constant for reaction of peroxyacetic acid with Ti^{3+}-EDTA at pH = 2 is *ca.* 6.57×10^2 mol^{-1} dm^3 s^{-1} and that the reaction of peroxyacetic acid with Fe^{2+}-EDTA proceeds more rapidly, with a rate constant estimated to be $\geq 2 \times 10^3$ mol^{-1} dm^3 s^{-1}. It has also been shown that Cu^+ formed by the reaction of Ti^{3+} with Cu^{2+} can react with peroxyacetic acid in a mixture of two ways - primarily to form the acetoxyl radical and hydroxide [reaction (2.1)], but also to form hydroxyl radicals and acetate anions [reaction (2.2)].

It is believed that the rapid generation of radicals by electron-transfer from a low-valent transition-metal ion to peroxyacid formulations may be responsible for their

bactericidal action and this will be investigated further in the forthcoming Chapters.

CHAPTER 3.

STUDIES OF PROTEIN DAMAGE INDUCED BY PEROXYACETIC ACID.

3.1. INTRODUCTION.

The previous Chapter described investigations of the reactions of peroxyacids with low-valent transition-metal ions utilising both EPR spin-trapping and EPR rapid-flow techniques. It was found that the reaction of peroxyacetic acid with Fe^{2+} proceeds very rapidly to produce acetoxyl radicals and hydroxide and that the corresponding reactions with copper(I) species depend upon the reducing species and ligand system. Hydrogen peroxide in the reaction mixtures reacts rapidly with Fe^{2+}-EDTA to produce hydroxyl radicals and again with copper(I) the nature of the reaction is highly dependent upon the individual system.

It was decided next to investigate the reactions of radicals derived from PAA in this way with proteins in order that possible damage in such systems caused by PAA could be characterised. Protein damage caused by free-radical species is believed to be involved in cell lysis of bacteria by leucocytes and several mammalian diseased states such as ageing, diabetes and atherosclerosis [185] It was therefore believed that studies of protein damage would provide an insight into possible mechanisms of protein damage in the biocidal action of PAA against *Escherichia coli* (see also Chapter Five).

The model protein to be utilised was chosen as Bovine Serum Albumin (BSA). BSA is a structurally well-characterised protein of molecular weight approximately 67,000. It has a well-defined structure, consisting of one continuous polypeptide chain which is arranged into nine disulfide double loops. It contains a binding site, principally for copper and nickel, at its N-terminus, as well as a marginally less well characterised binding site for gold, silver, mercury, cadmium, and to some extent copper, at Cys 34, the protein's only free cysteine residue. Anionic binding sites also exist, binding to species including long-chain fatty acids.[186,187]

BSA is also obtainable in relatively pure form, with antioxidants such as thymol removed, and is available cheaply in large quantities, unlike many bacterial proteins. In addition, the formation of radicals on BSA, induced by its reactions with the hydroxyl radical, have been studied in the context of examining degenerative radical processes which have been implicated in a number of diseased states, such as rheumatoid arthritis,

and ischemia reperfusion injury.[17,188] The nature of attack of hydroxyl radicals on BSA is therefore relatively well characterised. This should allow the relative contributions of hydroxyl radical attack on BSA and attack of other radical species, formed following one-electron reduction of peroxyacetic acid, to be assessed.

The work to be described in this Chapter involved the utilisation of several techniques, including EPR spin-trapping. Ancillary techniques to elucidate the sites of protein damage and the relative contributions of the peroxyacetic acid and hydrogen peroxide in the formulations included protease treatment of spin-adducts and catalase treatment of the peroxyacid samples as utilised in Chapter 2. In addition, oxidative stress was analysed by the measurement of carbonyl groups and reduced thiol groups on oxidised protein samples. The concentration of reduced thiol groups, either protein-bound or 'free' in the form of the important antioxidant glutathione is a good the overall oxidative state of a system. Studies on the fragmentation of oxidised protein and analysis of the susceptibility of the oxidised protein to enzymatic digestion were also to be undertaken.

Finally experiments were to be performed with cytochrome c in order to examine if the iron of the heme could react with the peroxyacid to generate radical species.

3.2. EPR SPIN-TRAPPING STUDIES OF THE REACTIONS OF PEROXYACETIC ACID WITH Fe^{2+}-EDTA AND BSA.

Damage to proteins and amino acids induced by the hydroxyl radical has been a topic for considerable research in recent years [reaction (3.1)],[188,189] but little attention has been paid to damage originating from the production of other radical species. Preliminary investigations have been reported on the reactions of proteins with $\cdot CH_3$, $N_3\cdot$ and $\cdot CH(CH_3)OH$.[188,190] However, the reactions of carbonyloxyl radicals have not been studied and only limited information is available regarding the reactions of alkyl radicals derived from them or subsequent radical products such as alkylperoxyl radicals [reactions (3.2) - (3.4)]

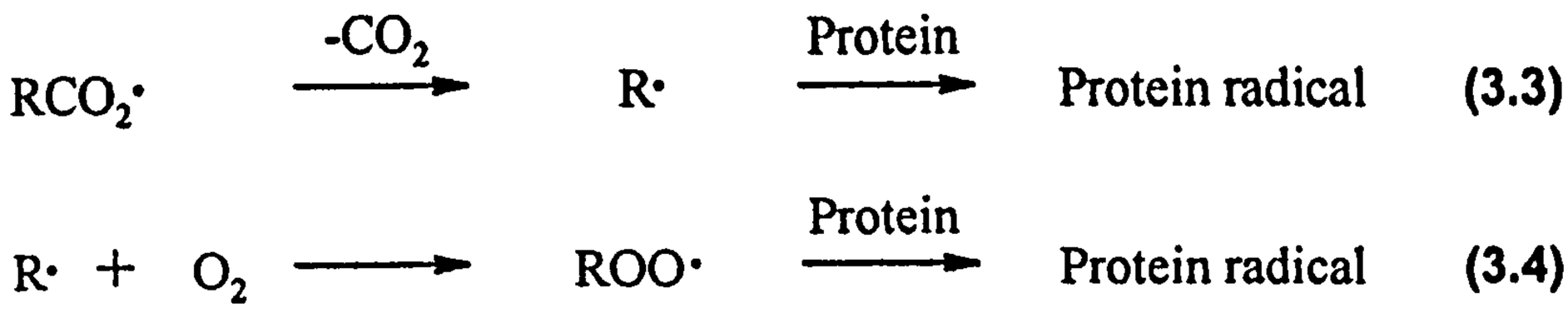

The aim of the work to be described was to analyse the extent and sites of damage on BSA by PAA / Fe^{2+}-EDTA mixtures. Iron was chosen, in preference to titanium for example, because of its biological significance, both in bacterial and mammalian systems. The principal technique employed was EPR spin-trapping because it is a sensitive method, enabling low steady-state radical concentrations to be detected (*eg.* in systems where their generation is slow). It also allows reactions to be performed on a small scale. It was intended to use both nitrone and nitroso spin-traps, since both can be employed to characterise initially formed radicals *e.g.* R·, RO· and macromolecular species. The particular traps chosen were DMPO, because it is water soluble and reacts with both carbon and heteroatom-centred radicals, and DBNBS, again for its water solubility and because it reacts very rapidly with a range of carbon-centred radicals to produce spin-adducts for which the splitting patterns are distinct for primary, secondary and tertiary carbon-centred radicals.[158,166-169]

The role of the cysteine 34 residue was also to be examined using EPR spin-trapping since it has been proposed that it may act as an 'oxidative sink', reducing the level of damage at other sites on the protein.[191,192]

3.2.1. Studies employing DBNBS.

Initial experiments employed mixtures containing of 0.1 M (total AvOx) 5% PAA (0.079 M CH_3CO_3H and 0.021 M in H_2O_2) and 0.002 M Fe^{2+}-EDTA in the presence of 5 $\times 10^{-4}$ M BSA and 0.002 M DBNBS. All reagents, with the exception of the Fe^{2+}-EDTA, were made up in 0.1 M phosphate buffer (pH 7.4) and all reagents were thoroughly purged with a stream of oxygen-free nitrogen. Care was taken to avoid frothing of the protein solution during degassing.

The EPR spectrum of the resulting mixture was very intense and anisotropic ($2a_I$ = 5.98 ± 0.05 mT), indicative of the trapping of a high molecular weight protein-derived radical (Figure 3.1.a).[188,190] The signal was observed to be stable for over sixty minutes after which slow decay was observed. No changes in the spectral features were observed over this time period. The signal was of comparable intensity and was found to have a similar value of $2a_I$ (5.98 ± 0.05 mT as compared to 5.84 ± 0.05 mT for ·OH) to that observed upon reaction of ·OH itself with BSA (see also refs. 188 and 190).

Background experiments, performed in the absence of the peroxyacid or the Fe^{2+}-EDTA produced low concentrations, estimated to be approximately 5% of the signal intensity observed for the reaction mixture containing all the components, of a broad, anisotropic signal ($2a_I$ = 6.22 ± 0.05 mT) attributed to the formation of a nitroxide spin-adduct through a non free-radical mechanism. It is believed that the mechanism for this reaction may be an 'ene' reaction since this is a well characterised reaction between alkenes and nitroso spin-traps [reactions (3.5 and (3.6)] and has been shown to occur between tryptophan residues and nitroso compounds.[141-144]

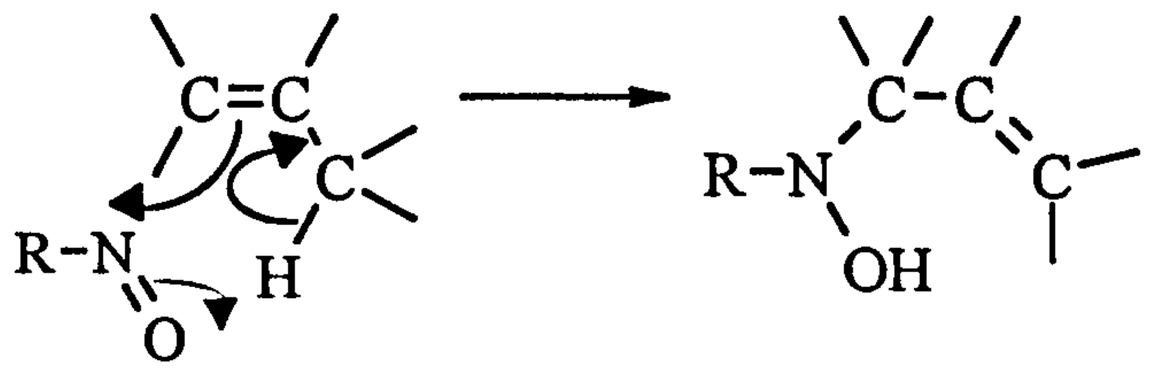

(3.5)

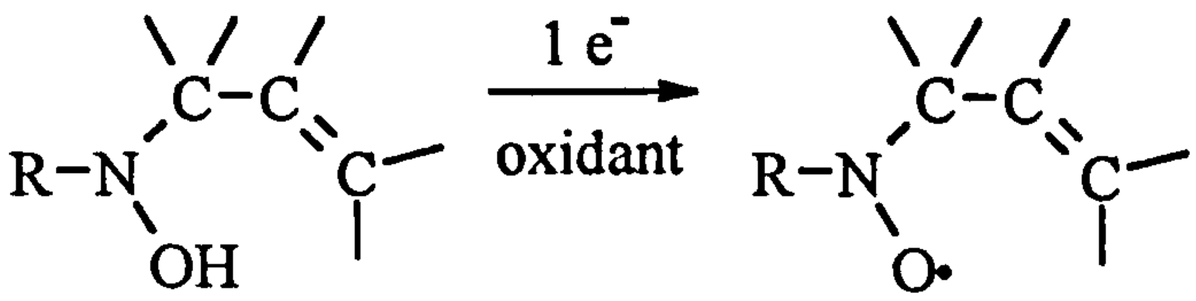

(3.6)

The possibility of the involvement of the 'ene' reaction, either in the system of interest or in the formation of adducts in the absence of one of the reagents, was further investigated by examining the signal produced by a mixture containing 5×10^{-4} M BSA, 0.0025 M DBNBS and 0.05 M potassium ferricyanide. This addition of ferricyanide to BSA and DBNBS facilitates the oxidation of the hydroxylamine product of the 'ene' reaction to a nitroxide spin-adduct. and comparison of the signal obtained with those obtained in other experiments can therefore be made. The EPR spectrum of this mixture was comprised of a weak, very broad, anisotropic signal with $2a_I = 6.25 \pm 0.05$ mT. It is believed, by comparison of the values obtained for $2a_I$ that the signals obtained when BSA reacts with DBNBS either in the absence of PAA or Fe^{2+}-EDTA are due to the 'ene' reaction. The spectrum of the reaction mixture containing BSA, 5% PAA, Fe^{2+}-EDTA and DBNBS was comprised of a signal which had a smaller $2a_I$ and hence it is believed that the signal is generated by genuine radical addition to the trap.

Another mechanism which does not involve direct radical addition to DBNBS has been found to generate BSA spin-adducts. Nucleophilic addition of the free sulfhydryl group of Cys 34 to the spin-trap followed by one-electron oxidation of the hydroxylamine product may occur [reactions (3.7) and (3.8)].[193] This reaction is promoted by the nucleophilicity of the thiol group in BSA, as it has an unusually low pK_a (5.9) for a thiol group and hence is a much better nucleophile than, for example glutathione which has a pK_a of 8.9 and cysteine which has a pK_a of 8.5.[186,187] However, it is unlikely that the signal observed in the absence of Fe^{2+}-EDTA or 5% PAA was attributable to this reaction since it does not resemble the characteristic signal of a thiyl spin-adduct which would be expected to be seen at slightly higher field and have a smaller $2a_I$.[193]

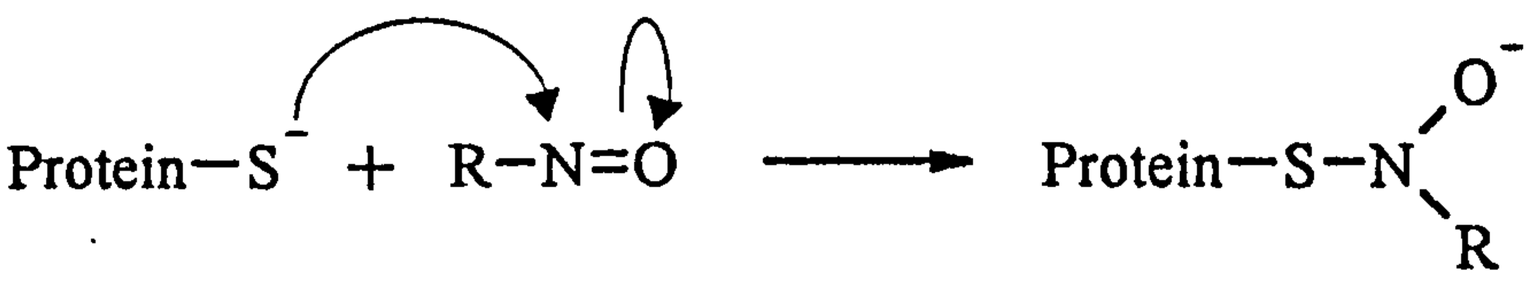

$$\text{Protein}-\text{S} + \text{R}-\text{N}=\text{O} \longrightarrow \text{Protein}-\text{S}-\text{N}(\text{O}^-)(\text{R}) \quad (3.7)$$

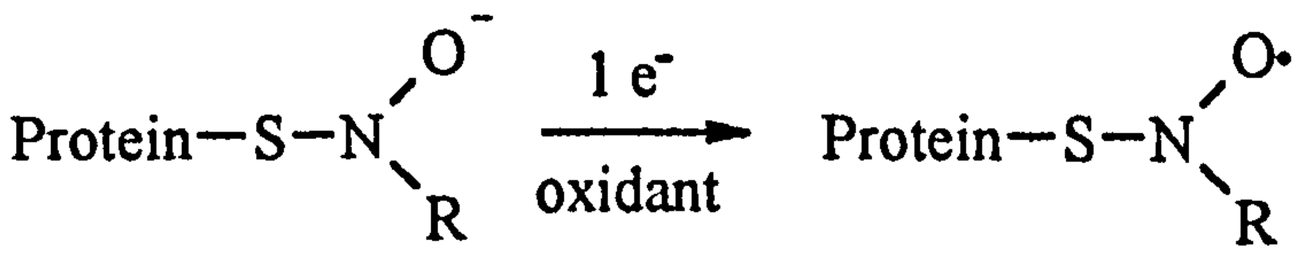

$$\text{Protein}-\text{S}-\text{N}(\text{O}^-)(\text{R}) \xrightarrow[\text{oxidant}]{1\ e^-} \text{Protein}-\text{S}-\text{N}(\text{O}\cdot)(\text{R}) \quad (3.8)$$

This experiment was next repeated employing 40% PAA at the same total AvOx (0.078 M CH_3CO_3H and 0.022 M H_2O_2). Again, a broad, anisotropic signal was observed ($2a_t = 5.98 \pm 0.05$ mT) indicating the formation of a high molecular weight protein spin-adduct.[188,190] The signal intensity was lower than that observed in the corresponding experiment with 5% PAA (Figure 2.1.b): this supports the importance of hydroxyl radicals generated from hydrogen peroxide in the generation of protein free-radicals. However, the appearance of a signal in the absence of high concentrations of hydrogen peroxide also suggests that radicals derived from peroxyacetic acid itself do play a role in the generation of protein radicals. Control experiments in the absence of Fe^{2+}-EDTA produced a very weak, very broad EPR signal ($2a_t = 6.22 \pm 0.05$ mT) again suggesting that a low concentration of nitroxide was generated by the 'ene' reaction, but that this was not significant in the system of interest.[141-144]

The nature of these spectra implies that identification of the site(s) of attack on the protein could not be made, as hyperfine coupling constants could not be determined. It was therefore decided to treat the spin-adducts with a non-specific protease, Pronase E, in order to examine further the nature of radical attack on BSA by PAA.[188,190] The spin-adducts were treated with protease (final concentration = 15 units ml^{-1}) for 30 min after which EPR spectra of the mixtures were recorded again. Protease treatment of the spin-adduct generated by the attack of Fe^{2+}-EDTA / 5% PAA on BSA resulted in an EPR spectrum (Figure 3.2.a) which consists of two signals, the major one, accounting for approximately 90% of the radical concentration, being a triplet ($a_N = 1.37 \pm 0.01$ mT) and the minor one being a doublet of triplets ($a_N = 1.42 \pm 0.01$ mT, $a_{\beta\text{-}H} = 0.80 \pm 0.01$ mT).[158,166-169] These signals are assigned to the trapping of a mixture of tertiary carbon-centred radicals and secondary carbon-centre radicals, respectively. It is believed that the tertiary carbon-centred radicals are largely a result of backbone attack [reaction (3.10)] on the protein (although attack of some amino acid side-chains such as isoleucine could lead to the generation of tertiary carbon-centred radicals) and the secondary carbon-centred radicals are formed as a result of side-chain attack [reaction (3.11)]. This result is similar to that observed in corresponding experiments with hydrogen peroxide and Fe^{2+}-EDTA, indicating the importance of the hydroxyl radical to radical generation on BSA by

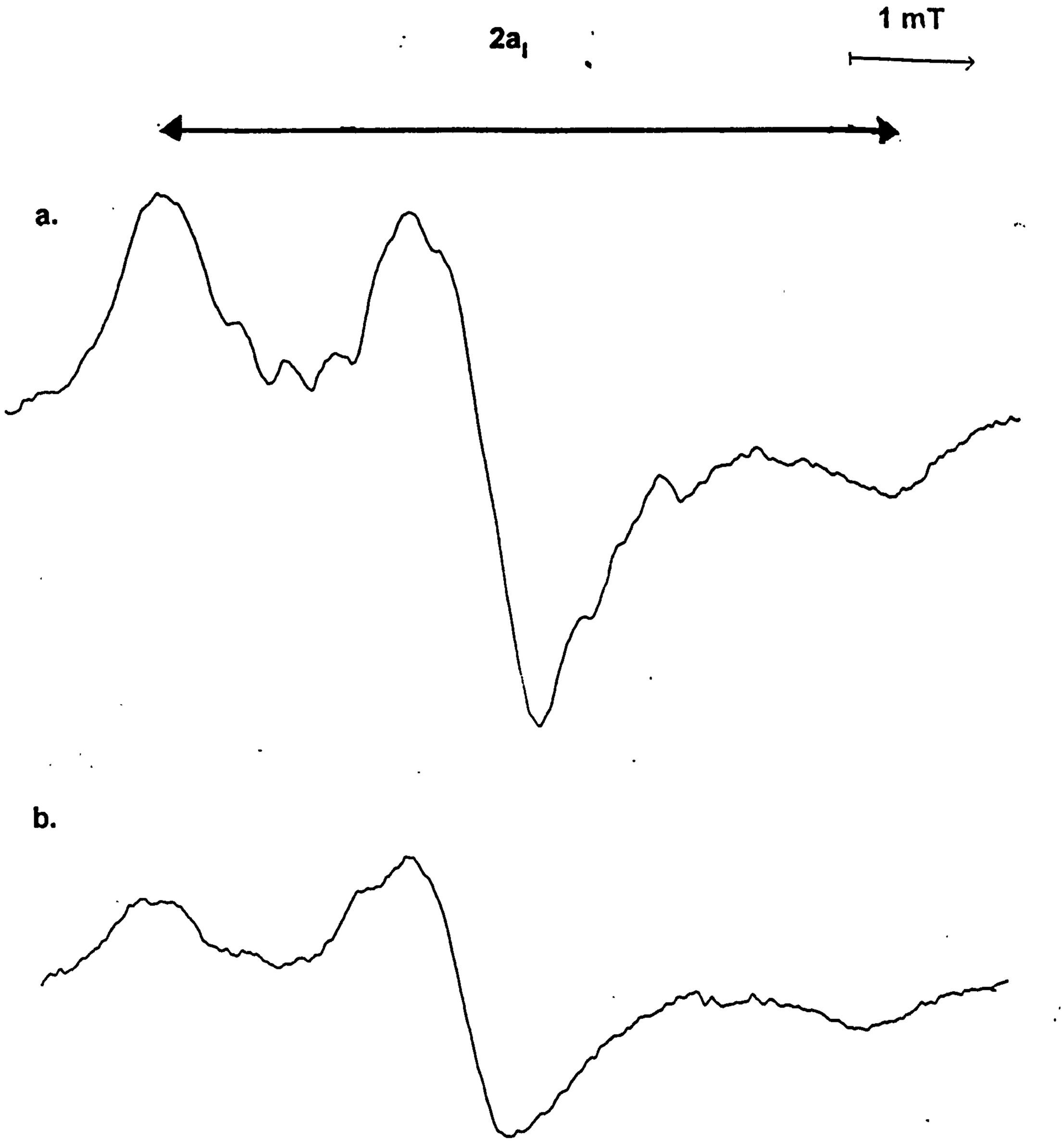

Figure 3.1.a. EPR spectrum showing a high yield of high molecular weight protein spin-adducts generated by the reaction between BSA, Fe^{2+}-EDTA, 5% PAA and DBNBS.

Figure 3.1.b. EPR spectrum showing a lower yield of high molecular weight protein spin-adducts generated with 40% PAA.

Concentrations employed:- BSA, 5×10^{-4} M, Fe^{2+}-EDTA, 0.002 M, PAA, 0.1 M (total AvOx) and DBNBS, 0.0025 M.

5% PAA.[188,190] This implies that the hydrogen peroxide is the component of the PAA formulation which is causing the majority of the damage, since it has already been shown in the previous Chapter that peroxyacetic acid does not react with Fe^{2+}-EDTA to produce hydroxyl radicals.

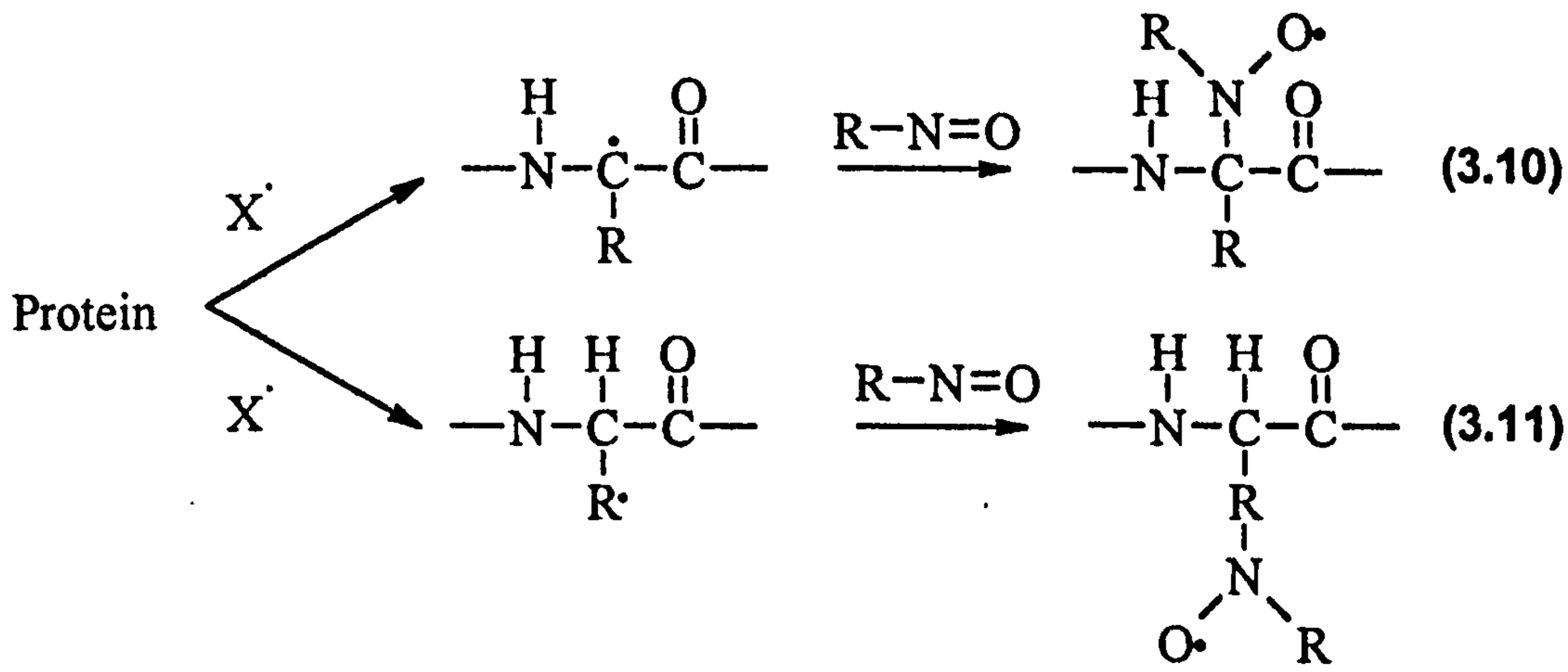

In contrast, when the spin-adduct generated by the reaction of BSA with Fe^{2+}-EDTA / 40% PAA and DBNBS was subjected to protease treatment no change was observed in the EPR spectrum after 30 min incubation (Figure 3.2.b). Increasing the length of time for which the spin-adduct was exposed to protease to sixty minutes had no effect and increasing the incubation time beyond 60 min only resulted in the gradual decay of the signal, as was observed in the absence of the protease.

It was believed there may be several explanations for the difference in observed behaviour between spin-adducts generated in the 5% PAA and 40% PAA systems. 40% PAA is known to be more damaging to cells than 5% PAA at the equivalent AvOx,[1] and although proteins have not been identified as a particular target for oxidation by PAA formulations, it is possible that the 40% PAA is damaging the protease as well as the BSA and therefore inactivating it. A second possibility is that the main attacking species is different in the reactions in which the peroxygen employed is 40% PAA: the primary attacking species may be the acetoxyl radical, the methyl radical or the methylperoxyl radical [see reactions (3.2) - (3.4)] as opposed to the hydroxyl radical [see reaction (3.1)]. In this case, the site(s) of attack would be expected to be more specific than the sites of attack by the hydroxyl radical, in which case the radicals may be formed at a site distant

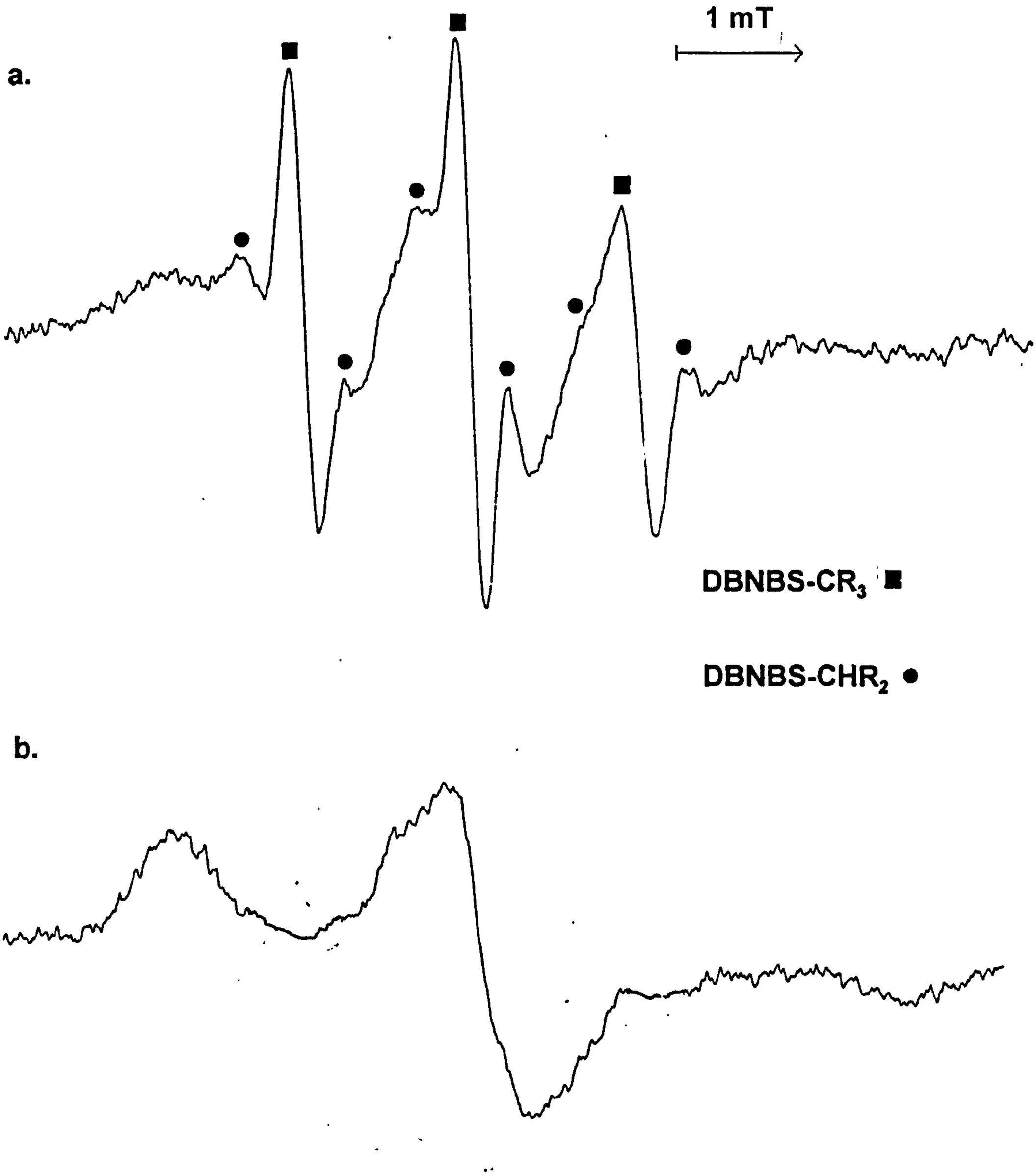

Figure 3.2.a. EPR spectrum showing a mixture of secondary and tertiary carbon-centred adducts generated by treatment of the reaction mixture containing BSA, Fe^{2+}-EDTA, 5% PAA and DBNBS with protease after 30 min.

Figure 3.2.b. EPR spectrum showing the undigested protein spin-adduct(s) generated with 40% PAA.

Concentrations employed:- BSA, 5×10^{-4} M, Fe^{2+}-EDTA, 0.002 M, PAA, 0.1 M (total AvOx) and DBNBS, 0.0025 M.

from the site of protease action.

It was decided to utilise size exclusion chromatography to investigate the role of peroxyacetic acid further. Sephadex PD10 - G25 size exclusion columns were employed. These facilitate the removal of any species with a molecular weight less than 12000 and would therefore be expected to remove any excess peroxyacetic acid as well as any excess DBNBS, Fe^{2+}-EDTA, hydrogen peroxide and small protein fragments from spin-adduct samples. A 0.5 ml sample of the reaction mixture containing BSA, DBNBS, Fe^{2+}-EDTA and 40% PAA was passed through the column which had been equilibrated with 0.1 M phosphate buffer (pH 7.4). 1 ml fractions were collected and by recording the EPR spectrum of each fraction and the use of Coomassie Blue protein binding dye it was found that the bulk of the protein eluted in fractions three and four. These fractions were combined and treated with protease (15 units ml^{-1}). After 30 minutes the spectrum of the reaction mixture was recorded and was found to display a mixture of a tertiary carbon-centred adduct and a secondary carbon-centred adduct, as was observed for the corresponding reaction mixture containing 5% PAA, thus indicating a mixture of backbone and side-chain attack had occurred, although the ratio of spin-adducts showed a higher relative concentration of the tertiary carbon-centred radical, and hence backbone attack. It may therefore be concluded that peroxyacetic acid was also attacking, and therefore inactivating the protease.

It is possible that the low molecular-weight species generated after protease treatment of the spin-adducts formed upon treatment of BSA with 5% PAA oxidising mixtures were spin-adducts of damaged protease. It is also possible that the protease had been prevented from *fully* digesting the BSA by damage caused by the oxidising mixture. After passing the mixture down a size exclusion column and protease treatment for thirty minutes the EPR spectrum was observed to be identical to that observed without removal of the oxidising species, indicating that the protease had not been affected by 5% PAA.

The role of peroxyacetic acid was further investigated by employing catalase treatment of the peroxyacetic acid samples before adding them to the reaction mixture as was employed in Chapter 2. On adding catalase-treated 5% PAA (total AvOx 0.1 M prior to catalase treatment) to a reaction mixture containing BSA, Fe^{2+}-EDTA and DBNBS an

anisotropic EPR signal was observed as previously. The notable difference in the spectrum was that the signal intensity was greatly reduced, reflecting the importance of hydrogen peroxide in the formulation, and therefore hydroxyl radical attack, on protein damage. In contrast, when the peroxygen employed was 40% PAA there was little discernible effect on the EPR spectrum when compared to that obtained in the presence of hydrogen peroxide, a reflection of the low concentration of hydrogen peroxide in the reaction mixture and hence the minor role of the hydroxyl radical.

The effect of protease on the spin-adducts of BSA generated by the reactions of catalase-treated PAA samples was next explored to examine if any differences in selectivity could be discerned between hydroxyl radical attack and attack by peroxyacetic acid derived radicals. Protease digestion of the spin-adduct formed on reaction of BSA with catalase treated 5% PAA, Fe^{2+}-EDTA and DBNBS resulted in the appearance of s spectrum comprising of a triplet (a_N= 1.37 ± 0.01 mT) and a triplet of doublets (a_N= 1.42 ± 0.01 mT, $a_{\beta\text{-}H}$ = 0.80 ± 0.01 mT)[158,166-169] as observed previously in experiments where the PAA had not been subjected to catalase treatment. However, the ratio of tertiary carbon-centred radicals to secondary carbon-centred radicals had *increased* when compared to the spectrum of the reaction mixture containing untreated 5% PAA, indicating a relative increase in backbone attack. On treatment of spin-adducts produced on reaction of BSA with catalase treated 40% PAA, Fe^{2+}-EDTA and DBNBS no release of small peptide fragments was observed. Again, this is believed to be a result of protease inactivation by excess peroxyacetic acid and hence the experiment was repeated after passage of the protein solution through a size exclusion column. After thirty minutes exposure to protease, the EPR spectrum of the reaction mixture displayed a mixture of a triplet and doublet of triplets as described previously, although as noted above a slight difference in the ratio of backbone to side-chain attack was observed.

From the results described above it is apparent that although hydroxyl radicals derived from hydrogen peroxide [reaction (3.1)] lead to the formation of radical species on BSA, radicals formed upon one-electron reduction of peroxyacetic acid also cause damage. It is unlikely that the attacking species is the acetoxyl radical, since it decarboxylates rapidly, hence this possibility was not investigated further. Although

methyl radicals are relatively unreactive in hydrogen-atom abstraction reactions or addition to double bonds when compared to the hydroxyl radical it is possible that methyl radicals lead to the formation of protein-derived radicals. In order to investigate the extent and nature of protein damage induced by methyl radicals the reaction of hydroxyl radicals with dimethyl sulfoxide was employed [reaction (3.12)].

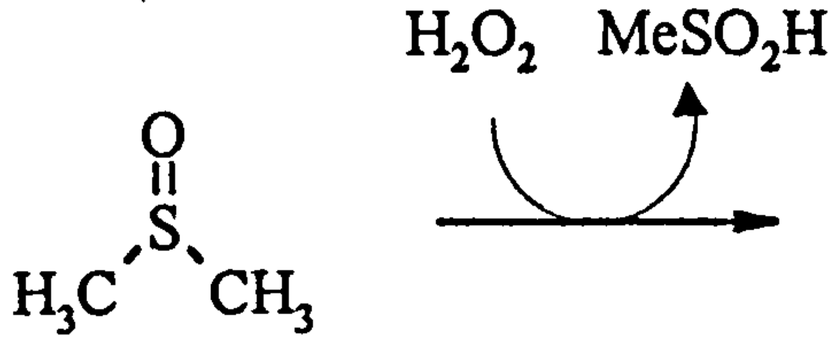

(3.12)

Experiments employed reaction mixtures containing 5×10^{-4} M BSA, 0.002 M Fe^{2+}-EDTA, 0.1 M hydrogen peroxide, 10% by volume (approximately 1 M) DMSO and 0.0025 M DBNBS. The EPR spectrum of this reaction mixture comprised of a signal corresponding to DBNBS-CH_3 ($a_N = 1.40 \pm 0.01$ mT, $a_{3\beta\text{-}H} = 1.40 \pm 0.01$ mT).[158,166-169] This indicates that the reaction solely of methyl radicals with BSA is not sufficiently fast to generate a detectable concentration of protein-centred radicals. In turn, this implies that the reactive species derived from peroxyacetic acid which leads to the formation of radicals on BSA may be the methylperoxyl radical, or possibly the acetylperoxyl or acetyl radicals generated by the reaction of Fe^{3+} with the peroxyacid [reactions (3.13) and (3.14)], which would not be trapped in this system since DBNBS does not trap oxygen-centred radicals very effectively.

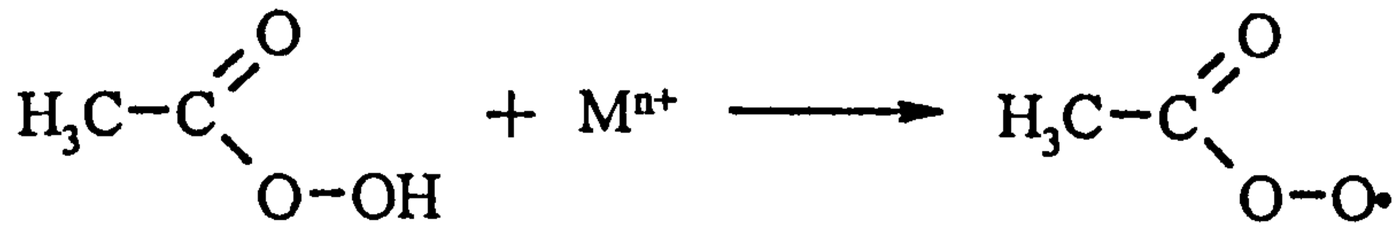

(3.13)

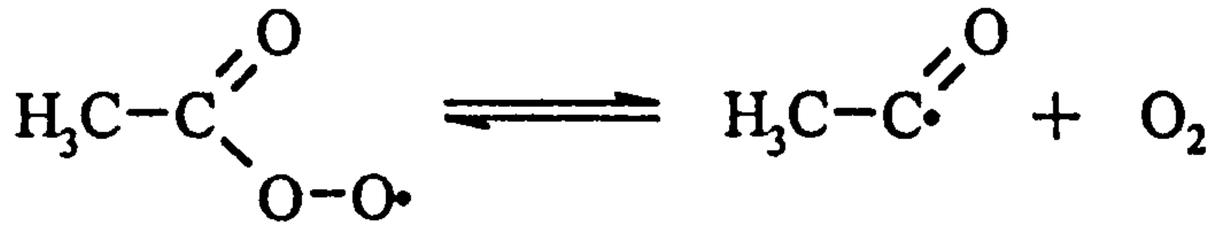

(3.14)

3.2.2. Studies employing DMPO.

It was next decided to investigate the reactions of BSA with Fe^{2+}-EDTA and PAA employing the nitrone spin-trap, DMPO. Initial experiments utilised mixtures including 5×10^{-4} M BSA, 0.002 M Fe^{2+}-EDTA, 0.1 M (total AvOx) 5% PAA and 0.01 M DMPO. The EPR spectrum of this reaction mixture consisted of a four-line signal characteristic of DMPO-OH only (Figure 3.3.a).[158] There was no evidence for the formation of high molecular weight protein-centred radicals or methyl radicals (although this was not unexpected on the basis of experiments described earlier in this Thesis). It was apparent that the hydroxyl radicals were being trapped before they could attack the protein. The experiment was therefore repeated with 0.002 M DMPO in an attempt to trap protein-derived radicals. The EPR spectrum of the mixture consisted of a very weak, anisotropic signal corresponding to a high molecular weight protein spin-adduct [188,190] and an isotropic element, also very weak, corresponding to DMPO-OH (Figure 3.3.b).[158] The spin-adducts were observed to be less long-lived than those formed with DBNBS, decaying beyond the detectable limit within approximately twenty minutes. As a result of this when protease treatment of the mixture was attempted the signal was found to decay before any small peptide fragments were released. Similar experiments were conducted on the reaction system containing 40% PAA. At high concentrations of DMPO, only signals due to DMPO-OH ($a_N = a_{\beta\text{-}H} = 1.49 \pm 0.01$ mT) and DMPO-CH_3 ($a_N = 1.64 \pm 0.01$ mT and $a_{\beta\text{-}H} = 2.34 \pm 0.01$ mT) were observed.[158] At lower concentrations of DMPO (0.002 M) no signals were seen whereas raising the concentration again to 0.004 M only caused the re-emergence of the isotropic DMPO-OH and DMPO-CH_3 signals.

It was next decided to investigate the role of the Cys 34 residue in damage to BSA produced by Fe^{2+}-EDTA / PAA oxidising systems. EPR spin-trapping was again employed to explore this.

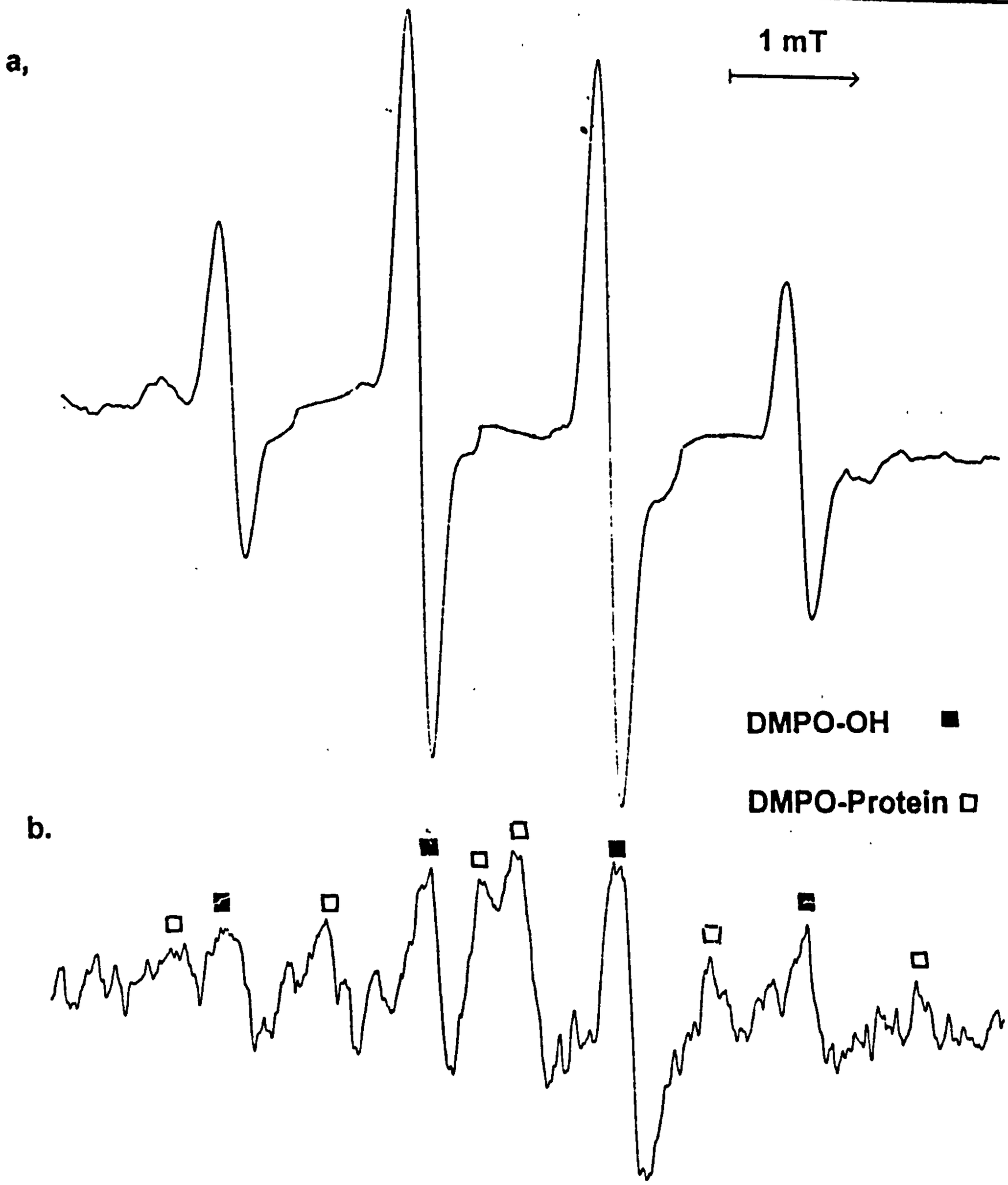

Figure 3.3.a. EPR spectrum showing a signal attributed to DMPO-OH, generated by the reaction of BSA with Fe^{2+}-EDTA, 5% PAA and 0.01 M DMPO.

Figure 3.3.b. EPR spectrum showing a signal attributed to DMPO-OH and a signal attributed to a high molecular weight protein radical generated with 0.002 M DMPO.

Concentrations employed:- BSA, 5×10^{-4} M, Fe^{2+}-EDTA, 0.002 M, PAA, 0.1 M (total AvOx), DMPO, as stated.

3.2.3. Examination of the role of the Cys-34 residue.

It has been suggested previously that the free sulfhydryl groups located on cysteine residues act as an 'oxidative sink' for damage to proteins in that when the protein is placed under oxidative stress, initial radical damage will be relocated via an electron-transfer mechanism to cysteine (tyrosine and tryptophan) residues.[194,195] It is also known that, especially under anoxic conditions, the formation of protein aggregates through disulfide bonds is indicative of oxidative stress.[194-196] It was therefore decided to examine the role of the Cys 34 residue in the reactions of BSA with PAA / Fe^{2+}-EDTA by experiments which involved blocking the residue with N-ethylmalemide (NEM) [reaction (3.15)].[197]

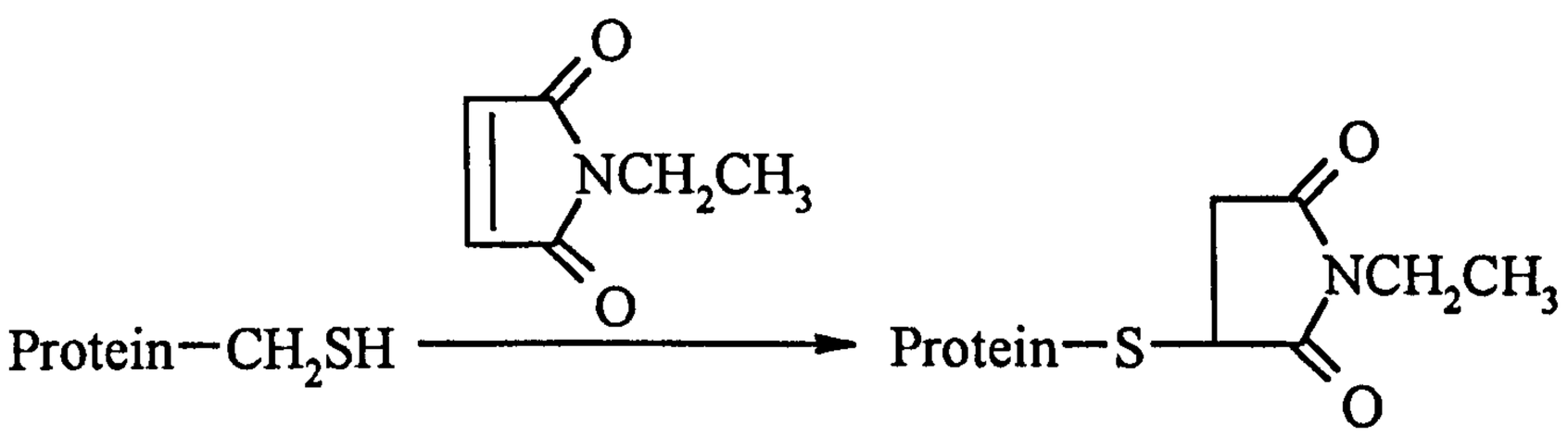

(3.15)

On reaction of 5×10^{-4} M thiol-blocked BSA with 0,1 M (total AvOx) 5% PAA, 0.002 M Fe^{2+}-EDTA and 0.0025 M DBNBS an EPR spectrum was observed comprising of a mixture of isotropic and anisotropic elements (Figure 3.4.a) which is markedly different to the spectrum observed for the native protein (see Figure 3.1.a) and very similar to that observed for the attack of ·OH on thiol-blocked BSA.[197] The isotropic elements of the spectrum are believed to correspond to DBNBS-CH_3[158,166-169] formed from the decomposition of the peroxyacetic acid and a mixture of secondary and tertiary carbon-centred radical adducts, similar to those formed on protease digestion of the spin-adducts formed by attack of 5% PAA / Fe^{2+}-EDTA on the native protein. It is believed that the appearance of these isotropic elements in the spectrum is indicative of protein fragmentation and / or denaturation, occurring due to the lack of the thiol group to act as an 'oxidative sink'. It is not believed that blocking the cysteine residue has led to the transfer of radical damage to other parts of the protein which have more local mobility, since the nature of radical attack (which is mainly hydroxyl radical attack for 5% PAA)

is probably random. It is also of significance that although the *total* radical concentration is similar to that observed in experiments with the native protein, the concentration of the anisotropic element is much *lower* than that observed with the native protein indicating that the formation of this species is dependent on the involvement of the thiol group.

Protease digestion of was performed in order to assign the site(s) of protein damage. In accord with the observations made above concerning the fragmentation / denaturation of the protein, protease treatment was effective over a shorter timescale than for the native BSA spin-adducts, typically ten minutes as opposed to thirty minutes. The spectrum of the protease-treated sample revealed a mixture of secondary and tertiary carbon-centred spin-adducts, as observed previously and as part of the signal in the untreated samples, indicating the formation of both side-chain and backbone radicals.

Catalase treatment of 5% PAA resulted in an EPR spectrum which consisted of a signal corresponding to DBNBS-CH_3 only.[158,166-169] This is in contrast to experiments carried out on reaction mixtures containing native BSA and catalase treated 5% PAA in which a protein-radical was observed. This implies that the reaction of hydroxyl radicals are crucial to the formation of protein radicals in the absence of a free thiol group.

The role of heterocentred radicals on the protein was next investigated employing the nitrone spin-trap, DMPO. This was employed at a concentration of 0.002 M since it has already been demonstrated that higher concentrations result in the trapping of peroxygen, not protein-derived, radicals. However, even at this concentration, reaction of thiol -blocked BSA with Fe^{2+}-EDTA and 5% PAA produced a spectrum consisting of only an isotropic elements, corresponding to the adduct DMPO-OH ($a_N = a_{\beta\text{-}H} = 1.49 \pm 0.01$ mT)[158]

When the reactions of thiol-blocked BSA with 40% PAA were examined in the presence of DBNBS the EPR spectrum consisted only of DBNBS-CH_3, in contrast to experiments on native BSA. This indicates the role of the thiol group is crucial in radical damage to BSA induced by peroxyacetic acid. When DMPO was employed (final concentration = 0.002 M) no spin-adducts were observed in concordance with results obtained with native BSA.

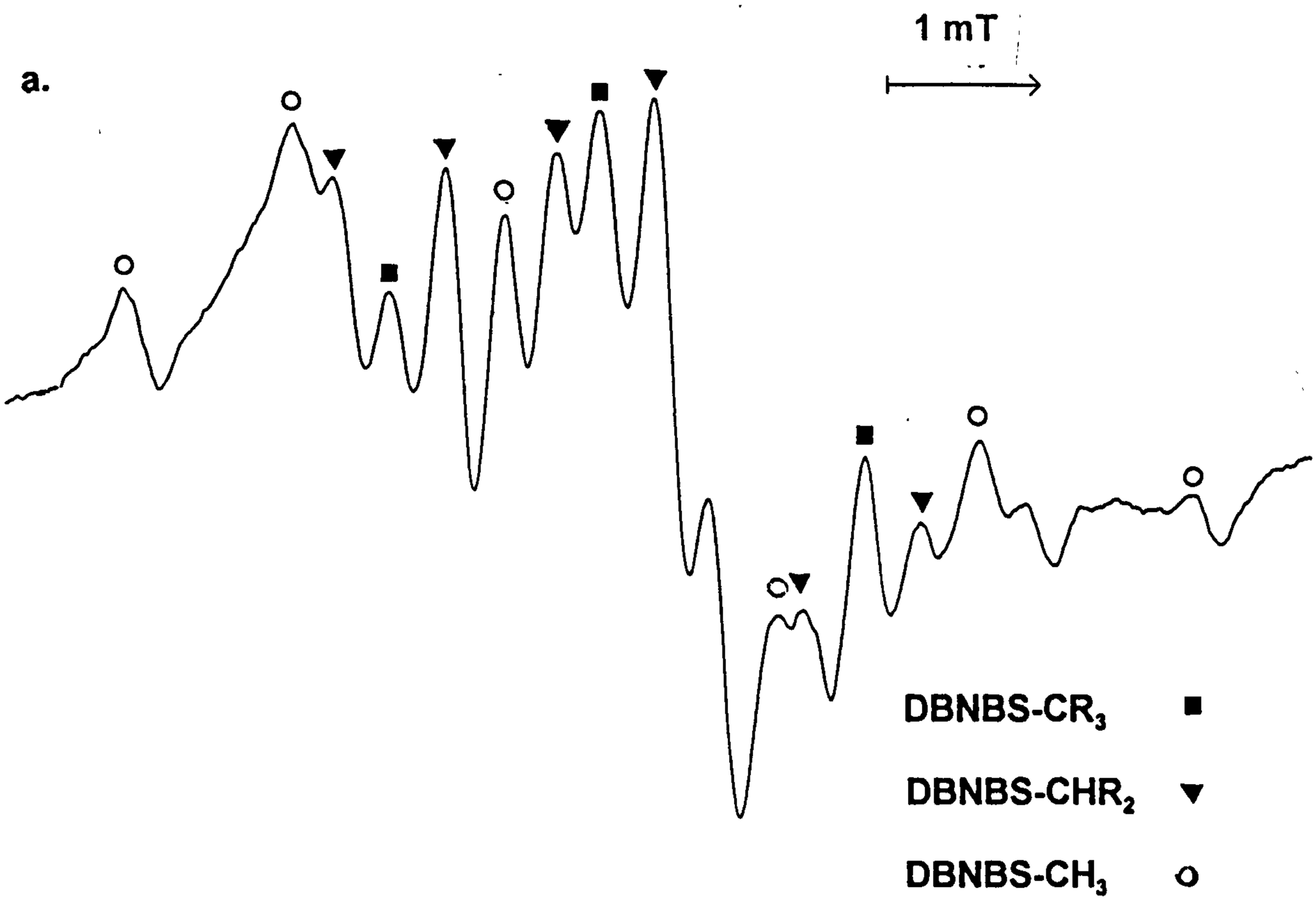

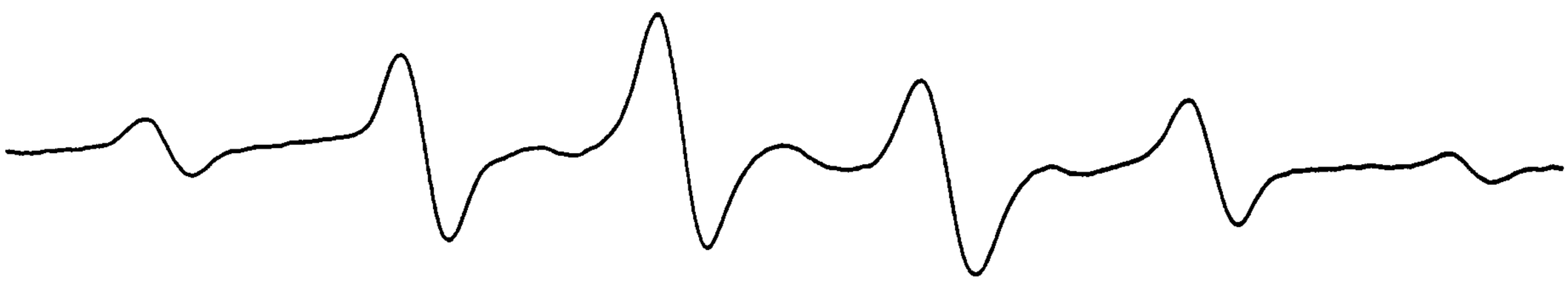

Figure 3.4.a. EPR spectrum showing an anisotropic signal attributed to a high molecular weight protein spin-adduct and isotropic signals assigned to DBNBS-CH_3 and DBNBS spin-adducts of secondary and tertiary carbon-centred protein radicals generated by the reaction of thiol- blocked BSA with Fe^{2+}-EDTA, 5% PAA and DBNBS.

Figure 3.4.b. EPR spectrum showing a signal attributed to DBNBS-CH_3, generated with 40% PAA.

Concentrations employed:- thiol blocked BSA, 5×10^{-4} M, Fe^{2+}-EDTA, 0.002 M, PAA, 0.1 M (total AvOx) and DBNBS, 0.0025 M.

3.2.4. Discussion.

It has been demonstrated that attack on BSA by PAA and Fe^{2+}-EDTA is largely a result of attack by hydroxyl radicals from hydrogen peroxide, the signal amplitude being approximately proportional to the concentration of hydrogen peroxide in the formulation. However, as was illustrated in experiments performed in the absence of hydrogen peroxide, peroxyacetic acid itself does play a role in the generation of protein-radicals. The radical species has not been identified, but it is not believed to be the acetoxyl radical, since this decarboxylates so rapidly, and it has been shown that under the conditions used it is unlikely to be the methyl radical. The attack, either by hydroxyl radicals or radical species derived from peroxyacetic acid has been shown to be random. Blocking the Cys 34 residue in BSA gave rise to spectra which contained isotropic elements. It is believed that the behaviour observed is a reflection, at least in part, of the denaturing effect of blocking the thiol group.

3.3. EPR STUDIES OF THE REACTIONS OF PAA WITH BSA IN THE PRESENCE OF Cu^{+} (OBTAINED FROM THE REACTION OF Cu^{2+} WITH L-ASCORBIC ACID).

It was next decided to investigate the reactions of Cu^{+} (generated by the reaction of Cu^{2+} with L-ascorbic acid) with BSA and PAA. Cu^{2+} ions in conjunction with L-ascorbic acid are known to generate a copper (I) species which may be reoxidised by hydrogen peroxide and other peroxides in a mechanism involving the formation of radical intermediates. It has also been demonstrated in the previous Chapter that the reaction of peroxyacetic acid with Cu^{2+} / L-ascorbic acid either occurs much more slowly than that with hydrogen peroxide (or primarily by a mechanism not involving free radicals). It was therefore decided to examine how the rate of radical generation and / or the overall radical yield from the PAA / metal system would affect the extent and nature of damage to BSA.

In addition, BSA has a binding site for Cu^{2+} ions at its N-terminus and a marginally less significant and well characterised binding site in the crevice containing the Cys 34

residue.[186,187] Hence, this provided an opportunity to examine how chelation of the metal ion would affect the magnitude and character of protein oxidation.

3.3.1. Spin-trapping studies.

Reaction of 0.004 M L-ascorbic acid and 0.002 M Cu^{2+} [as $CuSO_4 \cdot 5H_2O$ (aq)], (pre-mixed) with 5×10^{-4} M BSA, 0.0025 M DBNBS and 0.1 M (total AvOx) 5% PAA was examined. The EPR spectrum of this reaction mixture comprised an intense, broad, anisotropic signal ($2a_t = 5.80 \pm 0.05$ mT) which was dependent upon the presence of all the reactants and was unchanged over approximately sixty minutes after which slow decay was observed. It is believed that the intensity of the signal, which was approximately twice as intense as the corresponding spectrum for the reaction utilising Fe^{2+}-EDTA, possibly reflects the continual regeneration of Cu^{+} by reaction of Cu^{2+} with L-ascorbic acid. On protease treatment of the sample a triplet corresponding to protein backbone carbon spin-adducts was observed as was a low concentration of secondary carbon-centred adducts. Pre-treatment of the PAA with catalase led to some loss of signal intensity indicating that the peroxyacetic acid was producing radical species which were attacking the protein. A broad, anisotropic signal of much lower concentration was observed in the absence of the peroxygen or the Cu^{2+} / L-ascorbic acid and is believed to result from the 'ene' reaction (see section 3.2.1).

In corresponding experiments employing 40% PAA, a characteristic protein spin-adduct signal was observed. In contrast to the experiments performed on the reaction system in which Fe^{2+}-EDTA was employed as a one-electron reductant there was little discrepancy between the signal intensity observed in the spectra of the 5% PAA and 40% PAA oxidising mixtures. Catalase treatment again brought about slight signal reduction and protease treatment (after passage through a size exclusion column) produced a mixture of backbone and side-chain peptide spin adducts.

Additional studies, performed using DMPO (0.002 M) led to no detection of radical species.

3.3.2. Cu^{2+} EPR studies.

It was decided to investigate the nature of the copper species formed upon reaction of BSA with Cu^{2+} in order to examine if binding had occurred under the conditions used. Reaction mixtures containing 5×10^{-4} M BSA with equimolar Cu^{2+}(aq) were prepared and the copper EPR spectrum recorded and compared to that of Cu^{2+}(aq). It can be seen from the shift in *g*-value and the distortion in signal shape that binding occurs forming a completely different Cu^{2+} species (see Figure 3.5.a and 3.5.b).

3.3.3. Discussion.

The results described above indicate that Cu^{2+} / L-ascorbic acid (*i.e.* Cu^{+}) react with peroxygens in the presence of BSA to produce more protein damage that was observed with Fe^{2+}-EDTA. This is surprising since the reaction between Cu^{+} generated in this way and peroxyacetic acid was found to be either much slower than that observed the hydrogen peroxide in the reaction mixtures or occur via a mechanism not involving free radicals. It is believed that the increased yield of protein radicals may be a result of the continual regeneration of Cu^{+} by the reaction of Cu^{2+} with L-ascorbic acid followed by reoxidation by the excess hydrogen peroxide (or peroxyacetic acid).

It has also been demonstrated that the random nature of protein attack, producing mainly backbone radicals and a lower concentration of side-chain radicals, observed in the reactions with Fe^{2+}-EDTA is reproduced. The Cu^{2+} EPR spectra show that binding of (some of) the Cu^{2+} occurs to BSA but that this does not render it redox inert.

3.4. EPR STUDIES ON THE REACTIONS OF Cu^{2+} AND PAA WITH BSA.

It was next decided to investigate the redox activity of Cu^{2+} with BSA in the absence of an exogeneous reducing agent. On mixing BSA with Cu^{2+} (aq). 5% PAA and DBNBS the EPR spectrum of the resulting mixture was observed to consist of a typically broad protein spin-adduct ($2a_I = 5.95 \pm 0.05$ mT). The intensity of this signal was observed

a.

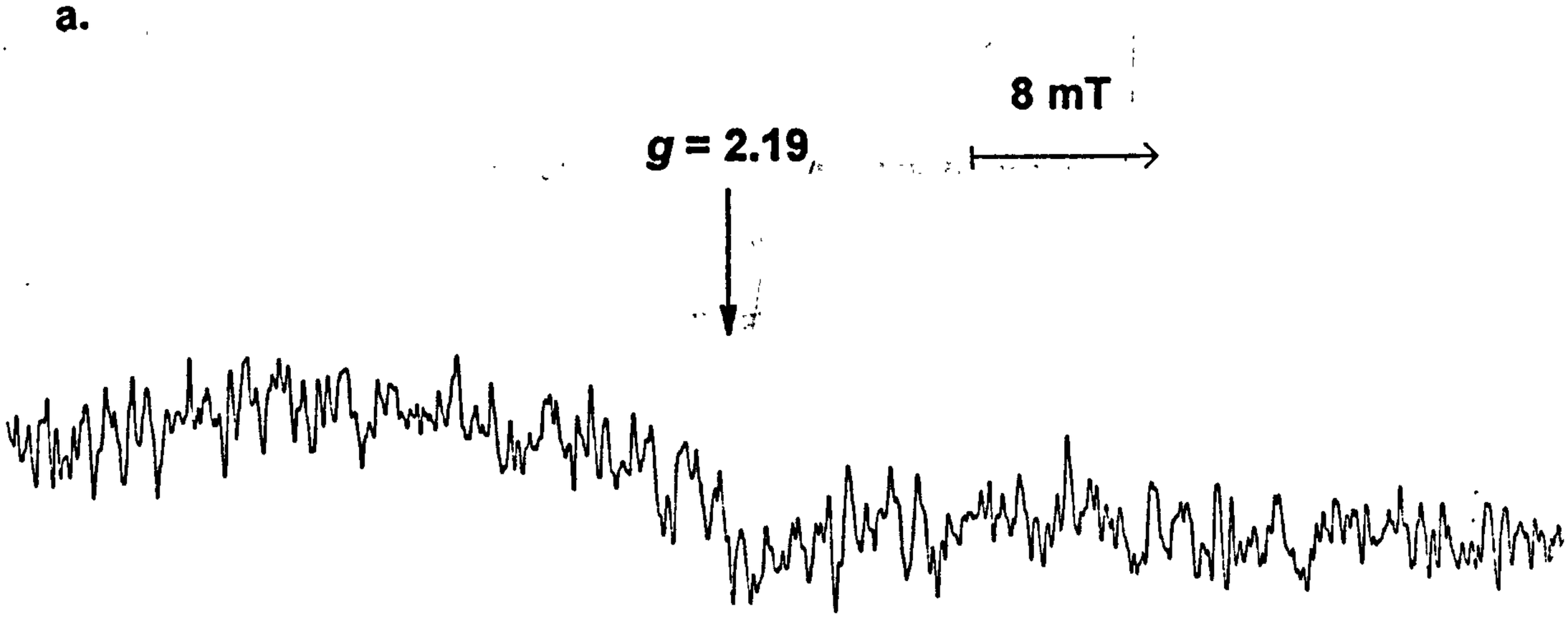

b.

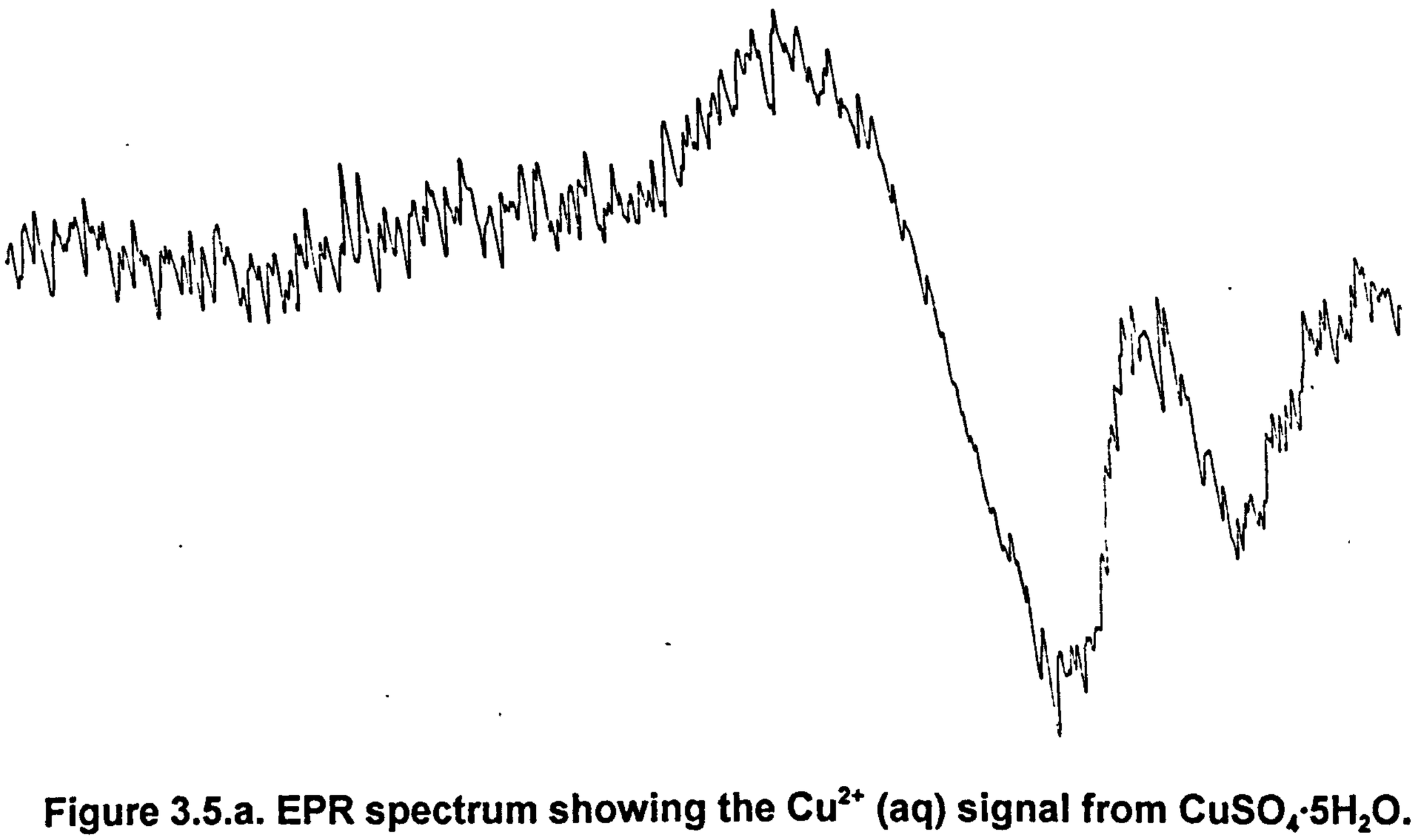

Figure 3.5.a. EPR spectrum showing the Cu^{2+} (aq) signal from $CuSO_4 \cdot 5H_2O$.

Figure 3.5.b. EPR spectrum showing *g*-shift and distortion of the Cu^{2+} (aq) signal by addition of BSA.

Concentrations employed:- BSA, 5×10^{-4} M, Cu^{2+} (aq), 5×10^{-4} M.

to be less intense than those observed in the presence of an exogenous reductant, but still more intense than those observed when Fe^{2+}-EDTA was employed. The signal was observed to be unchanged, both in intensity and in shape, over approximately one hour after which slow decay of the spin-adduct was observed. Catalase pre-treatment of the peroxyacid resulted in extensive reduction of signal intensity, as would be anticipated, but did not lead to a complete loss of signal. Incubation of the reaction mixture with a non-specific protease for thirty minutes resulted in the formation of small backbone and side-chain DBNBS spin-adducts, the backbone spin-adducts predominating. A broad, anisotropic signal of greatly reduced intensity was seen in the absence of either the peroxygen or the copper: this is assumed to be as a result of the 'ene' reaction (see section 3.2.1) since $2a_t = 6.25 \pm 0.05$ mT.

In analogous experiments in which 40% PAA was employed as an oxidant similar observations were made. This is in contrast to experiments in which Fe^{2+}-EDTA was employed for which the signal intensity was markedly greater when the oxidant employed was 5% PAA. Catalase treatment resulted in signal reduction which was approximately proportional to the concentration of hydrogen peroxide in the reaction mixture, while protease treatment resulted in the generation of small peptide spin-adducts corresponding to a mixture of backbone and side-chain protein attack.

EPR spin-trapping studies of these reactions in the presence of DMPO (0.002 M) were unsuccessful, concentrations of spin-adducts being sufficiently low that paramagnetic broadening due to Cu^{2+} became problematic when recording the spectra.

It is believed that radical generation may be the result of reduction of the Cu^{2+}(aq) by the free cysteine residue of BSA and subsequent reoxidation by PAA to form radicals. This was explored by conducting a series of experiments with thiol-blocked BSA [see reaction (3.15)], though very similar results were obtained, indicating that the thiol group is not involved in the generation of an active copper species.

Thus Cu^{2+}, with peroxygen compounds, has been shown to produce radicals on BSA. The mechanism of this reaction is unknown, but it has been demonstrated that interaction with Cys 34 is not significant. It is believed that reaction of Cu^{2+} with peroxyacetic acid may occur to produce $CH_3CO_3\cdot$ or that a high-valent copper species *e.g.*

Cu^{3+} may be involved.

3.5. OXIDATIVE ATTACK ON BSA BY PAA AS STUDIED BY A CARBONYL ASSAY.

It was next decided to explore the products of the reactions between PAA, Fe^{2+}-EDTA and BSA, using an assay for protein carbonyls. It is believed that attack by free-radical species on proteins leads to the formation of protein side-chain carbonyl formation and therefore it was hoped that comparisons could be made between the spin-trapping results already obtained and the results of the carbonyl study to examine the final products.

Several approaches have been developed for the examination of protein damage, including extent of fragmentation, quantification of bityrosyl / disulfide formation, analysis of proteolytic susceptibility and examination of protein side-chain carbonyl formation. Carbonyls have been widely used as markers for oxidative damage in proteins[7,129,185,199-202] and may be introduced into proteins by a variety of mechanisms (see Scheme 3.1). It has been demonstrated that transition-metal ions in conjunction with hydrogen peroxide can transform amino-acid side-chains into carbonyl derivatives as can other damaging processes.[7,129,185,199-202] The side-chains which have been found to be most susceptible to this type of damage are lysine, proline, arginine and histidine.[129] Carbonyl-group introduction into proteins has been shown to be highly damaging, leading to loss of catalytic activity of enzymes[7,200,201] and elevated levels of carbonyls have been found as a consequence of some diseased states.[15]

Many approaches have been taken to the determination of carbonyl content in proteins, the most common being reaction with 2,4-dinitrophenylhydrazine (2.4-DNPH) followed by spectrophotometric analysis of the resulting Schiff bases [reaction (3.16)][203] or reduction with tritiated sodium borohydride followed by analysis of tritium incorporation [reaction (3.17)].[203-205] Other methods which have been utilised are reaction with fluoresceinthiosemicarbazide [reaction (3.18)] or reaction with fluorescein amine followed by reduction with cyanoborohydride [reactions (3.19) and (3.20)].[203]

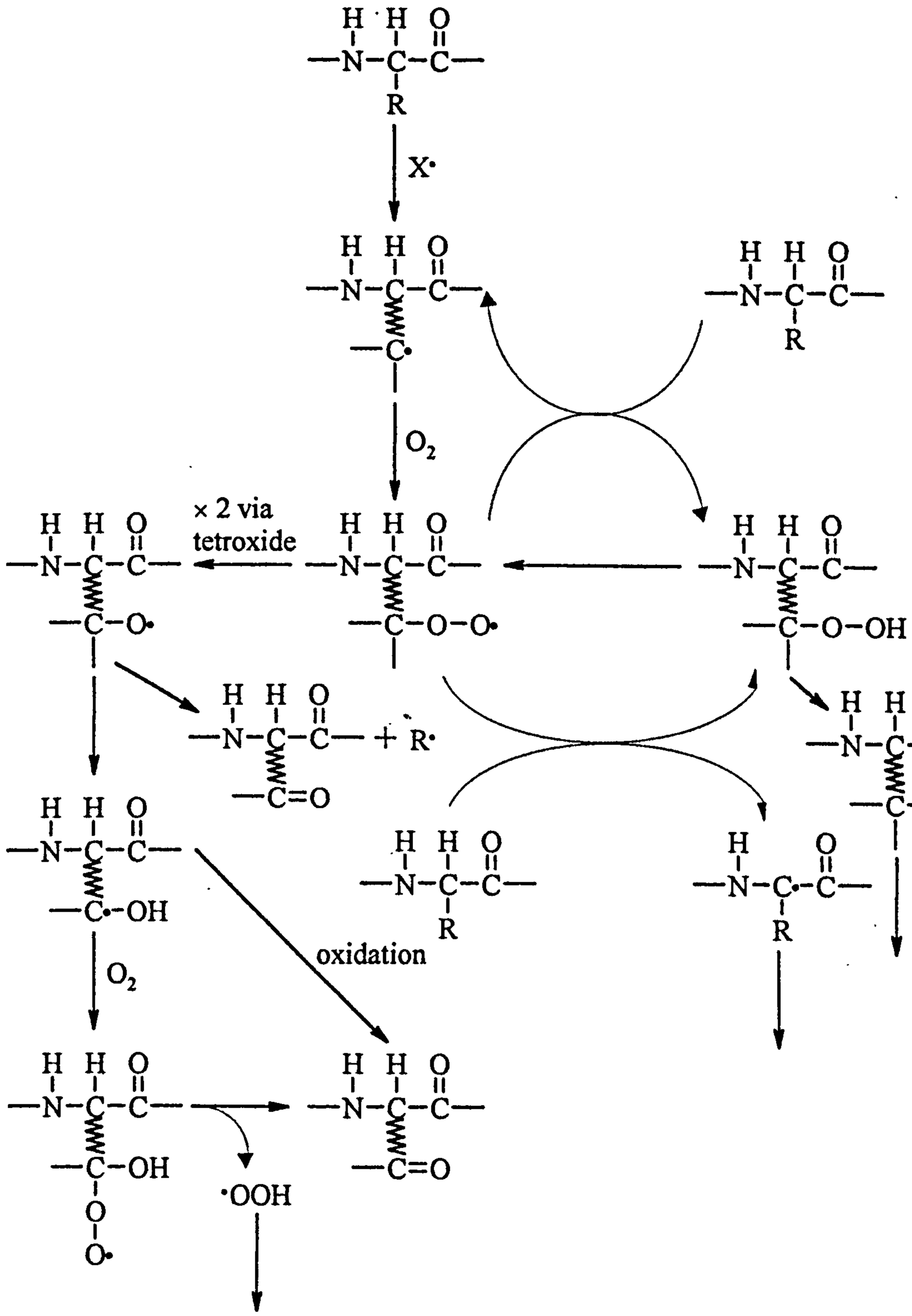

Scheme 3.1. Major reactions of aliphatic side-chain radicals formed during protein oxidation in the presence of oxygen, leading to the formation of carbonyl compounds (reproduced from reference 185).

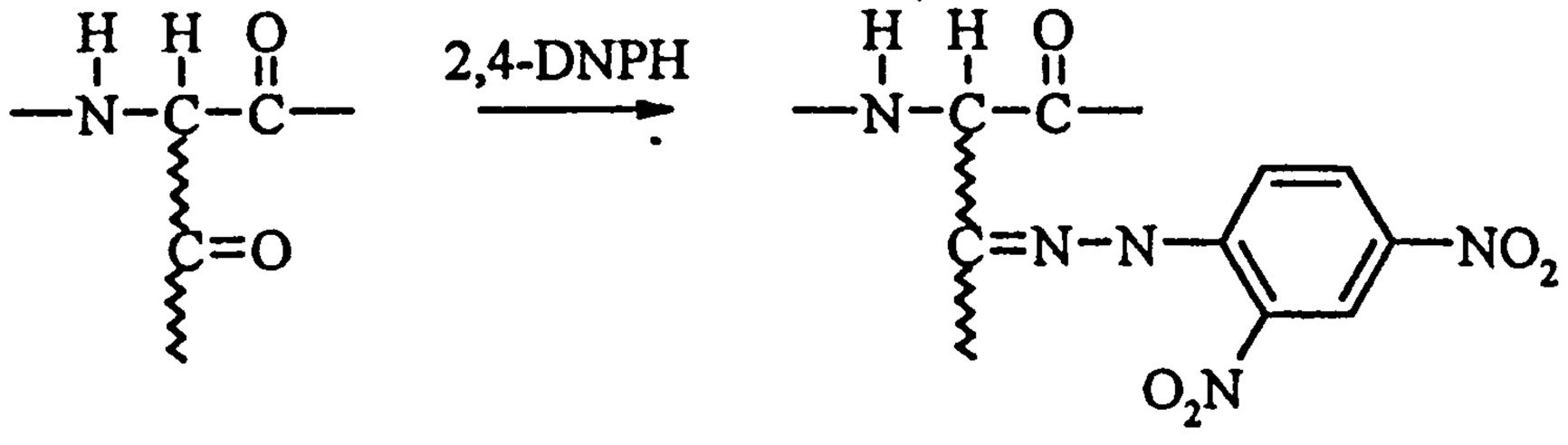

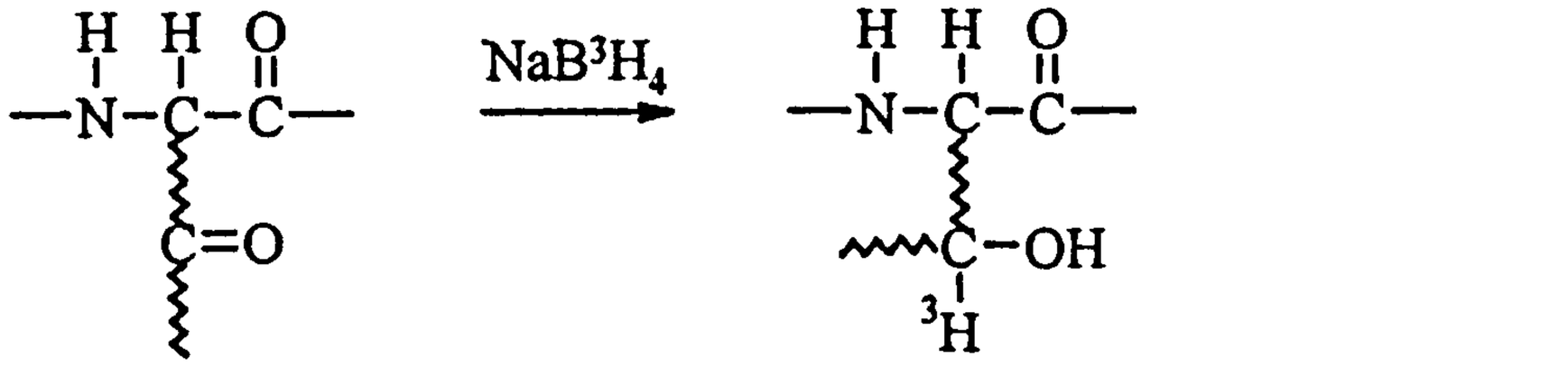

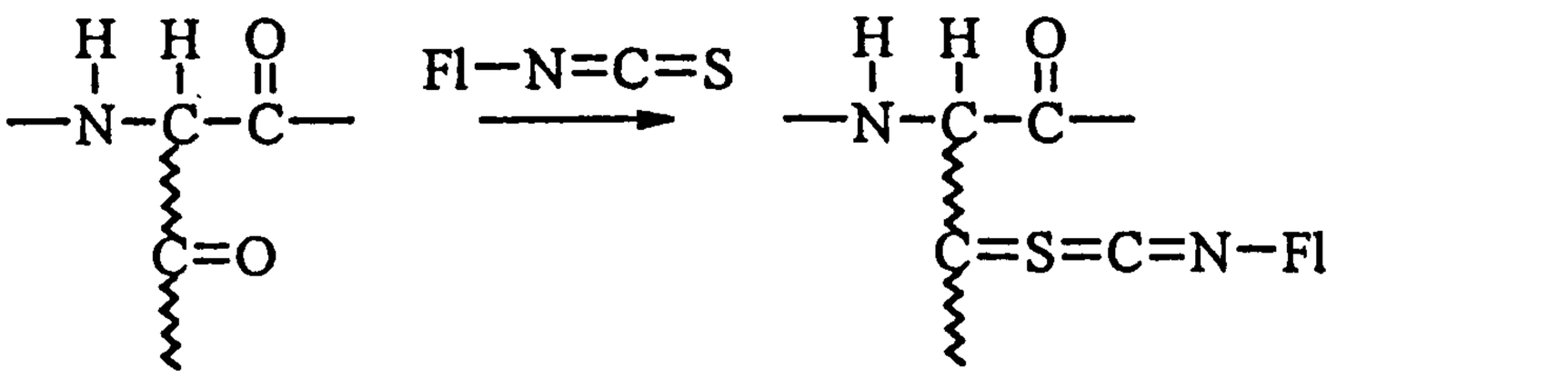

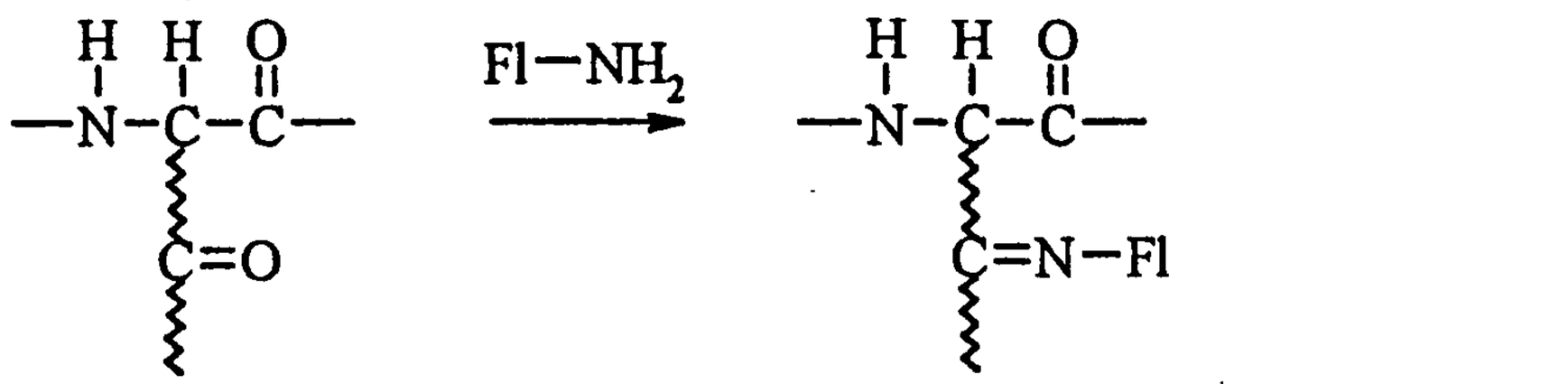

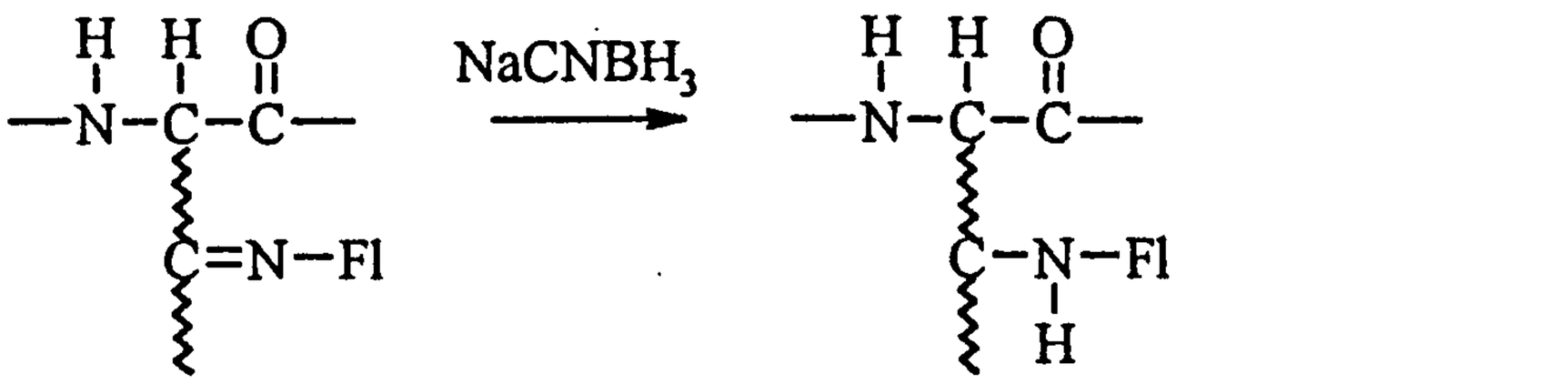

The method employed in this study was 2,4-DNPH derivatisation followed by spectrophotometric determination, as this is the most widely used and recognised procedure.[203-205] The protein hydrazones have λ_{max} between 355 and 390 nm and have an average extinction coefficient of 22000 M^{-1} cm^{-1} allowing easy quantification of low concentrations. The concentration of protein in each sample was determined using the bicinchoninic acid assay. This assay, an adaptation of the Lowry assay relies on the formation of a Cu^{+}-protein complex at high pH which exhibits a chromophore with λ_{max} = 562 nm.[206,207]

3.5.1. Studies of systems employing Fe^{2+}-EDTA.

The formation of carbonyl groups on BSA (0.0025 g ml^{-1} final concentration) on treatment with Fe^{2+}-EDTA / PAA couples at pH 7.4 for fifteen minutes was investigated using the 2,4-DNPH method, and the results are shown in Figure 3.6. It can be seen that a low concentration of carbonyl groups is detectable in untreated BSA; it is believed that this may be the result of autoxidation of transition-metals found in native BSA. On treatment of the protein with 1.25×10^{-3} M (final concentration) Fe^{2+} -EDTA the concentration of carbonyls was observed to increase, presumably as a result of autoxidation of the iron complex producing radicals. Addition of 0.02 M (total AvOx, final concentration) 5% PAA to BSA also caused an increase in the level of carbonyls over the baseline level observed, possibly due to reaction with transition-metal ions chelated to the native BSA. Similarly, addition of 40% PAA to BSA increased the concentration of side-chain carbonyl groups on the protein, to a level greater than that observed with the equivalent concentration of 5% PAA. This is also believed to be due to reaction of the PAA with adventitious transition-metal ions. Addition of Fe^{2+}-EDTA and 5% PAA to BSA resulted in a large increase in carbonyl content over the baseline level, but not as large as the increase as was observed when 40% PAA was combined with Fe^{2+}-EDTA. Catalase treatment of either 5% or 40% PAA before inclusion in the reaction mixture caused a decrease in the level of carbonyls observed, indicating the importance of H_2O_2.

The results of these experiments are in general agreement with those obtained in EPR experiments. Spin-adducts generated in the presence of all the reaction components produced far more intense spectra than those in which one of the components was missing, in which case the formation of any spin-adducts was attributed to an artifactual reaction. This is in agreement with the increase in the level of carbonyls observed when the iron complex and the PAA were present. However, the yield of carbonyls is *greater* in the reaction mixture containing 40% PAA, which is in contrast to the EPR results, in which the signal intensity was found to be *lower* for reaction mixtures containing 40% PAA. It is believed there may be two reasons for this. Firstly, the timescales of the experiments are different; the EPR spin-trapping experiments detect the first-formed protein-radicals

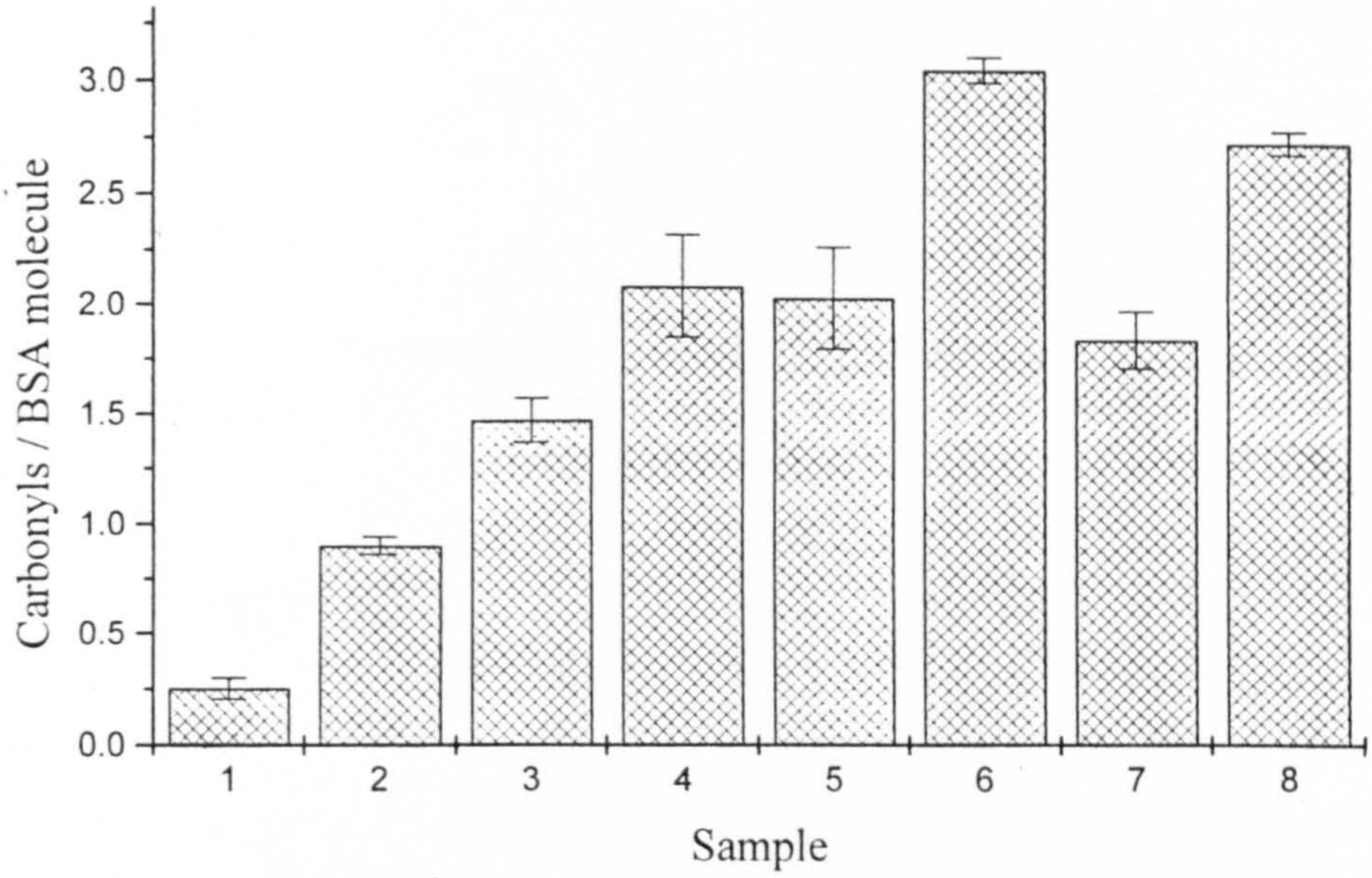

Figure 3.6. Formation of carbonyl groups (measured as 2,4-DNPH derivatives) on BSA (0.0025 g ml^{-1} on treatment with Fe^{2+}-EDTA (1.25×10^{-3} M) / PAA (0.02 M total AvOx) systems at pH 7.4. Results are displayed as the mean of triplicate determinations ± standard deviation.

1. **BSA.**
2. **BSA and Fe^{2+}-EDTA.**
3. **BSA and 5% PAA.**
4. **BSA and 40% PAA.**
5. **BSA, 5% PAA and Fe^{2+}-EDTA.**
6. **BSA, 40% PAA and Fe^{2+}-EDTA.**
7. **BSA, catalase treated 5% PAA and Fe^{2+}-EDTA.**
8. **BSA, catalase treated 40% PAA and Fe^{2+}-EDTA.**

where as the protein carbonyls are recorded after the reaction has been allowed to proceed for fifteen minutes. Secondly, it is possible that peroxyacetic acid may produce more *carbonyl specific* damage via the tentative mechanism proposed below (Scheme 3.2)

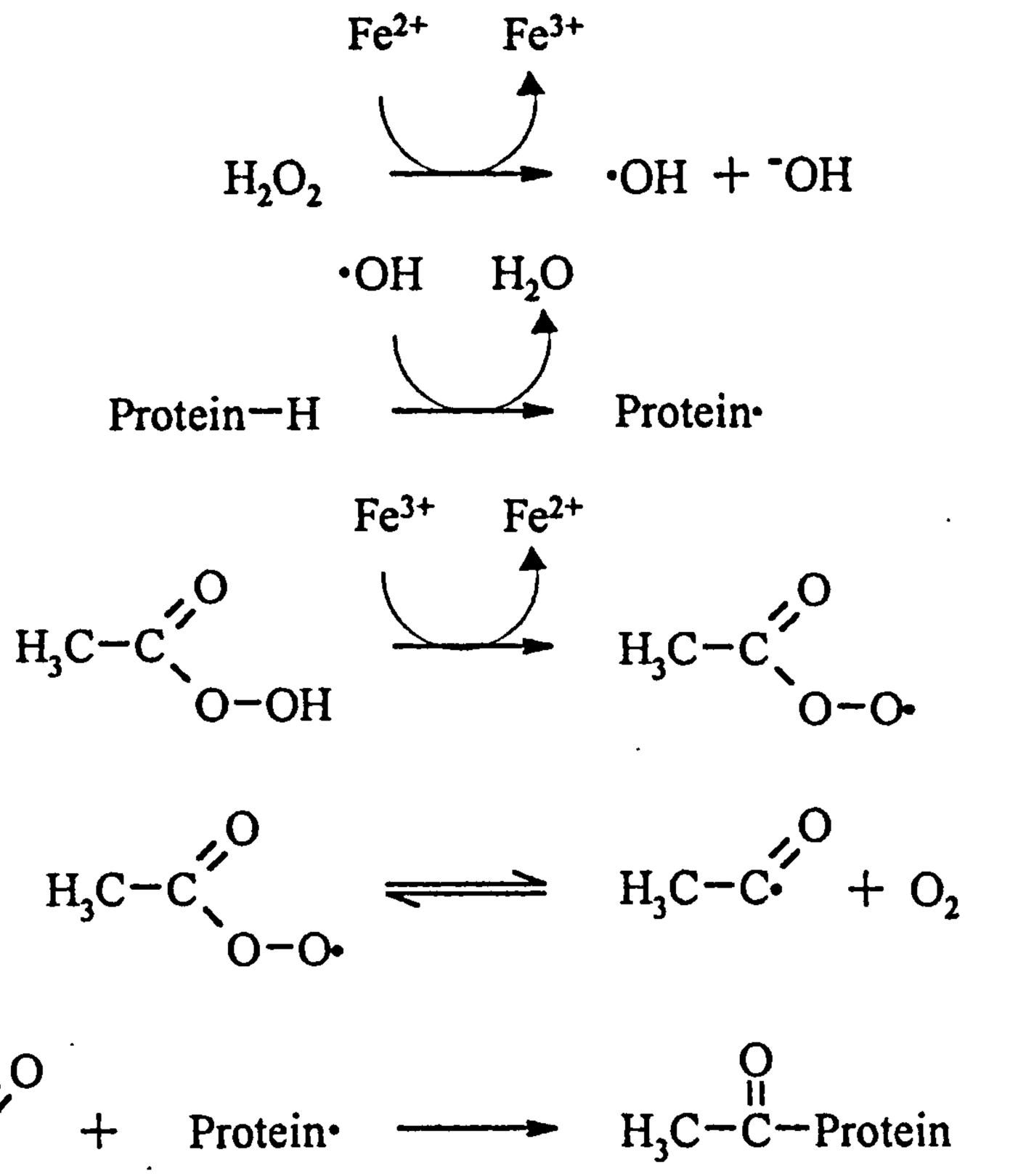

Scheme 3.2. Possible mechanism by which carbonyl groups are introduced into proteins by PAA.

Although it was not possible, using simple kinetic analysis, to determine the rate constant for the reaction between Fe^{2+}-EDTA and peroxyacetic acid, (see Chapter 2) it is anticipated that this will be slower than the reaction between Fe^{2+}-EDTA and hydrogen peroxide, by analogy with the reactions of Ti^{3+}-EDTA with hydrogen peroxide and peroxyacetic acid. It has been demonstrated that, even in the reaction mixtures in which 40% PAA is employed, *i.e.* when the concentration of hydrogen peroxide is low, hydrogen peroxide will be able to compete with the peroxyacetic acid to react with the Fe^{2+}-EDTA,

to produce a low concentration of hydroxyl radicals. It is known that hydroxyl radicals readily abstract hydrogen atoms from a variety of sites on proteins to produce protein radicals. The first-formed protein radicals can then undergo a variety of reactions. It is believed that it is possible that as the hydrogen peroxide reacts faster with Fe^{2+}EDTA than the peroxyacetic acid, there will not be a very high concentration of hydrogen peroxide remaining, but a surfeit of peroxyacetic acid. It is believed that peroxyacids can undergo reaction with Fe^{3+}-EDTA to produce $CH_3CO_3^{\cdot}$, which exists in equilibrium with the acetyl radical. Acetyl radicals may then add to the protein radicals to form protein side-chain ketones. Although the reaction of Fe^{3+}-EDTA with peroxyacetic acid is not rapid, only a low concentration of acetyl radicals needs to be generated in order to produce an observable difference in the concentration of protein side-chain carbonyl groups.

Catalase treatment of 5 / 40% PAA was found to lead to a reduction in carbonyl formation. In the reaction mixture containing 5% PAA, catalase treatment of the peroxygen led to a reduction in carbonyls from 2.03 ± 0.23 carbonyl groups per BSA molecule to 1.84 ± 0.13 carbonyl groups per BSA molecule whereas the concentration of carbonyl groups was reduced from 3.04 ± 0.06 to 2.71 ± 0.05 carbonyls per BSA molecule in the reaction mixture containing 40% PAA. It was significant that removal of the hydrogen peroxide, in either case, did not lead to a complete loss of carbonyl formation as this indicates the importance of peroxyacetic acid in protein damage.

The reactions were next monitored as a function of time. As expected when the mixtures were left for sixty minutes increased levels of carbonyls were observed in all of the reaction mixtures for example, in the reaction mixture containing Fe^{2+}-EDTA and 5% PAA the concentration of carbonyls was found to increase from 2.03 ± 0.23 carbonyls per BSA molecule after fifteen minutes to 2.64 ± 0.32 carbonyls per BSA molecule after sixty minutes. Similarly, in the reaction mixtures containing Fe^{2+}-EDTA and 40% PAA the concentration of carbonyls increased from 3.04 ± 0.06 to 3.64 ± 0.42 carbonyls per BSA molecule. Similar effects were observed on increasing the concentrations of the oxidants. This is attributed to the formation of higher concentrations of radical species, leading to the formation of higher concentrations of carbonyls.

3.5.2. Studies of systems employing Cu^{2+}.

Cu^{2+} (aq) caused little damage to BSA, whereas copper in conjunction with 5% PAA caused significant damage (2.20 ± 0.54 carbonyls per BSA molecule). The reaction of 40% PAA with Cu^{2+} generated an even higher concentration of carbonyls (2.94 ± 0.05 carbonyls per BSA molecule). The mechanism of formation of these species is not known, but it is believed that a high-valent copper species[42,43] or reaction of Cu^{2+} with the peroxygen compound may be involved. The reaction of the peroxyacid with Cu^{2+} may be expected to lead to more *carbonyl specific* damage in an analogous way to Fe^{3+} (see Scheme 3.2) although the involvement of a high-valent copper species is not ruled out..

3.5.3. Studies of systems employing Cu^{2+} / L-ascorbic acid.

The generation of carbonyl moieties on BSA from oxidation by Cu^{2+} / L-ascorbic acid (Cu^{+}) and peroxyacetic acid was next explored. As shown in section 3.3, this reaction mixture produced the most intense EPR spectra and therefore might be expected to produce high concentrations of carbonyls..

Treatment of BSA with L-ascorbic acid did not produce significant concentrations of carbonyl groups. However, addition of Cu^{2+} increased this concentration significantly, presumably a reflection of radical production as Cu^{+} is reoxidised. Addition of catalase to this mixture reduced the carbonyl concentration almost to baseline levels, indicating formation of hydrogen peroxide (and subsequently hydroxyl radicals) was critical to carbonyl formation on BSA. When either 5% PAA or 40% PAA was employed in conjunction with Cu^{2+} (aq) and L-ascorbic acid the carbonyl level was again observed to increase. The concentrations of carbonyls observed in these experiments were higher than those observed in either the experiments with Fe^{2+}-EDTA or Cu^{2+}(aq), in concordance with the EPR results. However, in contradiction to the EPR results 40% PAA was found to be more damaging. This is believed to possibly be a result of peroxyacetic acid generating more carbonyl specific damage, as outlined in Scheme 3.2.

Catalase pre-treatment of the peroxyacetic acid samples prior to their addition to

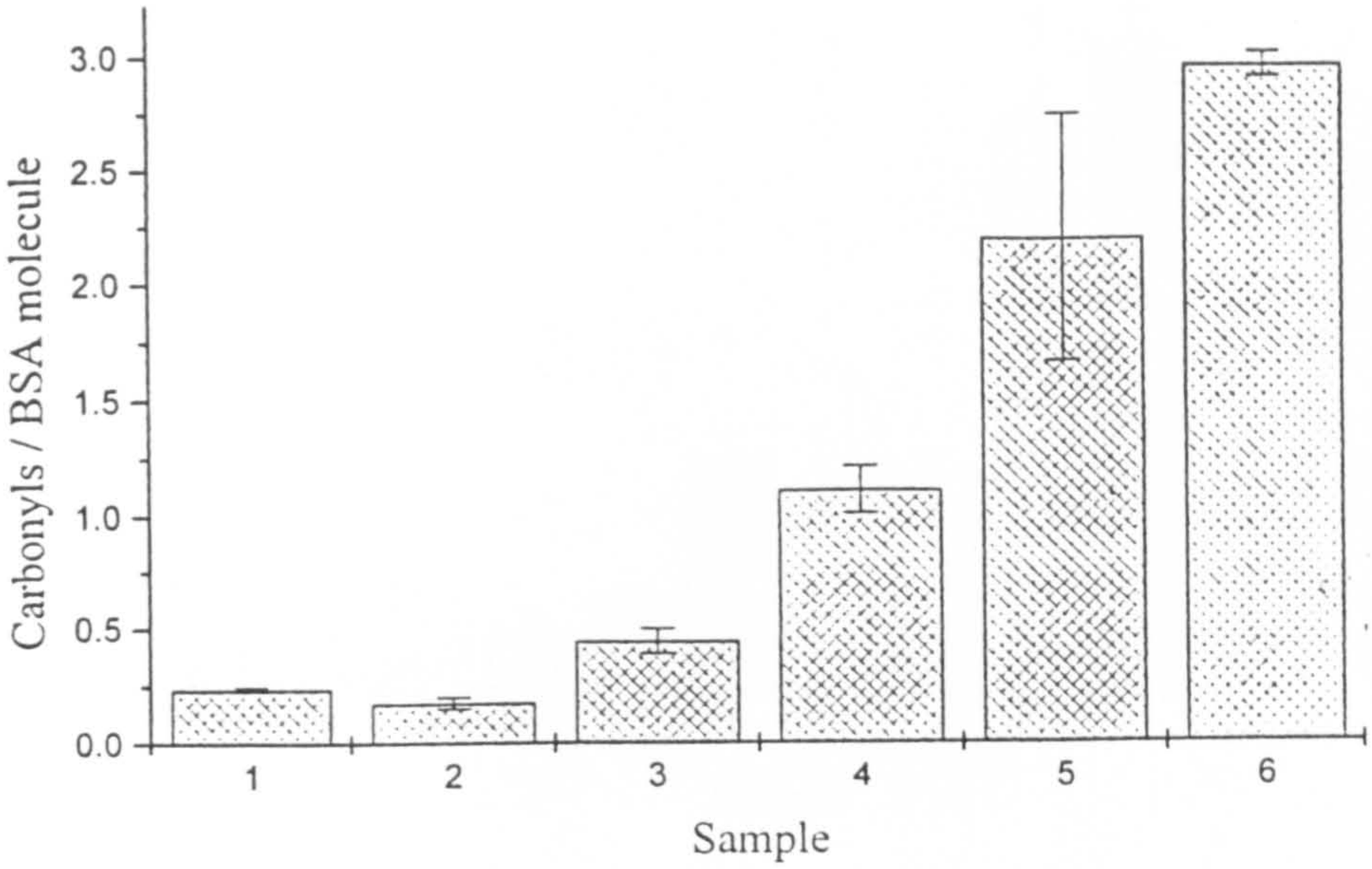

Figure 3.7. Formation of carbonyl compounds (measured as 2,4-DNPH derivatives on BSA (0.0025 g ml^{-1}) on treatment with Cu^{2+} (1.25×10^{-3} M) / PAA (0.02 M) oxidising systems. Results are displayed as mean ± standard deviation and are standardised against untreated BSA.

1. BSA.
2. BSA and Cu^{2+}(aq).
3. BSA and 5% PAA.
4. BSA and 40% PAA.
5. BSA, Cu^{2+}(aq) and 5% PAA.
6. BSA, Cu^{2+}(aq) and 40% PAA.

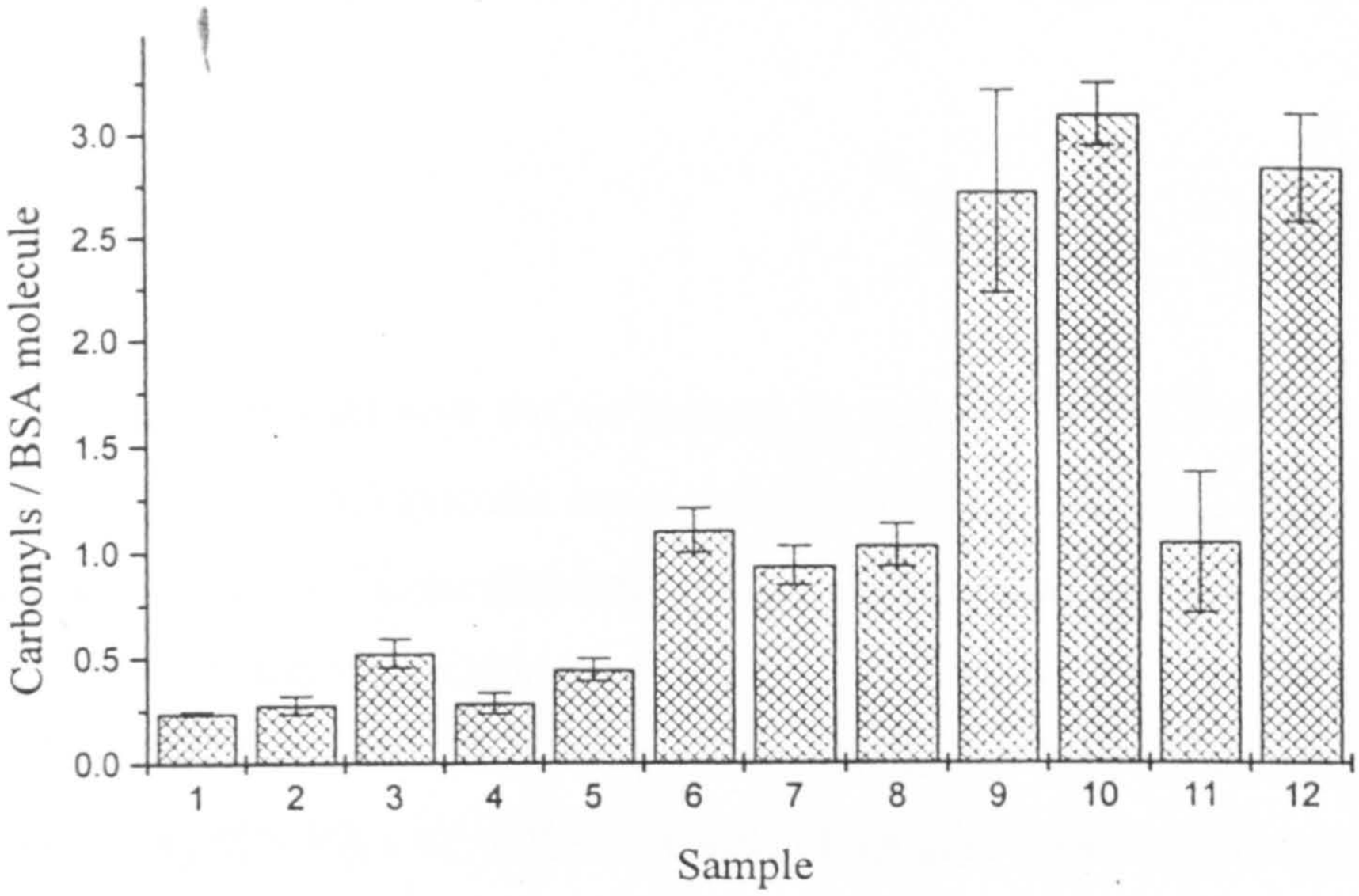

Figure 3.8. Formation of carbonyl compounds (measured as 2,4-DNPH derivatives on BSA (0.0025 g ml^{-1}) on treatment with Cu^{2+} (1.25 × 10^{-3} M) / L-ascorbic acid (0.0025 M) / PAA (0.02 M total AvOx) oxidising systems. Results are displayed as mean ± standard deviation and are standardised against untreated BSA.

1. BSA.
2. BSA and L-ascorbic acid.
3. BSA, L-ascorbic acid and Cu^{2+}(aq).
4. BSA, L-ascorbic acid Cu^{2+}(aq) and excess catalase.
5. BSA and 5% PAA.
6. BSA and 40% PAA
7. BSA, L-ascorbic acid and 5% PAA
8. BSA, L-ascorbic acid and 40% PAA.
9. BSA, L-ascorbic acid, Cu^{2+}(aq) and 5% PAA.
10. BSA, L-ascorbic acid, Cu^{2+}(aq) and 40% PAA.
11. BSA, L-ascorbic acid, Cu^{2+}(aq) and catalase treated 5% PAA.
12. BSA, L-ascorbic acid, Cu^{2+}(aq) and catalase treated

the BSA with Cu^{2+} and L-ascorbic acid resulted in reductions in the concentrations of carbonyl groups formed approximately proportional to the concentration of hydrogen peroxide in the sample.

3.5.4. Discussion.

The results obtained here are, in general, in agreement with the EPR findings. Thus, transition metal / PAA systems cause significant damage to BSA, as measured by the carbonyl assay, the Cu^{2+} / L-ascorbic acid system producing the highest carbonyl yields and most intense EPR spectra, followed by the Fe^{2+}-EDTA system and finally the system in which Cu^{2+} was employed. However, in contrast to the EPR results the reaction mixtures containing 40% PAA led to the formation of a higher concentration of carbonyls than the corresponding mixtures in which 5% PAA was employed. It may be possible that peroxyacetic acid acts via a mechanism outlined in Scheme 3.2 in order to produce higher concentrations of carbonyls. Catalase treatment of the PAA samples prior to their addition to BSA in the presence of transition-metal ions consistently led to a reduction in the levels of carbonyls observed, although this was not always directly proportional to the concentration of hydrogen peroxide in the reaction mixtures. PAA samples, in the absence of added transition-metal ions were found to produce significant levels of carbonyls. This is attributed to reaction of the PAA with adventitious transition-metal ions. However, this does not explain why no EPR signals attributable to spin-trapped protein radicals were observed in these systems.

3.6. OXIDATIVE ATTACK ON BSA AS MEASURED BY AN ASSAY FOR REDUCED THIOL GROUPS.

It was next decided to explore the oxidation of the Cys 34 residue by PAA / Fe^{2+}-EDTA oxidising systems since it is believed that cysteine residues in proteins are sites of particular vulnerability to oxidation, and as described previously[191,192] often act as "oxidative sinks " The loss of free thiol groups is therefore often used as marker for

oxidative stress.[208,209] There are two well recognised pathways by which thiol oxidation can occur by peroxides, one of which is transition-metal independent [reaction (3.21)] and the other of which is transition-metal dependent [reactions (3.22) - (3.25)].

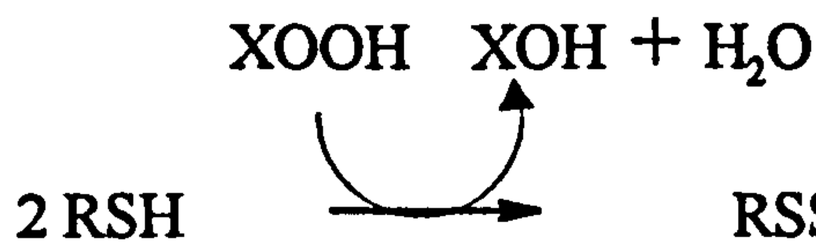

(3.21)

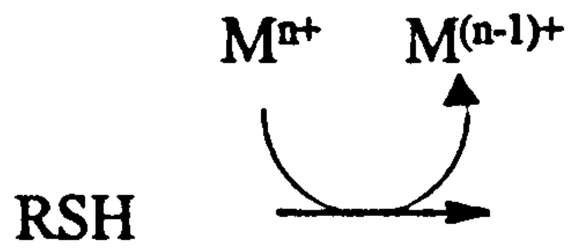

(3.22)

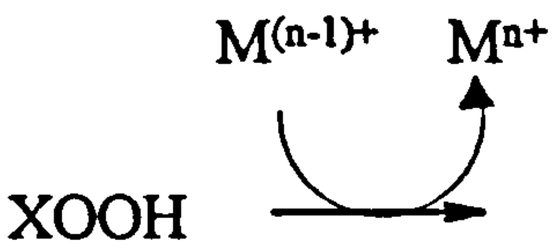

(3.23)

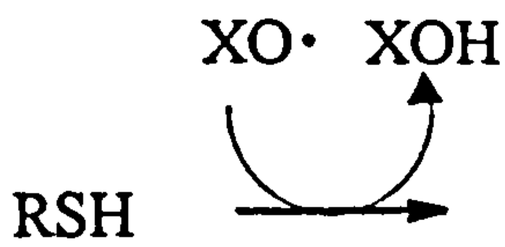

(3.24)

(3.25)

Free thiol groups on BSA were analysed using the reaction with 5,5'-dithio-bis(2-nitrobenzoic acid) (Ellmans Reagent, DTNB).[208,209] This reacts with free thiol groups [reaction (3.26)] producing a mixed disulfide and 2-nitro-5-thiobenzoate which has λ_{max} = 412 nm and an extinction coefficient of 13600 $M^{-1}cm^{-1}$. Since this reaction is highly pH dependent, all the reagents excluding the Fe^{2+}-EDTA were made up in 0.1 M phosphate buffer (pH 7.4) and experiments were performed with very low concentrations of peroxyacid, not only to prevent false results, but because it was believed that only low concentrations would be required for oxidation of the thiol group to occur.

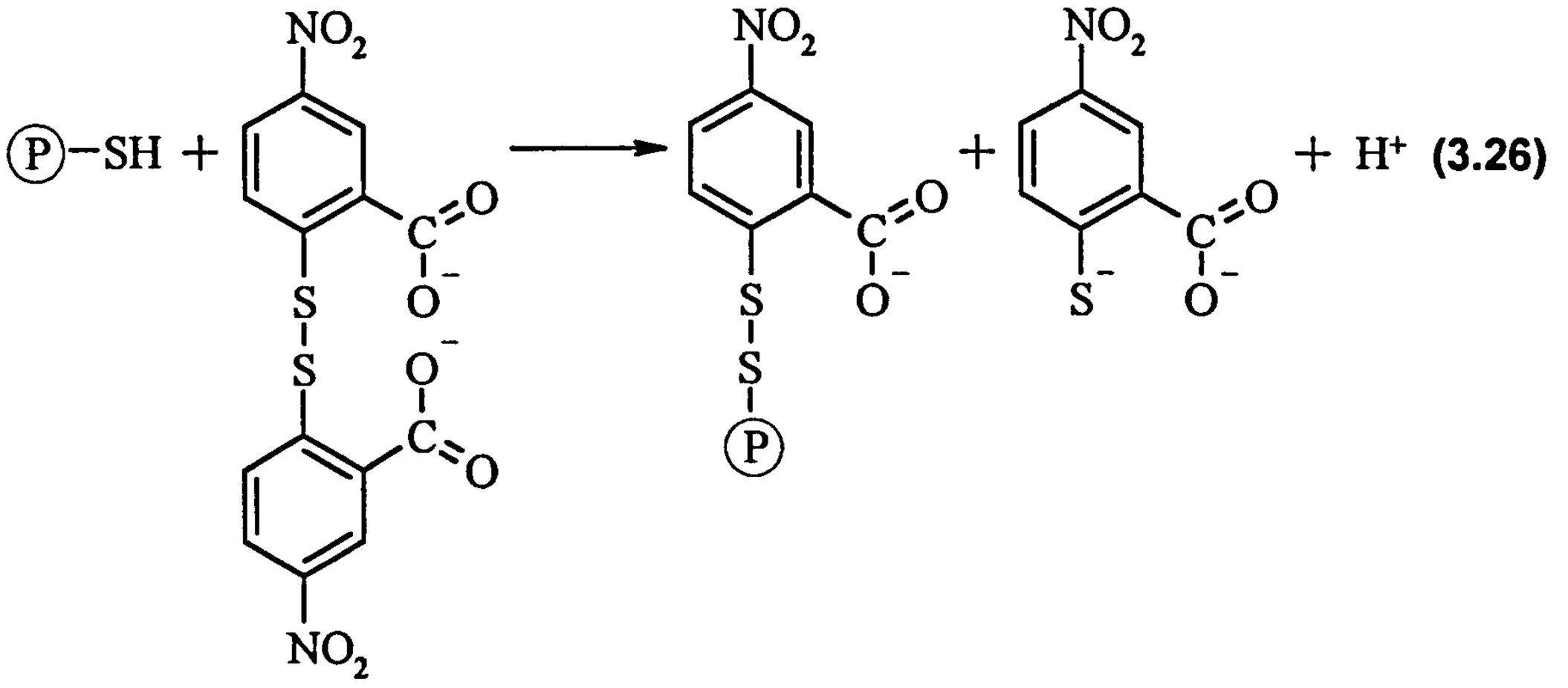

(3.26)

3.6.1. Systems employing PAA only.

Treatment of BSA (final concentration 0.0025 g ml^{-1}) with either 0.001 M, (final concentration, total AvOx) 5% or 40% PAA for fifteen minutes led to a dramatic loss in free thiol groups. The reduction can be seen (Figure 3.9) to be the same within standard deviation for the two peroxygens. Addition of catalase to the peroxygen compounds prior to their addition to the BSA leads to a marked reduction in the concentration of thiol groups oxidised by 5% PAA , but very little difference in the concentration of thiol groups oxidised by 40% PAA, reflecting the difference in overall oxidising equivalents.

It is apparent from these results that both hydrogen peroxide and peroxyacetic acid are effective oxidants of thiol groups in the absence of transition-metal ions..

3.6.2. Systems employing Fe^{2+}-EDTA and PAA.

Addition of 2×10^{-4} M Fe^{2+}-EDTA to BSA led to a slight loss in the number of free thiol groups presumably as a result of autoxidation of the iron complex leading to radical production (Figure 3.10). Treatment with Fe^{2+}-EDTA and either 5% PAA or 40% PAA caused a dramatic loss in free thiol groups, similar to that observed in the absence of the exogenous transition-metal ion, but presumably occurring via a radical mechanism as outlined in reactions (3.22) - (3.25). Catalase-treated 5% PAA in conjunction with Fe^{2+}-

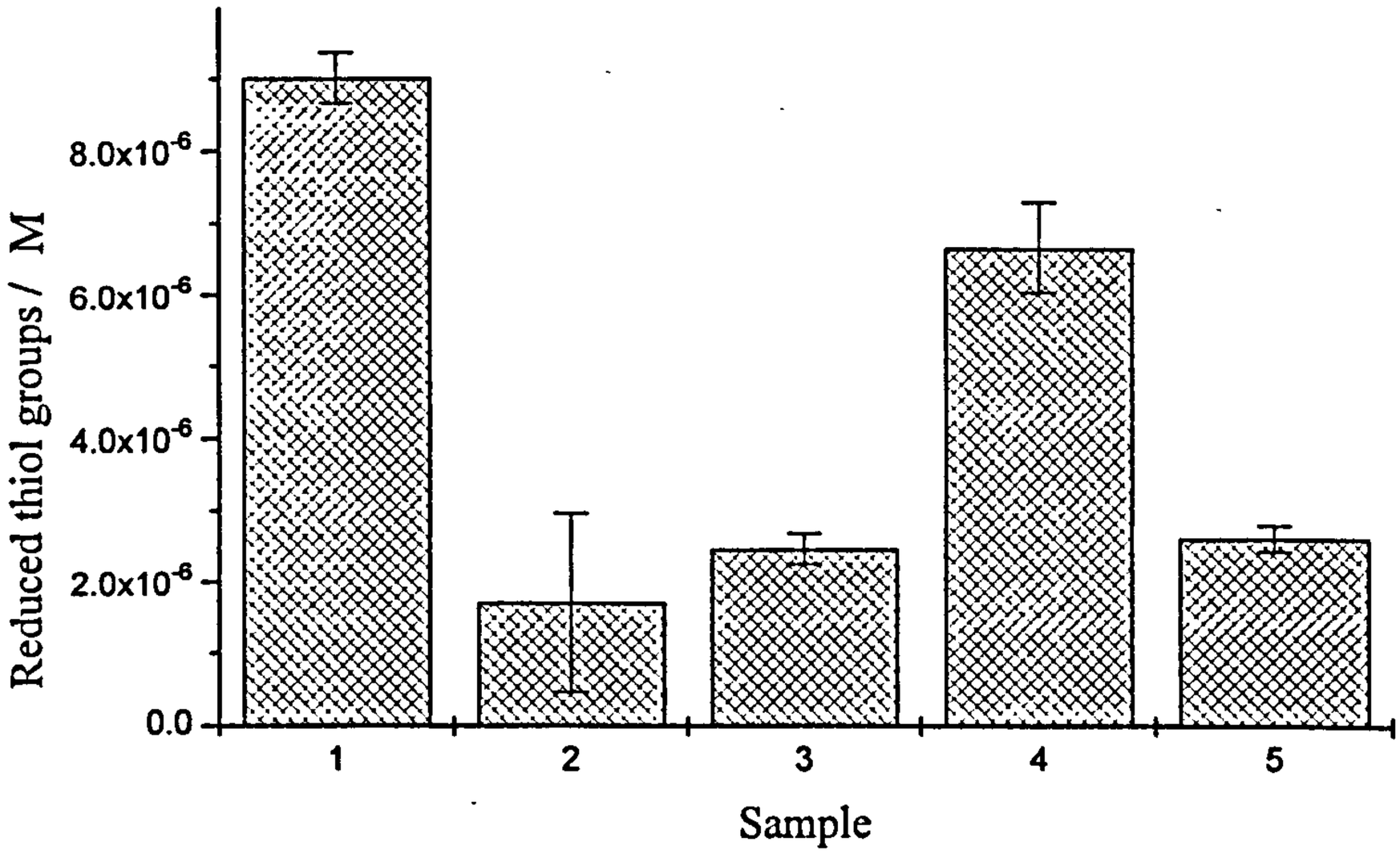

Figure 3.9. Concentration of free thiol groups on BSA as measured by DTNB derivatisation after treatment with PAA (0.001 M total AvOx) oxidising systems at pH = 7.4. Results are displayed as mean of triplicate determinations ± standard deviation.

1. **BSA.**
2. **BSA and 5% PAA.**
3. **BSA and 40% PAA.**
4. **BSA and catalase treated 5% PAA**
5. **BSA and catalase treated 40% PAA.**

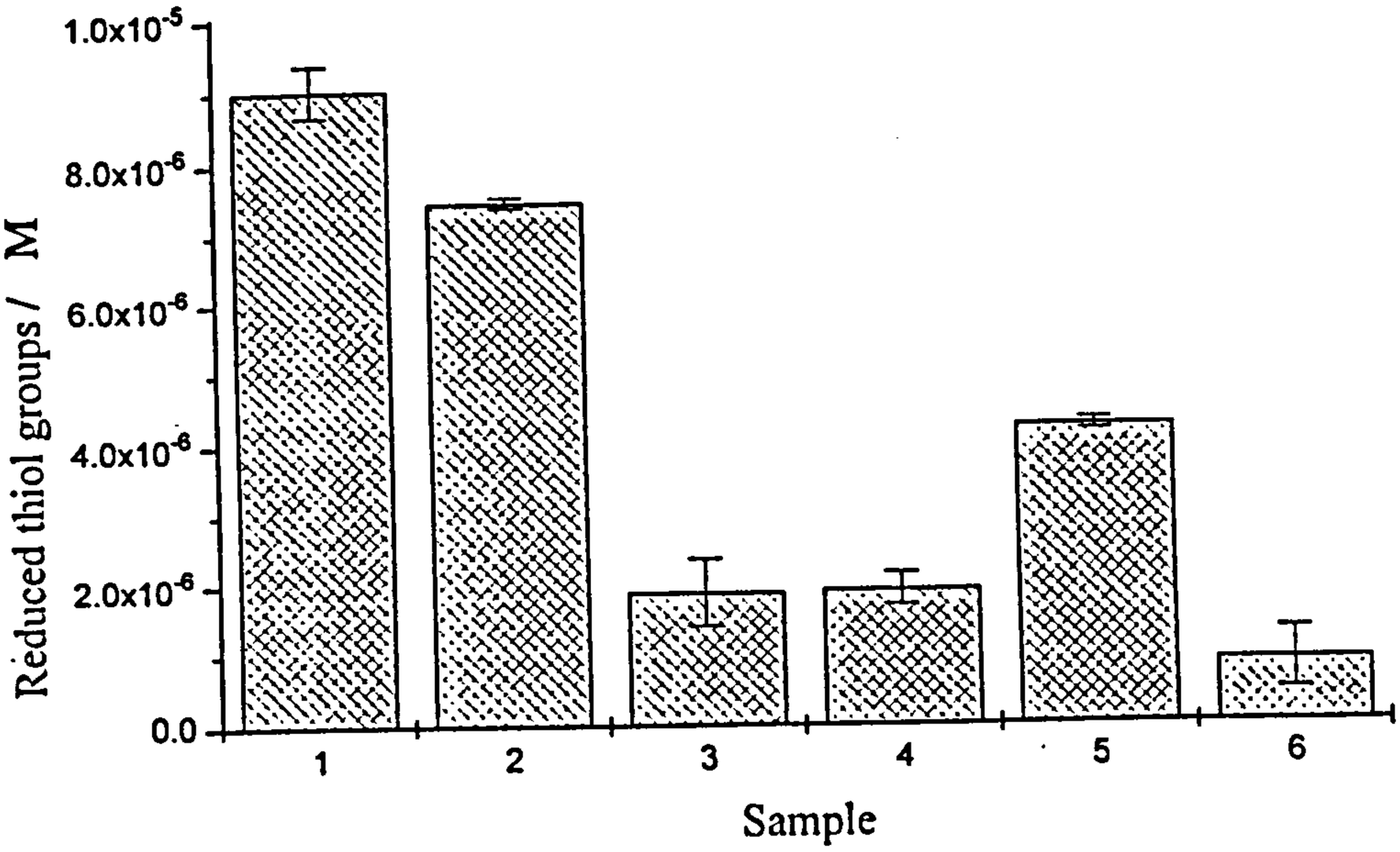

Figure 3.10. Concentration of free thiol groups on BSA as determined by DTNB derivatisation after treatment with Fe^{2+}-EDTA (2×10^{-4} M) / PAA (0.001 M) systems at pH = 7.4. Results are displayed as the mean of triplicate determinations ± standard deviation and are standardised against untreated BSA.

1. BSA.
2. BSA and Fe^{2+}-EDTA.
3. BSA, Fe^{2+}-EDTA and 5% PAA.
4. BSA, Fe^{2+}-EDTA and 40% PAA.
5. BSA, Fe^{2+}-EDTA and catalase treated 5% PAA.
6. BSA, Fe^{2+}-EDTA and catalase treated 40% PAA.

EDTA was not as effective as oxidising thiol groups as the corresponding system employing untreated 5% PAA. This is in contrast to the reaction system containing catalase-treated 40% PAA and Fe^{2+}-EDTA which was as effective (within error) at oxidising thiol groups as the corresponding system containing untreated 40% PAA, reflecting the relatively low concentration of hydrogen peroxide in the formulation.

3.6.3. Discussion.

The results described above indicate that both hydrogen peroxide and peroxyacetic acid are effective oxidants of the Cys 34 residue in BSA. Catalase treatment of 5% PAA prior to its addition to BSA reduced its ability as an oxidant, $6.67 \times 10^{-6} \pm 0.63 \times 10^{-6}$ reduced thiol groups remaining as opposed to $1.72 \times 10^{-6} \pm 1.25 \times 10^{-6}$ reduced thiol groups in the absence of catalase, whereas catalase treatment of 40% PAA had little effect on its ability to oxidise the free thiol group. This indicates the importance of both the hydrogen peroxide and the peroxyacetic acid in the formulations in the oxidation process. Addition of transition metals, to produce radicals, gave broadly comparable results, but it is anticipated that the reaction occurs via the mechanism outlined in reactions (3.22) - (3.25) as opposed to a molecular mechanism [reaction (3.21)].

3.7. FRAGMENTATION OF BSA BY Fe^{2+}-EDTA / PAA OXIDISING SYSTEMS.

In addition to the formation of carbonyl moieties,[7,129,185,199-202] the loss of reduced thiol groups,[208,209] and the formation of protein peroxides,[65,210] oxidation of proteins can lead to drastic modifications in structural properties. These include increases in hydrophobicity, alterations in susceptibility to protease digestion (see later) and either fragmentation or aggregation.[7,129,211] Aggregation often occurs under anaerobic conditions, mainly through cysteine and tyrosine residues, whereas under aerobic conditions fragmentation tends to predominate.[7,129,211]

Fragmentation of BSA was examined after exposure to oxidising treatments for fifteen minutes at 37 °C. The concentration of small peptides was measured using the BCA

assay after removal of large protein fragments.

When 0.0025 g ml^{-1} (final concentration) BSA was incubated with 0.02 M (final concentration, total AvOx) 5% PAA for fifteen minutes a high concentration of small peptides was released (see Figure 3.11). Addition of 1.25×10^{-4} M Fe^{2+}-EDTA led to a slight increase in the concentration of small peptides released. In contrast, when the experiments were repeated in reaction mixtures containing 40% PAA, very little evidence for fragmentation was observed, either in the presence or absence of added Fe^{2+}-EDTA. This observed difference in the reactions of 5 and 40% PAA oxidising mixtures was observed to be maintained over sixty minutes, although there was a marginal increase in fragmentation for each of the oxidising mixtures.

These findings support results obtained in the EPR experiments which suggested that the hydrogen peroxide causes more damage to the protein than peroxyacetic acid. However, the results of the carbonyl assay suggested that peroxyacetic acid caused more damage than hydrogen peroxide, which is in contrast to these results.

Initial studies employing MALDI-TOF mass spectrometry, a mass spectrometry technique particularly useful for the examination of high molecular weight species, showed that no large protein fragments were generated by treatment of BSA with PAA formulations either in the presence or absence of added Fe^{2+}-EDTA. Peaks were only observed for the molecular ion at approximately 67,000 and for the m/z = 2 peak at around 34,000. This suggested that largely random protein attack had occurred, leading to the release of small peptide fragments.

3.8 SUSCEPTIBILITY OF BSA TO PROTEASE DIGESTION AFTER TREATMENT WITH PAA / Fe^{2+}-EDTA OXIDISING SYSTEMS.

Protein oxidation often leads to an increase in susceptibility to proteolytic digestion.[7,129,185,199,211] However, there have been reports that proteins which have been extensively oxidised become less susceptible to proteolytic degradation.[129,185,211] These changes in proteolytic susceptibility have been demonstrated both in model systems [7,185,199] and in intact cells,[185,211] where protein turnover is markedly increased in cells that have

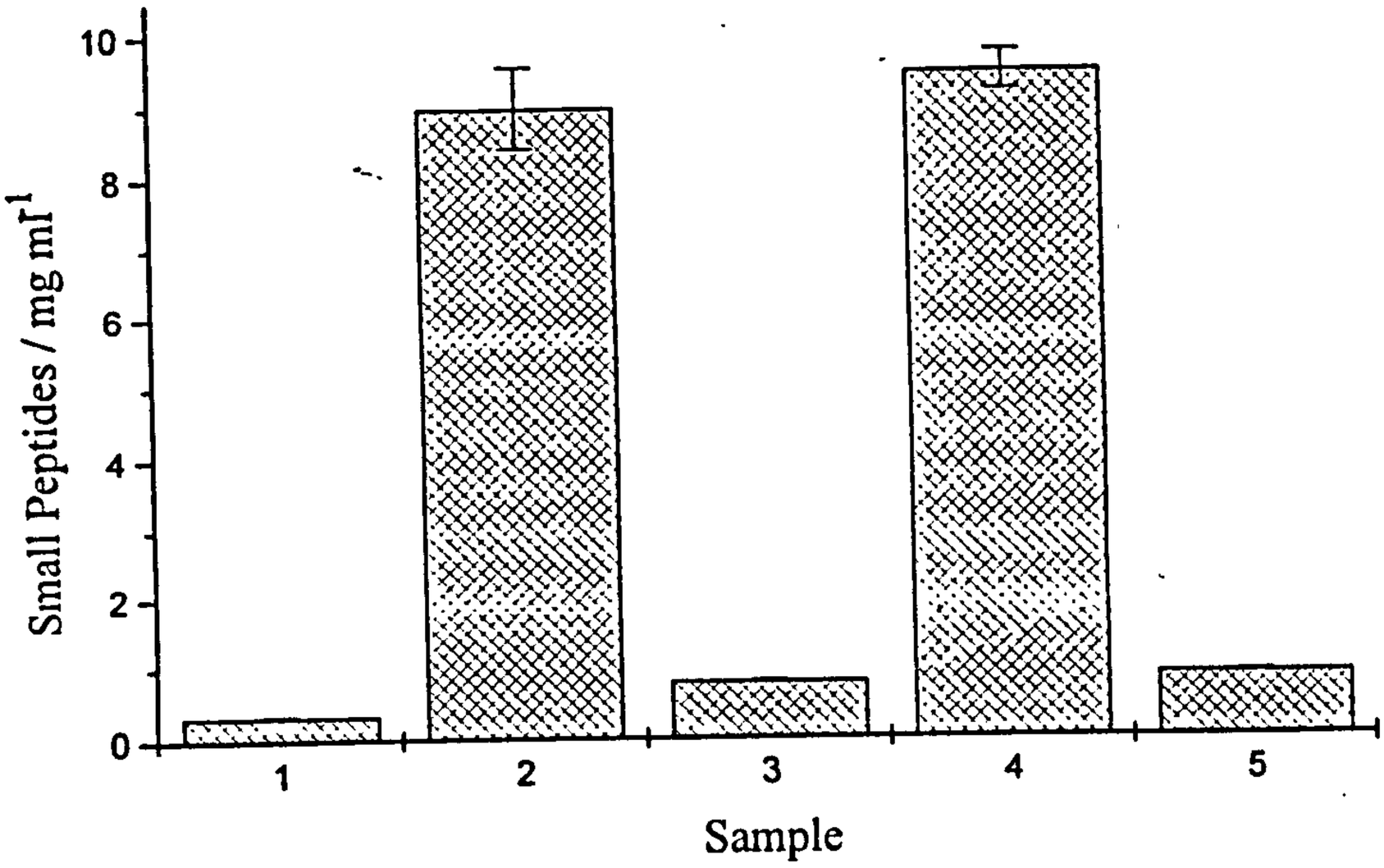

Figure 3.11. Release of small peptide fragments from BSA (0.0025 g ml^{-1}) treated with PAA (0.02 M) / Fe^{2+}-EDTA (1.25×10^{-3} M) oxidising systems as measured by the BCA assay. Results are displayed as mean of triplicate determinations ± standard deviation.

1. BSA.
2. BSA and 5% PAA.
3. BSA and 40% PAA.
4. BSA, 5% PAA and Fe^{2+}-EDTA.
5. BSA, 40% PAA and Fe^{2+}-EDTA.

been subjected to oxidative stress.

The proteolytic susceptibility of BSA after treatment with PAA / Fe^{2+}-EDTA oxidising systems was therefore investigated. This was achieved by incubating BSA with various oxidising mixtures for fifteen minutes at 37 ^{0}C, after which each sample was passed through a Sephadex G25 PD 10 size exclusion column, to remove small protein fragments generated by the oxidising treatment, and to remove excess peroxygen, which has already been shown to have a detrimental effect on the action of proteases. 1 ml fractions were collected and fractions three and four were recombined, (as these had been found to contain the majority of the protein by Coomassie Blue staining) then subjected to protease treatment for thirty minutes at 37 ^{0}C. After this large protein fragments and intact protein were removed by trichloroacetic acid precipitation and centrifugation and the supernatants were analysed for small peptide fragments using the BCA assay.

Native BSA underwent slight digestion with the protease to produce a small concentration of TCA soluble peptides (see Figure 3.12). However, on addition of 5% PAA this concentration increased over five-fold. Addition of Fe^{2+}-EDTA did not appear to affect the proteolytic susceptibility. When 40% PAA was added to native BSA an increase in proteolytic susceptibility over the native protein was observed, but this was not nearly as great as that observed with 5% PAA. Addition of Fe^{2+}-EDTA , again did not have much effect on the ability of the protease to digest the BSA.

These results indicate that peroxyacetic acid itself does not cause changes in the protein that make it more susceptible to protease digestion. However, when high concentrations of hydrogen peroxide are present in the reaction mixture the protein becomes much more susceptible to protease digestion either in the presence or absence of added iron.

The findings are in accord with the EPR results which suggest 5% PAA is more damaging than 40% PAA, and with the results of the fragmentation study. The higher level of carbonyls observed in protein which was treated with 40% PAA is believed to be a result of PAA leading to *carbonyl specific* damage

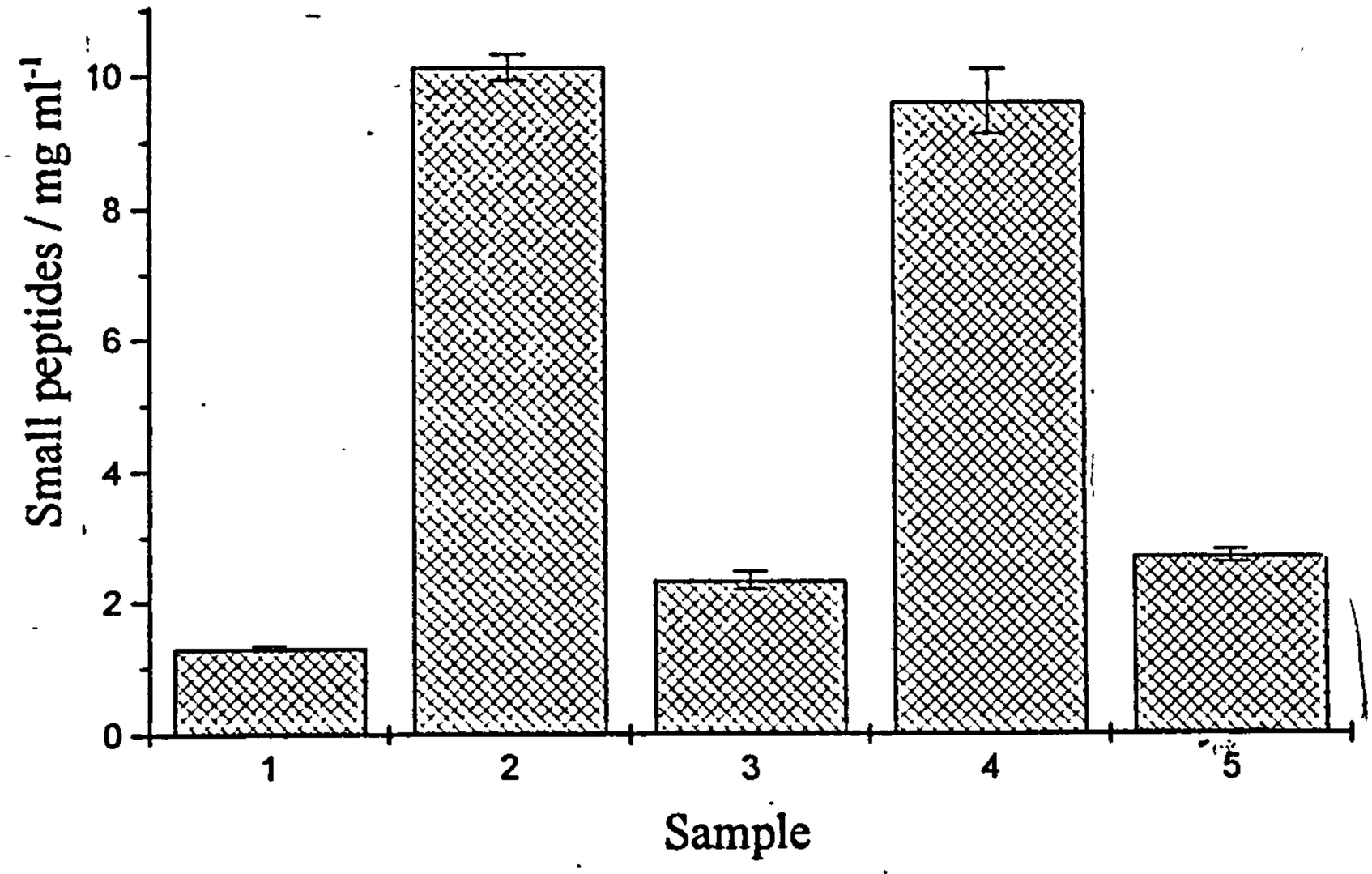

Figure 3.12. Generation of small TCA soluble peptides after protease treatment of BSA (0.0025 g ml^{-1}) treated with Fe^{2+}-EDTA (1.25×10^{-3} M) / PAA (0.02 M) systems as measured by the BCA assay. Results are displayed as the mean of triplicate determinations ± standard deviation.

1. BSA.
2. BSA and 5% PAA.
3. BSA and 40% PAA.
4. BSA, 5% PAA and Fe^{2+}-EDTA.
5. BSA, 40% PAA and Fe^{2+}-EDTA.

3.9. INVESTIGATIONS OF THE REACTIONS OF CYTOCHROME C WITH PAA.

The possible generation of radicals from PAA by reaction with *endogeneous* iron was next investigated, employing the membrane heme protein cytochrome c. This was employed because it is a well characterised, readily available protein, and is an important constituent of the electron-transport chain, shuttling electrons from the cytochrome reductase to the cytochrome oxidase complex.[86] Clearly if radicals are generated upon reaction of cytochrome c with peroxyacids damage to the protein itself or to surrounding cellular constituents may result.

Initial experiments employed the spin-trap DMPO, since it is known to trap a variety of carbon and heteroatom-centred radical species.[158] A mixture consisting of 4×10^{-4} M ferricytochrome c with 4×10^{-4} M (total AvOx) 5% PAA and 0.072 M DMPO resulted in a spectrum of DMPOX ($a_N = 0.71 \pm 0.01$ mT and $a_{2\gamma\text{-}H} = 0.41 \pm 0.01$ mT) (see Chapter Two, page 46).[158] This could be produced by the reaction of oxygen-centred radicals with the trap followed by further oxidation. Neither raising the concentration of the trap (up to 0.36 M) nor reducing the concentration of the peroxygen had any effect on the spectra observed. Similarly, addition of 40% PAA to ferricytochrome c in the presence of DMPO led to the formation of DMPOX.[158] Reduction of the ferricytochrome c to ferrocytochrome c (using sodium dithionite) prior to the addition of the spin-trap and peroxygen led to similar results. These results are in contrast to those obtained with alkyl hydroperoxides, in which alkyl, alkoxyl and alkylperoxyl radicals have been detected by spin-trapping.[212,213]

The species responsible for oxidation of the spin-trap here is not known. It could be, for example, either a protein radical / porphyrin radical cation or ferryl iron [$(Fe{=}O)^{2+}$] [see reactions (3.27)]. Ferryl iron, for example, is believed to be formed at some heme centres by the addition of peroxides[212,214] and is believed to be formed at the heme centre of cytochrome c by some workers, who have performed both mechanistic studies[213] and studies of substrate oxidation.[215] However, thus far no spectrophotometric evidence for the formation of ferryl iron has been observed for cytochrome c, unlike other heme proteins.[213]

In addition, the iron at the heme centre of cytochrome c is known to be fully co-ordinatively saturated, so that displacement of the axial methionine would have to occur for the formation of ferryl iron to be possible.[213]

$$\text{Protein}-Fe^{3+} \xrightarrow[/\,H_2O_2]{CH_3CO_3H} \text{Protein}-Fe^{4+}=O + \begin{matrix}\text{porphyrin} \\ \text{radical cation}\end{matrix} \Big/ \begin{matrix}\text{protein} \\ \text{radical}\end{matrix} \quad \textbf{(3.27)}$$

If the oxidising species is a protein radical it would be expected to be short-lived, hence addition of the spin-trap *after* the peroxide should not lead to trap oxidation. Addition of DMPO one minute after mixing the protein with the peroxygen again produced the characteristic spectrum of DMPOX.[158] This implies that the oxidising species is not a protein radical.

UV-visible spectrophotometry of 1:1 peroxygen / cytochrome c mixtures was next employed in an attempt to deduce the oxidation state of the iron. However, over sixty minutes only slow quenching of the Soret band, (λ_{max} = 410 nm) was observed, indicating destruction of the porphyrin ring, together with an increase in absorbance between 520 and 548 nm, indicative of a change in the interaction between the porphyrin ring and the iron centre were observed.[213] No evidence was seen for the formation of ferryl iron, which would be expected to lead to shifting of the Soret band.[213] Increasing the concentration of the peroxygen led only to more rapid and extensive quenching of the Soret band and a greater increase in absorbance between 520 and 548 nm.

Utilisation of an alternative spin-trap, α-(4-pyridyl-1-oxide) *N*-tertbutyl nitrone [4-POBN, was next explored. It was anticipated that this may be less susceptible to oxidation, whilst retaining the ability to trap a variety of radical species and being highly soluble in aqueous systems. Reaction mixtures containing 4×10^{-4} M (total AvOx) 5% PAA, 0.072 M 4-POBN and 4×10^{-4} M ferricytochrome c produced EPR spectra comprising of a nitrogen splitting of 1.49 ± 0.01 mT, a further nitrogen splitting of 0.19 ± 0.01 mT and a β-hydrogen splitting of 0.18 ± 0.01 mT. It is believed that this is due to the trapping of a nitrone-derived species by 4-POBN itself. In addition, a second signal was evident which was comprised of a quartet ($a_N = a_{\beta\text{-}H}$ = 1.44 ± 0.01 mT) indicative of the formation of

MNP-H (*t*-BuNHO) which is typically formed by the reduction of MNP (*t*-BuNO) which itself could be formed by fragmentation of a 4-POBN adduct (see Figure 4.13.a). Similar spectra have been observed in systems in which peroxidases were employed.[216]

Employing a mixture of DMPO (0.18 M) and 4-POBN (0.072 M) in these experiments (Figure 4.23.b) led to the production of a signal with a nitrogen splitting of 1.36 ± 0.01 mT, a second nitrogen splitting of 0.46 ± 0.01 mT and a β-hydrogen splitting of 1.58 ± 0.01 mT assigned to a nitrogen-centred species trapped by DMPO.[216] Substitution of pyridine-*N*-oxide for 4-POBN led to the production of no EPR-active species. This suggests that the radical of the 4-POBN species is located on the nitrone nitrogen, not the nitrogen of the pyridine-*N*-oxide ring, although this was not pursued further.

Although it has not been proved spectrophotometrically, it is believed that ferryl iron may be produced upon reaction of cytochrome c with PAA. This is a highly oxidising species and may be responsible for damage to surrounding molecules in bacterial cells. It is therefore possible that damage to the protein itself (degradation of the porphyrin ring was observed in UV-visible experiments) may be of importance in cell death, since it is a key molecule in the electron-transfer chain. In addition if the protein is damaged to such an extent that the iron is released it may then react with PAA in the manner already explored in Chapter Two and thus generate damaging radical species.

3.10. CONCLUSIONS.

The results described here with BSA indicate that both peroxyacetic acid and hydrogen peroxide, in the presence of Fe^{2+}-EDTA, lead to the formation of protein radicals, which are both backbone and side-chain derived. Reaction mixtures containing 5% PAA lead to the generation of higher concentrations of protein-derived radicals. This implies that hydroxyl radicals from the hydrogen peroxide are more effective at generating protein radicals than radicals derived from the peroxyacetic acid. The reaction of BSA with PAA is not only catalysed by Fe^{2+}-EDTA but also Cu^{2+} / L-ascorbic acid (*i.e.* Cu^{+}) and Cu^{2+}. Cu^{2+} / L-ascorbic acid systems produced the highest concentration of protein

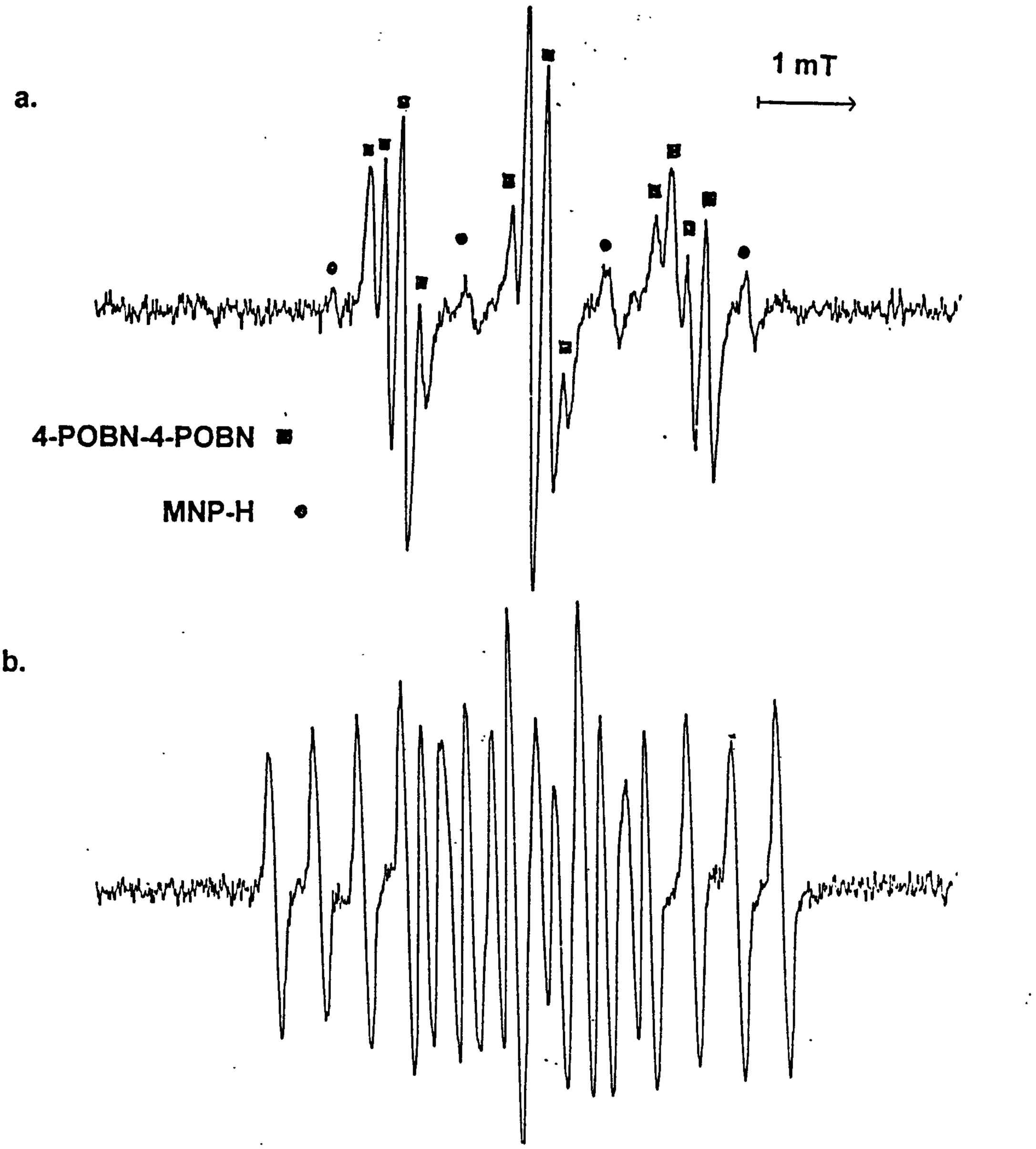

Figure 4.13.a. EPR spectrum generated by the reaction of ferricytochrome c with 5% PAA and 4-POBN.

Figure 4.13.b. EPR spectrum generated by the reaction of ferricytochrome c with 5% PAA, 4-POBN and DMPO.

Concentrations employed:- ferricytochrome c, 4×10^{-4} M, 5% PAA, 4×10^{-4} M, 4-POBN, 0.072 M, DMPO, 0.18 M

radicals, as a result of the continual regeneration of Cu^{+} by reduction of the Cu^{2+} with L-ascorbic acid.

Reaction mixtures in which Fe^{2+}-EDTA is utilised give spectra which were observed to be markedly different when the thiol group of BSA was blocked. The spectra showed much more hyperfine structure and the spin-adducts were much more readily digested by protease. This is believed to be a reflection of the denaturing effect of blocking the thiol group.

Determination of protein-bound carbonyls showed that, in the presence of Fe^{2+}-EDTA, Cu^{2+} (aq) or Cu^{+} (generated by the reaction of Cu^{2+} (aq) with L-ascorbic acid) 40% PAA led to the formation of higher concentrations of protein-bound carbonyls than 5% PAA. This is in contrast to the EPR results, which showed that higher concentrations of protein radicals were generated in systems in which 5% PAA was employed. It is possible that peroxyacetic acid-derived radicals, although not as effective as hydroxyl radicals from hydrogen peroxide, in generating protein radicals, could lead to a higher concentration of carbonyls on the protein possibly via the mechanism proposed earlier. The Cu^{2+} / L-ascorbic acid system generated the highest concentration of carbonyl groups.

Nucleophilic oxidation of the thiol group of Cys 34, in the absence of Fe^{2+}-EDTA, and radical oxidation in the presence of Fe^{2+}-EDTA are facile with very low concentrations of peroxygen compounds and transition-metal ions causing extensive thiol oxidation. This implies that PAA may seriously reduce the antioxidant capability of bacterial cells and possibly contribute to cell-death.

It has also been found that extensive fragmentation of BSA occurs when it is treated with 5% PAA either in the presence or absence of added Fe^{2+}-EDTA, where as the corresponding treatments with 40% PAA led to release of only low concentrations of small peptide fragments. Similarly, digestion of oxidised BSA by protease has been demonstrated to be far more effective when the BSA has been oxidised by 5% PAA oxidising mixtures than with 40% PAA oxidising mixtures.

Thus, the EPR study, protein fragmentation results and proteolytic digestion results suggest that 5% PAA causes more damage to BSA than 40% PAA (this is surprising given the more effective bactericidal action of peroxyacetic acid). [1,109-111] However, studies on the

formation of carbonyl groups on protein side-chains showed that 40% PAA is more damaging. As it is known that introduction of carbonyl groups into proteins can lead to a loss of catalytic activity,[7,200,201] the formation of high concentrations of carbonyls by 40% PAA may provide an insight into its greater biocidal activity.

In a second area of study, the reactions of cytochrome c with PAA have been shown to generate a highly oxidising species, possibly ferryl iron, which leads to extensive spin-trap oxidation. Degradation of the heme by PAA has also been demonstrated using UV-visible spectrophotometry. Degradation of the heme itself, reaction of the oxidising species with surrounding biomolecules or ultimate release of the iron from the heme centre may all be of importance in the bactericidal action of peroxygens

The reactions of PAA with proteins will be explored further in Chapter Five, in intact bacterial cells. The next Chapter will describe studies of the effects of PAA on model lipid systems to gain a further insight into their bactericidal action.

CHAPTER 4.

CHEMICAL AND STRUCTURAL CHANGES IN LIPIDS INDUCED BY PEROXYACETIC ACID.

4.1. INTRODUCTION.

Radical production from peroxyacetic acid as the result of electron-transfer from low-valent transition-metal ions was discussed in Chapter Two. This was shown to be a rapid process, especially in the case of Fe^{2+}-EDTA: with Cu^{+} the rate and direction of the reaction are dependent upon a number of factors, not least ligand and reducing species. In Chapter Three it was demonstrated how the reaction of peroxyacids and transition metals with proteins can lead to the formation of protein-derived radicals and of other protein-derived species characteristic of oxidative stress. The research described in this Chapter aimed to complement this information by examining how peroxyacetic acid, both in the presence and absence of exogenous transition-metal ions, might lead to oxidative modification of lipids. It is possible this may be of importance in the bactericidal action of PAA.

The lipids to be examined are model fatty acids, phospholipid mixtures in solution and liposomes; transition-metal independent modification of lipids will be examined as alkenes are known to react readily with peroxyacids to form epoxides.[20-28] It is possible that in areas of the bacterial membrane where there is limited access to transition-metal ions *epoxidation* of the membrane may be of significance. However, it is believed that in the presence of transition-metal ions, for example in the form of membrane heme proteins which have been found to be potent promoters and initiators of lipid peroxidation,[126,212-214] that *peroxidation* will predominate. The structural effects of lipid peroxidation on membranes are relatively well characterised both by spin-probe and fluorescence techniques;[217-219] however membrane epoxidation has not previously been considered, apart from the low degree of epoxidation that occurs in the course of lipid peroxidation.[5,220]

The methods to be employed in this work were standard synthetic procedures to examine epoxidation in model fatty acids, phospholipid mixtures in solution and in liposomes. In addition, EPR spin-probe studies were to be employed to examine the effects of epoxidation on liposome structure, and peroxidation was to be assessed using the 2-thiobarbituric acid assay and spin-probe studies.

4.2. EPOXIDATION OF MODEL FATTY ACIDS.

Peroxygen compounds, in particular *m*-chloroperoxybenzoic acid and peroxyacetic acid are widely utilised for the epoxidation of alkenes.[20-28] The reaction is well understood and has been found to be quantitative, or nearly so, for a variety of substrates. The mechanism of the reaction is believed to be concerted, proceeding through a planar bicyclic transition-state (Scheme 4.1).

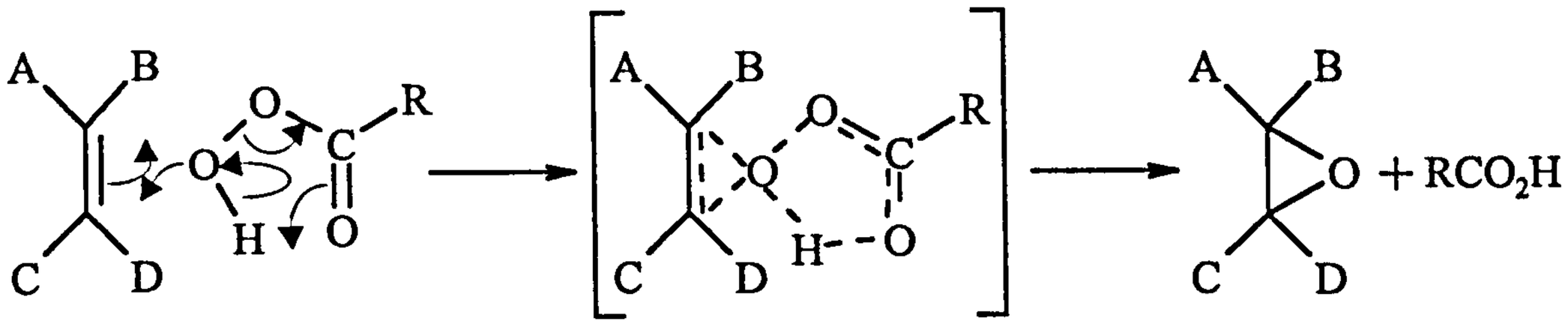

Scheme 4.1. Mechanism of epoxidation of alkenes with peroxyacids.

As would be expected from this reaction mechanism, the reaction proceeds with *syn* stereochemistry: thus cis alkenes will produce *cis* epoxides and *trans* alkenes are converted into the corresponding *trans* epoxides Further support is provided for this mechanism by the observations that the reaction is accelerated by the presence of electron-donating substituents, such as alkyl groups, on the alkene, and the presence of electron-withdrawing substituents on the peroxyacid. This is illustrated by the relative rates of reaction for the following alkenes:-

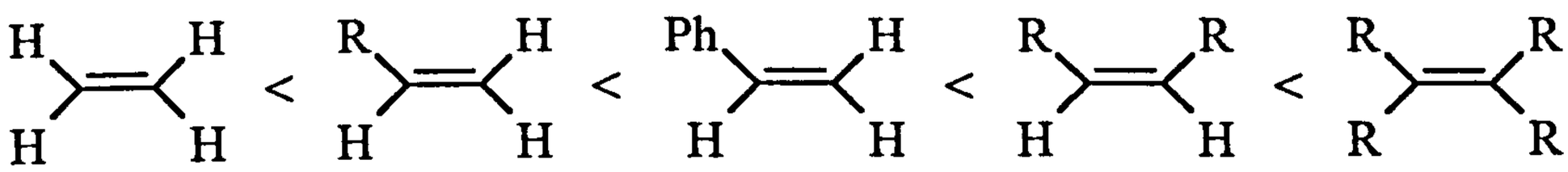

and similarly for the peroxyacids:-

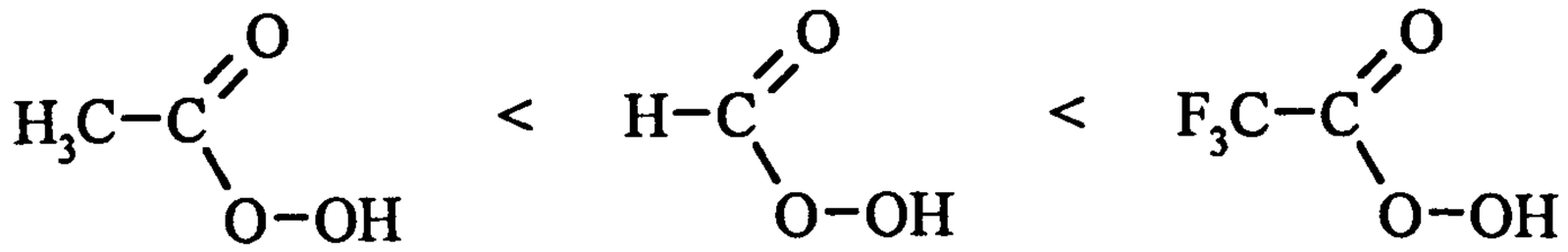

The epoxide product is usually sensitive to the presence of catalytic quantities of acid or base (see Scheme 4.2), undergoing ring opening to form the corresponding diol.

Attack occurs on the opposite side to the oxacycyclopropane ring and hence this method has been used to facilitate *anti* dihydroxylation, in contrast to, for example the reaction of potassium permanganate which facilitates *syn* dihydroxylation.

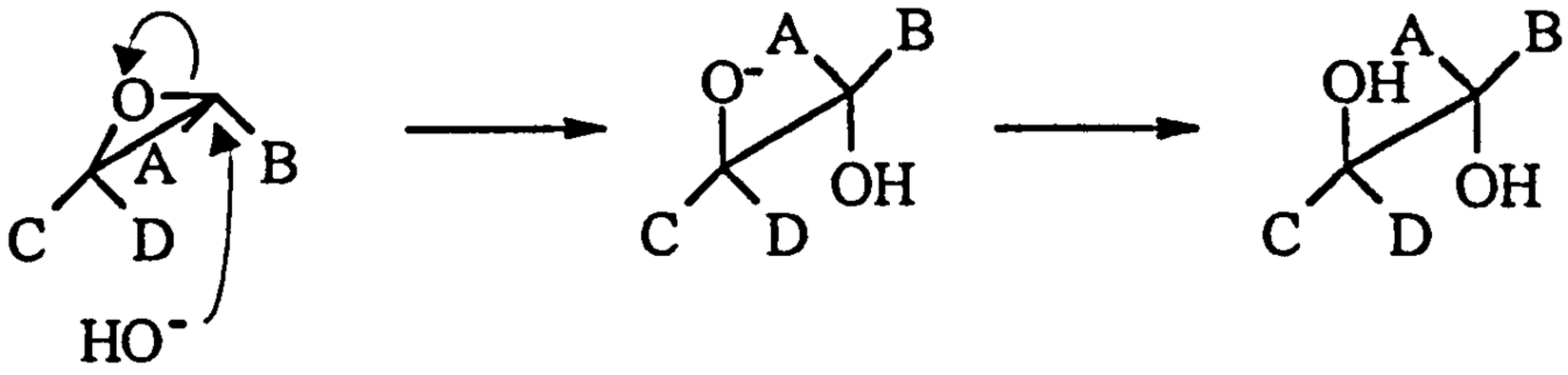

Scheme 4.2. Ring opening of an epoxide by catalytic base.

Epoxides are of particular biological relevance. In mammalian systems, they are formed upon reaction of fatty acids with cytochrome P-450 epoxygenase and have been found to be effective vasilodilators and stimulators of prolactin release, although they have also been found to be highly toxic; for example the carcinogenic action of butadiene has been attributed to the di-epoxide which is derived from it.[221,222] In bacterial systems, although they have not been identified as being associated with a particular process, they are known have bactericidal activity; for example ethylene oxide is one of the few gases that is highly bactericidal.[1,223]

Initial experiments were undertaken to ascertain whether simple fatty acids in organic solution could undergo epoxidation with both peroxyacetic acid and the classical epoxidation reagent, *m*-chloroperoxybenzoic acid (4.1).

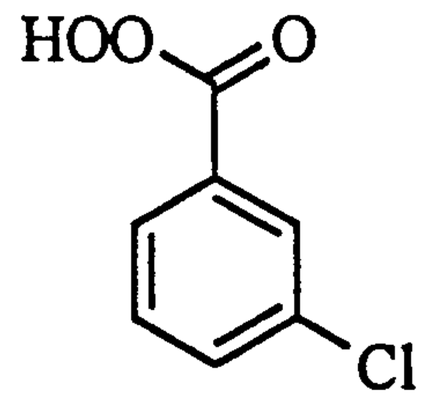

(4.1)

The fatty acids chosen for this initial study were oleic acid [octadec-9-enoic acid,

(4.2)] and linoleic acid [octadec-6,9-dienoic acid, (4.3)], chosen because they are typical of the fatty acids found in cell membranes. They contain an even number of carbon atoms; the carbon-chain of fatty acids is typically between twelve and twenty-four carbons in length and contains an even number of carbon atoms. The stereochemistry about the double bonds is also always *cis* in membrane fatty acids; the degree of unsaturation, which at least in part, controls the flexibility of the membrane varies, some fatty acids being completely saturated and others containing up to four double bonds.[86]

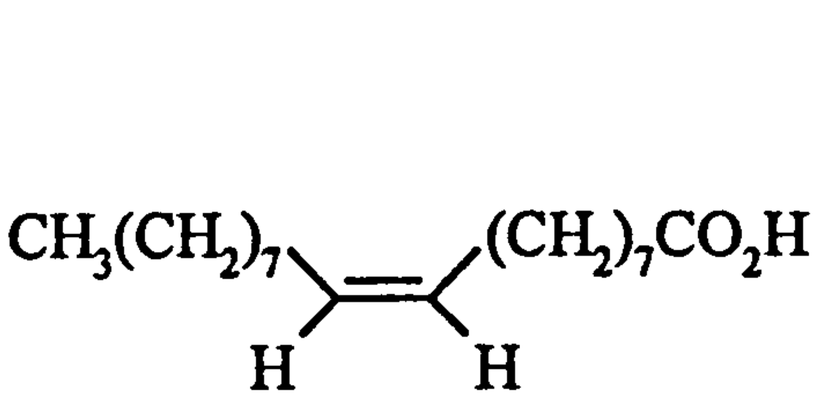

(4.2)

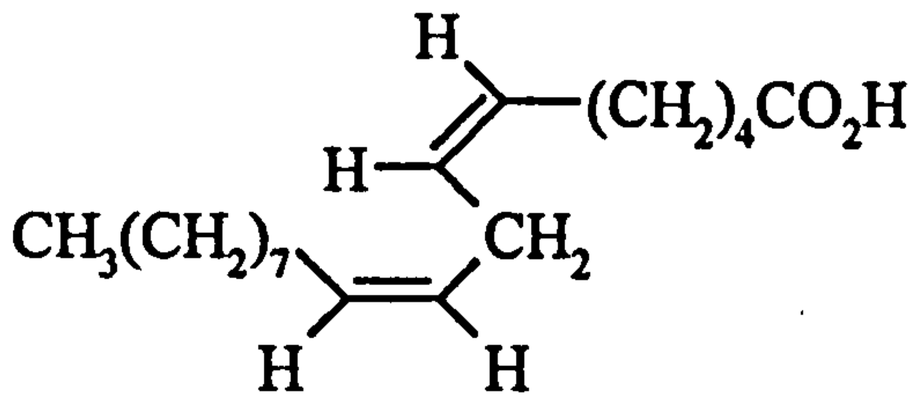

(4.3)

4.2.1. Epoxidation employing *m*-CPBA.

A typical procedure is as follows: 0.006 mol *m*-CPBA was added to a stirred dichloromethane solution containing 0.005 mol of the colourless oil (4.2) and stirred under nitrogen at room temperature overnight (see Chapter Six for full experimental detail). The product, a white solid, was isolated in 95% yield. The ^{1}H NMR spectrum of this compound, when compared to that of the starting material, showed loss of the alkene CH resonance [doublet of triplets (2 H) at $\delta = 5.4$] and the allylic resonance [multiplet (4 H) $\delta = 2.1$] as well as the appearance of a characteristic peak at $\delta = 3.0$ ppm (2 H) indicating epoxide formation. The ^{13}C NMR (fully proton decoupled) provided similar information, the alkene resonances observed at $\delta = 130$ ppm in the starting material were not apparent and a peak corresponding to epoxide at $\delta = 57$ ppm had appeared. These observations were confirmed by the off resonance ^{13}C NMR spectrum which indicated the formation of epoxide (4.4).[224]

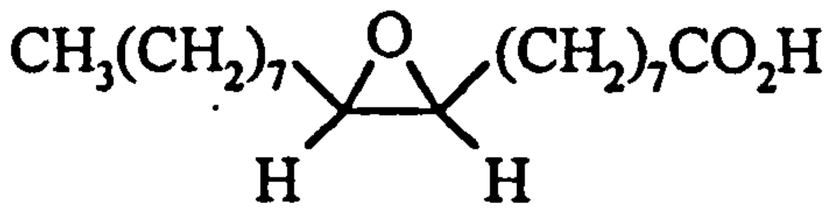

(4.4)

Corresponding experiments with the colourless oil (4.3) were similarly facile. Thus 0.0123 moles of *m*-CPBA was added to a stirred dichloromethane solution of 0.005 moles of linoleic acid (4.3); the product was isolated as a white powder in 93% yield and had an ^{1}H NMR spectra consistent with the formation of the di-epoxide (4.5). The resonances observed in the spectrum of the starting material, corresponding to the allylic protons [multiplet (4 H) $\delta = 2.2$ and triplet (2 H) $\delta = 2.9$] were lost as were those corresponding to the alkene protons [multiplet (4 H) $\delta = 5.45$]. These were replaced by signals at $\delta =$ 3.05 ppm and 3.2 ppm corresponding to the di-epoxide. In the ^{13}C NMR spectrum the resonances associated with the alkene carbons in the starting material ($\delta = 128$ and $\delta =$ 130 ppm) had disappeared. These were replaced by two signals at $\delta = 55$ ppm and $\delta = 58$ ppm corresponding to the four epoxide carbons. This NMR data is consistent with that already reported (for full detail see Chapter Six).[224]

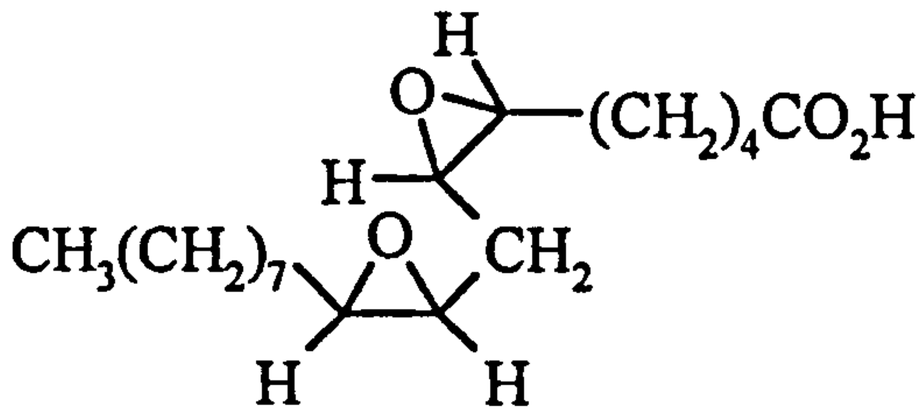

(4.5)

4.2.2. Epoxidation employing buffered 40% PAA.

It was next decided to investigate the reactions of oleic and linoleic acid with 40% PAA. The reaction conditions were broadly the same as used for the *m*-CPBA reactions, with some notable exceptions. As 40% PAA is a mixture containing sulfuric acid and acetic acid, and further acetic acid is produced on epoxidation, equimolar sodium carbonate was added to the reaction mixture to prevent any opening of the epoxide ring

to form side-products. This was not necessary when the reagent was *m*-CPBA since *m*-chlorobenzoic acid is insoluble in dichloromethane. The procedure is described fully in Chapter Six.

When 0.0096 moles (total AvOx) 40% PAA was mixed with 0.0025 moles oleic acid (4.2) and 0.0075 moles sodium carbonate and treated as described, a white solid was isolated in 95% yield. The ^{1}H and ^{13}C NMR characteristics of this compound were identical to those obtained previously and in concordance with the literature data available (see Figure 4.1.a and 4.1.b).[221] In the corresponding reaction with linoleic acid (4.2) a white solid was isolated in 76% yield. This structure of this compound was assigned, on the basis of ^{1}H and ^{13}C NMR data, to the epoxide (4.5) [224]

4.2.3. Epoxidation employing buffered 5% PAA.

Although 5% PAA is seldom used in epoxidation reactions it was decided to investigate if whether or not it could bring about epoxidation of the model fatty acids (4.2) and (4.3). 0.68 moles (total AvOx) of 5% PAA was added to a stirred dichloromethane solution of oleic acid (00025 moles) with 0.075 moles of sodium carbonate to buffer the mixture. The mixture was treated as for the reactions which employed 40% PAA and a white solid was isolated in 83% yield. ^{1}H and ^{13}C NMR analysis of the compound showed that it was the epoxide (4.4), although a trace of unreacted alkene was still evident. Similarly, reaction of linoleic acid (4.3) with 1.36 moles (total AvOx) 5% PAA yielded the di-epoxide compound (4.5) in 78% yield. No unreacted alkene was observed.

4.2.4. Discussion.

The synthesis of the epoxides (4.4) and (4.5) from oleic acid (4.2) and linoleic acid (4.3), respectively, has been demonstrated to be facile, using 5% PAA, 40% PAA and *m*-CPBA, producing high yields of essentially pure products. In the presence of sodium carbonate (as buffer), the epoxides formed by the reaction of either 5% or 40% PAA have been shown to be stable to ring opening. However, when PAA formulations are used as

a.

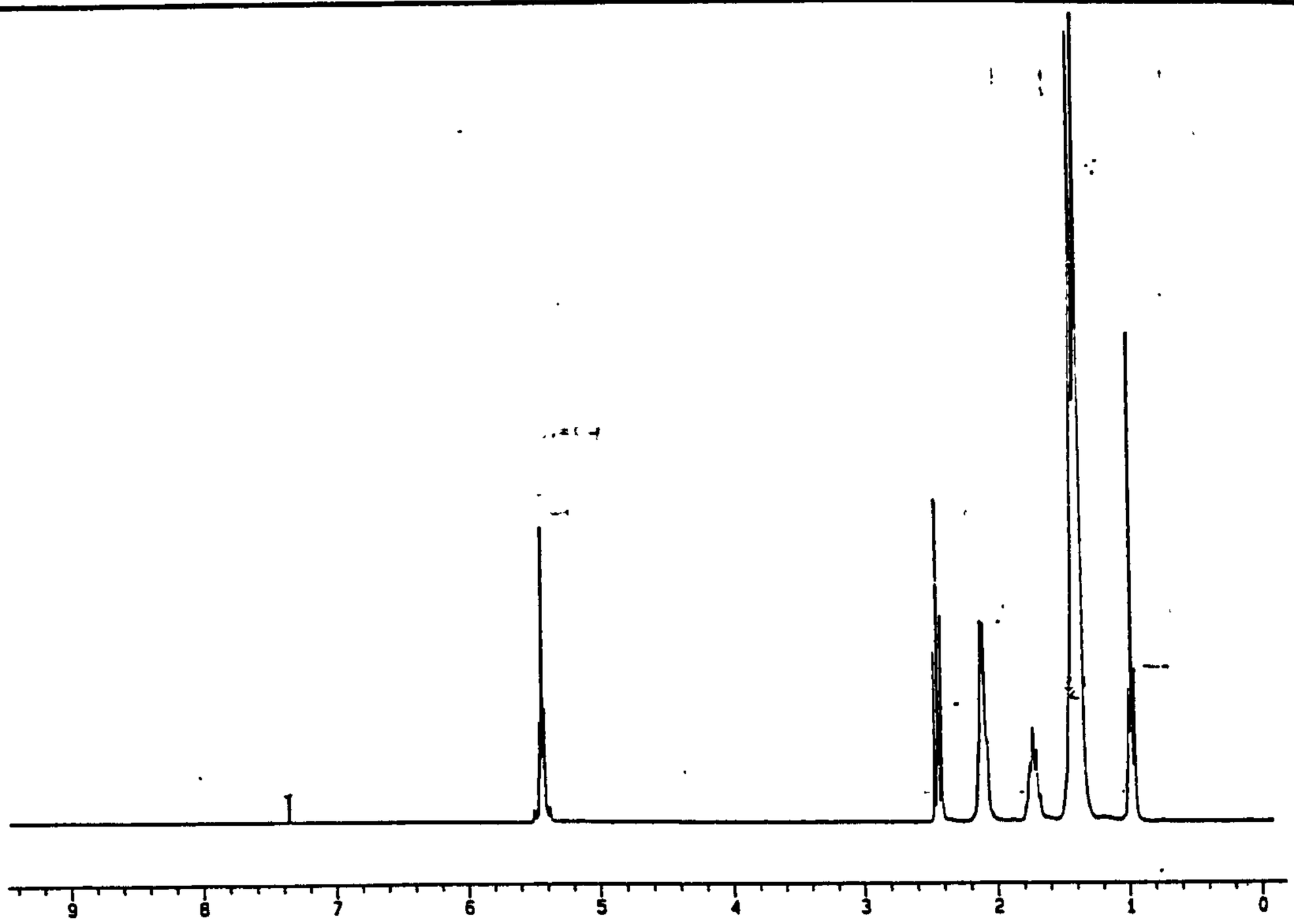

b.

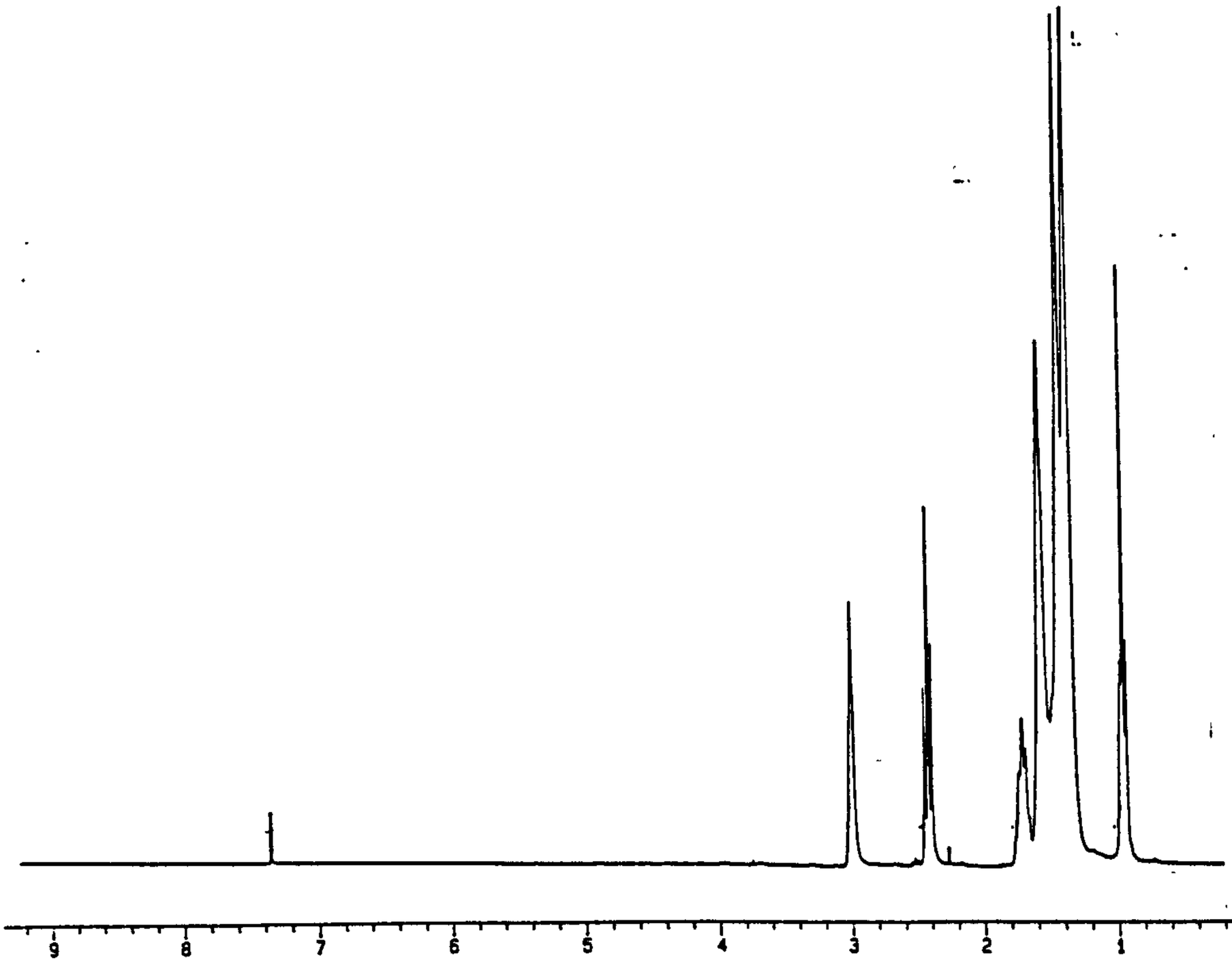

Figure 4.1.a. ^{1}H NMR spectrum of oleic acid showing characteristic alkene and allylic resonances.

Figure 4.1.b. ^{1}H NMR spectrum of oleic acid epoxide, synthesised using buffered 40% PAA, showing epoxide resonances and loss of allylic and alkene resonances.

biocides they are not buffered. Therefore, the reactions of oleic and linoleic acid with 5% and 40% PAA in the absence of buffer was next investigated to enable the stability of the epoxides to ring opening under more realistic conditions to be determined.

4.2.5. Epoxidation employing unbuffered 40% PAA.

Reaction of oleic acid (4.2) with 40% PAA, under identical reaction conditions as previously described (except without the sodium carbonate buffer), yielded epoxide (4.4) as a white solid in 97% yield. There was no evidence in the ^{1}H and ^{13}C NMR spectra that any ring opened products had been formed. Epoxidation of linoleic acid (4.3) yielded di-epoxide (4.5) in 81% yield. Again no evidence of ring opened products was found in the NMR spectra.

4.2.6. Epoxidation employing unbuffered 5% PAA.

Reaction of 5% PAA with oleic acid (4.2), utilising the reaction conditions previously defined, in the absence of sodium carbonate buffer led to the formation of a white solid in 90% yield. However, NMR analysis of this product showed that it was not pure epoxide (4.4), but a mixture of approximately 90% epoxide and 10% of a compound believed to be the diacetate ester (4.6).

This compound displayed resonances in the ^{1}H NMR spectrum at $\delta = 3.75$ and 3.95 which are believed to be due to the methyl protons of the ester and a resonance at $\delta = 5.1$ which is believed to be due to the CH protons. This is substantiated by the ^{13}C NMR spectrum which contains an extra methyl carbon resonance at $\delta = 18$ ppm, thought to correspond to the methyl carbon of the ester and a resonance at $\delta = 105$ ppm believed to be due to the chain carbons attached to the ester groups.

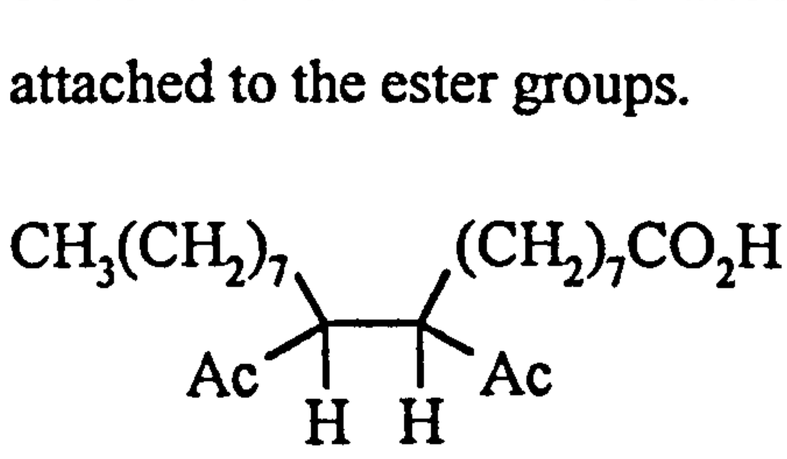

(4.6)

When this experiment was conducted with linoleic acid, the di-epoxide was isolated in a 60% yield (pure by ^{1}H and ^{13}C NMR analysis).

4.2.7. Discussion.

Reaction of oleic acid (4.2) and oleic acid (4.3) with unbuffered 40% PAA produce epoxide (4.3) and di-epoxide (4.5), respectively, in good yield without any evidence of ring-opened products. However, with unbuffered 5% PAA, (which contains more acetic acid) some of the epoxide had undergone ring-opening to form what is believed to be the corresponding diacetate ester. The di-epoxide (4.5) was not ring-opened under these conditions. It is therefore concluded that the synthesis of epoxide derivatives of fatty acids is straightforward, and, in general, produces high yields of pure epoxide although low concentrations of ring opened products have been seen in the case of unbuffered 5% PAA epoxidation of oleic acid. The results are summarised in Table 4.1

Reagent	Yield (4.4) / %	Yield (4.5) / %
2 eq. *m*-CPBA	95	93
3 eq. in PAA buffered 40% PAA	83	78
3 eq. in PAA buffered 5% PAA	95	76
3 eq. in PAA 40% PAA	90[a]	60
3 eq. in PAA 5% PAA	97	81

a. This product was estimated to be a 10:1 mixture of epoxide (4.5): diacetate ester (4.6) by NMR.

Table 4.1. Yields of oleic and linoleic acid epoxides using the reagents indicated.

4.3. EPOXIDATION OF PHOSPHATIDYLCHOLINE.

The epoxidation of cellular phospholipids was next investigated in order to explore the ease of the reaction on these substrates. Cell membranes contain phospholipids in two forms, phosphatidylcholine (4.7) and phosphatidylethanolamine (4.8), where R^1 and R^2 are fatty acid chains. In mammalian cells the majority of cellular phospholipid is in the form of phosphatidylcholine, whereas as in bacterial systems the majority of the phospholipid is in the form of phosphatidylethanolamine.[86]

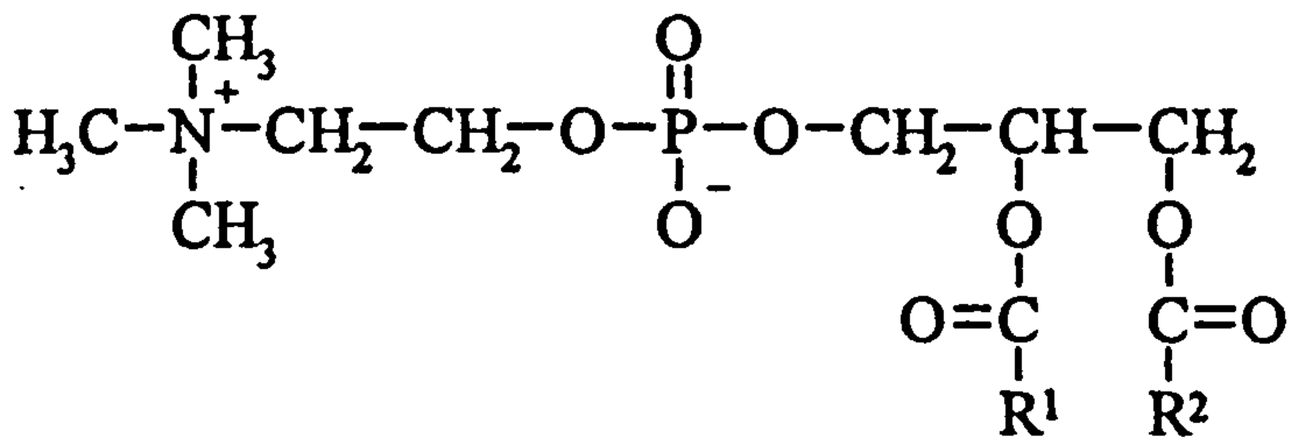

(4.7)

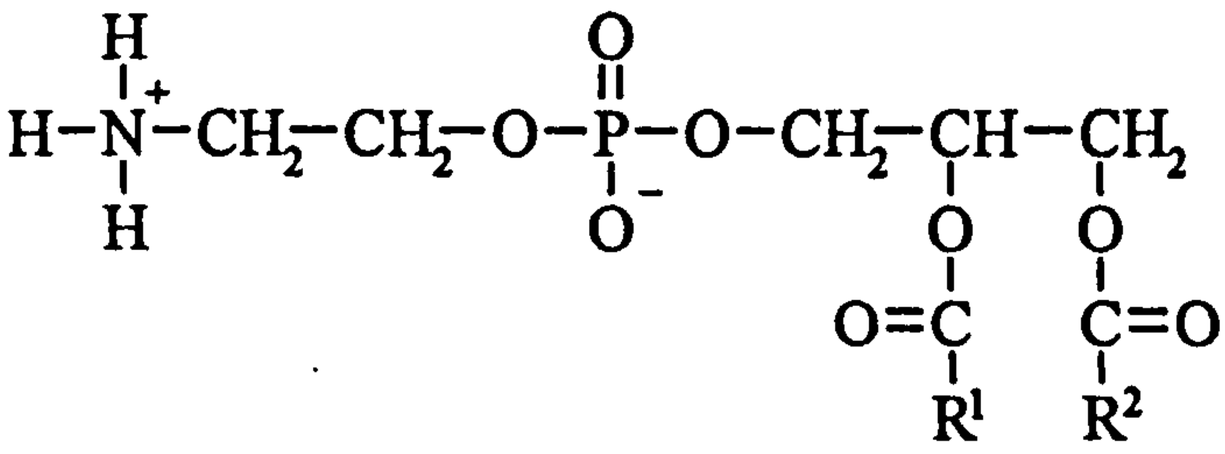

(4.8)

Despite the predominance of phosphatidylethanolamine in bacterial cells, phosphatidylcholine was used in this study since it is more readily available. It was obtained as a mixture of compounds with varying fatty acid moieties.

4.3.1. Epoxidation using *m*-CPBA.

Phosphatidylcholine was obtained as an essentially pure mixture of phospholipids in chloroform solution (100 mg ml^{-1}). A 1 ml aliquot was removed and the solvent was removed under reduced pressure to leave a sticky pale yellow oil. This was redissolved in 2 ml of dichloromethane and 0.002 moles of *m*-CPBA was added. The reaction mixture

was stirred overnight and worked up as described previously to yield a sticky yellow oil. (The yield was not determined since the exact composition of the starting material was not known).

The ^{1}H NMR spectrum displayed several differences when compared to that of the starting material. The resonances in the ^{1}H NMR spectrum at δ = 2.0 ppm corresponding to the allylic resonances were not evident in the product. The resonances corresponding to the alkene protons at δ = 5.25 ppm were also lost. A peak at δ = 3.0 ppm was seen which is believed to correspond to the phosphatidylcholine epoxides. The fully decoupled ^{13}C NMR spectrum displayed these differences with greater clarity. The resonances corresponding to the alkene carbons (δ = 128 -130 ppm) were not evident but a new peak was observed at δ = 57 ppm which is believed to correspond to the phosphatidylcholine epoxides. This was verified by the off resonance ^{13} C NMR spectrum which showed that this peak was due to CH protons.

4.3.2. Epoxidation employing 40% PAA.

The reaction was repeated employing 40% PAA. 0.0038 moles (total AvOx) of PAA were added to a stirred solution of the phosphatidylcholine in dichloromethane. The reaction was treated and worked up as previously described and the product was isolated as a sticky yellow oil. ^{1}H and ^{13}C NMR (see Figure 4.1.a and 4.1.b) spectroscopy showed that the product was a pure mixture of phosphatidylcholine epoxides. No evidence for either unreacted starting materials or ring opened products was observed.

The reaction was next repeated employing unbuffered 40% PAA to see determine whether evidence for any ring opened products could be obtained. Analysis of the product by NMR spectroscopy showed that it was a pure sample of the epoxidised mixture.

4.3.3. Epoxidation employing 5% PAA.

0.03 moles (total AvOx) of 5% PAA was added to a stirred solution of phosphatidylcholine and the reaction treated as previously described. Upon work up the

a.

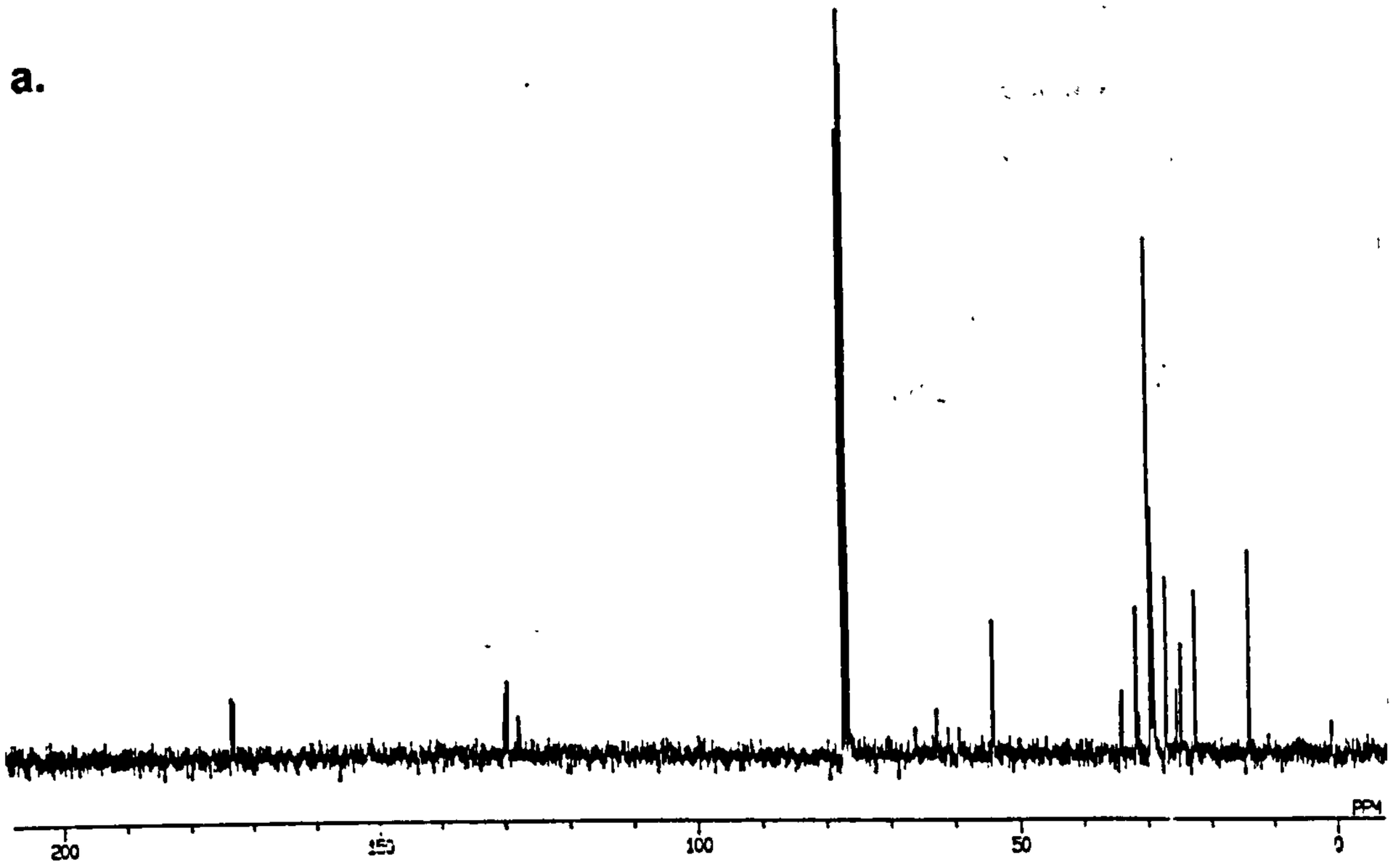

b.

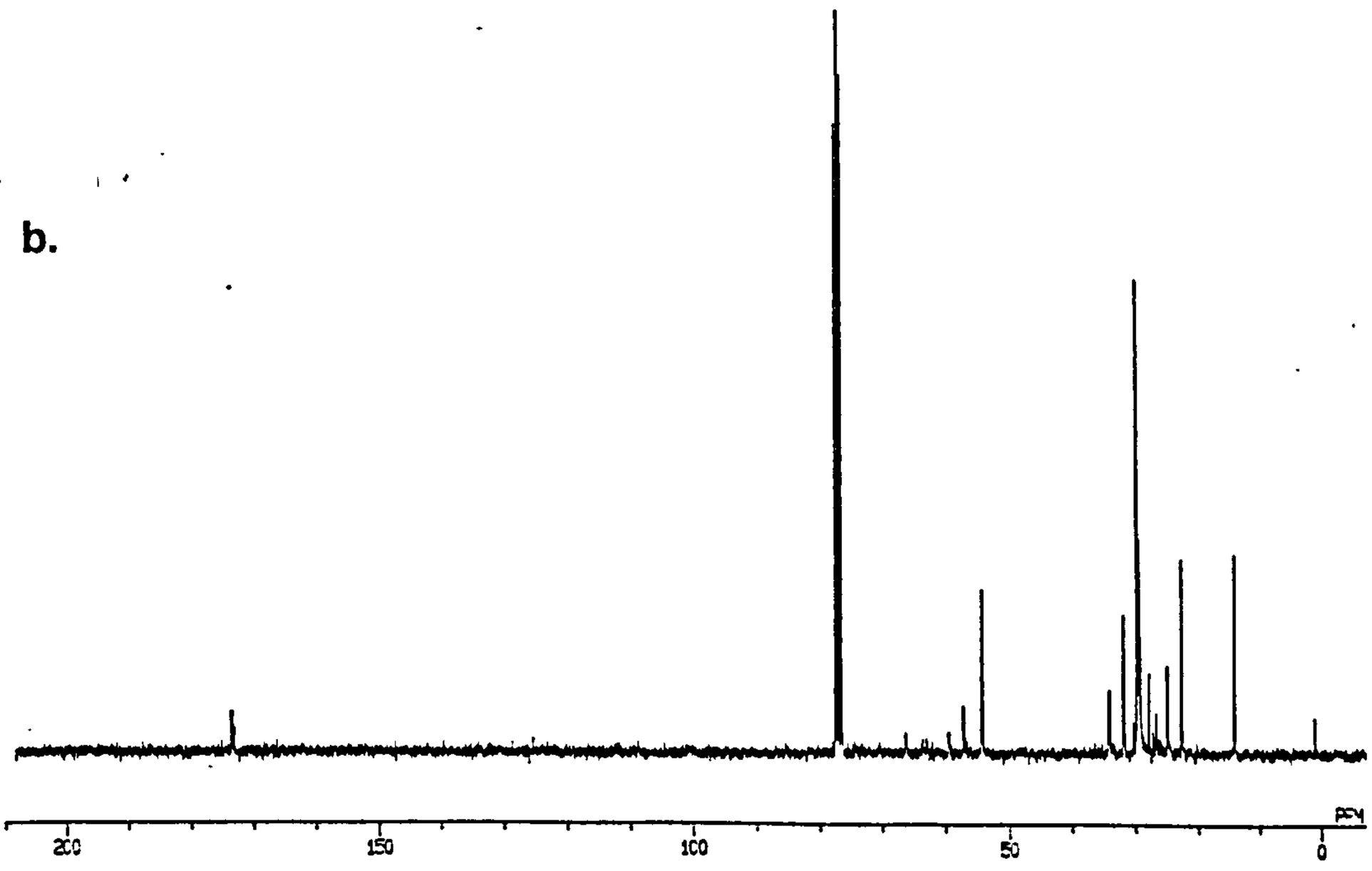

Figure 4.2.a. ^{13}C NMR spectrum (fully proton decoupled) of phosphatidylcholine showing alkene resonances.

Figure 4.2.b. ^{13}C NMR spectrum (fully proton decoupled) of phosphatidylcholine epoxide, synthesised using buffered 40% PAA, showing epoxide resonances and loss of alkene resonances.

product was isolated as a sticky yellow oil. The ^{1}H and ^{13}C NMR spectra of this product showed that a trace of phosphatidylcholine remained, but that the epoxide predominated in the reaction mixture. It was not possible to work out an exact ratio of alkene:epoxide since the exact composition of the materials was not known.

Experiments in which unbuffered 5% PAA was employed led to the production of pure epoxide. This is slightly surprising given that oleic acid epoxide was found to undergo ring opening under these conditions, and therefore some of the epoxides formed in phosphatidylcholine would be expected to undergo ring-opening. However, if they only form a small proportion of the reaction mixture it is possible they may not be seen. In addition, the exact alkene:peroxyacid ratio is not known in the reactions with phosphatidylcholine so it is possible that there may be insufficient acid present to ring open the epoxide.

4.3.4. Discussion.

The epoxidation of phosphatidylcholine is easily accomplished with both 5 and 40% PAA and with *m*-CPBA. Isolation of the products and ^{1}H and ^{13}C NMR spectroscopy showed that the products were essentially mixtures of pure epoxides.

4.4. EPOXIDATION OF UNILAMELLAR LIPOSOMES.

It was next decided to investigate whether epoxidation could still occur if the phospholipids were formed into unilamellar liposomes. This would allow an insight to be gained into the possibility of epoxidation occurring in bacterial cell membranes. Liposomes are well-defined models for biological membranes (see Figure 4.3) and offer the advantage over real biological membranes that the composition can be easily controlled, for example molecules such as spin-probes may easily be incorporated (see later).

10 ml of 0.01g ml^{-1} unilamellar liposomes in 0.05 M Chelex-treated Na_2SO_4 were prepared as described in Chapter 6. 0.002 moles of *m*-CPBA was added and the reaction

a.

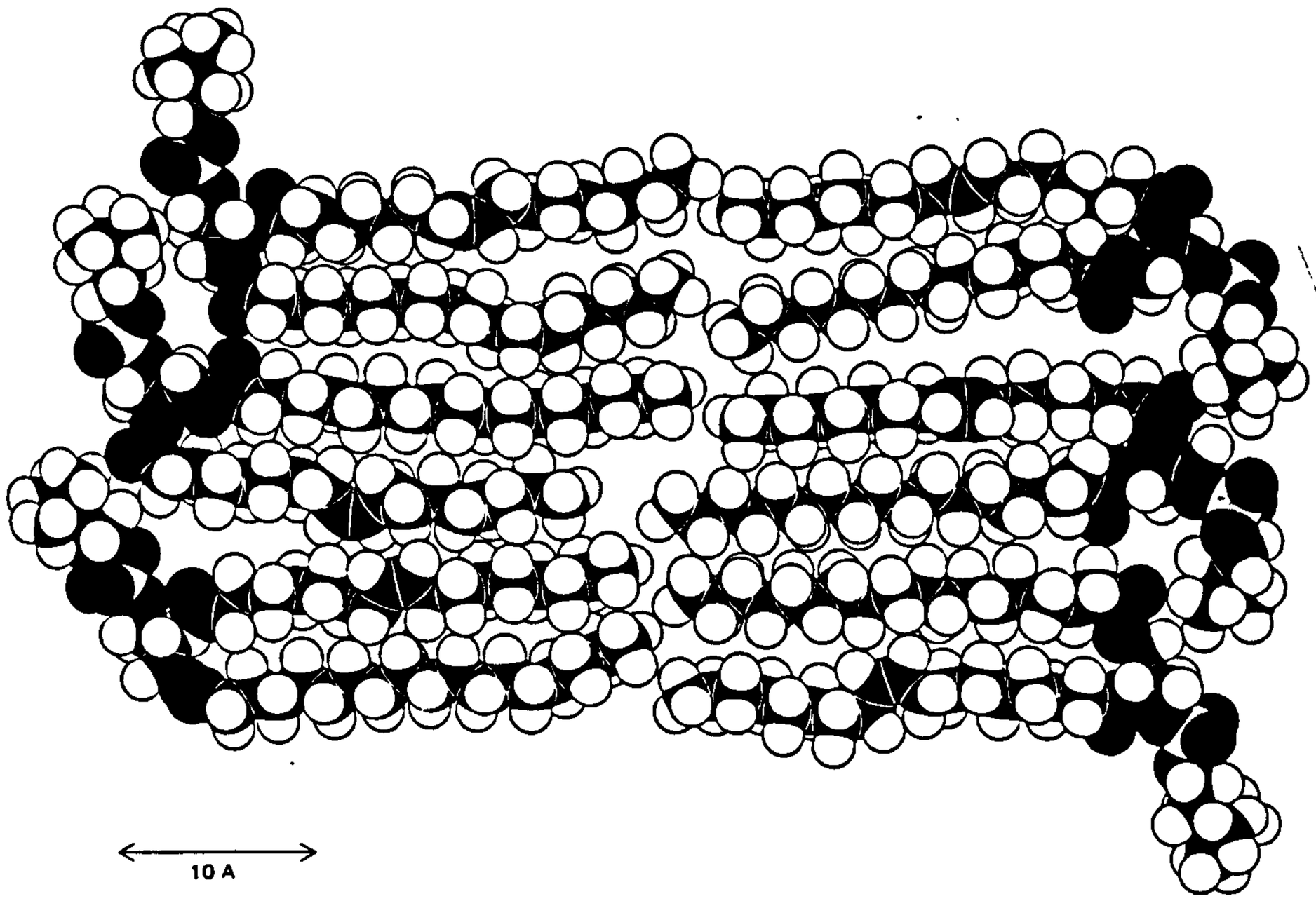

b.

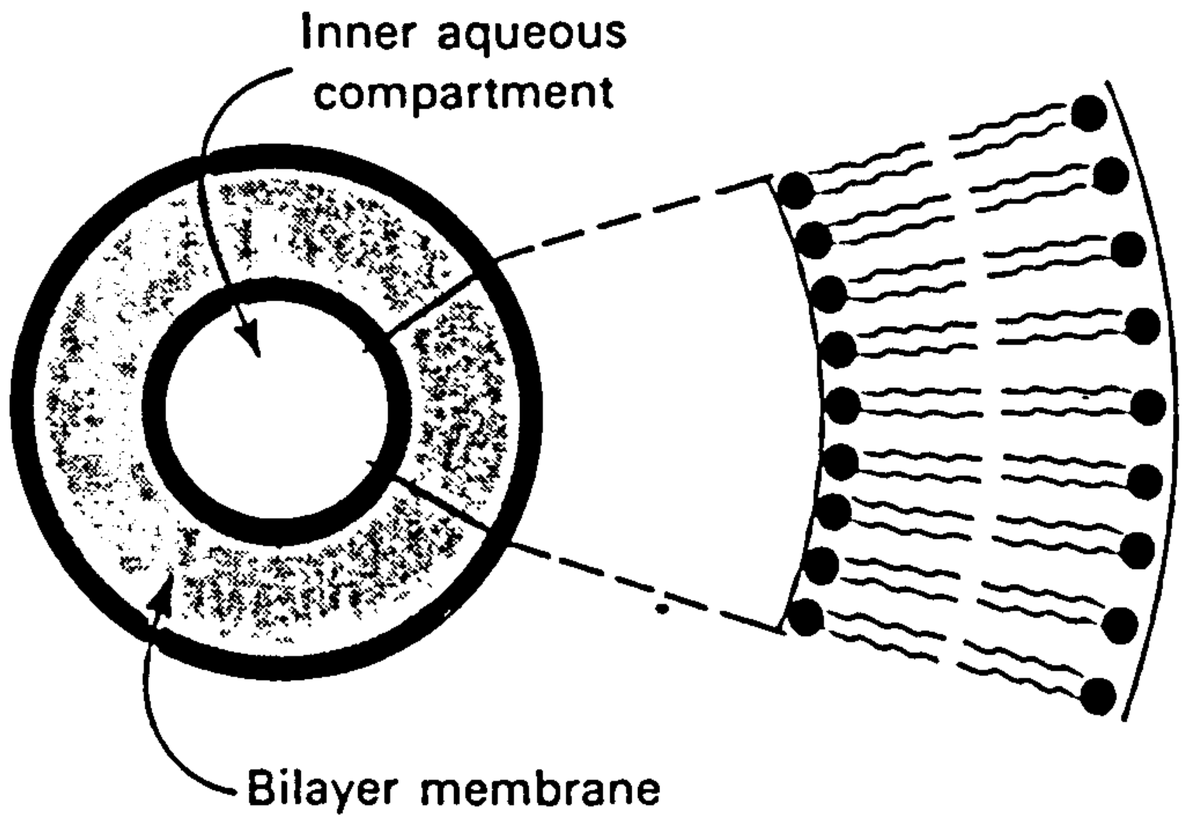

Figure 4.3.a. Space-filling model of a section of a phospholipid bilayer.

Figure 4.3.b. Representation of a unilamellar liposome.

Both diagrams are reproduced from reference 86.

mixture stirred under nitrogen overnight. It was noted that the *m*-CPBA was not very soluble in the sodium sulfate, but it was believed that enough would dissolve to facilitate the reaction. Upon extraction of the lipid material with diethyl ether and subsequent work up, the NMR spectrum of the reaction mixture comprised of signals attributable only to unreacted phospholipid. It was decided not to repeat this reaction with a higher concentration of *m*-CPBA since the aqueous solvent used in the experiments was already saturated.

Unilamellar liposomes were then mixed with 0.0038 moles (total AvOx) of 40% PAA and 0.003 moles of sodium carbonate and stirred under nitrogen overnight. The lipid was extracted with diethyl ether and worked up as previously described. Initial experiments on this reaction system led only to the recovery of unreacted phospholipid. This may be a result of dilution of the peroxygen by the aqueous liposome preparation, as well as the organised structure of the liposomes protecting the phospholipids from attack by the PAA. The experiment was therefore repeated using 0.038 moles (total AvOx) of 40% PAA (and 0.03 moles of sodium carbonate). After extraction and work up the lipid material was isolated as a viscous yellow oil. The NMR spectra of this reaction mixture showed that some conversion of the phospholipid to phospholipid epoxide had occurred, although a small amount of unreacted phospholipid remained. This reaction was repeated in the absence of buffer in order to examine ring opening of the phospholipid epoxides. NMR analysis of the reaction products provided no evidence for ring opened phospholipid epoxides.

Treatment of unilamellar liposomes with 0.03 moles (total AvOx) 5% PAA and 0.02 moles of sodium carbonate gave, upon extraction and work up, a sticky yellow oil. ^{1}H and ^{13}C NMR analysis of this mixture showed that it contained only unreacted phospholipid. Attempts at repeating this reaction at higher concentrations of 5% PAA were unsuccessful. This was due to the lipid mixture forming a thick, soapy foam with the high concentrations of 5% PAA and sodium carbonate buffer making extraction of the lipid impossible. However, the reaction was repeated with a higher concentration of 5% PAA [0.3 moles (total AvOx] in the absence of sodium carbonate buffer. Isolation and analysis of this product mixture showed it to be comprised only of unreacted phospholipid.

4.4.1. Discussion.

Evidently, due to its lack of solubility in aqueous systems, *m*-CPBA does not lead to epoxidation of phospholipids in liposomes. 5% PAA in moderate and high concentrations does not lead to the epoxidation of liposomal membranes. However, it has been demonstrated that although it is more difficult to accomplish, the reaction of phospholipids, in the form of liposomes, with 40% PAA yields a high concentration of phospholipid epoxides, either in the presence or absence of sodium carbonate buffer.

This has important consequences for the reactions of PAA in cells. It is anticipated that peroxidation of lipid membranes will predominate in the presence of redox-active transition-metals. However, in areas of the membrane which contain low concentrations of transition-metal ions, or where the transition-metal ions have been rendered redox inactive by sequestration, the introduction of epoxides into membranes may be involved in peroxygen toxicity towards bacteria. It was therefore decided next to investigate if introduction of epoxide groups into membranes in the place of double bonds had any effect on the structural integrity of the membrane, using the spin-probe technique.

4.5. SPIN-PROBE STUDY INTO THE EFFECTS OF EPOXIDATION ON MEMBRANE FLUIDITY.

The spin-probe technique has been widely used for the assessment of physical properties in a variety of contexts. The technique has been employed for the determination of oxygen concentration,[225] measurements of local motion[218,226-232] and polarity measurements.[226,227,230-233] The spin-probe, usually a nitroxide, must be inert to chemical modification in the medium in which it is to be used and must not cause perturbation to the property of the system which is to be determined. Examples are shown [(4.9) - (4.12)] which include those to be utilised here.

Spin-probes can be designed so that they can be used in a variety of environments. For example they may be hydrophobic [eg. (4.9) and (4.12)], hydrophilic [eg. (4.11)] or amphiphilic [eg. (4.10)]. The doxyl stearic acid series is particularly useful when

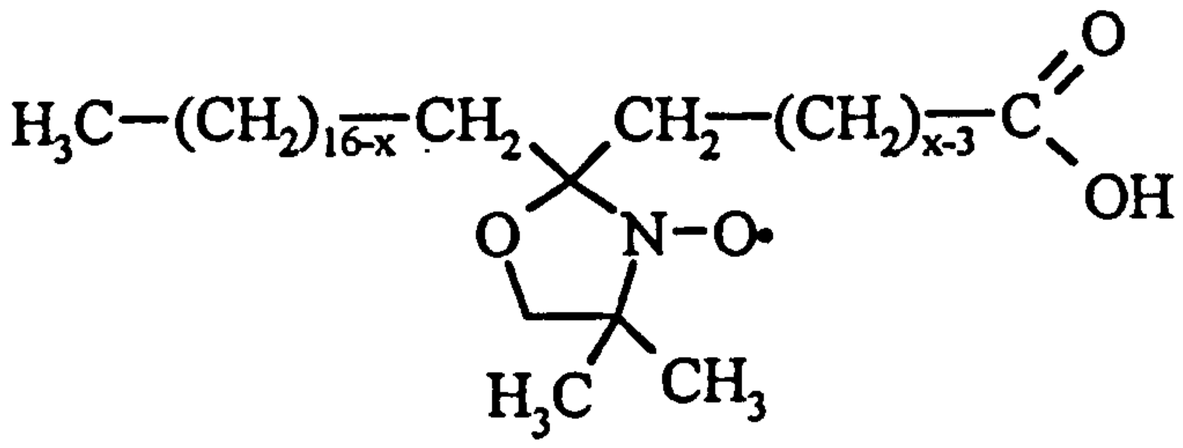

x = 5, 7, 10, 12, 16

x-doxyl stearic acid (x-DSA)

(4.9)

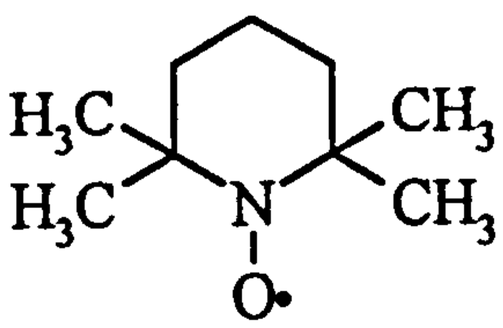

2,2,6,6-tetramethyl-piperidine -1-oxide (TEMPO)

(4.10)

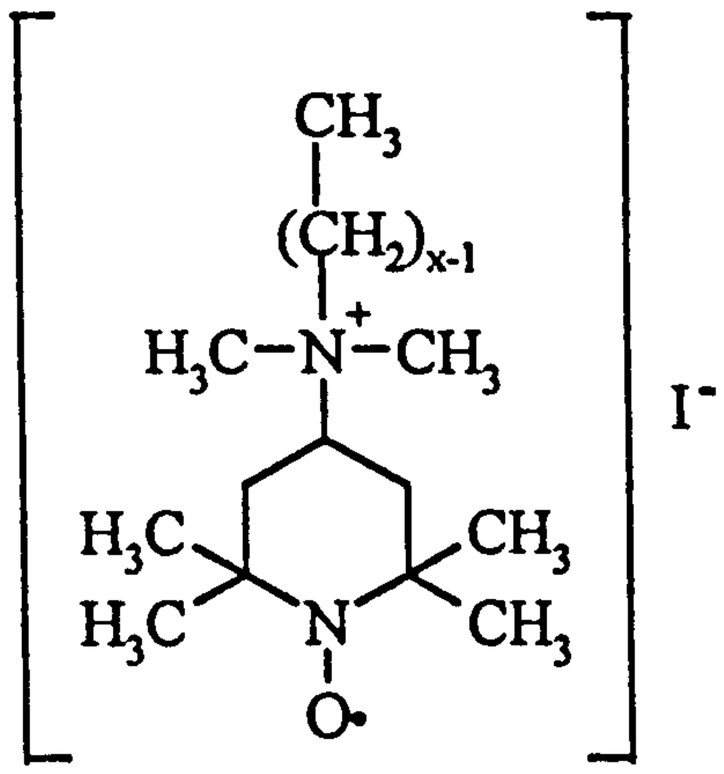

x = 4, 8, 11, 16

(4-[*N,N*-dimethyl-*N*-(methylene)$_x$] ammonium-2,-6,6-tetramethyl-piperidine-1-oxyl iodide (CAT-x)

(4.11)

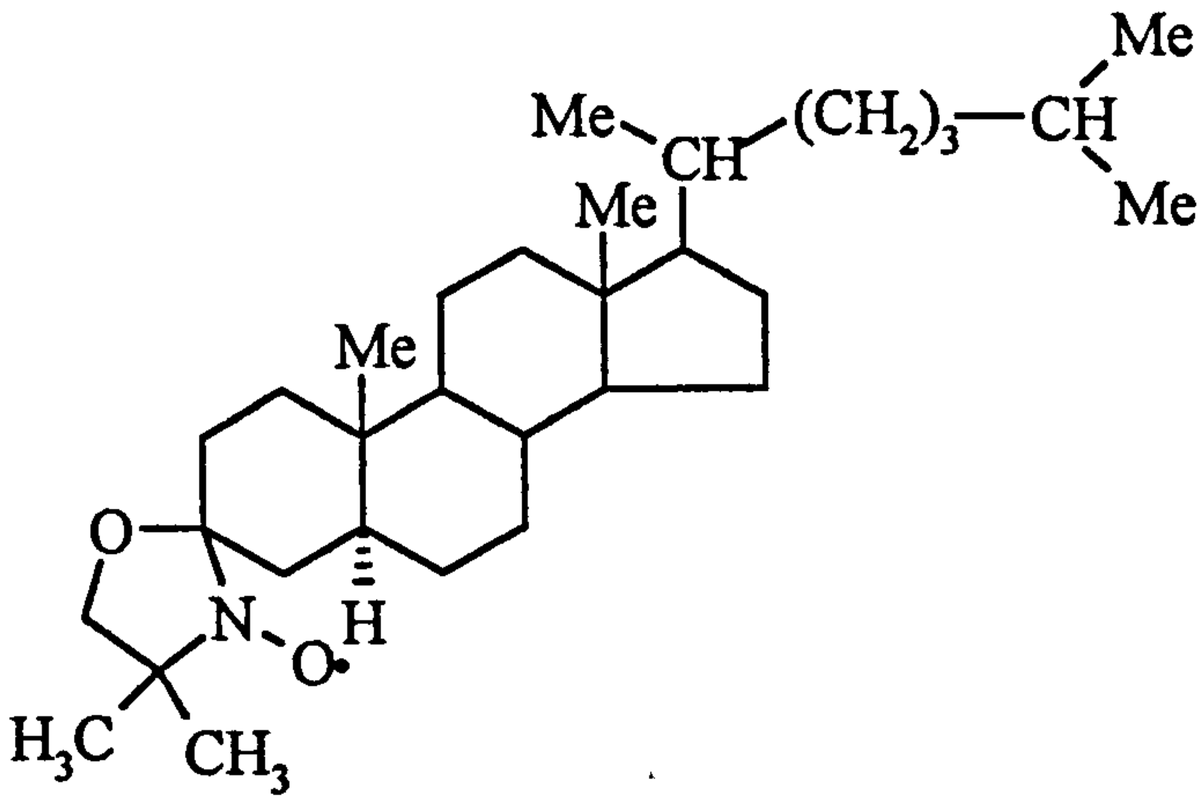

3-β-doxyl 5-α-cholestane

(4.12)

examining membranes, because they align so that their long axes are parallel to the long axes of the fatty acid chains of the membrane.[218] Since doxyl stearic acids may be obtained with their nitroxide groups at various positions along the chain, this allows the membrane to be examined along the entire length of the fatty acid chains, hence providing detailed information about localised changes within the membrane.

Much information concerning the physical properties of a system can be gleaned from the EPR spectra of spin-probes. The relative polarity of a solvent may be determined by the nitrogen splitting of the nitroxide.[227] In solvents of lower polarity the nitrogen splitting is low than in solvents of high polarity as the resonance structure (4.13) is of greater significance, whereas in more polar solvents the resonance structure (4.14) is more important. In this structure spin density is located on the nitrogen atom and hence the nitrogen splitting will be observed to increase with increasing solvent polarity.[227]

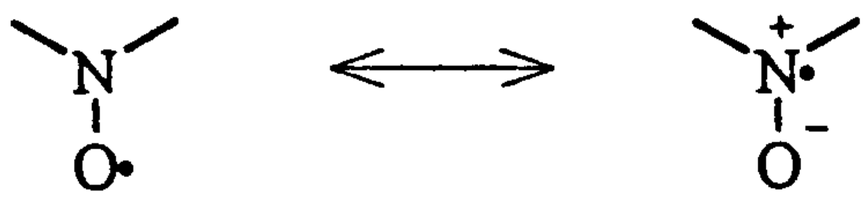

(4.13) **(4.14)**

Secondly, the linewidth may be determined in order to assess the oxygen concentration in a system; the linewidth increasing as the oxygen concentration increases.[225] This occurs because oxygen is paramagnetic and therefore reduces the spin-spin relaxation time so increasing the uncertainty of the energy levels of the unpaired electron. Paramagnetic broadening also occurs as a consequence of the presence of high concentrations of other paramagnetic species, including the probe itself, hence care needs to be exercised when examining these systems.

As the movement of the nitroxide becomes more restricted the EPR spectra become increasingly anisotropic due to incomplete averaging of all the orientations of the nitroxide in the magnetic field.[134] However this does not prevent useful information being gained from the spectra.

Spin-probe spectra are characterised in a number of ways. If the spectra are largely isotropic in appearance they may be characterised by τ_c which is the average time taken for the spin-probe to complete one complete rotation and is calculated as shown in

equation (4.1) from spectral measurements illustrated in Figure 4.4.a as described by McConnell *et al.*[227] Values of τ_c typically range between 10^{-11} s for a freely-tumbling nitroxide and 10^{-7} s for a nitroxide which is experiencing severe motional restriction. Measurement of τ_c has been used to examine the properties a wide number of systems including polymers,[232] mitochondria,[226] liposomes,[218] polypeptides[227] and proteins.[227]

$$\tau_c = 6.51 \times 10^{-10}\, \Delta H(0)\, [\{h(0)/h(1)\}^{½} + \{h(0)/h(-1)\}^{½}] \qquad \textbf{Eqn. 4.1}$$

where

$\Delta H(0)$ is the linewidth of the central line in Gauss

$h(-1)$, $h(0)$, and $h(1)$ are the heights of the low, mid and high field lines, respectively

However, when the spectra are more anisotropic in nature, difficulties arise in measuring the linewidth and peak heights with any degree of accuracy. EPR spectra of this nature are usually interpreted in terms of their *order parameter*, S which is related to the mean angular deviation of the spin-probe from its average orientation; for example in a host crystal where the motional anisotropy is maximal, S = 1 and in an isotropic environment S = 0.[235] S can be easily calculated as shown in equation (4.2) from the measurement of spectral features as indicated in Figure 4.4.b. The order parameter has been used to characterise the motion of a nitroxide in systems including liposomes,[218,230] reverse micelles,[231] and various mammalian cells.[228,229]

$$S = A_{\parallel} - A_{\perp} / A_{zz} - ½(A_{xx} + A_{yy}) \qquad \textbf{Eqn. 4.2}$$

where

$A_{\parallel}$ and $A_{\perp}$ are the half distances between the outer and inner extrema of the experimental spectra, respectively

A_{xx}, A_{yy} and A_{zz} are the principal elements of the A tensor in the absence of molecular motion

The aim of this study is therefore to characterise the structure of unilamellar liposomes comprised of phosphatidylcholine epoxide relative to those comprised of

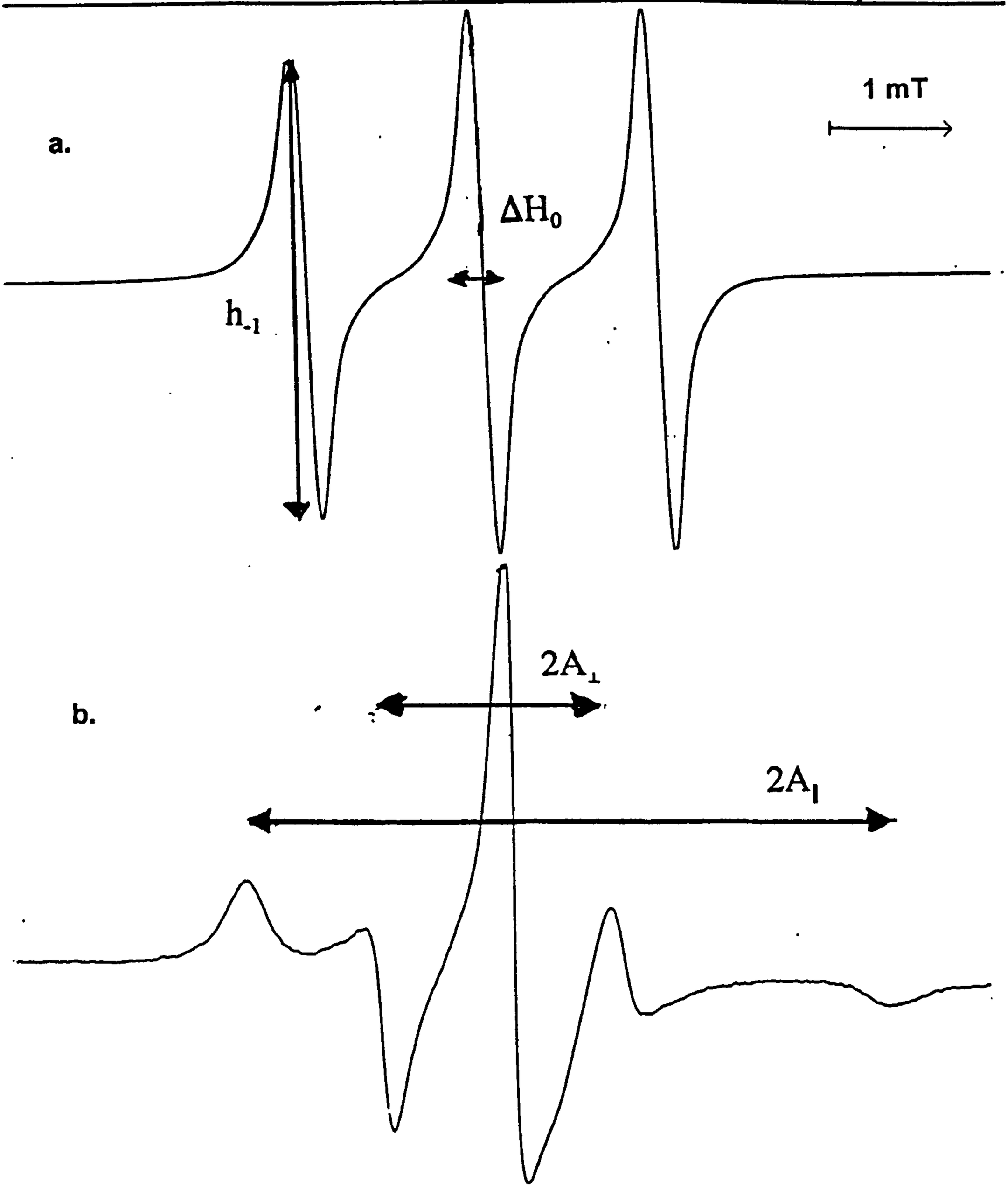

Figure 4.4.a. Isotropic EPR spectrum of 5-doxyl stearic acid in $CHCl_3$ showing the measurements required to calculate the rotational correlation time, τ_c the length of time taken for the spin-probe to complete a single rotation.

Figure 4.4.b. Anisotropic EPR spectrum of 5-doxyl stearic acid in a liposome showing the measurements required to calculate the order parameter, S, a measurement relating to the mean angular deviation of the spin-probe from its average orientation.

phosphatidylcholine using the spin-probe technique. The structure will be characterised in terms of the rotational correlation time (τ_c) when it is believed that this can be calculated with accuracy and the order parameter, S. It is also proposed to examine the polarity throughout the membrane structure by comparing the values of a_N, the nitrogen hyperfine splitting. Where this cannot be determined directly from the experimental spectra with any great degree of accuracy, it will be calculated using equation 4.3.

$$a_N = \frac{1}{3}(A_{\parallel} + 2A_{\perp}) \qquad \textbf{Eqn. 4.3.}$$

The spin-probes to be employed in this study are the doxyl series of probes (4.9), since the model membrane may be examined along its entire depth by employing this series of probes and studies of both model systems[218,231,232] and intact cells[226,228,229] which have employed this series of probes have proved to be very informative.

The doxyl stearic acid series of spin-probes allows changes in membrane characteristics to be monitored along the depth of the membrane. 5-Doxyl stearic acid has its nitroxide group closest to the polar carboxylate group of the probe and hence the nitroxide is located closest to the membrane surface. In contrast, in 16-doxyl stearic acid the nitroxide is located at the opposite end of the chain to the acid moiety and hence is located deep within the hydrophobic core of the membrane, where its motional freedom is greatest.[218] The EPR spectra of this species when it is located in a membrane are therefore almost isotropic in appearance This observable difference in spectral characteristics, implying a difference in membrane properties throughout the depth of the membrane has been termed the *transmembrane fluidity gradient.*[218,228]

4.5.1. Examination of the transmembrane fluidity gradient and the transmembrane polarity gradient.

Experiments involved the synthesis of phosphatidylcholine epoxide from phosphatidylcholine as described in 4.3.2 and in detail in Chapter Six, using buffered 40% PAA. 0.02 mg ml^{-1} unilamellar phosphatidylcholine / phosphatidylcholine epoxide

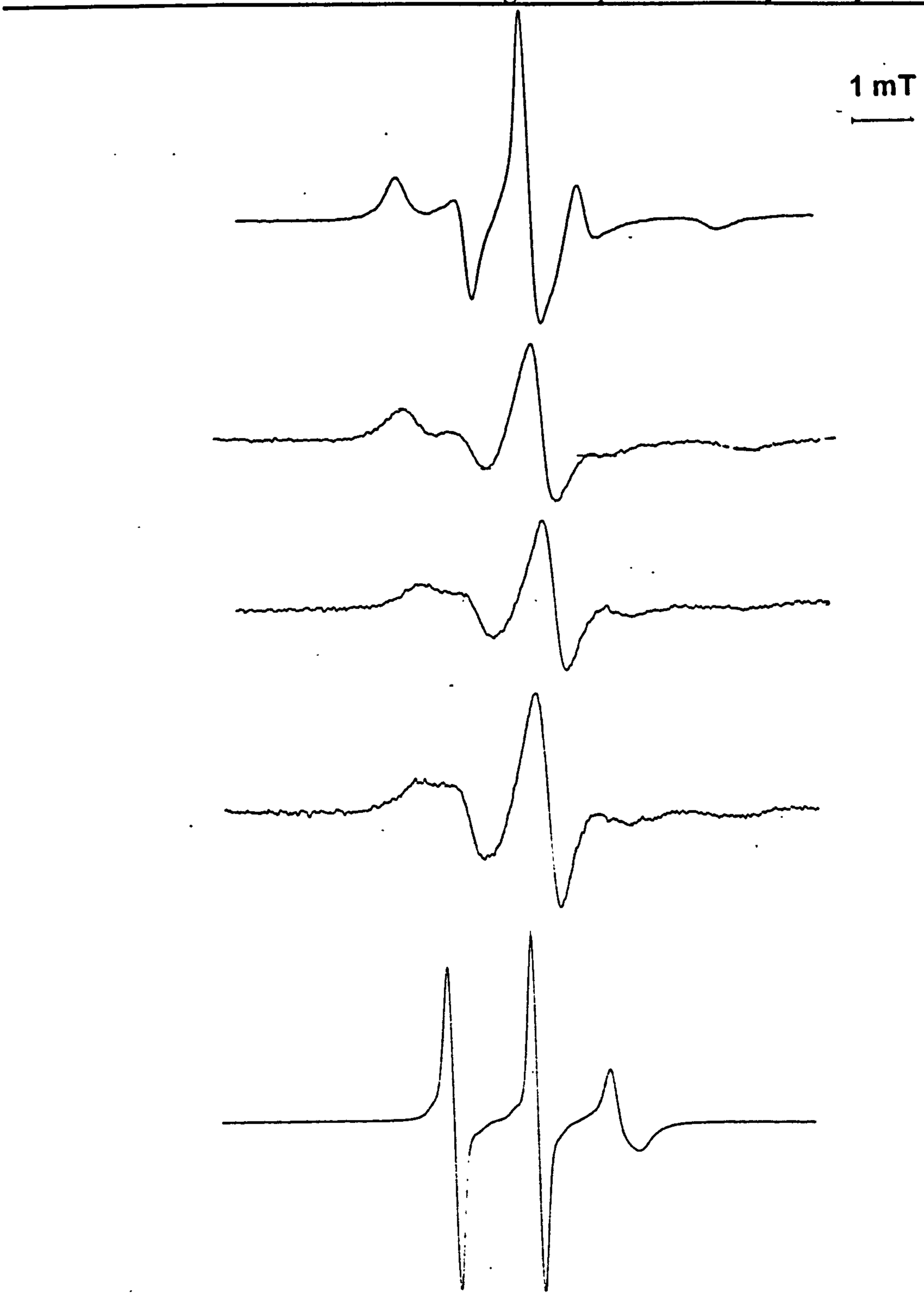

Figure 4.5. EPR spectra showing the increase in motional freedom experienced by the nitroxide groups of doxyl stearic acids in unilamellar phosphatidylcholine liposomes as the nitroxide group is moved from the 5 to the 16 position on the fatty acid chain.

liposomes in the presence of the spin-probes 5, 7, 10, 12 and 16-doxyl stearic acid, at a spin probe to lipid ratio of approximately 1:250 w/w, were formed as described in Chapter Six. EPR spectra of the resulting translucent mixtures were recorded as soon after preparation as possible. In all cases the spectra were characterised by their order parameter, S. The values for A_{xx}, A_{yy} and A_{zz}, the components of the A tensor in the x, y and z directions respectively were taken as 0.63 mT, 0.58 mT and 3.35 mT respectively.[234] The spectra in which 16 doxyl stearic acid was employed showed mainly isotropic motion, hence the inner exterma were not resolved. In this instance it was necessary to set $A_{\parallel} + A_{\perp} = 4.45$ mT as described by Gaffney[228] and calculate $A_{\perp}$ from this. The large degree of isotropic motion observed in the case of 16-doxyl stearic acid also allowed calculation of the rotational correlation time, τ_c.

Ir can be seen (Figure 4.5) that the difference in membrane fluidity as the membrane is traversed is clearly reflected in the EPR spectra. Examination of the spectrum in which the spin-probe employed is 5-doxyl stearic acid shows that the motion of the nitroxide group of the spin-probe is very restricted. This is reflected by the order parameter of 0.60 ± 0.03. Although an increase in order is observed on changing the spin-probe from 5 to 7-doxyl stearic acid, the general trend that is observed is that the order parameter decreases as the nitroxide group becomes closer to the hydrophobic core of the bilayer, the order parameter being 0.29 ± 0.01 for 16-doxyl stearic acid (see Figure 4.6). This is as expected, the motional freedom of the nitroxide, as measured by the degree of "wobble" about its long axis increases as the nitroxide gets further from the conformationally restricted outer face of the membrane.

Calculation of the rotational correlation time for 16-doxyl stearic acid in unilamellar liposomes gives a value of $1.62 \times 10^{-9} \pm 0.15 \times 10^{-9}$ s, which indicates fairly rapid rotation of the spin-probe around its long axis. This is a reflection of fairly rapid tumbling of the nitroxide close to the core of the membrane. However it is evident, by comparison to the value of τ_c obtained for the nitroxide in chloroform ($2.39 \times 10^{-10} \pm 0.28 \times 10^{-10}$ s) that the nitroxide is still located in the membrane.

Comparison of the spectra obtained with those obtained from liposomes comprised of phosphatidylcholine epoxide show a similar trend, in that the transmembrane fluidity

gradient is maintained. The order parameter for 5 doxyl stearic acid is 0.65 ± 0.05 which is similar to that obtained for 'normal' liposomes. Similarly, in the hydrophobic core of the membrane the order parameter was very similar to that obtained in phosphatidylcholine liposomes, 0.34 ± 0.005 as opposed to 0.29 ± 0.01 However, calculation of the order parameters for spin-probes with the nitroxide groups in the 7,10 and 12 positions reveal that the amplitude of motion of the nitroxide had decreased more in the middle of the fatty acid chain as compared to 'normal' liposomes, a phenomenon which has previously been observed for peroxidised liposomes.[227] This is the area in which double bonds are located in liposomes comprised of phosphatidylcholine and therefore the area in which the epoxides are situated. This increase in rigidity of the membrane at the centre of the fatty acid chains is substantial, typical differences in the order parameter being ≥ 0.05 (Figure 4.6) and may be of consequence in the bactericidal action of peroxygen biocides.

The rotational correlation time for 16 doxyl stearic acid in unilamellar phosphatidylcholine liposomes was also calculated to be $1.75 \times 10^{-9} \pm 0.27 \times 10^{-9}$ s. This is the same, within error, as that observed for 'normal' liposomes and is believed to be a result of the reduced effect of epoxidation at the 'ends' of the fatty acid chains as compared to the middle.

The polarity of the membranes was next investigated by examining the values for a_N. Where appropriate these were measured directly form the spectrum, but where this was precluded by anisotropy this was calculated using equation 4.3. Examination of the spectra of spin-probes in phosphatidylcholine liposomes show that when the probe is changed from 5 to 7-doxyl stearic acid an increase in a_N is observed, indicating an increase in polarity. However, as the probe is changed to 10, 12 and 16-doxyl stearic acid the a_N decreased (see Figure 4.7). This is believed to be a reflection of the nitroxide group of the probe residing deeper in the hydrophobic core of the bilayer.

These results can be compared to those obtained with phosphatidylcholine epoxide liposomes. Similar values for a_N were found at either end of the fatty acid chains, the mean values being within 0.02 mT of the values obtained for liposomes comprised of phosphatidylcholine. However, the values of a_N obtained for 7, 10 and 12 doxyl stearic

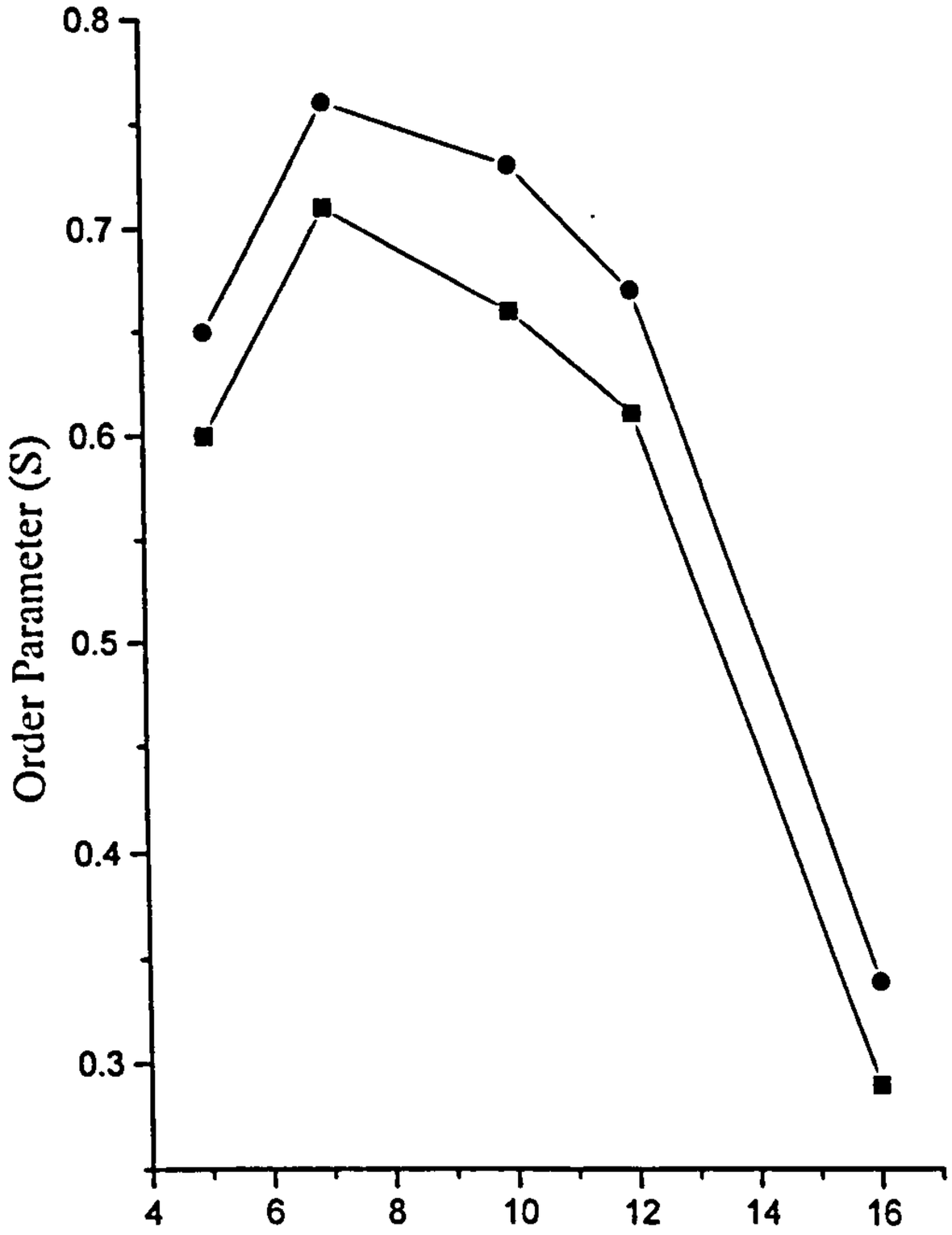

Figure 4.6. The change in membrane fluidity as measured by the change in order parameter, S, of doxyl stearic acids in liposomal membranes comprised of phosphatidylcholine and phosphatidylcholine epoxide

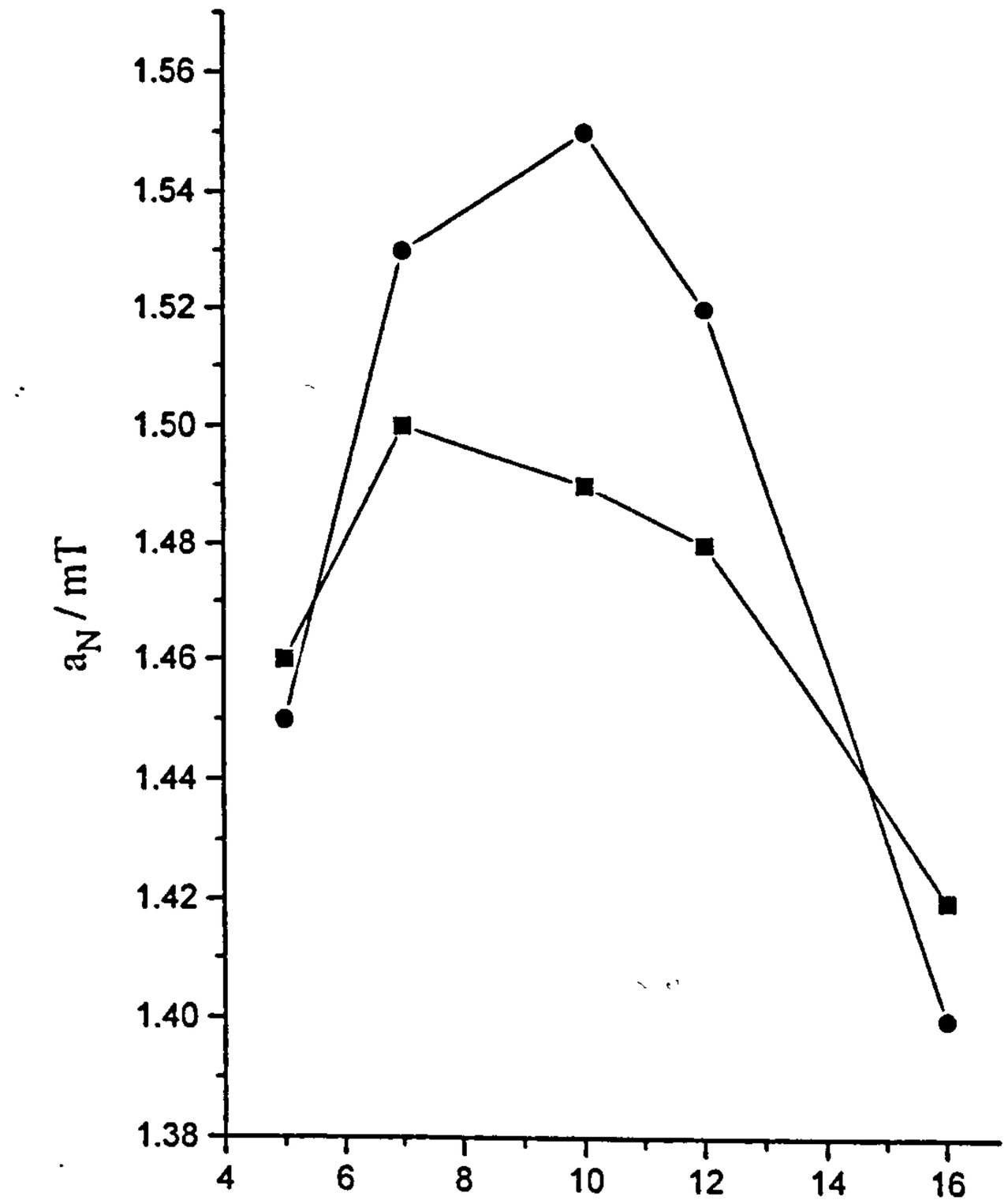

Figure 4.7. The change in polarity of the environment of doxyl stearic acid spin-probes, as measured by a_N, as the liposome composition is changed from phosphatidylcholine to phosphatidylcholine epoxide

acids in liposomes were much higher than those obtained in 'normal' liposomes, indicating a substantial increase in polarity in the middle of the fatty acid chains (see Figure 4.7). This is not unexpected, since the double bonds have been transformed into epoxides and would therefore be expected to be more polar.

4.5.2. Discussion.

The results obtained show that when liposomes are comprised of epoxidised phosphatidylcholine the fluidity of the membrane, as measured by the order parameter of doxyl stearic acid spin-probes, is reduced. The reduction is not entirely uniform however, the greatest difference being observed for 7, 10 and 12 doxyl stearic acids, which have their nitroxide groups situated in the middle of the fatty acid chains in the areas in which the double bonds of the membrane phospholipids are situated..[215,216]

Similarly epoxidation of phosphatidylcholine leads to a significant difference in polarity, as measured by the values of a_N, in the middle of the fatty acid chains. This is as expected since the double bonds, or epoxide groups of the fatty acids are located in this area of the membrane. The results are summarised in Table 4.2.

It is believed that the changes observed in membrane fluidity and polarity may be of importance in the bactericidal action of peroxygens, since it may have an impact on membrane function and this will be examined in Chapter Five. It was next decided to examine transition-metal / PAA dependent damage to model phosphatidylcholine liposomes.

Probe	S_{normal} [a,b]	$S_{epoxide}$ [a,b]	$\tau_{c\ normal}$ / s [a,c]	$\tau_{c\ epoxide}$ / s [a,c]	$a_{N\ normal}$ / mT [a,d]	$a_{N\ epoxide}$ / mT [a,d]
5-DSA	0.60	0.65	-	-	1.46	1.45
7-DSA	0.71	0.76	-	-	1.50	1.53
10-DSA	0.66	0.73	-	-	1.49	1.55
12-DSA	0.61	0.67	-	-	1.48	1.52
16-DSA	0.29	0.34	1.62×10^{-9}	1.75×10^{-9}	1.42	1.40

a. values are determined from the average of between three and six spectra.

b. typical errors for the measurement of the order parameter, S, are ± 0.005 - ± 0.01

c. typical errors for the measurement of the rotational correlation time, τ_c, are ± 0.15 - ± 0.30×10^{-9} s

d. typical errors in a_N are ± 0.005 - ± 0.02 mT

Table 4.2. Results obtained in spin-probe experiments with 'normal' and 'epoxidised' liposomes showing values obtained for τ_c, S and a_N.

4.6. A STUDY OF PEROXIDATION IN LIPOSOMES INDUCED BY TRANSITION METAL / PAA SYSTEMS.

Damage to lipids by lipid peroxidation has been implicated in a number of diseased states in mammals.[13-16] The process is initiated by any species capable of abstracting an allylic hydrogen atom.[5,17,64] There is much debate about the exact mechanism of lipid peroxidation in metal-containing systems,[5,64,236,237] some believing that it is initiated by high-valent iron species, while others claim that hydroxyl radicals are the initial attacking species. The mechanism is very difficult to establish conclusively, since most of the evidence indicating that lipid peroxidation has occurred is from product studies, after extensive lipid damage has occurred.

However, assays for the end products of lipid peroxidation are still informative about the levels of bulk damage inflicted upon a system and are the most widely used

indicators of lipid peroxidation. Many techniques have been developed to assess lipid peroxidation. These include spectrophotometric determination of conjugated dienes,[5,64,238] spectrophotometric / fluorescence determination of malondialdehyde, either as the native molecule[5,64,239] or as its derivative either with thiobarbituric acid[5,64,238,239] [reaction (4.1)] or an amine [reaction (4.2)].[5,64] The sensitivity of these assays in complex biological systems has sometimes been enhanced by the use of HPLC techniques.[64,240] Other assays which have been developed for the assessment of lipid peroxidation include assays for the detection of lipid hydroperoxides which involve their reactions with enzymes or iodine,[5,64] or HPLC[241] or GC-MS[242] based methods. Methods which have found limited use are the measurement of oxygen uptake, measurement of pentane and ethane evolution, determination of light emission from singlet oxygen and excited carbonyls and examination of alterations in the lipid profile using GC.[5,64]

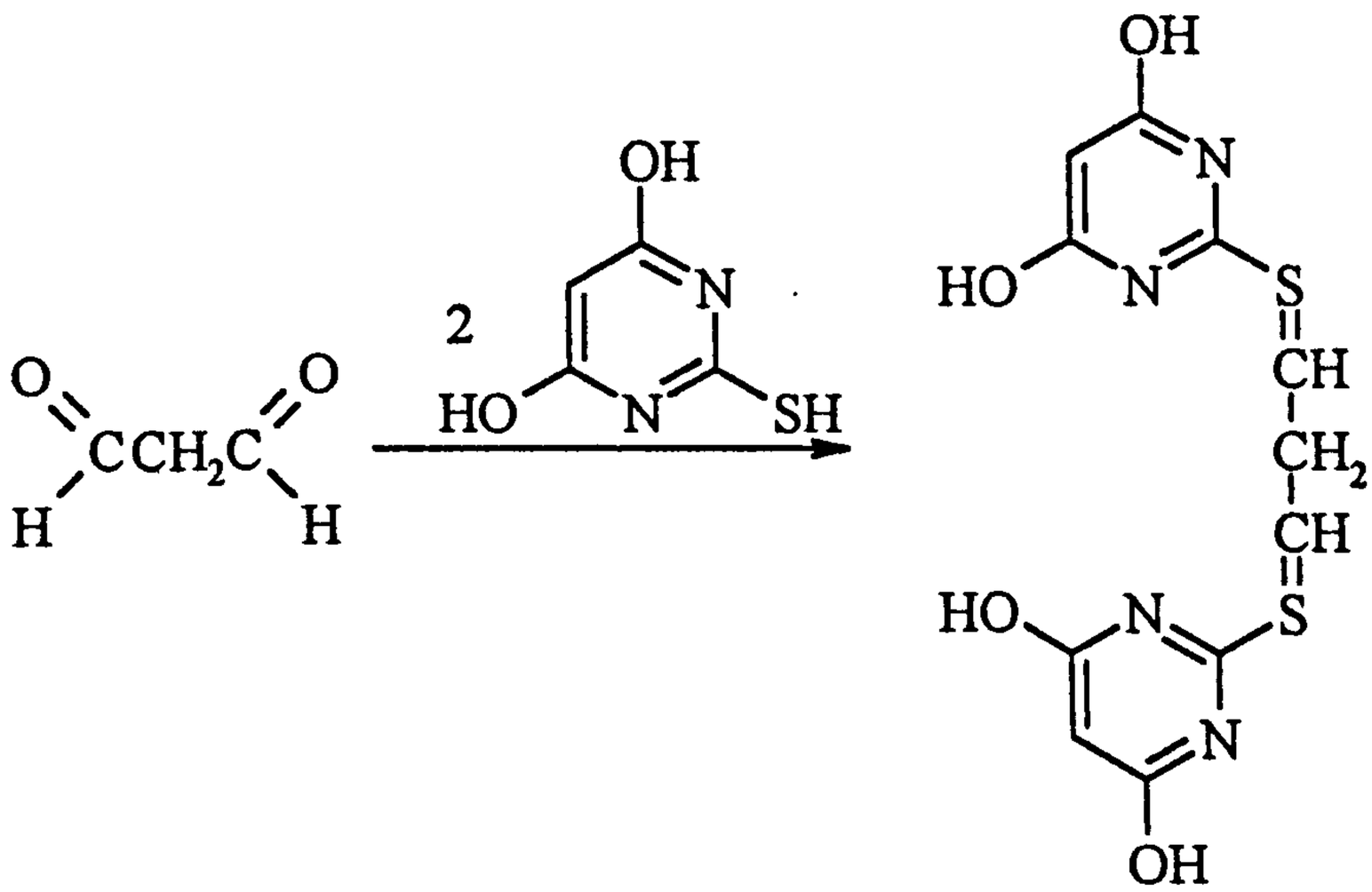

(4.1)

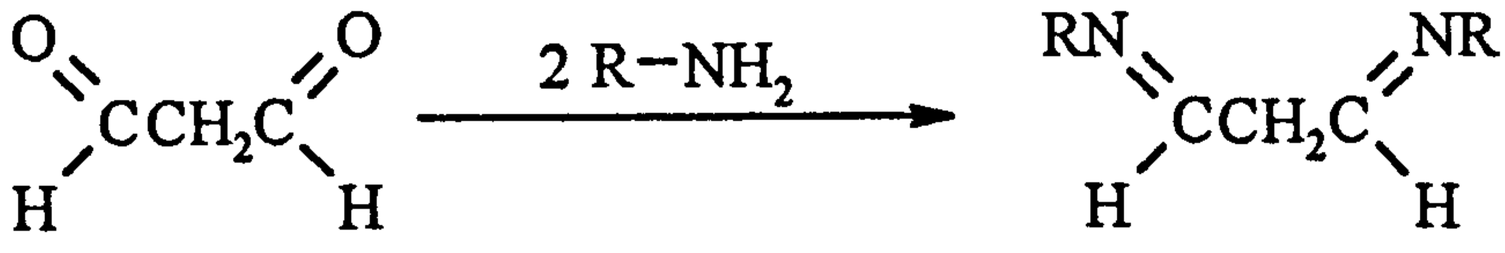

(4.2)

Despite problems experienced with the TBA test, it is still the most widely used indicator of lipid peroxidation and is of great use especially in well-defined systems, and where adequate measures are taken to avoid the formation of MDA during the acid heating stage of the test.

It was therefore decided to use this assay to examine peroxidation in unilamellar

phosphatidylcholine liposomes induced by various PAA / transition metal oxidising systems.

4.6.1. Peroxidation induced by Fe^{2+}-EDTA systems.

Initial experiments were performed using Fe^{2+}-EDTA. Reaction mixtures containing 5×10^{-4} g ml^{-1} unilamellar liposomes and various oxidising systems of either PAA alone (0.001 M total AvOx), Fe^{2+}-EDTA alone (2×10^{-4} M), or combinations of the two were incubated at 37 ^{0}C for one hour. After this they were derivatised with 2-thiobarbituric acid (TBA) as described in Chapter Six and the absorbance recorded against a blank at 532 nm. Special care was taken adjust the pH of the reaction mixture to greater than 2 if necessary since although the mixture needs to be acidic, colour development has been found to be inhibited at pH below 2.[240] The TBA_2-MDA concentration was determined by comparison with a standard plot generated by the reaction of 1,1,3,3-tetramethoxypropane and reactions were performed in triplicate.

Analysis of the mixture containing untreated liposomes showed that a low concentration of MDA was formed in the absence of any added oxidising agent (see Figure 4.8). It is believed that this is a result of decomposition of pre-existing phospholipid hydroperoxides. Addition of 2×10^{-4} M Fe^{2+}-EDTA increased the concentration of MDA formed, presumably as a result of autoxidation of the iron complex leading to radical production, although it is acknowledged that other mechanisms may be operating, possibly involving high-valent iron species or an iron-oxo complex.[5,64,236,237] The addition of either 5% PAA or 40% PAA in the absence of the iron complex did not generate concentrations of MDA above the baseline level. This was as expected since no transition metal was present. Addition of 5% PAA in conjunction with Fe^{2+}-EDTA led to the production of a high concentration of TBA_2-MDA ($2.76 \times 10^{-9} \pm 0.44 \times 10^{-9}$ mol mg^{-1}). It is believed that this is a result of radical production by reaction of PAA with Fe^{2+}-EDTA, although again it is acknowledged that other mechanisms may be occurring.[5,64,233,234] Repetition of this reaction with 40% PAA led to the generation of an even greater concentration of MDA ($3.96 \times 10^{-9} \pm 0.12 \times 10^{-9}$ mol mg^{-1}). The reason for this is not known but it is believed that

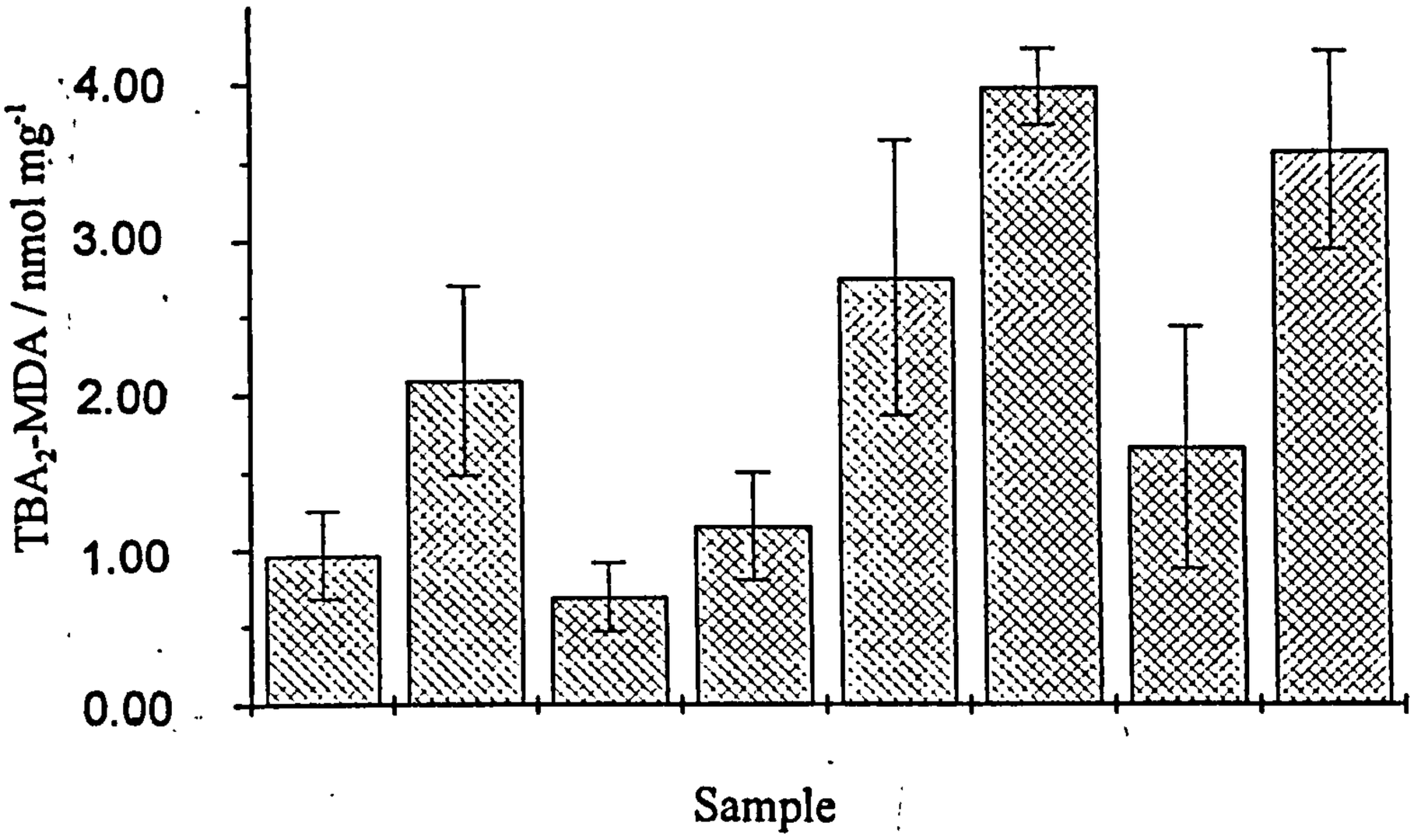

Figure 4.8. Extent of lipid peroxidation in liposomes (5×10^{-4} g ml^{-1}) caused by Fe^{2+}-EDTA (2×10^{-4} M) / PAA (0.001 M total AvOx) oxidising systems as measured by the TBA test.

1. Liposomes.
2. Liposomes and Fe^{2+}-EDTA.
3. Liposomes and 5% PAA.
4. Liposomes and 40% PAA.
5. Liposomes, Fe^{2+}-EDTA and 5% PAA.
6. Liposomes, Fe^{2+}-EDTA and 40% PAA.
7. Liposomes, Fe^{2+}-EDTA and catalase treated 5% PAA.
8. Liposomes, Fe^{2+}-EDTA and catalase treated 40% PAA.

it may involve the mechanism outlined in reactions (4.2) - (4.8). Although the reaction of peroxyacetic acid with Fe^{2+}-EDTA is slower than that with hydrogen peroxide, some of the peroxyacetic acid has been found to compete with the hydrogen peroxide to react with the metal complex (see Chapter 2). The first-formed carbonyloxyl radical decarboxylates rapidly[78,156] and is believed to add to molecular oxygen more readily than it will to an alkene / lipid radical or dimerise.[243] The methyl peroxyl radical will react rapidly with the alkene moieties of the phospholipids either by hydrogen abstraction from allyilic positions or addition to the double bonds. In cases where addition to a double bond occurs, this radical is likely to undergo rapid cyclisation producing a lipid epoxide and the methoxy radical.[244] This radical rearranges rapidly to form the hydroxymethyl radical which is an effective reducing agent for Fe^{3+}.[135] It is therefore possible that peroxyacetic acid promotes lipid peroxidation through being a source of an effective reducing species for Fe^{3+}. Although it is not anticipated that this is a major contributing mechanism to the peroxidation of lipids by PAA mixtures, only low concentrations of peroxyacetic acid need to react by this route to promote the regeneration of low-valent iron and hence the propagation of the chain reaction. It is also believed that peroxyacetic acid is more membrane soluble than hydrogen peroxide (see section 4.8) and that this will lead to higher levels of peroxidation being observed in reaction mixtures in which high concentrations of peroxyacetic acid are present.

$$CH_3CO_3H \xrightarrow{Fe^{2+} \rightarrow Fe^{3+}} CH_3CO_2^{\bullet} + {}^{-}OH \qquad (4.2)$$

$$CH_3CO_2^{\bullet} \longrightarrow {}^{\bullet}CH_3 + CO_2 \qquad (4.3)$$

$$^{\bullet}CH_3 + O_2 \longrightarrow CH_3OO^{\bullet} \qquad (4.4)$$

$$^{\bullet}OH + \text{alkene} \longrightarrow \text{HO-alkyl}^{\bullet} + \text{allyl}^{\bullet} \qquad (4.5)$$

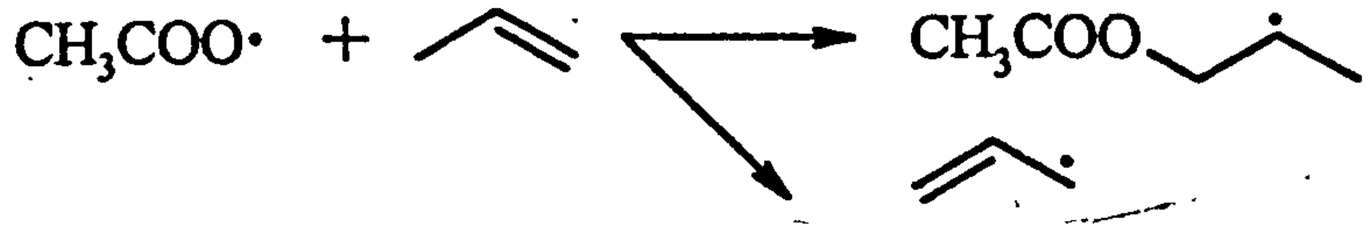

(4.6)

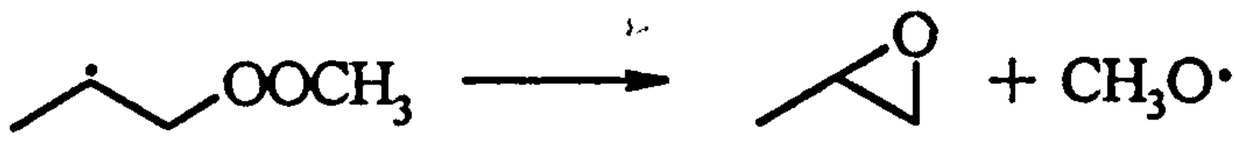

(4.7)

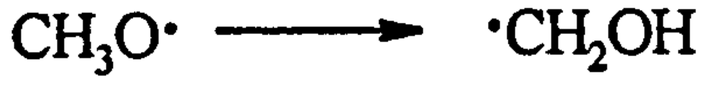

(4.8)

Addition of catalase to the PAA samples prior to their addition to the reaction mixture led to a reduction in the level of MDA observed, both in the case of 5% PAA and in the case of 40% PAA. This reduction in MDA is approximately proportional to the concentration of hydrogen peroxide in the reaction mixtures and indicates that both the hydrogen peroxide and peroxyacetic acid in the formulations are of importance in leading to lipid peroxidation.

Incubation of the liposomes with Fe^{2+}-EDTA / PAA oxidising mixtures over longer periods of time (up to two hours) led to slight increases in the levels of peroxidation, as measured by the TBA test. However, increasing the concentrations of the oxidants was shown to have a much more dramatic effect. Incubation of liposomes with 0.002 M Fe^{2+}-EDTA led to the formation of $6.64 \times 10^{-9} \pm 0.03 \times 10^{-9}$ mol mg^{-1} MDA. Addition of 0.01 M 5% PAA and Fe^{2+}-EDTA increased the concentration of TBA_2-MDA observed to $1.14 \times 10^{-8} \pm 0.03 \times 10^{-8}$ mol mg^{-1} MDA, while addition of 40% PAA and Fe^{2+}-EDTA led to the formation of $1.92 \times 10^{-8} \pm 0.05 \times 10^{-8}$ mol mg^{-1} MDA. Addition of catalase to the PAA prior to its addition to the reaction mixtures again led to the reduction on the concentration of MDA observed for both 5% and 40% PAA oxidising mixtures, in accordance with the concentrations of hydrogen peroxide in the formulations.

4.6.2. Peroxidation induced by Cu^{2+}(aq) and Cu^{2+}(aq) / L-ascorbic acid (*i.e.* Cu^{+}) systems.

The role of copper(II) / PAA in peroxidation of liposomes was next investigated

Initial experiments involved the treatment of unilamellar phosphatidylcholine liposomes with 2×10^{-4} M Cu^{2+}. This caused a small increase over the baseline level of TBA_2-MDA detected and is attributed to the copper catalysed decomposition of pre-formed phospholipid peroxides. Addition of either 5% PAA or 40% PAA to the reaction mixtures did not lead to the formation of significant concentrations of TBA reactive species. It is believed that the lack of TBA-reactive species observed in these systems is a reflection of the relative redox inactivity of copper(II) in the liposomes.

It was therefore decided to examine whether addition of L-ascorbic acid to the system, in order to produce copper(I), would lead to an increase in lipid peroxidation (see Figure 4.9). Addition of 4×10^{-4} M L-ascorbic acid to the reaction mixture containing liposomes and Cu^{2+}(aq) led to the production of $2.12 \times 10^{-9} \pm 0.32 \times 10^{-9}$ mol mg^{-1} MDA. This is believed to be a result of radical generation as a consequence of the continual regeneration of the low-valent copper species. Addition of 5% PAA to this reaction mixture produced a sharp increase in the concentration of MDA observed ($3.94 \times 10^{-9} \pm 0.19 \times 10^{-9}$ mol mg^{-1}).This is significantly higher than the concentration of MDA observed in the corresponding system which employed Fe^{2+}-EDTA. It is known (see Chapter Two) that Cu^{2+}/ L-ascorbic acid reacts readily with hydrogen peroxide to produce radicals, but that its reaction with peroxyacetic acid is either much slower, or proceeds without the generation of high concentrations of radical species. It is therefore believed that the increase in TBA-reactive species observed when Cu^{2+} / L-ascorbic acid is employed, as opposed to Fe^{2+}-EDTA reflects continual regeneration of the low-valent copper species to react with any remaining peroxide. Similarly when 40% PAA was employed in conjunction with Cu^{+}, a large increase in the concentration of TBA reactive species ($4.18 \times 10^{-9} \pm 0.10 \times 10^{-9}$ mol mg^{-1}) over the concentration in the corresponding reaction with Fe^{2+}-EDTA was observed and this is attributed to the continual regeneration of Cu^{+}.

Catalase treatment of 5% PAA before its addition to the reaction mixture led to a decrease in TBA_2-MDA detected, thus indicating the importance of the hydrogen peroxide in peroxidation. However, complete loss of peroxidation was not observed, suggesting that peroxyacetic acid does contribute to the process. Similarly when 40% PAA was catalase-treated prior to its reaction with Cu^{+} in the presence of liposomes, a decrease in TBA_2-

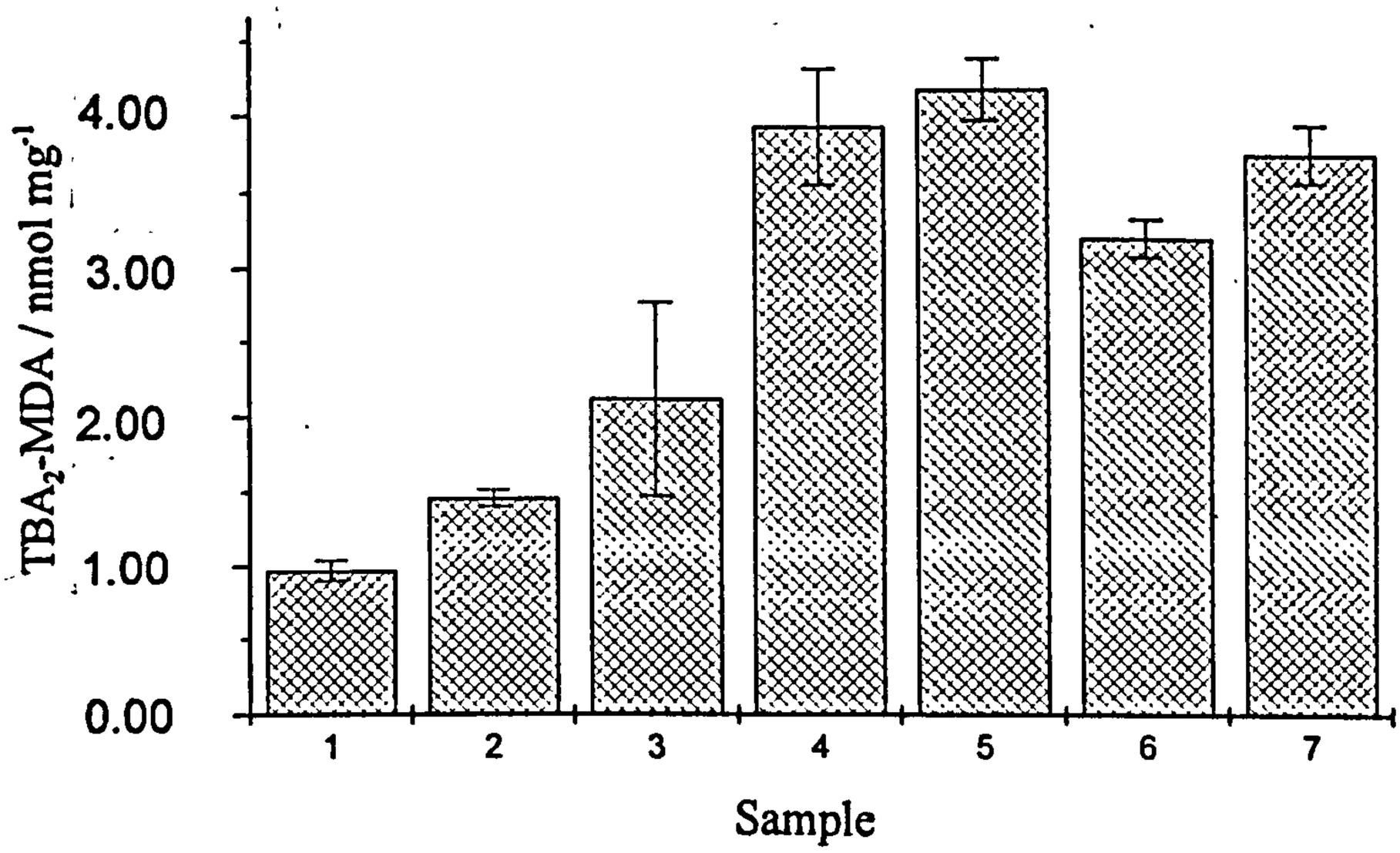

Figure 4.9. Extent of lipid peroxidation in liposomes (5×10^{-4} g ml^{-1}) caused by Cu^{2+} (2×10^{-4} M) / L-ascorbic acid (4×10^{-4} M) / PAA (0.001 M total AvOx) oxidising systems as measured by the TBA test.

1. Liposomes.
2. Liposomes and Cu^{2+} (aq).
3. Liposomes, Cu^{2+} (aq) and L-ascorbic acid.
4. Liposomes, Cu^{2+}, L-ascorbic acid and 5% PAA.
5. Liposomes, Cu^{2+}, L-ascorbic acid and 40% PAA.
6. Liposomes, L-ascorbic acid and catalase treated 5% PAA.
7. Liposomes, L-ascorbic acid and catalase treated 40% PAA.

MDA was observed. This decrease was not as large as that observed in the corresponding reaction mixture with 5% PAA. This is as expected and is a result of the lower concentration of peroxyacetic acid in the reaction mixture. Failure of catalase treatment of the PAA samples to reduce damage to liposomes to the level caused by Cu^{2+} / L-ascorbic acid alone suggests that peroxyacetic acid does have a role in damage caused in this manner. Since it believed that radical production from the reaction between Cu^{2+} / L-ascorbic acid and peroxyacetic acid occurs only in low concentration and is not very rapid, it is believed that the relatively high yields of TBA_2-MDA found in these systems reflects the longer timescale of the experiments as compared to the spin-trapping experiments.

4.6.3. Discussion.

It has been found that both Fe^{2+}-EDTA and Cu^{+} (generated by the reaction of Cu^{2+} with L-ascorbic acid) in conjunction with PAA led to the peroxidation of liposomes. Peroxyacetic acid alone did not cause any peroxidation of liposomes. It was found that peroxidation was dependent, not only on hydrogen peroxide, but also on peroxyacetic acid in the PAA formulations. In general, systems in which Cu^{2+} / L-ascorbic acid were employed caused more damage than those in which Fe^{2+}-EDTA were employed. It is believed that this is due to the continual regeneration of redox active Cu^{+}. In the case of the reactions which employed Fe^{2+}-EDTA 40% PAA produced much higher concentrations of TBA reactive species than 5% PAA. This is attributed to the generation of hydroxymethyl radicals from the peroxyacetic acid [reactions (4.2) - (4.8)] which reduce Fe^{3+} effectively and therefore propagate the chain reaction. It is also believed that this may be due to the greater lipid solubility of peroxyacetic acid than hydrogen peroxide. The difference between the ability of 5% PAA and 40% PAA to cause lipid peroxidation was far less marked in reaction systems in which Cu^{2+} / L-ascorbic acid was employed. And this is believed to reflect the slower reaction of peroxyacetic acid with Cu^{+}, although it is obviously still significant since catalase treatment in these systems did not eradicate damage caused by the PAA.

4.7. EPR SPIN-PROBE STUDY ON THE PEROXIDATION OF LIPOSOMES.

It was next decided to investigate the effect of lipid peroxidation on membrane fluidity. It is known that peroxidation leads to an eventual decrease in membrane fluidity,[218,219] but this has never been monitored whilst peroxidation is in progress. It was therefore decided to conduct a series of experiments in which liposomes were prepared containing the spin-probe 3-β-doxyl 5-α-cholestane. The EPR spectrum was then monitored over time after the addition of 0.002 M Fe^{2+}-EDTA and 0.02 M PAA. 3-β-Doxyl 5-α-cholestane was chosen because of its lipophilicity and because the use of doxyl stearic acids in systems in which high concentrations of acid are present can lead to complex spectra as a result of the spin-probe being in a mixture of its protonated and deprotonated form and these possessing different partition characteristics.[245]

EPR spectra of these reaction mixtures were recorded over approximately eighteen hours. However, the only difference seen in the spectra was a slight reduction in signal amplitude. It is believed that the nitroxide was able to scavenge the carbon-centred lipid radicals, therefore preventing lipid peroxidation and leading to gradual loss of the nitroxide signal [reaction (4.9)].[246]

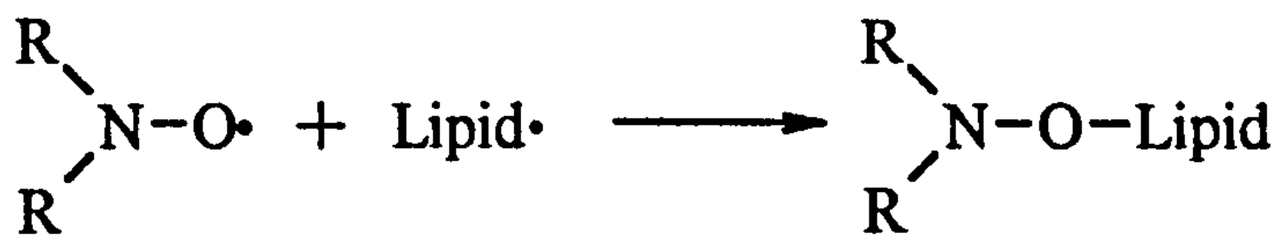

(4.9)

It was next decided to examine the membrane solubility of peroxyacetic acid relative to hydrogen peroxide so that the importance of accessibility in the mechanism of peroxidation by peroxyacetic acid could be examined.

4.8. DETERMINATION OF THE 1-OCTANOL:WATER PARTITION COEFFICIENTS FOR PEROXYACETIC ACID AND HYDROGEN PEROXIDE.

Experiments were developed to estimate the membrane solubility of peroxyacetic acid and hydrogen peroxide although it should be noted that pre-saturation of the solvents

with the other solvent of interest and pH effects were not considered. 1 ml of PAA was added to a vial containing 3 ml of water and 3 ml of 1-octanol.. The mixture was rigorously shaken then left to stand for 10 min. after which 0.1 ml samples were removed from each layer. The peroxyacetic acid concentration was determined by titration with acidified ceric sulfate and the hydrogen peroxide concentration was determined by titration with sodium thiosulfate as described in Chapter Six. This procedure was undertaken for 5% and 40% PAA so that any possible effects of the increased overall acidity of the 5% PAA formulation could be accounted for.

On addition of 5% PAA to the 1-octanol / water mixture it was found that the water layer contained 0.153 ± 0.004 M peroxyacetic acid and 1.893 ± 0.006 M hydrogen peroxide and that the 1-octanol layer contained 0.044 ± 0.001M peroxyacetic acid and 0.114 ± 0.004 M hydrogen peroxide. This leads to values for the 1-octanol:water partition coefficient of 0.288 ± 0.015 for the peroxyacetic acid and 0.060 ± 0.002 for the hydrogen peroxide. On repetition with 40% PAA it was found that the concentration of peroxyacetic acid in the aqueous phase was 1.026 ± 0.005 M and in the organic phase was 0.328 ± 0.001 M whereas the concentration of hydrogen peroxide was found to be 0.472 ± 0.014 M in the aqueous phase and 0.030 ± 0.002 M in 1-octanol. The partition coefficients were therefore calculated to be 0.320 ± 0.002 for peroxyacetic acid and 0.063 ± 0.005 for hydrogen peroxide. These values show that the partition of the peroxyacetic acid and hydrogen peroxide is not drastically affected by the composition of the formulation.

Although it is apparent from these results that both peroxyacetic acid and hydrogen peroxide prefer to be in the aqueous phase peroxyacetic acid is approximately five times more lipophilic than hydrogen peroxide. It is believed that this may account, at least in part, for the increased levels of peroxidation that occur in mixtures containing transition metal / 40% PAA oxidising systems than 5% PAA / Fe^{2+}-EDTA oxidising systems. The results are summarised in Table 4.3.

Formulation	5%	40%
$[H_2O_2]_{water}$ / M[a]	1.893	0.472
$[H_2O_2]_{octanol}$ / M[a]	0.114	0.030
H_2O_2 partition coefficient[b]	0.060	0.063
$[CH_3CO_3H]_{water}$ / M[a]	0.153	1.026
$[CH_3CO_3H]_{octanol}$ / M[a]	0.044	0.328
CH_3CO_3H partition coefficient[b]	0.288	0.320

a. typical errors in concentrations are ± 0.001 - ± 0.014 M

b. typical errors in partition coefficients are 0.002 - 0.015

Table 4.3. Determination of octanol:water partition coefficient for hydrogen peroxide and peroxyacetic acid in PAA formulations.

4.9. CONCLUSIONS.

It has been shown that transition-metal independent epoxidation of fatty acids and phospholipids in organic solution is easily accomplished with a range of epoxidising agents. Similarly it has been demonstrated that under certain circumstances it is possible to epoxidise phospholipids when they have been formed into liposomes. The structural effects of epoxidation of liposomes have been assessed using a spin-probe technique and it has been shown that epoxidation leads to a loss of membrane fluidity, as measured by the order parameter, S, especially in the centre of the phospholipid chains. Similarly it has been found that epoxidation leads to a large increase in membrane polarity, as measured by the nitrogen hyperfine splitting, and that this increase is also localised around the centre of the phospholipid chains. This is as expected since it is this area of the chains that contain the highest density of alkenes / epoxides. It is possible that this could be a contributing factor in cell damage.

It has also been shown that in the presence of Fe^{2+}-EDTA or Cu^{+} (generated by reaction of Cu^{2+} with L-ascorbic acid) peroxyacetic acid will induce lipid peroxidation.

It has been found that Cu^{2+} / L-ascorbic acid is more effective than Fe^{2+}-EDTA in generating TBA reactive species and this is attributed to the continual regeneration of redox active Cu^{+} by reduction with L-ascorbic acid. 40% PAA has been found to be more effective at leading to lipid peroxidation than 5% PAA and this attributed to the greater lipid solubility of peroxyacetic acid (peroxyacetic acid was found to be approximately fives times more lipid soluble than hydrogen peroxide) and in the case of initiation with Fe^{2+}-EDTA the possible participation of a mechanism that regenerates the low-valent transition metal.

It is believed that in areas of the membrane in which either there is a surfeit of transition-metal ions, or the transition-metal ions are chelated in such a way that they are rendered redox inactive, epoxidation may be of importance in cellular lipid damage inflicted by PAA. However, in areas of the membrane in which there is an ample supply of redox active transition-metal ions it is believed that peroxidation will predominate. The nature of lipid damage by PAA will be examined further in the next Chapter where the reactions of bacterial cells with PAA will be considered.

CHAPTER 5.

REACTIONS OF PEROXYGENS WITH *ESCHERICHIA COLI.*

5.1. INTRODUCTION.

The research in the previous Chapters described the reactions of peroxyacids, both in the presence and absence of low-valent transition-metal ions, with proteins and lipids. In the research described within this Chapter the impact of these reactions on a model strain of *Escherichia coli* has been investigated and an insight gained into the importance of lipid and protein damage in the bactericidal action of peroxyacetic acid. *E. coli* was chosen since it has been widely used in tests for bactericidal activity,[247] for example by Solvay, and its defence mechanisms against oxidative stress (for example its superoxide dismutase and catalase) are relatively well characterised.[112,115]

Some peroxyacids are known to be potent bactericides,[1,109-111] but their mechanism of action is not clear. It has been postulated on the basis of cell-kill and some spin-trapping studies that they may reacts with intracellular transition-metal pools to generate radicals and that these that are the toxic species.[100-102] This is supported by radiolysis studies which have shown that radicals are highly toxic to bacteria.[99] However, only preliminary studies on the generation of radicals in bacteria have been undertaken thus far in this department,[102] (see also reference 248) and damage to proteins and lipids in intact cells has not been examined, hence relevant information on the mechanism of action of peroxyacetic acid is extremely limited.

The aim of the research contained in this Chapter was therefore to seek evidence for *in situ* radical generation from peroxyacids, with particular emphasis on PAA, in *E. Coli* and to examine the impact, if any, of radical generation on important cellular components. The techniques employed, therefore, include EPR spin-trapping to examine radical formation in *E. coli,* using a variety of spin-traps, and ancillary techniques such as the use of paramagnetic broadening agents and scavengers. A spin-probe technique was also to be employed to examine changes in membrane fluidity induced by treatment of *E. coli* by peroxygens. Protein and lipid damage has been measured using the TBA (see Chapter Four) and DNPH (see Chapter Three) assays, respectively, to assess if the generation of carbonyl groups on protein side-chains and the formation of MDA from lipids is of importance in the bactericidal activity of PAA. The role of endogenous and

exogenous iron in these processes has also been examined.

5.2. EPR SPIN-TRAPPING STUDIES OF THE REACTIONS OF PEROXYGENS WITH *ESCHERICHIA COLI* EMPLOYING DMPO.

5.2.1. Initial experiments.

Initial studies employed DMPO which was chosen because it is soluble in aqueous systems and also slightly soluble in organic solvents (octanol:water partition coefficient = 0.08) and it is therefore believed that a reasonable concentration will be able to traverse the bacterial membrane.[141]

E. Coli were grown overnight and isolated as described in Chapter Six. Reaction mixtures for these initial experiments contained 2.0×10^9 cfu ml^{-1} *E. coli*, up to 3.6×10^{-4} M (total AvOx) 5% PAA and 0.066 M DMPO. The EPR spectrum of this comprised a weak signal attributed to DMPO-OH ($a_N = a_{\beta\text{-}H} = 1.49 \pm 0.01$ mT)[158] which remained unchanged with time. The signal amplitude was greatest when the concentration of 5% PAA was 5×10^{-5} M (total AvOx) (see Figure 5.1.a).The presence of the signal required the presence of all the reactants. Raising the concentration of the peroxygen above 3.6×10^{-4} M sometimes led to the detection of the well characterised DMPO oxidation product, DMPOX ($a_N = 0.71 \pm 0.01$ mT, $a_{2\gamma\text{-}H} = 0.41 \pm 0.01$ mT)[158] and was therefore not investigated further.

Repetition of this reaction with 40% PAA at equivalent AvOx also produced a weak signal of DMPO-OH. Variation of the concentration of peroxygen did not lead to any improvement in the signal-to-noise ratio; in fact at elevated concentrations ($\geq 3.6 \times 10^{-4}$ M total AvOx) of peroxygen, DMPOX was sometimes observed. No carbon-centred radical adducts were observed, which is rather surprising given the results obtained earlier (see Chapter Two). However, these observations are in agreement with those obtained by Clapp *et al*[102] in spin-trapping experiments involving a range of peroxygen compounds.

On replacement of PAA by MMPP, DMPO-OH was again observed. The signals were generally of greater intensity than those observed for PAA and were of maximum

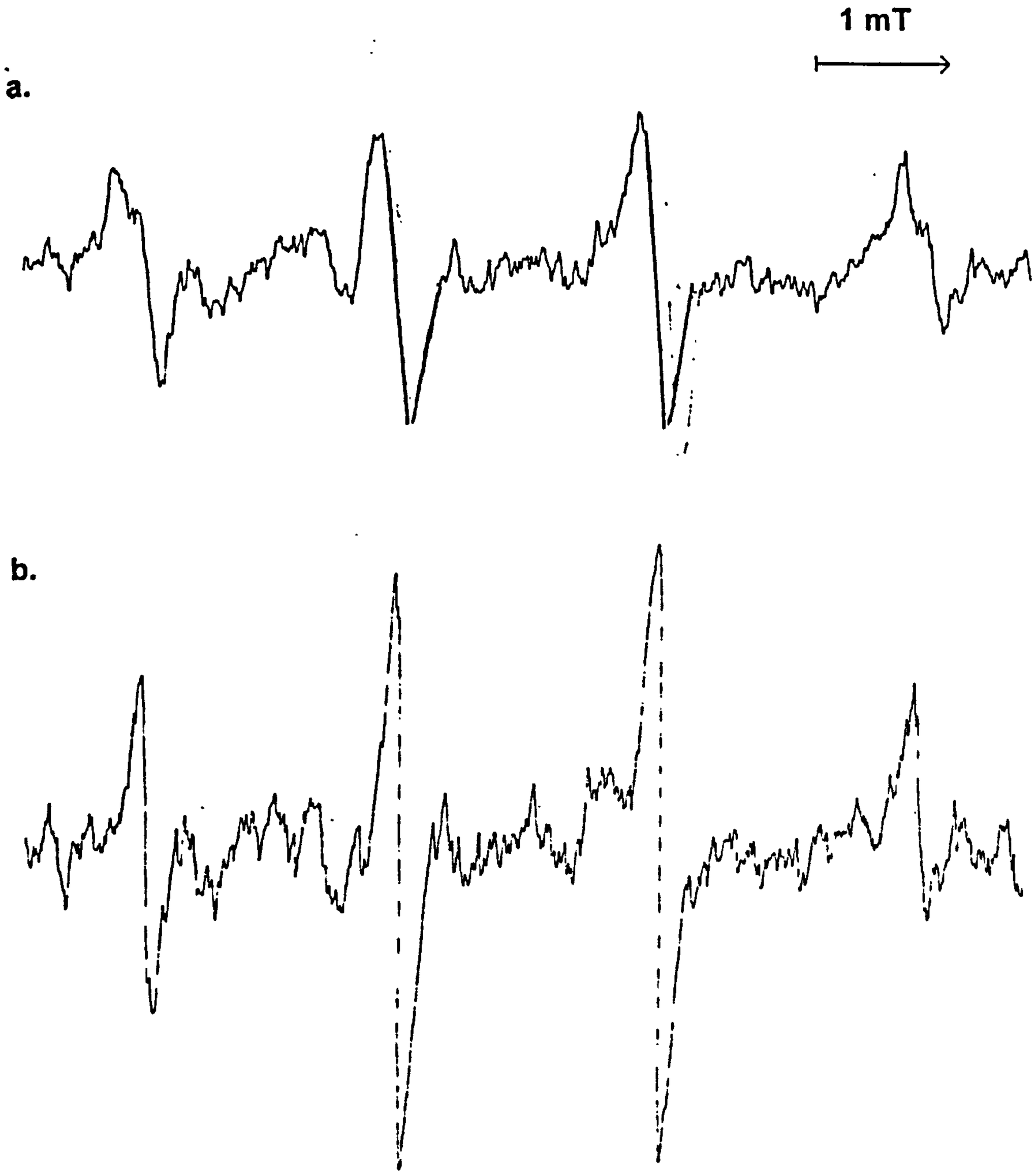

Figure 5.1.a. EPR spectrum showing the low concentration of DMPO-OH adduct generated by the reaction between *E. coli* with 5% PAA in the presence of DMPO.

Figure 5.1.b. EPR spectrum showing the higher concentration of DMPO-OH generated by the reaction of MMPP with *E. coli* in the presence of DMPO. Concentrations employed:- *E. coli*, 2×10^9 cfu ml^{-1}, 5% PAA, 5×10^{-5} M (total AvOx) or MMPP, 3.6×10^{-4} M, DMPO, 0.066 M.

intensity when the concentration of peroxygen was 3.6×10^{-4}M. The signal was somewhat stronger than those observed for reactions which employed PAA (see Figure 5.1.b) but there was still no evidence for the formation of carbon-centred (or arylcarbonyloxyl) radical adducts as would be expected on the basis of studies of the reactions of MMPP with low-valent transition-metal ions (see Chapter Two and reference 77). However, similar results have been obtained previously in spin-trapping experiments of the reaction between *Escherichia coli* and MMPP.[102,248]

Experiments in which hydrogen peroxide was used were next performed. It was found that the signals were generally of greater intensity than those observed for peroxyacetic acid, but of lower intensity than those observed for MMPP. The signal intensity was maximum at the experimental limit of 3.6×10^{-4} M. These results are in accord with the results of studies previously undertaken on the reactions of a variety of peroxygens with bacteria within this department.[102] A summary of these results is provided in Table 5.1.

Peroxygen	Concentration at which maximum signal amplitude was observed / 10^{-4} M	Relative signal intensity / arbitrary units
H_2O_2	3.6	++
5% PAA[a]	0.5	+
40% PAA[a]	0.5	+
MMPP	3.6	+++++++

a. total AvOx

Table 5.1. Optimum concentrations for observation of EPR signals and relative signal intensities of DMPO-OH adducts in the reactions between *E. coli* and peroxygens in the presence of DMPO.

5.2.2. Experiments exploring the nature of the bacterial culture.

The signal-to-noise ratio in the spectra obtained so far was poor and it is believed this may be for a number of reasons. Firstly, the concentrations of peroxygen employed were rather low, but use of higher concentrations was precluded by spin-trap oxidation. The use of an alternative trap may therefore be useful (see section 5.3). Secondly, it is also possible that the spin-trap is not traversing the membrane as effectively as anticipated; this was also explored using an alternative trap (see section 5.3). Further experiments to ensure that a sufficient concentration of the trap was inside the cells were also performed. The bacterial suspension was therefore incubated at 37 ^{0}C for up to twenty minutes to ensure that an adequate concentration was attained inside the cell. However, this did not lead to any increase in signal-to-noise ratio.

In addition, it was thought possible that the cells may have to be actively metabolising to be affected by the peroxide. Therefore 0.055 M α-D glucose was added to the suspension and incubated at 37 ^{0}C for up to 1 h before addition of the peroxygen and spin-trap to ensure that the cells used in the experiments were actively metabolising.[223] This also did not lead to an increase in signal amplitude.

Finally, it was believed that intracellular antioxidants such as glutathione and L-ascorbic acid may be reducing any nitroxides formed to EPR-silent hydroxylamines [see reactions (5.1 and (5.2)]. It is well known that mammalian cells metabolise spin-adducts to form their corresponding EPR-silent hydroxylamines,[248-250] but it is not known if bacterial cells can metabolise these compounds in an analogous way.[247-250] The reducing ability of *E. Coli* was therefore examined. DMPO-CH_3 and DMPO-OH were prepared using the reaction between 0.005 M Fe^{2+}-EDTA, 0.005 M hydrogen peroxide and 0.066 M DMPO either in the presence or absence of 1.1 M DMSO. Then, a sonicated suspension of *E. coli* (final concentration 2×10^{9} cfu ml^{-1}) was added and the EPR spectrum observed over 20 min. This was repeated in the absence of the latter in order to see how they affected the decay of the EPR signal. It was found that the signal was not significantly affected by the presence of the sonicated *E. coli*. This indicates that the cells' antioxidant defences are not reducing the spin-adducts to hydroxylamines. However, it is

acknowledged that the concentration of radicals generated in these experiments is relatively high and therefore may not be noticeably affected by the presence of the *E. coli* and also that sonication of the *E. coli*, whilst ensuring that the spin-adducts were accessible to the antioxidants, may have reduced the antioxidant capabilities of the cells, therefore reducing their ability to react with the nitroxides.

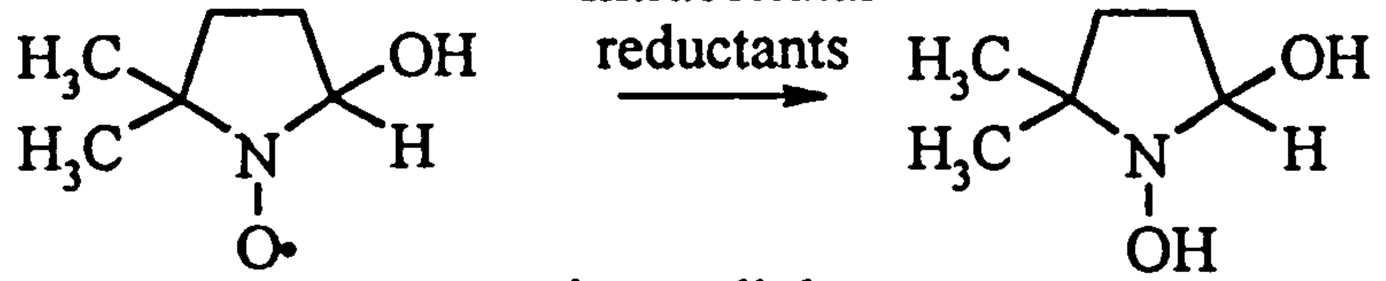

(5.1)

(5.2)

The effect of the age of the bacterial culture employed was next investigated, since it is known that spores which start to develop during the stationary phase are more resistant to damage by peroxygen compounds than vegetative cells that predominate in the exponential phase.[1,109-111] Bacteria were isolated at various stages of growth, throughout the exponential and stationary phases and the spin-trapping experiments were repeated; the signal intensity was found to be independent of the age of the bacterial culture.

5.2.3. Experiments investigating the location and mechanism of formation of the spin-adducts.

The location of formation of the spin-adducts was next examined using the membrane-impermeable line-broadening agent, potassium ferricyanide. If the spin-adducts are formed extracellularly the EPR signal should be broadened by the addition of ferricyanide, whereas if the spin-adducts were formed intracellularly no line broadening would occur. Addition of 0.05 M ferricyanide had no effect on the EPR spectra indicating that the spin-adducts were formed *intracellularly*.

The origin of the spin-adducts was then examined using the hydroxyl-radical

scavenger, DMSO; this was chosen in preference to, for example, sodium formate because it is membrane permeable. On addition of up to 10% by volume DMSO the DMPO-OH signals persisted, but no signals attributable to DMPO-CH_3 were observed. Pre-incubation of the bacteria for up to twenty minutes with DMSO to ensure that the DMSO was crossing the membrane did not lead to the formation of DMPO-CH_3. The concentration of DMSO was not increased further as it is anticipated that high concentrations of DMSO may lead to disruption of the membrane.

5.2.4.Discussion.

The concentration of spin-adducts formed in *E. coli* upon treatment with peroxygen compound has been found to be rather low although MMPP leads to signals of greater intensity than hydrogen peroxide which in turn produces a higher concentration of spin-adducts than either 5% or 40% PAA. The use of potassium ferricyanide has shown that the radical adducts are generated intracellularly whilst the use of the hydroxyl radical scavenger, DMSO has shown that the spin-adducts are not generated by the trapping of hydroxyl radicals. As discussed previously (see Chapter Two) many mechanisms exist by which spin-adducts may be formed apart from spin-trapping, including the Forrester-Hepburn mechanism,[145] inverse spin-trapping[151,152] and nucleophilic substitution of the first-formed spin-adduct,[153] although it is not known which, if any, of these mechanisms is responsible for the formation of spin-adducts in peroxygen-treated *E. coli*.

5.3. EPR SPIN-TRAPPING STUDIES OF THE REACTIONS OF PEROXYGENS WITH *E. COLI* EMPLOYING PBN.

Use of the trap, PBN was next explored as this may be less prone to oxidative modification and is believed to be more membrane permeable than DMPO (octanol:water partition coefficient = 10.40).[141] It was expected that the combination of these factors may lead to the observation of higher concentrations of spin-adducts formed through conventional mechanisms, if these are occurring.

Initial experiments involved mixing 2×10^9 cfu ml^{-1} *E. coli* with 0.042 M PBN and 4.8×10^{-4} M (total AvOx) 5% PAA. No signals were observed. Similarly on addition of either 40% PAA or hydrogen peroxide no signals were detected. Addition of MMPP, however led to the production of a low concentration of PBN-OH ($a_N = 1.54 \pm 0.01$ mT and $a_{\beta\text{-}H} = \pm 0.28 \pm 0.01$ mT.[158] It is known that the PBN-OH signal is short-lived when compared to that of DMPO-OH so the experiments were repeated in the presence of 1.1 M DMSO. No signals were detected upon addition of DMSO to the reaction mixtures containing 5% PAA. 40% PAA and hydrogen peroxide. On addition of DMSO to the reaction mixture containing MMPP, the PBN-OH signal persisted and there was no evidence of methyl radical production., indicating that the hydroxyl radical spin-adduct is formed via a non-conventional mechanism, not by the trapping of hydroxyl radicals.

It may therefore be concluded that the signals observed in the experiments employing DMPO are not due to a classical spin-trapping reaction. It is believed that oxidation of the spin-trap by the Forrester-Hepburn mechanism,[145] 'inverse spin-trapping'[151,152] or an alternative mechanism, possibly involving generation of ferryl iron at heme centres by reaction with PAA, may be involved in spin-adduct generation.

It was finally decided to employ DEPMPO as this was found (see Chapter Two and reference 179) to provide a useful probe for the mechanism of spin-adduct formation, where DEPMPO is oxidised directly without hydroxyl radical formation.

5.4. EPR SPIN-TRAPPING STUDIES OF THE REACTIONS OF *E. COLI* WITH PEROXYGENS EMPLOYING DEPMPO.

Oxidation of spin-traps in aqueous solution often leads to the production of the hydroxyl radical spin-adduct.[145,148-153] When DEPMPO is employed under these conditions an additional signal is observed in the EPR spectrum (see ref. 179 and Chapter Two). This can be tentatively attributed to the rearrangement product of a radical cation intermediate formed by one-electron oxidation of the spin-trap (see ref. 179). A mechanism has been suggested by which this may be formed and it has also been suggested that this could be used as a powerful mechanistic probe.

It was therefore considered appropriate to investigate the reactions of peroxygen compounds with *E. coli* using DEPMPO to see this second signal could be seen. Initial experiments involved mixing 2×10^9 cfu ml^{-1} *E. coli* with 5×10^{-5} M (total AvOx) 5% PAA and 0.05 M DEPMPO. The EPR signal of the mixture was extremely weak , but it was possible to see a signal attributable to DEPMPO-OH ($a_P = 4.66 \pm 0.01$ mT, $a_N = a_{\beta\text{-}H} = 1.36 \pm 0.01$ mT)[172,173] and a second very weak signal comprised of a phosphorus splitting of 4.60 ± 0.01 mT, a nitrogen splitting of 1.45 ± 0.01 mT and a hydrogen splitting of 2.20 $\pm$ 0.01 mT.[179] Similarly, the EPR spectra of reaction mixtures containing 40% PAA, hydrogen peroxide or MMPP and *E. coli* in the presence of DEPMPO were comprised of two signals corresponding to DEPMPO-OH and the DEPMPO-derived radical (see Figure 5.2).

5.4.1 Discussion.

It can therefore be concluded that the reactions of *E. coli* with peroxygens *under the conditions used* does not lead to the formation of a detectable concentration of radicals, although their involvement in the bactericidal action of peroxyacetic acid cannot be ruled out. An oxidising species, is made upon reaction of peroxygen compounds with the bacteria and this species leads to the formation of spin-adducts through non-conventional mechanisms.

5.5. EPR SPIN-TRAPPING STUDIES OF THE REACTIONS OF ALKYL HYDROPEROXIDES WITH *ESCHERICHIA COLI.*

The reactions of hydroperoxides with *Escherichia coli* were next investigated as these compounds are also believed to kill bacteria via a radical mechanism.[106,107] In addition, they are less likely to lead to direct spin-trap oxidation and their reactions with heme proteins, which are possibly believed to be involved with the formation of radical species, are relatively well understood.[212,213] The hydroperoxides chosen for this study were *t*-butyl hydroperoxide (5.1) and cumene hydroperoxide (5.2)

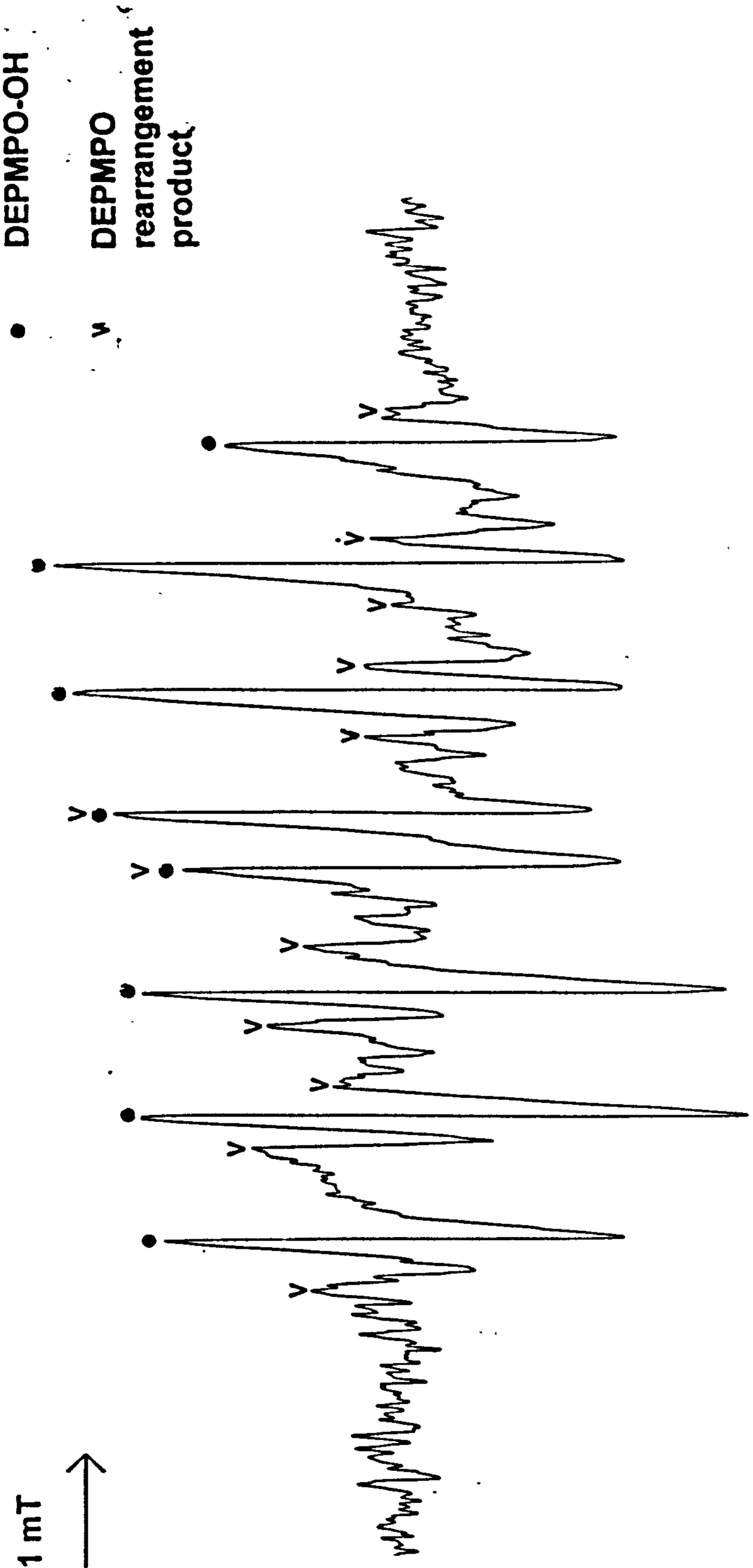

Figure 5.2. EPR spectrum showing signals attributed to DEPMPO-OH and the rearrangement product of the DEPMPO radical cation generated by the reaction of *E. coli* with MMPP in the presence of DEPMPO. Concentrations employed:- *E. coli*, (2×10^9 cfu ml^{-1}), MMPP (3.6×10^{-4} M), DEPMPO, (0.05 M).

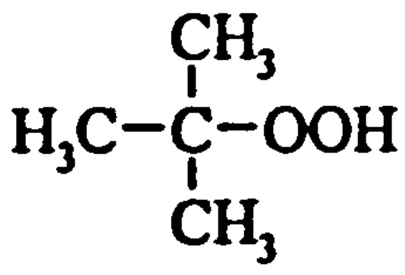

(5.1)

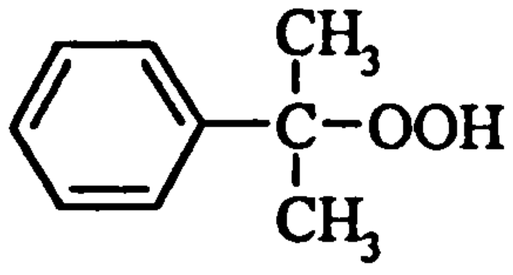

(5.2)

Initial experiments involved the mixing of *E. coli* with 3.6×10^{-4} M *t*-BuOOH and 0.066 M DMPO. No signals were detected under these conditions. However, when the experiments were repeated with higher concentrations of *t*-BuOOH (up to 0.036 M) very weak signals were evident. These are assigned as DMPO-OH ($a_N = a_{\beta\text{-}H} = 1.49 \pm 0.01$ mT)[158] and DMPO-CH_3 ($a_N = 1.64 \pm 0.01$ mT, $a_{\beta\text{-}H} = 2.34 \pm 0.01$ mT).[158] Similarly, when cumene hydroperoxide (5.2) was employed, no signals were observed at low concentrations (3.6×10^{-4}M) but at higher concentrations of hydroperoxide (0.036 M) very weak signals became evident that can be assigned to DMPO-CH_3 and DMPO-OH on the basis of the observed hyperfine splittings.[158] The production of methyl radicals is attributed to the β-scission of the alkoxyl radical formed upon reaction of the hydroperoxide with intracellular low-valent transition-metal ions [for *t*-BuOOH see reactions (5.3) and (5.4)]. The rate of β-scission is very fast (2.9×10^4 s^{-1} for *t*-$BuO^{\cdot}$ [251] and 3.7×10^5 s^{-1} for $PhC(CH_2)_2O^{\cdot}$ [252]) hence explaining alkoxyl radical spin-adducts were not evident in the EPR spectra.

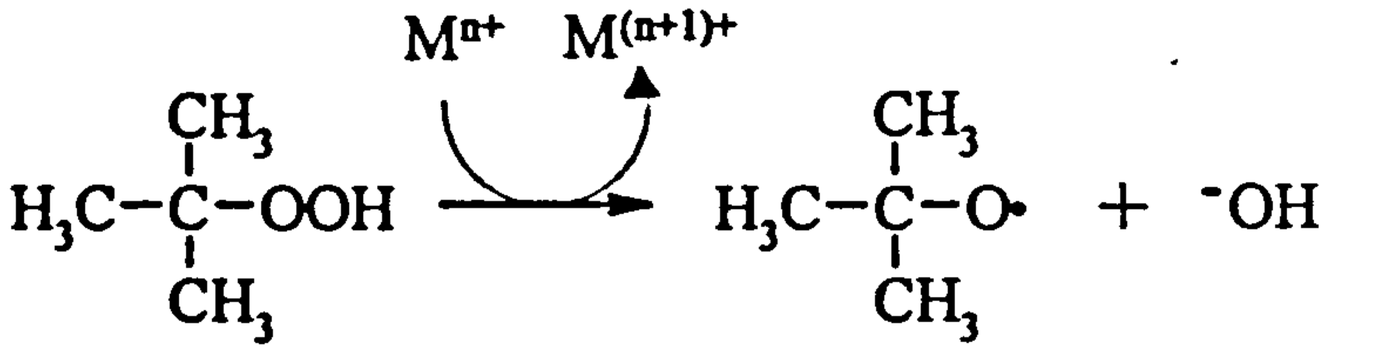

(5.3)

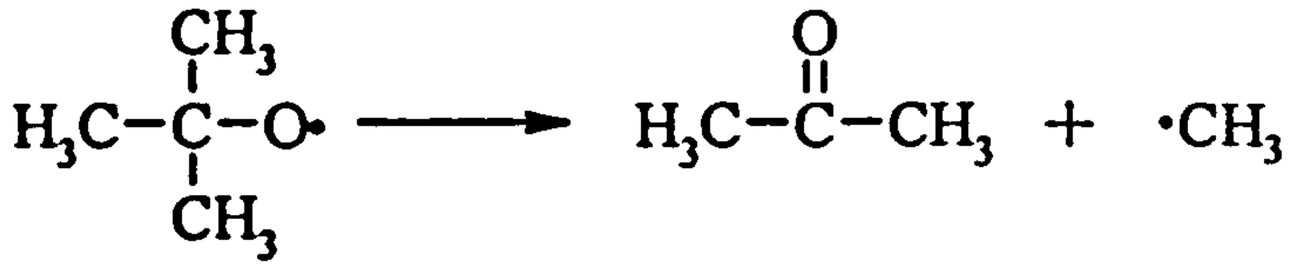

(5.4)

This provides evidence that, at least in the case of alkyl hydroperoxides, low concentrations of radicals are generated on addition of these types of compound to *E. coli*. It is believed this may be a result of reaction of intracellular transition-metal ions with the

hydroperoxides, which has been suggested to account for their biocidal action.[106,107]

5.6. EXPERIMENTS EMPLOYING TRANSITION-METAL SUPPLEMENTED *E. COLI.*

In experiments described thus far, measures have been taken to exclude transition-metal ions from the experimental system, since these would obviously lead to artefactual results. However, in real situations where peroxygens are used as biocides, bacteria will not have been subjected to these stringent growth conditions and hence may be expected to contain higher concentrations of transition-metal ions such as iron or copper. It is believed that although high-valent transition metal ions such as Cu^{2+} and Fe^{3+}do not react particularly rapidly with peroxyacids they will be able to undergo reduction intracellularly to produce their more redox-active forms (Cu^{+} and Fe^{2+}, respectively). It was therefore decided to examine the reactions of *E. coli* grown with elevated concentrations of iron and copper with peroxygens, employing the spin-trapping technique.

5.6.1.Iron supplemented *E. coli.*

E. coli were grown as described earlier in the presence of 5×10^{-4} M $FeSO_4 \cdot 7H_2O$. Removal of extracellular iron before EPR experiments was ensured by repeated washing in 0.05 M Chelex treated Na_2SO_4. Initial experiments involved mixing iron-enriched *E. coli* with 3.6×10^{-4} M 5% PAA in the presence of 0.066 M DMPO. The EPR spectrum showed a signal attributed to DMPO-OH ($a_N = a_{\beta\text{-}H} = 1.49 \pm 0.01$ mT).[158] The signal was stronger than that produced in the absence of added iron and was found to be scavengable on addition of 1.1 M DMSO, providing evidence for the formation of hydroxyl radicals intracellularly (see Figures 5.3.a and 5.3.b).

Addition of 40% PAA to the iron-enriched bacteria in the presence of DMPO also led to the formation of DMPO-OH. The signal amplitude was greater than that observed in the absence of the iron; addition of DMSO led to the detection of DMPO-CH_3 providing evidence for the formation of hydroxyl radicals. However, it is interesting to note that no

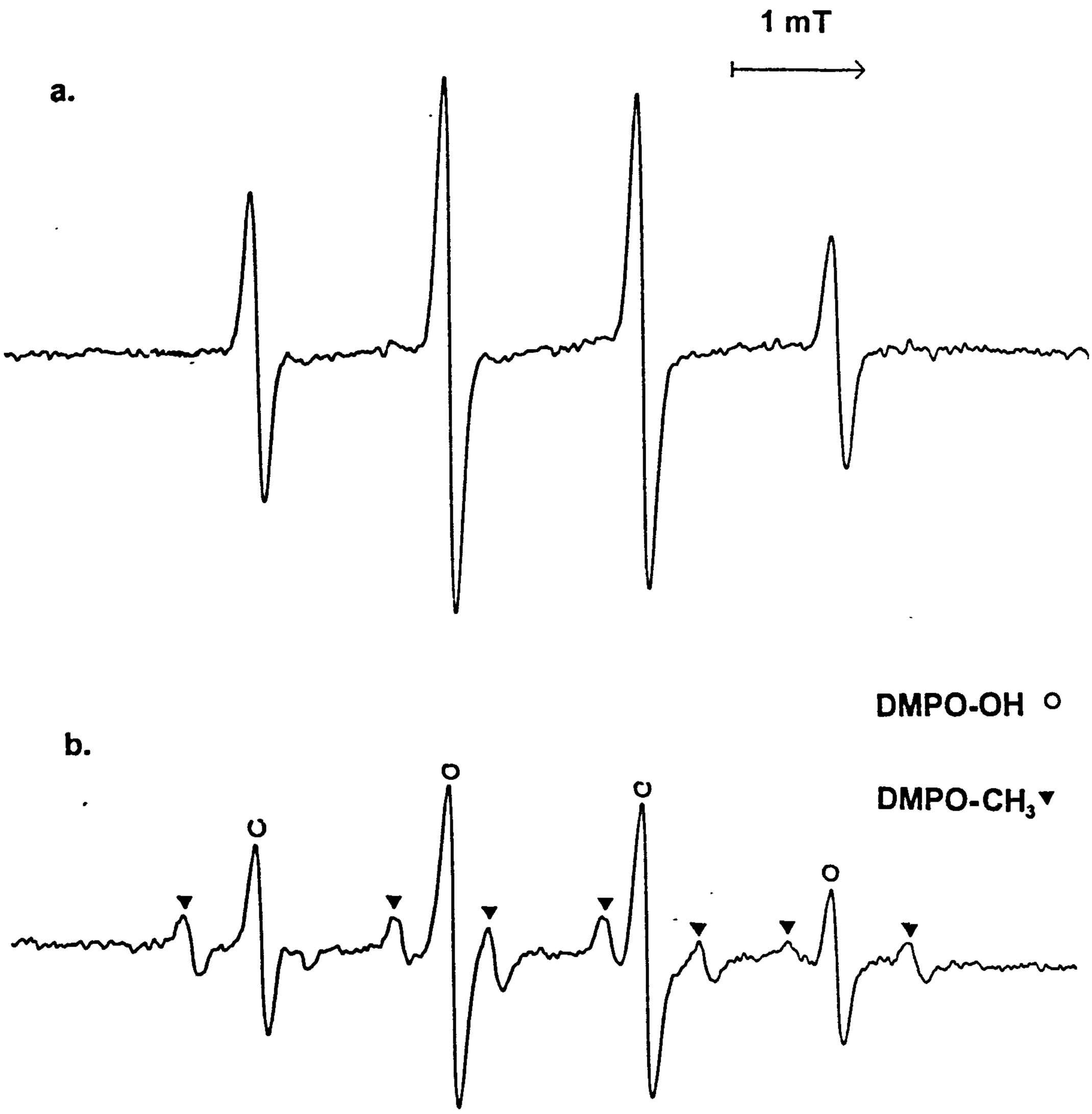

Figure 5.3.a. EPR spectrum showing the DMPO-OH adduct generated upon reaction of iron-enriched *E. coli* with 5% PAA and DMPO.

Figure 5.3.b. EPR spectrum showing the DMPO-OH and DMPO-CH_3 adducts generated upon reaction of iron-enriched *E. coli* with 5% PAA, DMSO and DMPO.

Concentrations employed:- *E. coli*, 2×10^9 cfu ml^{-1}, 5% PAA, 3.6×10^{-4} M, DMPO, 0.066 M, DMSO, 1.1 M

signal attributable to a carbon-centred radical adduct was observed, which is again surprising given the results described earlier in this Thesis (see Chapter Two). It is possible that the metal may be chelated intracellularly in such a way that it reacts with the peroxyacid by an outer-sphere rather than an inner-sphere mechanism thus leading to the formation of the thermodynamically-preferred hydroxyl radicals and acetate anions, rather than acetoxyl radicals [see reactions (5.5) and (5.6)]. It is also believed that the hydroxyl radicals observed are in part be due to the reaction of hydrogen peroxide in the reaction mixtures.

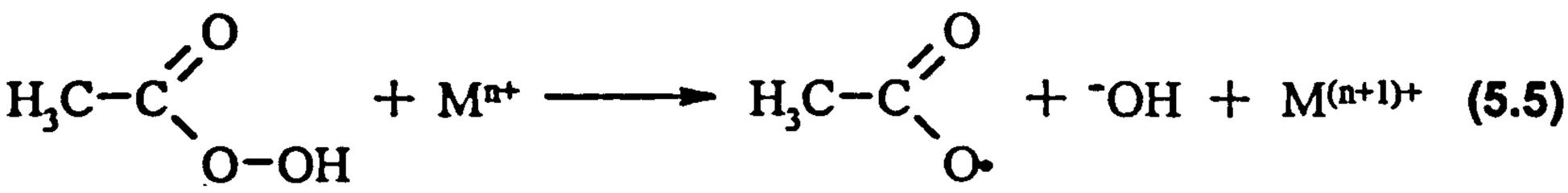

$$H_3C-C(=O)-O-OH + M^{n+} \longrightarrow H_3C-C(=O)-O\cdot + {}^{-}OH + M^{(n+1)+} \quad \textbf{(5.5)}$$

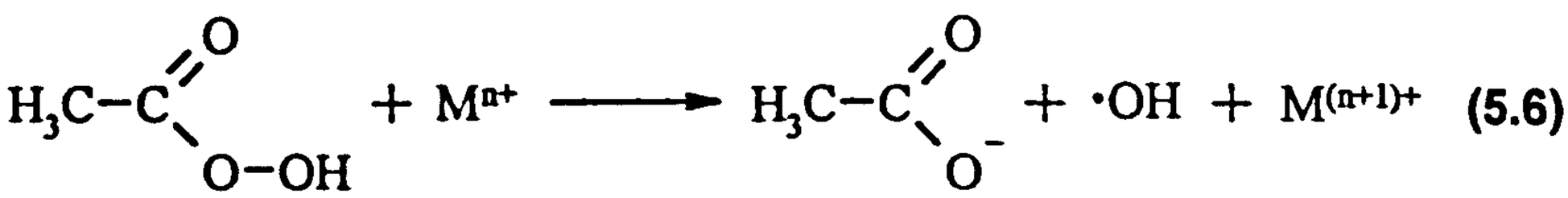

$$H_3C-C(=O)-O-OH + M^{n+} \longrightarrow H_3C-C(=O)-O^{-} + {}^{\cdot}OH + M^{(n+1)+} \quad \textbf{(5.6)}$$

On addition of MMPP to the iron-enriched bacteria signals attributable to DMPO-OH and DMPO-Ar were observed. Addition of DMSO led to partial scavenging of the DMPO-OH signal indicating the formation of a low concentration of hydroxyl radicals, but the DMPO-OH signal is largely attributed to spin-trap oxidation.

Addition of hydrogen peroxide led to the production of DMPO-OH. Addition of DMSO prior to the addition of the peroxide led to the detection of DMPO-CH_3 indicating that hydroxyl radicals are formed.

5.6.3. Copper supplemented *E. coli.*

E. coli were grown in the presence of 5×10^{-4} M $CuSO_4 \cdot 5H_2O$. Initial experiments involved the mixing of copper-enriched *E. coli* with DMPO and 5% PAA. The EPR spectrum observed was of DMPO-OH. Addition of DMSO did not lead to the conversion of this signal into DMPO-CH_3 indicating that the spin-adduct is formed through an alternative oxidative mechanism to classical spin-trapping. Similarly, addition of 40%

PAA, MMPP and hydrogen peroxide to the copper-enriched *E. coli* led to the formation of hydroxyl-radical adducts which were shown to have been formed by non-conventional mechanisms by the use of DMSO (see above).

5.6.3. Discussion.

The results described here show that radical production on *E. coli* can be promoted by addition of intracellular iron, but not by the addition of intracellular copper. It has also been shown that reaction of PAA with iron-enriched *E. coli* leads to the formation of hydroxyl radicals rather than acetoxyl radicals. This is somewhat surprising given the results obtained earlier, and has tentatively been attributed to the iron being chelated in such a way that it can react via an outer-sphere mechanism to produce the thermodynamically preferred hydroxyl radical and acetate anion [see reactions (5.5) and (5.6)]. It was next decided to examine the modification of cellular components in intact cells caused by oxidation with PAA (and transition-metal ions).

5.7. EPR SPIN-PROBE STUDIES OF THE REACTIONS OF PEROXYGENS WITH *ESCHERICHIA COLI.*

The effect of peroxygens on the structure of the bacterial membrane was next investigated using an EPR spin-probe technique, employing the doxyl stearic acid series of spin-probes. It was believed that, as only low concentrations of peroxygen were to be used, there would not be a problem with acidity leading to partitioning of the protonated and deprotonated forms of the spin-probe into different areas of the membrane.

Experiments were performed with 5 and 16-doxyl stearic acids. In all cases the spectra were comprised of an anisotropic and an isotropic element, although the relative concentration of each component varied. The anisotropic element was broad and featureless indicating that the nitroxide signal is being broadened by another paramagnetic species (possibly other nitroxides or paramagnetic metal centres) or the spin-probe is slow-tumbling at varying rates. The isotropic element was a typical nitroxide (a_N typically

1.39 mT). Attempts were made to examine the spectra again after the addition of peroxygens (final concentration 3.6×10^{-4} M). Again, inconsistencies were observed. On some occasions the signal intensity was seen to increase. It is believed that this may be a result of oxidation of EPR silent hydroxylamines (produced by the reaction of the spin-probe with cellular antioxidants) by the peroxygen. On other occasions the signal was seen to decrease. The reason for this is not known, since it is believed (from the spin-trapping experiments) under the conditions used radicals are not formed.

In conclusion, no gross changes were observed in the spectra of *E. coli* containing doxyl stearic acid spin-probes after the addition of peroxygens.

5.8. EXAMINATION OF PROTEIN DAMAGE IN *ESCHERICHIA. COLI* TREATED WITH PAA OXIDISING SYSTEMS.

Protein damage (as assessed by protein carbonyls)[7,129,185,199-202] has already been assessed for a model protein, BSA, (see Chapter Three) and was found to be extensive, especially when 40% PAA was employed in conjunction with transition-metal ions. Therefore it was decided to examine protein oxidation in intact bacterial cells using this method, both in the presence and absence of exogenous transition-metal ions.

A bacterial suspension (final concentration 3×10^{10} cfu ml^{-1}) was treated with a variety of oxidising mixtures for one hour and the appearance of the suspensions noted. After this, the soluble protein fraction was isolated (see Chapter Six). The concentration of protein recovered was examined to allow the degree of cell lysis caused by the oxidising mixtures to be estimated and to ensure that the protein concentration was high enough to proceed with the derivatisation step. The protein was then analysed for the concentration of side-chain carbonyl groups formed, employing the 2,4-DNPH method,[203] and the concentration of protein reanalysed to determine how many carbonyls were formed per mg of protein.

The appearance of the suspensions after treatment was found to differ depending upon the oxidising treatment used. The suspension containing untreated cells was unchanged after one hour, being of uniform turbidity. Suspensions which were treated

with 5% PAA oxidising mixtures were slightly more turbid at the bottom than the top. However, the samples which had been treated with 40% PAA oxidising mixtures were almost clear at the top, where as a thick layer of cell debris was seen at the bottom, providing an indication that extensive cell-death was caused by these mixtures.

It was found that the concentration of protein recovered from cells which had been treated with 0.01 M (total AvOx) 5% PAA, either in the presence or absence of Fe^{2+}-EDTA was approximately equal to the concentration of protein recovered from untreated cells. This implies that cell lysis was not significant when the bacteria were treated with 5% PAA oxidising mixtures as the majority of the protein remained in intact cells and therefore was not removed by centrifugation of the treated suspension and removal of the supernatant. However, the yield of protein which was recovered from cells exposed to 40% PAA oxidising treatments was much lower, indicating that significant cell lysis had occurred.

Upon derivatisation with 2,4-DNPH the protein recovered from untreated cells was found to contain a low concentration of protein carbonyl groups (see Figure 5.4). Addition of either 0.01 M (total AvOx) 5% PAA did not lead to the production of a significant concentration of carbonyl groups. This suggests that the role of intracellular transition-metal ions in radical generation is minimal. It is believed low levels of protein damage are detected because detected hydrogen peroxide is not very membrane-soluble and therefore only low concentrations reach transition-metal ion centres. In addition, if only low concentrations of the peroxygen are crossing the membrane the cells antioxidant defences may well be able to overcome the low levels of oxidative stress. Addition of 0.001 M Fe^{2+}-EDTA to 5% PAA to generate radicals, did not lead to the production of significant concentrations of carbonyl groups. This is surprising given the results obtained in Chapter Three although, again this possibly reflects hydrogen peroxide being less lipophilic than peroxyacetic acid and therefore intracellular proteins being less accessible to damage.

Treatment of *E. coli* with 40% PAA only led to the detection of low concentrations of carbonyl groups, indicating that the role of intracellular transition-metal ions in radical generation was not important. The reasons for this are unknown. However, addition of exogenous Fe^{2+}-EDTA and 40% PAA to the bacterial suspension led to the formation of

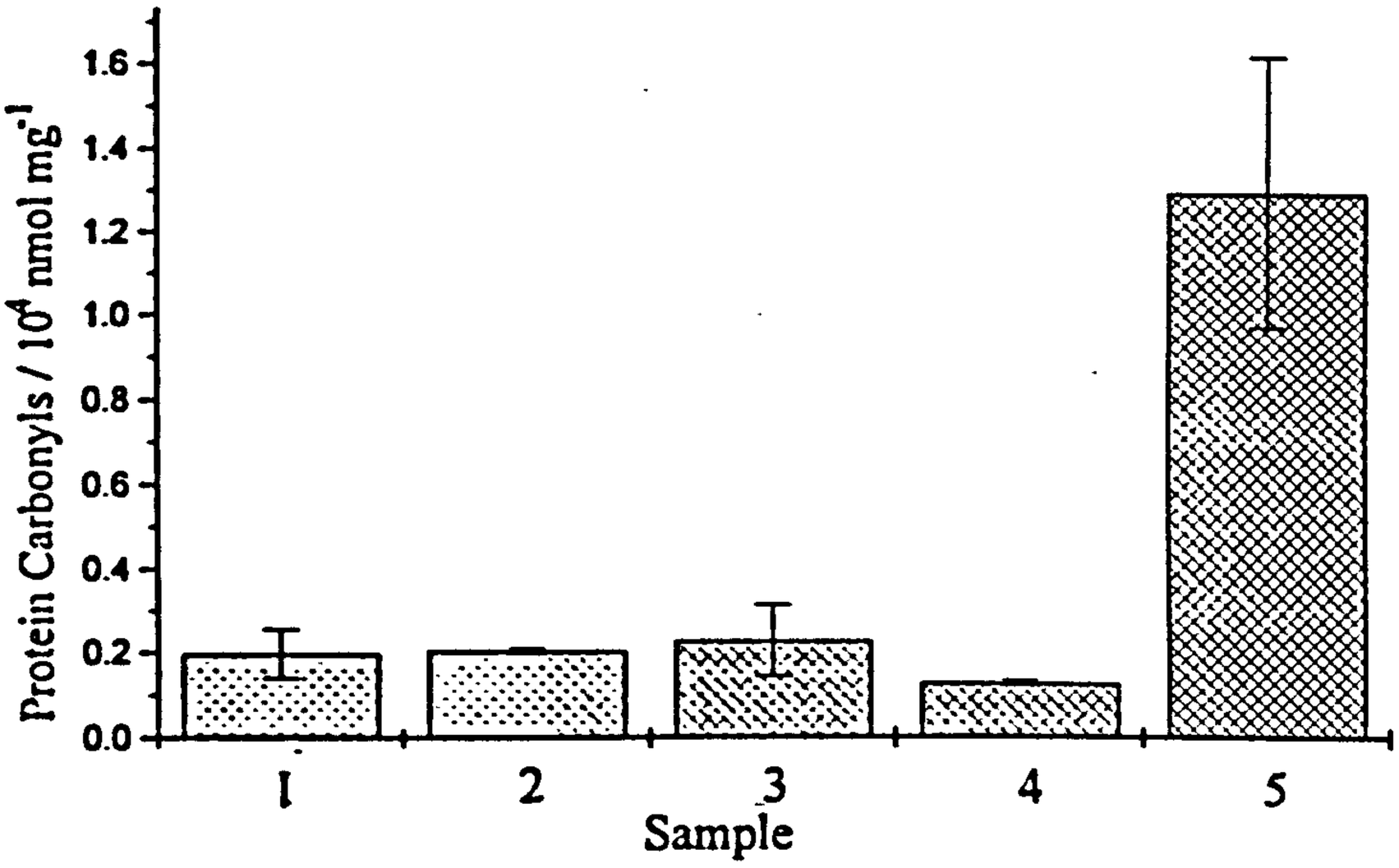

Figure 5.4. Determination of protein carbonyls generated on bacterial proteins by treatment with various Fe^{2+}-EDTA (0.001 M) / PAA (0.01 M total AvOx) oxidising treatments as measured by derivatisation with 2,4-DNPH:-

1. **Untreated *E. coli.***
2. ***E. coli* and 5% PAA.**
3. ***E. coli* and 40% PAA.**
4. ***E. coli*, Fe^{2+}-EDTA and 5% PAA.**
5. ***E. coli*, Fe^{2+}-EDTA and 40% PAA.**

1.29 ± 0.32 protein carbonyls per mg of protein. This is in agreement with the results obtained in Chapter Three that showed that this mixture led to extensive carbonyl formation on BSA. It indicates that the combination of the greater lipophilicity of the peroxyacetic acid combined with a stimulated radical burst leads to extensive protein carbonyl formation.

5.8.1.Discussion.

It is clear that extensive cell lysis is caused by treatment of bacterial suspensions with 40% PAA, both in the presence and absence of Fe^{2+}-EDTA. This is in agreement with studies which have found that formulations containing higher concentrations of peroxyacetic acid are better biocides.[1,109-111] In addition, it has also been shown that formation of carbonyl groups on side-chains of bacterial proteins is considerable when intact cells are treated with Fe^{2+}-EDTA and 40% PAA. This is in agreement with earlier work (see Chapter Three) which suggested that 40% PAA / Fe^{2+}-EDTA caused the most damage to BSA. However, significant levels of damage were also observed when BSA is treated with 5% PAA / Fe^{2+}-EDTA. It is believed that this was not repeated in the bacteria for two reasons. Firstly, it has been shown that hydrogen peroxide (the main component in 5% PAA) does not dissolve as readily in membrane-type solvents (see Chapter Four) and therefore might not be found intracellularly in such high concentrations. Secondly, bacteria are much better equipped to remove hydrogen peroxide than peroxyacetic acid, and hence it might be anticipated that formulations containing higher concentrations of peroxyacetic acid are more damaging. The reasons for 40% PAA alone causing little damage are unclear.

Since treatment of bacteria with PAA alone[1,109-111] leads to cell death, it is concluded that the formation of carbonyls on proteins may not be crucial, either as a part of bactericidal action or as a consequence. However, in situations where cells might be expected to be exposed to higher levels of transition-metal ions this type of radical damage may become more important.

5.9. EXAMINATION OF LIPID PEROXIDATION IN *ESCHERICHIA. COLI* TREATED WITH PAA OXIDISING SYSTEMS.

Experiments examining lipid peroxidation in bacteria were next carried out to examine if lipid peroxidation (as measured by the TBA test)[5,64,238,239] could be initiated by the reactions of PAA with endogenous transition-metal ions or whether lipid peroxidation could be induced by the addition of exogenous transition-metal ions.

Initial experiments involved the mixing of *E. coli* (final concentration 3×10^9 cfu ml^{-1}) with 0.01 M (total AvOx) 5% PAA followed by incubation at 37° C for one hour. After this, the pH was adjusted to between 2.0 and 2.5 by addition of NaOH if necessary, and the mixtures treated as described in Chapter Six. This treatment did not produce any change in the concentration of TBA_2-MDA produced over the baseline level (see Figure 5.5). Addition of the equivalent concentration of 40% PAA led to a small increase in the concentration of TBA reactive species formed. It is believed this reflects the greater lipophilicity of peroxyacetic acid, low concentrations being able to permeate the membrane. Addition of Fe^{2+}-EDTA, to stimulate radical production led to a dramatic rise in the concentration of TBA_2-MDA observed in both the 5% PAA and 40% PAA systems, although the difference between the two was not as marked as it was in the liposomes.

The generation of only low concentrations of TBA reactive material in these reactions in the absence of added transition-metal ions suggests that lipid peroxidation is not of great significance in the bactericidal action of PAA. However, it is believed that it may contribute in situations where bacteria have been exposed to transition-metal ions.

5.10. CONCLUSIONS.

The results described in this Chapter suggest that the generation of spin-adducts from peroxyacid / *E. coli* reactions is not indicative of radical formation, but possibly indicative of the formation of some other highly oxidising species. However, addition of iron to the growth medium does stimulate radical production. Conversely, reaction of alkyl hydroperoxides with *E. coli* leads to radical formation, at least at elevated concentrations.

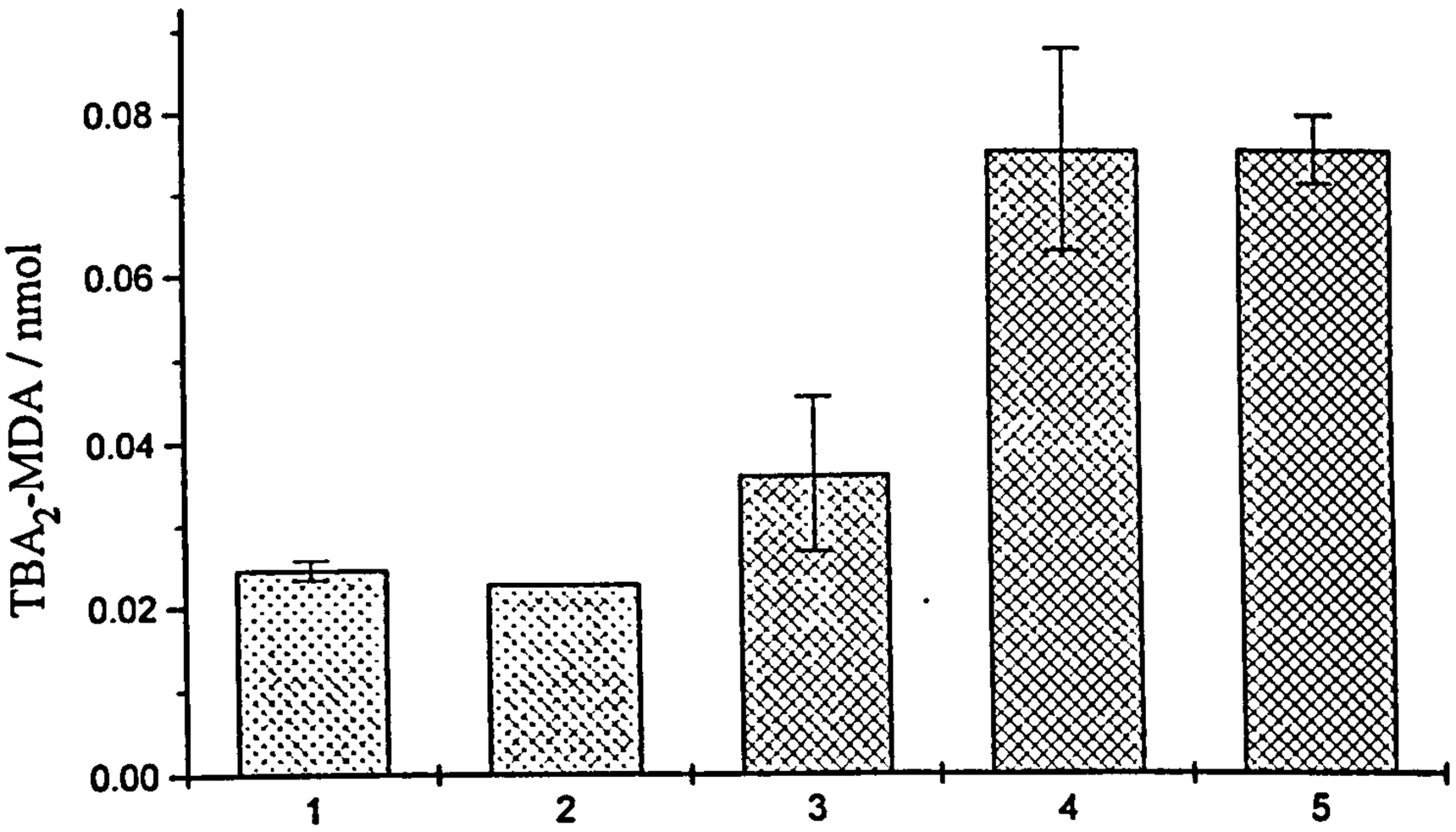

Figure 5.5. Lipid peroxidation in *E. coli* caused by PAA (0.01 M total AvOx) / Fe^{2+}-EDTA systems as measured by the TBA test.

1. ***E. coli*.**
2. ***E. coli* and 5% PAA.**
3. ***E. coli* and 40% PAA**
4. ***E. coli*, Fe^{2+}-EDTA and 5% PAA.**
5. ***E. coli*, Fe^{2+}-EDTA and 40% PAA.**

Damage to both proteins and lipids in bacterial cells is brought about by, in particular, 40% PAA in the presence of Fe^{2+}-EDTA. However, the significance of these reactions in bactericidal action is questionable, since it is known that PAA is bactericidal in the absence of exogenous transition-metal ions.[1.109-111]

The results described here are in partial agreement with those described in previous Chapters, and this provides some insight into the complex mechanism of action of peroxygen biocides; the conclusions are reviewed at this stage in the context of the earlier results. For example, the reaction between Ti^{3+}-EDTA / Fe^{2+} -EDTA and peroxyacetic acid is rapid and yields carbonyloxyl radicals, whereas the reaction between Cu^{+} and peroxyacetic acid is much more complex, as shown in Chapter Two. Radical generation in iron-enriched *Escherichia coli* also occurs, although the nature of the radicals produced is different, possibly as a result of intracellular chelation of the iron.

Modification to BSA induced by the action of transition-metal / PAA couples includes the generation of side-chain and backbone radicals, loss of reduced thiol groups, increased susceptibility to enzymatic digestion, protein fragmentation and side-chain carbonyl formation. All of these processes are more extensive when 5% PAA oxidising systems are employed, except for the generation of side-chain carbonyl groups, which are found to be more prevalent when 40% PAA oxidising systems are employed. This is in agreement with the results of protein-bound carbonyl determinations conducted upon *Escherichia coli*. Damage to proteins as measured by the generation of side-chain carbonyl moieties may be of significance in bactericidal action, although PAA is known to lead to cell-death at the concentrations employed in the absence of added iron.[109]

From the findings described in Chapter Four it is concluded that lipid peroxidation is more extensive in the presence of 40% PAA / transition-metal systems than in the presence of 5% PAA / transition metal systems; a result which was reproduced in the bacteria. However, it is not envisaged that this is an important mechanism in cell death since the concentrations of TBA_2-MDA generated are very low. This is in accord with previous suggestions which stated that the lipid profile of *Escherichia coli* is not perturbed by treatment with lethal doses of peroxygen compounds.[248]

It is believed that a range of processes including generation of radical species and

other oxidising species, lipid damage, protein damage and damage to antioxidant defences in a variety of processes generally referred to as oxidative stress contribute to the bactericidal action of peroxyacetic acid.

It is concluded from results described here and elsewhere that peroxyacetic acid is a more effective biocide than other peroxyacids and hydrogen peroxide itself. Although no definitive evidence has been obtained here, membrane permeability, generation of $MeCO_2^{\cdot}$, $^{\cdot}CH_3$ and reduction in overall antioxidant defences may be of importance in the bactericidal action of peroxyacetic acid.

There is much scope for future research into the bactericidal action of peroxyacetic acid especially in transition-metal containing systems. In model systems, the reactions of peroxyacetic acid with amino acids and small peptides could be investigated to gain an insight into their specific reactions with proteins. The effects of more lipophilic peroxyacids on peroxidation, both in liposomes and in bacteria would be particularly informative as would the relation of this information to cell-death studies, both in *Escherichia coli* and other organisms.

CHAPTER 6.

EXPERIMENTAL.

6.1. CHEMICALS.

All chemicals were supplied by Sigma Aldrich Co. apart from hydrogen peroxide and 5% peroxyacetic acid samples which were a gift of Solvay and 40% PAA which was a gift of Degussa. DEPMPO and OPMPO were both gifts of Prof. Paul Tordo. Coomassie Blue protein-binding dye was purchased form Pierce. *Escherichia coli* (NCIMB 9517, ATCC 11229) were obtained as a freeze dried culture from the NCIMB. The culture was reconstituted in 1 ml nutrient broth / glycerol and stored at -80 °C until required. Nutrient broth and nutrient agar were obtained from Oxoid.

All chemicals were used as supplied, with the exception of DMPO which was made up in aqueous solution and then stirred with activated charcoal for twenty minutes to remove paramagnetic impurities. The solutions was then filtered and stored at -20 °C before use.

All aqueous solutions were prepared in ultra high purity deionised water and (for EPR studies and elsewhere when necessary) were purged with a stream of oxygen-free nitrogen before use. Solutions of MNP and OPMPO were made up in approximately 70% v/v water (or buffer where stated) and 30% v/v acetonitrile to ensure complete dissolution. All buffer solutions were treated with Chelex chelating resin for twenty minutes then filtered to remove adventitious transition metal ions before use.

Peroxygen solutions were made up immediately before use. The concentrations of hydrogen peroxide and peroxyacetic acid were determined as described later (6.5).

6.2. INSTRUMENTATION.

6.2.1.EPR spectroscopy.

EPR spectra were recorded either with a Jeol JES RE1X EPR spectrometer equipped with an X band Gunn Diode and 100 kHz modulation or a Bruker ESP 300 equipped with a X band klystron and 100 kHz modulation and a Bruker ER035 gaussometer for field calibration. For studies of freely tumbling organic species the modulation amplitude was

typically set between 0.025 and 0.1 mT. Acquisition of copper EPR spectra or EPR spectra of protein-derived free radicals were typically made with modulation amplitude between 0.25 and 0.4 mT. The microwave power was typically set at 10 mW.

EPR flat cells (with internal dimensions of approximately 60 × 8 × 0.26 mm) constructed in the department from high quality quartz glass were employed for studies of aqueous solutions. Hyperfine splittings were determined directly from the field scan and where necessary were confirmed by spectral simulation. *g*-values were obtained by using the machine field scan and frequency.

6.2.2.Continuous-flow system.

The flow system employed for the direct detection of radicals from peroxyacetic acid employed a specially designed EPR cell and mixing chamber allowing simultaneous mixing of three reagent streams in the range of 20 - 100 ms (for experiments described in this Thesis typically 30 - 40 ms) before entering the EPR cell; the flow was controlled and maintained using a Watson- Marlow 502S peristaltic pump positioned on the inlet tubing. The pH of the reaction mixtures was monitored by a pH meter placed in the effluent stream; the pH was adjusted where necessary by the addition of concentrated sulfuric acid or concentrated ammonia to the metal ion stream. Typical experiments employed a metal concentration of 0.0017 M, a peroxyacetic acid concentration of between 0.0083 and 0.033 M (total AvOx) and a concentration of reagent (where used) of 3.3% by volume. All concentrations are quoted after mixing. All streams were deoxygenated by purging with nitrogen-free oxygen prior to and during the experiments.

6.2.3.Photolysis

Photolysis of samples in the cavity of the EPR spectrometer employed an ILC302 UV xenon high intensity light source (0-300 W variable power, $\lambda \leq 390$ nm) directed by a liquid light guide.

6.2.4.UV-visible spectrophotometry.

UV-visible spectra were recorded on a Hitatchi U-3000 spectrophotometer using a 1 cm path length quartz cells with internal volume of either 1 or 4 cm^3 or for studies of proteins or bacterial suspensions disposable silica cells of internal volume 1 cm^3.

6.2.5.NMR spectroscopy.

^1H and ^{13}C NMR (both fully and partially decoupled) spectra were recorded on a Jeol EX 270 spectrometer, Chemical shifts are quoted in δ (ppm). Samples were prepared in solutions of deuterochloroform.

6.2.6.Spectral simulations.

Spectral assignments and splittings were sometimes verified by spectral simulation using a program originally written by Dr. M.F. Chiu and subsequently adapted by Dr. A.C. Whitwood (both of the Department of Chemistry, University of York) to run on a Viglen 486 P.C. This program allows simulation of isotropic spectra containing up to ten species. Variations in linewidth, concentration, exchange processes and second-order effects may also be accounted for. Simulations were carried out with a range of parameters until the best visual fit was obtained between experimental and simulated spectra.

6.3. SYNTHESES AND PREPARATIONS.

6.3.1.DBNBS.

DBNBS was synthesised according to the standard literature procedure[166,167] and recrystallised from hot ethanol. Samples were stored at -20 °C before use.

6.3.2.Preparation of oleic and linoleic acid epoxides using PAA.

Typically 0.015 moles of 5% PAA or 40% PAA was added to a stirred dichloromethane solution containing 0.005 moles of either linoleic or oleic acid. In buffered reaction systems Na_2CO_3 was added in either an equimolar quantity (40% PAA) or at a ten-fold molar excess (5% PAA). Reaction mixtures were stirred overnight under nitrogen atmosphere before the organics were extracted into dichloromethane and washed three times (20 cm^3) with saturated sodium bicarbonate and three times (20 cm^3) with water. The organic layer was dried using anhydrous magnesium sulfate and the solvent was removed under reduced pressure. The product was redissolved in $CDCl_3$ and analysed by ^1H and ^{13}C NMR spectroscopy. Purity is quoted on the basis of NMR evidence only.

NMR data:-

oleic acid epoxide; δ_H(270 MHz; $CDCl_3$) 3.0 (2 H, br s, epoxide CH), 2.4 (2 H, t, CH_2CO_2H) 1.8 - 1.3 (26 H, br m, CH_2) 0.98 (3 H, t, CH_3); δ_C(67.9 MHz: $CDCl_3$) 180.0 (C=O) 57.5 (C-O) 35.0, 32.5, 30.3, 29.9, 29.8, 28.0, 27.5, 25.0, 22.5 (CH_2), 14.0 (CH_3)

oleic acid diacteate ester; δ_H(270 MHz; $CDCl_3$) as for oleic acid epoxide except 5.1 (2 H, m, CH-O-C=O) 4.95 (3 H, m, CH_3C=O) 4.75 (3 H, m, CH_3C=O); δ_C(67.9 MHz; $CDCl_3$) as for oleic acid epoxide except 104.2 (C-Ac) 18.0 (CH_3).

linoleic acid epoxide; δ_H(270 MHz; $CDCl_3$) 3.2 (2 H, m, epoxide CH) 3.05 (2 H, br s, epoxide CH) 2.4 (2 H, t, CH_2CO_2H), 1.9 -1.3 (22 H, br m, CH_2) 0.98 (3 H, t, CH_3); δ_C(67.9 MHz; $CDCl_3$) 180.0 (C=O) 58.0 (C-O) 54.0 (C-O) 34.0, 31.5, 29.9, 29.85, 28.0, 27.9, 27.85, 27.0, 26.85 (CH_2) 14.0 (CH_3).

6.3.3.Preparation of oleic and linoleic acid epoxides using *m*-CPBA.

0.01 Moles *m*-CPBA was added to a stirred solution containing 0.005 moles of oleic or linoleic acid in dichloromethane. The reaction mixture was stirred under nitrogen overnight. The organic components were then extracted into dichloromethane and washed three times with 10% w/v sodium sulfite (20 cm^3) and three times with 5% w/v sodium bicarbonate (20 cm^3) before finally washing three times with water (20 cm^3). The organic

layer was dried with anhydrous magnesium sulfate and the solvent removed under reduced pressure to isolate the product. The product was analysed using ^{1}H and ^{13}C NMR spectroscopy (for details see 6.3.2). Quoted purities are based upon NMR data only.

6.3.4.Preparation of epoxyphosphatidylcholine in organic solvent using PAA.

Typically 1 ml of a 100 mg/ml solution of fresh egg yolk phosphatidylcholine in $CHCl_3$ was taken and the solvent removed under vacuum. The residue was dissolved in 1 ml CH_2Cl_2 and 0.03 moles (total AvOx) 5% PAA or 0.0038 moles (total AvOx) 40% PAA was added. 0.03 moles of sodium carbonate was added in experiments where buffered 5% PAA was required and 0.003 moles of sodium carbonate was added in experiments in which buffered 40% PAA was required. The reactions were stirred overnight under nitrogen before the organics were extracted into CH_2Cl_2. The organic layer was washed three times with saturated sodium bicarbonate (20 cm^3), then three times with water (20 cm^3) before drying with anhydrous magnesium sulfate. The product was isolated by removal of the solvent under reduced pressure then redissolved in $CDCl_3$ and analysed by NMR spectroscopy.

NMR data:-

δ_H(270 MHz; $CDCl_3$) 5.15 (br s, CH_2-O-C=O) 4.3, 4.05, 3.85, 3.75 (br s/m CH_2-O) 3.2 (br s, $N^+(CH_3)_3$) 3.0 (br s, epoxide CH) 2.85 (br s, $(CH_3)_3N^+CH_2$), 2.2, 1.95, 1.6 - 1.15 (br m, CH_2); δ_C(67.9 MHz; $CDCl_3$) 173.5 (C=O) 69.0 (C-O) 67, 63.5, 63.0, 60.0 (CH_2-O) 57.5 (epoxide C-O) 54.2 ($N^+(CH_3)_3$) 34.3, 34.0, 31.8, 31.5, 29.7, 29.5, 29.3, 29.2, 29.1, 27.2, 25.6, 24.9, 24.8, 22.6, 22.5 (CH_2) 14.1 (CH_3).

6.3.5.Preparation of epoxyphosphatidylcholine in organic solvent using *m*-CPBA.

0.002 Moles *m*-CPBA was added to a stirred solution of phosphatidylcholine (0.1 g) in dichloromethane. The reaction was stirred under nitrogen overnight before extraction

of the organics into dichloromethane. This was washed three times with 10% w/v sodium sulfite (20 cm^3), then three times with 5% w/v sodium bicarbonate (20 cm^3) and three times with water (20 cm^3). The organic layer was dried with anhydrous magnesium sulfate, filtered and the solvent removed under reduced pressure. The residue was redissolved in $CDCl_3$ and analysed by ^1H and ^{13}C NMR spectroscopy (for details see 6.3.4)..

6.3.6.Preparation of liposomes.

Samples of 0.01 g ml^{-1} (for lipid epoxidation or lipid perooxidation studies) phosphatidylcholine liposomes were prepared as follows: an aliquot of 0.1 g ml^{-1} phosphatidylcholine in chloroform was pipetted into a 15 ml test tube and the solvent removed by bubbling with a stream of oxygen-free nitrogen. The appropriate volume of Chelex-treated 0.05 M Na_2SO_4 and several small washed glass beads were added and the mixture vortex mixed under nitrogen for approximately 60 s. The opaque mixtures were left under nitrogen, on ice in the dark for 1 h after which they were exposed to sonic oscillation in a sonic bath for approximately 30 minutes at 25 ^0C, until the mixtures became translucent.

6.3.7.Liposome epoxidation studies using PAA.

10 ml Samples of 0.01 g ml^{-1} liposomes were prepared as described above. 0.03 - 0.3 moles (total Av)x) 5% PAA or 0.0038 - 0.038 moles (total AvOx) 40% PAA was added to the liposome preparation. In addition where specified, sodium carbonate was added (0.03 - 0.3 moles for experiments employing 5% PAA and 0.003 - 0.03 moles for experiments employing 40% PAA). The reaction mixture was stirred overnight under nitrogen. The lipid was extracted into diethyl ether prior to work up which involved washing three times with 5% w/v sodium bicarbonate (20 cm^3) and three times with water (20 cm^3). The organic layer was dried with anhydrous magnesium sulfate and the solvent removed under reduced pressure. The mixture was redissolved in $CDCl_3$ and analysed by

^{1}H and ^{13}C NMR spectroscopy (for details see 6.3.4).

6.3.8.Liposome epoxidation studies using *m*-CPBA.

10 ml Samples of 0.01 g ml^{-1} liposomes were prepared as described in 6.3.5. and 0.02 moles of *m*-CPBA were added. The mixture was stirred under nitrogen overnight and the lipid extracted into diethyl ether. The organic layer was washed three times (20 cm^3) with 10% w/v sodium sulfite, three times (20 cm^3)with 5% w/v sodium bicarbonate and three times with water. The organic layer was then dried using anhydrous magnesium sulfate and the solvent removed under reduced pressure. The residue was redissolved in $CDCl_3$ for analysis by ^{1}H and ^{13}C NMR spectroscopy (for details see 6.3.4).

6.3.9.Preparation of liposomes for spin-probe studies.

Liposomes were prepared for spin-probe studies as follows: 0.2 ml 0.1 g ml^{-1} phosphatidylcholine in chloroform was placed in a 15 ml test tube. 0.4 ml of 5×10^{-4} M x-doxyl stearic acid (where x is 5, 7, 10, 12 or 16) in chloroform was added and the solvent removed by bubbling with a stream of oxygen-free nitrogen. After this the procedure was identical to that described above (6.3.6).

6.3.10.Preparation of thiol-blocked BSA.

A 0.005 M solution of BSA was made up in a 0.1 M solution of N-ethylmalemide (NEM). The solution was transferred to washed dialysis tubing and dialysed overnight against 4 l of water at 4 ^{0}C to remove any excess NEM.[196]

6.3.11.Preparation of bacterial cultures.

Streak plates were prepared on sterile (autoclaved for 15 min at 121 ^{0}C) nutrient agar from the stock culture (see 6.1). The plates were incubated (upside down) overnight

at 37 °C then kept at 4 °C for up to two weeks. Liquid cultures were prepared from these plates as required. A colony was isolated from the agar plate with a sterile loop and used to inoculate a sterile (autoclaved for 15 min at 121 °C) solution (usually 100 ml) of nutrient broth in a 500 ml conical flask. The flask was loosely stoppered using a sterile cloth bung and incubated in an orbital shaker overnight at 37 °C. The bacteria were isolated by centrifugation at 4000 rpm for 10 min, after which they were washed three times in Chelex treated 0.05 M sodium sulfate and finally resuspended in a little of this solution. The concentration of the bacteria was calculated by the absorbance of an appropriately diluted sample of the suspension at 620 nm against a sodium sulfate blank and application of equation 6.1:-

$$\text{Conc. of diluted } \textit{E. coli} \text{ suspension / cfu ml}^{-1} = x(2 \times 10^8 / 0.16) \quad \textbf{Eqn. 6.1.}$$

where

x absorbance of diluted suspension at 620 nm.

The undiluted suspension was then used to make up a suspension of the required concentration.

All equipment used to handle bacteria and all used cultures were sterilised either by autoclaving at 121 °C for 30 min or, when this was not practical, immersion in a 20% solution of sodium hypochlorite overnight. Good microbiological practice was observed throughout.

Transition-metal supplemented *E. coli* were prepared by addition of the metal salt to the nutrient broth before inoculation. Bacteria containing spin-probes were prepared by inoculating a bacterial culture in the usual way and incubating at 37 °C until turbid. After this 1.4 ml of labelling mixture (0.01 g doxyl stearic acid in 2 ml ethanol, 0.5 ml 0.1 M NasOH and 5 ml 5×10^{-4} g ml^{-1} human serum albumin) was added for every 100 ml of nutrient broth and the culture incubated as usual.

6.3.12.Preparation of crude protein extracts from *E. coli*.

Intact bacteria (concentration after treatment approximately 5×10^9 cfu ml^{-1}) were exposed to oxidising mixtures as described in the text. After this the oxidant mixtures were removed from the intact bacteria by centrifugation at 4000 rpm for 10 minutes. The pellets were washed three times then resuspended in 0.05 M Chelex treated Na_2SO_4. The cells were lysed using 0.025 ml 0.01 g ml^{-1} lysozyme followed by incubation for 30 minutes at 37 °C. After this the bacteria were mixed with 0.1 ml 10% w/v streptomycin sulfate, to precipitate out DNA and 0.01 ml 5×10^{-4} g ml^{-1} RNase to degrade the RNA and incubated for 15 minutes at 37 °C. The mixtures were then centrifuged at 6500 rpm for 10 min to remove cell debris. To ensure that all the DNA and RNA has been removed the absorbance of samples was then recorded at 260 and 280 nm. If A_{280}/A_{260} was ≤ 1 another aliquot of streptomycin sulfate and RNase was added, the mixture incubated again and the precipitated DNA removed by centrifugation. The ratio of A_{280}/A_{260} of the supernatant was examined again to ensure removal of interfering substances. The crude protein extract was then removed to be analysed for carbonyl content and protein concentration.

6.4. METHODS OF ANALYSIS.

6.4.1.Protein Carbonyl Determination.

The method employed was based upon that outlined in references 203 - 205. Damage to proteins was initiated by the addition of oxidising mixtures to a solution of BSA in phosphate buffer (0.1 M pH 7.4) to give a concentration of protein of 0.0025 g ml^{-1}. After incubation for the desired time 4 × 0.5 ml aliquots of the protein solution were removed and placed in 1 ml Eppendorf tubes. 0.01 M 2,4-DNPH in 2.5 M HCl was added to three of the tubes and 0.5 ml 2.5 m HCl was added to the fourth tube. The tubes were incubated in the dark for 15 min before the addition of 0.1 ml 100% trichloroacetic acid. The tubes were stood in an ice bath for 10 min before centrifuging at 13000 rpm for five min. The supernatant were discarded and the protein precipitates washed once with 0.5

ml 10% v/v TCA then three times with 0.5 ml 1:1 ethyl acetate: ethanol. The protein pellets were air dried then redissolved in 1 ml 6 M guanidine hydrochloride.

The absorbance spectrum between 355 and 390 nm of each sample was recorded, using a solution of 6 M guanidine hydrochloride as a reference, and the absorbance at λ_{max} noted. The carbonyl concentration was determined. The concentration of carbonyls was determined using Eqn 6.2.

$$\text{Carbonyl concentration / nmol ml}^{-1} = \text{Abs at } \lambda_{max} / 22000 \qquad \textbf{Eqn 6.2.}$$

The concentration of the protein samples was determined from the blanks using one of the methods described below.

6.4.2.Protein Concentration Determination - the Bicinchoninic Acid Assay.

This method of protein concentration determination is based upon the method outlined in references 206 and 207. Reagent solutions A (1% w/v BCA, 2% w/v sodium carbonate, 0.16% w/v sodium tartrate, 0.4% w/v NaOH, 0.95% w/v sodium bicarbonate - pH adjusted to 11.25 by the addition of NaOH if necessary) and B (4% w/v $CuSO_4 \cdot 5H_2O$) were prepared and stored at room temperature; these solutions are stable for months. The working reagent was prepared by addition of 1 ml of reagent solution B to 50 ml of reagent solution A and was used within two hours of mixing. 0.05 ml of the protein solution was added to 1 ml of the working regent and was incubated at 37 °C for 30 min. The samples were then cooled and the absorbance recorded at 562 nm against a blank of phosphate buffer (0.1 M pH 7.4). The protein concentration was determined by comparison with a standard curve generated using known concentrations of protein between 0 and 0.001 g ml^{-1} prepared in parallel with the protein samples being determined. All samples were run in triplicate.

6.4.3.Protein Concentration Determination - the Coomassie Blue Assay.

This assay relies upon the binding of a dye to the protein leading to the formation of a chromophore.[207] Although it is not as strictly quantitative as the BCA assay it suffers from less problems with interfering substances which makes its use more appropriate when crude biological extracts are being used. 0.025 ml of the protein solution was added to 1.25 ml of the stain and mixed thoroughly. The absorbance at 595 nm was recorded against a blank of phosphate buffer (0.1 M, pH 7.4). The concentration of the protein was determined by comparison to a standard curve generated using protein samples of known concentration between 0 and 0.001 g ml^{-1}. All samples were run in triplicate.

6.4.4.Determination of reduced thiol groups.

The concentration of reduced thiol groups was determined using the method developed by Ellman, employing 5,5'-dithio-bis(2-nitrobenzoic acid) (DTNB) as outlined in references 208 and 209. All solutions (except Fe^{2+}-EDTA were prepared in phosphate buffer (0.1 M, pH 7.40 as the assay is known to be highly pH dependent. 0.5 ml aliquots of protein (0.005 g ml^{-1}) exposed to oxidising mixtures were taken and mixed with 0.125 ml o.002 M DTNB and 0.375 ml phosphate buffer (0.1 M, pH 7.4) and left for 30 minutes in the dark to react. After this the absorbance of the samples at 412 nm was recorded against a phosphate buffer as a reference. The absorbance of blanks, prepared in the absence of either protein or DTNB was recorded and subtracted from the original reading. The concentration of free thiol groups was determined using the extinction coefficient of 13600 M^{-1} cm^{-1}.

6.4.5.Determination of MDA.

0.01 g ml^{-1} unilamellar liposomes were treated with oxidising treatments as stated in the text to give a final concentration of 5×10^{-4} g ml^{1} lipid. Lipid peroxidation in bacteria was assessed employing a final concentration of *E. coli* of approximately 3×10^{9}

cfu ml^{-1}. Peroxidation was examined by a modification of the TBA test.[64,235,236] After incubation at 37 °C with the oxidants the reaction was quenched by the addition of 0.025 ml 0.2% w/v butylated hydroxytoluene in ethanol. 1 ml 10% v/v trichloroacetic acid and 2 ml 2% 2-thiobarbituric acid in 0.5 M NaOH. The mixtures were heated in a boiling water bath for 15 minutes, then cooled on ice. The TBA_2-MDA adduct was extracted into 2 ml of butan-1-ol and the organic layer removed. The organic layer was centrifuged to remove any solids (5 min, 6500 rpm) and the absorbance recorded against a butan-1-ol blank at 532 nm. The concentration of TBA_2-MDA was determined by comparison wit a standard curve generated by the reaction of 1,1,3,3 tetramethoxypropane (TMP) with TBA to produce TBA_2-MDA.

6.5. DETERMINATION OF PEROXYGENS.

6.5.1.Hydrogen peroxide.

The concentration of hydrogen peroxide in commercial samples was determined titration with potassium permanganate [see reaction (6.1)]. Approximately 100 ml sulfuric acid was placed in a 500 ml conical flask. 0.1 m potassium permanganate was added dropwise until a faint pink colour was seen. 0.2 - 0.25 g hydrogen peroxide was added and titrated against 0.1 M potassium permanganate solution until the faint pink colour reappeared. Titrations were performed in triplicate.

$$2\,MnO_4^- + 5\,H_2O_2 + 6\,H^+ \longrightarrow 2\,Mn^{2+} + 8\,H_2O + 5\,O_2 \quad \textbf{(6.1)}$$

6.5.2.Hydrogen peroxide in PAA.

Hydrogen peroxide in PAA formulations was determined by titration with acidified ceric sulfate [see reaction (6.2)]. Approximately 100 ml of 5% v/v sulfuric acid was placed in a 500 ml conical flask. Enough crushed ice was added to keep the temperature below 10 °C for the duration of the titration. When the temperature of the solution dropped below

10 °C a few drops of ferroin indicator was added and 0.1 m ceric sulfate solution was added dropwise until a faint blue colour appeared. 0.1 - 0.2 ml PAA was added and the solution titrated against the ceric sulfate until the faint blue colour became evident again. Titrations were performed in triplicate.

$$2\,Ce^{4+} + H_2O_2 \longrightarrow 2\,Ce^{3+} + 2\,H^+ + O_2 \qquad \textbf{(6.2)}$$

6.5.3.Peroxyacetic acid in PAA.

Peroxyacetic acid was determined by titration of liberated iodine from the reaction between peroxyacetic acid and potassium iodide against sodium thiosulfate [see reactions (6.3) and (6.4)]. 50 ml methanol was mixed with 50 ml 10 g l^{-1} potassium iodide in a 500 ml conical flask. Solid carbon dioxide pellets were added until the solution temperature fell to below 0 °C. A known volume between 0.5 - 0.7 ml of PAA was added to the flask. The iodine liberated was titrated against sodium thiosulfate until the solution becomes colourless.

$$2\,I^- + 2\,H^+ + CH_3CO_3H \longrightarrow I_2 + CH_3CO_2H + H_2O \qquad \textbf{(6.3)}$$

$$I_2 + 2\,S_2O_3^{2-} \longrightarrow S_4O_6^{2-} + 2\,I^- \qquad \textbf{(6.4)}$$

REFERENCES.

1. S.S Block, in "Disinfection, Sterilisation and Preservation", (ed. S.S Block), Lea and Febiger, London, 1983, 1.
2. R.B. Seymour and C.E. Carraher, "Polymer Chemistry, An Introduction", Marcel Dekker Inc, New York, 1992.
3. J.C. Bevington, "Radical Polymerisation", Academic Press, London and New York, 1961.
4. A.P. James and I.S. Mackirdy, *Chemistry and Industry*, 1990, 641.
5. J.M.C. Gutteridge and B. Halliwell, *TIBS*, 1990, **15**, 129.
6. K.J.A. Davies, *J. Biol. Chem.*, 1987, **262**, 9895.
7. R.L. Levine, *J. Biol. Chem.*, 1983, **258**, 11833.
8. H.R. Griffiths, J. Unsworth, D.R. Blake and J. Lumec, in "Free Radicals: Chemistry, Pathology and Medicine", (eds. C.A. Rice-Evans and T. Dormandy), Richlieu Press, London, 1988, 439.
9. B. Halliwell and O.L. Aruoma, *FEBS Lett.*, 1991, **281**, 9.
10. A.P. Breen and J.A. Murray, *Free Rad. Biol. Med.*, 1995, **18**, 1033.
11. R.H. Burdon, in "Free Radical Damage and its Control", (eds. C.A. Rice-Evans and R.H. Burdon), Elsevier Science, Amsterdam, 1993, 155.
12. B. Halliwell and J.M.C. Gutteridge, *Arch. Biochem. Biophys.*, 1986, **246**, 502.
13. B. Halliwell, *FASEB J*, 1988, **2**, 2867.
14. J.M. McCord, *Science*, 1974, **185**, 529.
15. M.L. Wolbarsht and I. Fridovich, *Free Rad. Biol. Med.*, 1989, **6**, 61.
16. H. Nakazawa and N. Fukuyama, *Redox Report*, 1995, **1**, 177.
17. B. Halliwell and J.M.C. Gutteridge, "Free Radicals in Biology and Medicine", Clarenden Press, Oxford, 1989.
18. A.I. Tauber and B.M. Babior, *Adv. Free Rad. Biol. Med.*, 1985, **1**, 265.
19. D. Cremer in "The Chemistry of Functional Groups: Peroxides", (ed. S. Patai), John Wiley and Sons, New York, 1983, 1.
20. Y. Sawaki in "Organic Peroxides", (ed. W. Ando), John Wiley and Sons, London, 1992, 425.
21. A.G. Davies, "Organic Peroxides", Butterworths, London, 1961.

22. J.O. Edwards in "Peroxide Reaction Mechanisms", (ed. J.O. Edwards), John Wiley and Sons, London and New York, 1962, 67.

23. R. Curci and J.O. Edwards in "Organic Peroxides - Volume 1", (ed. D. Swern), Wiley-Interscience, New York, 199.

24. S.N. Lewis in "Oxidation - Volume 1", (ed. R.L. Augustine), Marcel Dekker, New York, 1969, 213.

25. R. Hiatt in "Oxidation - Volume 2", (eds. R.L. Augustine and D.J. Trecker), Marcel Dekker, New York, 1971, 113.

26. D. Swern in "Organic Peroxides - Volume 2", (ed. D. Swern), Wiley Interscience, New York, 1971, 355.

27. G. Bouillon, C. Lick and K. Schank in "The Chemistry of Functional Groups: Peroxides", (ed. S. Patai), John Wiley and Sons, New York, 1983, 279.

28. B. Plesnicar in "The Chemistry of Functional Groups: Peroxides", (ed. S. Patai), John Wiley and Sons, New York, 1983, 521.

29. C.A. Bunton in "Peroxide Reaction Mechanisms", (ed. J.O. Edwards), John Wiley and Sons, London and New York, 1962, 11.

30. H.J.H. Fenton, *J. Chem. Soc.*, 1894, **65**, 899.

31. H.J.H. Fenton, *Proc. Chem. Soc.*, 1899, **15**, 224.

32. F. Haber and J.J. Weiss, *Proc. Roy. Soc. London Series A*, 1934, **147**, 332.

33. J.D. Rush and W.H. Koppenol, *J. Biol. Chem.*, 1986, **261**, 6730.

34. S. Pahaal and W. Richter, *J. Am. Chem. Soc.*, 1988, **110**, 3126.

35. T. Shiga, *J. Phys. Che*m., 1965, **69**, 3805.

36. J.D. Rush and W.H. Koppenol, *J. Inorg. Biochem.*, 1987, **29**, 199.

37. G. Sosnovsky and D.J. Rawlinson in "Organic Peroxides", (ed. D. Swern), Wiley Interscience, New York, 1971, 269.

38. Y. Ogata, K. Tomizawa and K. Furuta in "The Chemistry of Functional Groups: Peroxides", (ed. S. Patai), John Wiley and Sons, New York, 1983, 711.

39. A. Samuni, D. Meisel and G. Czapski, *J. Chem. Soc., Dalton Trans.*, 1972, 1273.

40. G.R.A. Johnson, N.B. Nazhat and R.A. Saadalla-Nazhat, *J. Chem. Soc., Faraday Trans. 1*, 1988, **84**, 501.

41. A. Bakac and J.H. Espénson, *Inorg. Chem.*, 1983, **22**, 779.

42. M. Masarwa, H. Cohen, D. Meyerstein, D.L. Hickman, A. Bakac and J.H. Espénson, *J. Am. Chem. Soc.*, 1988, **110**, 4293.

43. G.R.A. Johnson, N.B. Nazhat and R.A. Saadalla-Nazhat, *J. Chem. Soc, Faraday Trans. 1*, 1988, **84**, 501.

44. V.A. Luneok-Burmakina, G.G. Lerzina, V.B. Emel'yanov and A.G. Miroshnichenko, *Zh. Fiz. Khim.*, 1977, **51**, 2831, [*(Russ. J. Phys. Chem. (Engl. Trans.)*, 1977, **51**, 1650].

45. B.C. Gilbert and J.K. Stell, *J. Chem. Soc., Perkin Trans. 2*, 1990, 1281.

46. P. Maruthamuthu and P. Neta, *J. Phys. Chem.*, 1977, **81**, 937.

47. C. Marsh, Z. Zhang and J.O. Edwards, *Aust. J. Chem.*, 1990, **43**, 321.

48. J.E. Bennett, B.C. Gilbert and J.K. Stell, *J. Chem. Soc., Perkin Trans. 2*, 1991, 1105.

49. S. Steenken in 'Free Radicals: Chemistry, Pathology and Medicine', (eds. C.A. Rice-Evans and T. Dormandy), Richlieu Press, London, 1988, vol 3, 51.

50. M.J. Davies and B.C. Gilbert, *J. Chem. Soc., Perkin Trans. 2*, 1984, 1809.

51 G. Manivannan and P. Maruthamuthu, *Eur. Polymer J.*, 1987, **23**, 311.

52. P.Kanakaraj and P. Maruthamuthu, *Int. J. Chem. Res.*, 1983, **15**, 1301.

53. S. Fronaeus, *Acta Chem. Scand.*, 1986, **A40**, 172.

54. P. Neta and V. Madhavan, H. Zemel and R.W. Fessenden, *J. Am. Chem. Soc.*, 1977, **99**, 163.

55. F. Minisci and A. Cittero, *Acc. Chem. Res.*, 1983, **16**, 27.

56. B.C. Gilbert and J.K. Stell, *J. Chem. Soc., Perkin Trans. 2*, 1988, 1867.

57. R.O.C. Norman, P.M. Storey and P.R. West, *J. Chem. Soc. B*, 1970, 1099.

58. M.J. Davies, B.C. Gilbert and R.O.C. Norman, *J. Chem. Soc., Perkin Trans. 2*, 1984, 503.

59. R.G.R. Bacon and J.R. Doggart, *J. Chem. Soc.*, 1960, 1332.

60. P. Maruthamuthu and P. West, *J. Phys. Chem.*, 1977, **81**, 937.

61. I.I. Creaser and J.O. Edwards, *Topics in Phosphorus Chemistry*, 1972, **7**, 379.

62. P. Maruthamuthu, *J. Chem. Soc., Faraday Trans. 1*, 1985, **81**, 1979.

63. A.A. Green Jr, J.O. Edwards and P. Jones, *Inorg. Chem.*, 1986, **5**, 1858.

64. B. Halliwell and S. Chirico, *Am. J. Clin. Nutr.*, 1993, **57**, 715.

65. M.J. Davies, S. Fu and R.T. Dean, *Biochem. J.*, 1995, **305**, 643.

66. R. Hiatt in "Organic Peroxides - Volume 1", (ed. D. Swern), Wiley-Interscience, New York, 1971, 1.

67. N.A. Porter, in "Organic Peroxides", (ed. W. Ando), John Wiley and Sons, London, 1992, 101.

68. S. Matsugo and I. Santo, in "Organic Peroxides", (ed. W. Ando), John Wiley and Sons, London, 1992, 157.

69. G. Sosnovsky and D.J. Rawlinson in "Organic Peroxides - Volume 2", (ed. D. Swern), Wiley Interscience, New York, 1971, 153.

70. A.C. Baldwin in "The Chemistry of Functional Groups: Peroxides", (ed. S. Patai), John Wiley and Sons, New York, 1983, 97.

71. J.K. Kochi and A. Bemis, *Tetrahedron*, 1968, **24**, 5099.

72. W.L. Reynolds and R. Lumry, *J. Chem. Phys.*, 1955, **23**, 2560.

73. S. Hasegawa, N. Nishimura, S. Mitsumoto and K. Yokoyama, *Bull. Chem. Soc. Jpn*, 1963, **36**, 522.

74. C.E.H. Bawn and J.B. Williamson, *Trans. Faraday Soc.*, 1951, **47**, 721.

75. S.S. Levush, Z.P. Prisyazhnyuk and A.M. Kovalskaya, *Kinet. Katal.*, 1983, **24**, 1294.

76. R.A. Sheldon and J.K. Kochi, *Oxidation and Combustion Reviews*, 1973, **5**, 135.

77. B.C. Gilbert, J.K. Stell, C. Halliwell and W.R. Sanderson, *J. Chem. Soc., Perkin Trans. 2*, 1991, 629.

78. BC. Gilbert, R.G.G. Holmes, P.D.R. Marshall and R.O.C. Norman, *J. Chem. Res, (S)*, 1977, 172.

79. B. Ashworth, B.C. Gilbert, R.G.G. Holmes and R.O.C. Norman, *J. Chem. Soc., Perkin Trans. 2*, 1978, 951.

80. J.K. Stell, *D.Phil.Thesis, University of York*, 1990.

81. E. Heckel, *J. Phys. Chem.*, 1976, **80**, 1274.

82. P.D. Bartlett and R.R. Hiatt, *J. Am. Chem. Soc.*, 1958, **80**, 1398.

83. L.A. Singer, in "Organic Peroxides - Volume 1", (ed. D. Swern), Wiley-Interscience, New York, 1969, 265.

84. J.K. Kochi, *J. Am. Chem. Soc.*, 1963, **85**, 1958.

85. G. Sosnovsky and D.J. Rawlinson, in "Organic Peroxides - Volume 1", (ed. D. Swern), Wiley-Interscience, New York, 1969, 561.

86. L. Stryer, "Biochemistry", W.H. Freeman and Co., New York, 1988.

87. S.G. Sligar, J.D. Lipscombe, P.G. Debrunner and I.C. Gunsalus, *Biochem. Biophys. Res. Commun.*, 1982, **61**, 290.

88. T.F. Slater and B.C. Sawyer, *Biochem. J.*, 1984, **123**, 805.

89. G. Powis, *Free. Rad. Biol. Med.*, 1985, **6**, 63.

90. P. Reichard and A. Ehrenberg, *Science*, 1983, **221**, 514.

91. W.A. Vanderdonk, G.X. Yu, D.J. Silva and J.A. Stubbe, *Biochemistry*, 1996, **35**, 8381.

92. S. Yoshikawa, *Biochem. Soc. Trans.*, 1999, **27**, 351.

93. R.A. Miller and B.E. Brittigan, *J. Invest. Med.*, 1995, **43**, 39.

94. A.I. Tauber and B.M. Babior, *Adv. Free Rad. Biol. Med.*, 1985, **1**, 265.

95. R.L. Baehner, L.A. Boxer and L.M. Ingerham, in "Free Radicals in Biology - Volume 5", (ed. W.A. Pryor), Academic Press, New York, 1982, 91.

96. C.C. Winterbourne, *Biochim. Biophys. Acta*, 1985, **840**, 204.

97. J.M. Zgliczynski and T. Stelmaszynska, *Eur. J. Biochem.*, 1975, **56**, 157.

98. J.E. Harrison and S. Schultz, *J. Biol. Chem.*, 1976, **251**, 1371.

99. R.G. Wolcott, B.S. Franks, D.N. Hannum and J.K. Hurst, *J. Biol. Chem.*, 1994, **269**, 9721.

100. G. Brandi, F. Cattabeni, A. Albano and O. Cantoni, *Free Rad. Res. Commun.*, 1989, **6**, 47.

101. J.E. Repine, R.B. Fox and E.M. Berger, *J. Biol. Chem.*, 1981, **256**, 7094.

102. P.A. Clapp, M.J. Davies, M.S. French and B.C. Gilbert, *Free Rad. Res.*, 1994, **21**, 147.

103. J.A. Imlay, S.M. Chin and S. Linn, *Science*, 1988, **240**, 640.

104. J.A. Imlay and S. Linn, *Science*, 1988, **240**, 1302.

105. J.A. Imlay and S. Linn, *J. Bacteriol.*, 1986, **166**, 519.

106. B. Setlow, C.A. Setlow and P. Setlow, *J. Indust. Microbiol. Biotech.*, 1997, **18**, 384.

107. S.V. Shin and R.G. Marquis, *Arch. Microbiol.*, 1994, **161**, 184.

108. T.Akaike, K. Sato, S. Jiri, Y. Miyamoto, M. Khono, M. Ando and H. Maeda, *Arch. Biochem. Biophys.*,1992, **294**, 55.

109. M.G.C. Baldry, *J. App. Bacteriol.*, 1983, **54**, 417.

110. R.E. Marquis, G.C. Rutherford, M.M. Faraci and S.Y. Shin, *J. Indust. Microbiol.*, 1995, **15**, 486.

111. A. Alasri, C. Roques, G. Michel, C. Cabassud and P. Aptel, *Can. J. Microbiol.*, 1992, **38**, 635.

112. H.M. Hassan and I. Fridovich, *J. Biol. Chem.*, 1978, **253**, 6445.

113. A. Bast, G.R.M.M. Haenen and C.J.A. Doelman, *Am. J. Med.*, 1991, **91**, 3C.

114. I. Fridovich, *Science*, 1978, **201**, 875.

115. H.M. Hassan and I. Fridovich, in "The Biology and Chemistry of Active Oxygen", (eds. J.V. Bannister and W.H. Bannister), Elsevier, New York, Amsterdam and Oxford, 1984, 128.

116. C. von Sonntag and H.P. Schuchmann, in "Sulfur-Centred Reactive Intermediates in Chemistry and Biology", (eds. C. Chatgilialoglu and K.D. Asmus), Pleman Press, New York, 1990, 409.

117. B. Halliwell and J.M.C. Gutteridge, *Arch. Biochem. Biophys.*, 1990, **280**, 1.

118. B. Halliwell and J.M.C. Gutteridge, *TIBS*, 1986, **11**, 372.

119. G.W. Burton and K.U. Ingold, *Acc. Chem. Res.*, 1986, **19**, 194.

120. E. Niki, A. Kawakami, Y. Yamamoto and Y. Kamiya, *Bull. Chem. Soc. Jpn.*, 1985, **58**, 1971.

121. V. Braun, *Biol. Chem.*, 1997, **378**, 779.

122. P.M. Harrison and P. Arosio, *Biochim. Biophys. Acta*, 1996, **1275**, 161.

123. S.C. Andrews, *Adv. Microbial Physiol.*, 1998, **40**, 281.

124. M. Yasuda and T. Fijita, *Japan J. Pharmacol.*, 1977, **27**, 429.

125. E.R. Stadtman, *Free Rad. Biol. Med.*, 1990, **9**, 315.

126. M. Maiorino, F. Ursini and E. Cadenas, *Free Rad. Biol. Med.*, 1994, **16**, 661.

127. R. Paryu, *Physiol. Rev.* 1994, **74**, 139.

128. K.J.A. Davies, *J. Biol. Chem.*, 1987, **262**, 9895.

129. E.R. Stadtman, *Annu. Rev. Biochem.*, 1993, **62**, 797.

130. K.J.A. Davies, *J. Biol. Chem.*, **262**, 9902.

131. C. von. Sonntag, "The Chemical Basis of Radiation Biology", Taylor and Francis, London, 1988, 153.

132. R.O.C. Norman and B.C. Gilbert, *Adv. Phys. Org. Chem.*, 1967, **5**, 53.

133. B.C. Gilbert, *Essays in Chemistry*, 1972, **3**, 61.

134. W.G. Miller in"Spin Labelling II Theory and Applications", (ed. L.J. Berliner), Academic Press, 1979, 173.

135. S. Croft, B.C. Gilbert, J.R. Lindsay Smith and A.C.Whitwood, *Free Rad. Res. Comms.*, 1992, **17**, 21.

136. E.G. Janzen, *Acc. Chem. Res.*, 1971, **4**, 31.

137. E.G. Janzen and D.L. Haire, *Adv. Free Rad. Chem.*, 1990, **1**, 253.

138. P. Graceffam *Arch. Biochem. Biophys.*, 1983, **225**, 802.

139. M.J. Davies, *Biochim. Biophys. Acta.*, 1988, **964**, 24.

140. M.J. Davies, L.G. Forni and S.L. Shuter, *Chem. Biol. Interact.*, 1987, **61**, 177.

141. M.J. Davies and G.S. Timmins, in "Biomedical Applications of Spectroscopy", (eds. R.J.H. Clark and R.E. Hester), John Wiley and Sons, London 1996, 217.

142. R.P. Mason, B. Kalyanaraman B.E. Tainer and T.E. Eling, *J. Biol. Chem.*, 1980, **255**, 5019.

143. C. Motley and R.P.Mason, im "Spin Labelling; Theory and Applications, Biological Magnetic Resonance - Volume 8", (eds. L.J. Berliner and J. Reuben), Plenum Press, New York, 1989, 489.

144. R.A. Floyd, L.M. Soong, M.A. Stuart and D.L. Reigh, *Arch. Biochem. Biophys.*, 1978, **185**, 450.

145. A.R. Forrester and S.P. Hepburn, *J. Chem. Soc. (C)*, 1971, 701.

146. L. Eberson and O. Persson, *J. Chem. Soc., Perkin Trans. 2*, 1997, 893.

147. L. Eberson, J.J. MacCullough and O. Persson, *J. Chem. Soc., Perkin Trans. 2*,

1997, 133.

148. K. Makino, T. Hagiwara, A. Hagi, M. Nishi and A. Murakami, *Biochem. Biophys. Res. Comm.*, 1990, **172**, 1073.

149. P.M. Hanna, W. Chamulitrat and R.P. Mason, *Arch. Biochem. Biophys.*, 1992, **296**, 640.

150. Y. Miura, J. Ueda and T. Ozawa, *Inorg. Chim. Acta.*, 1993, **234**, 169.

151. L. Eberson and O. Persson, *J. Chem. Soc., Perkin Trans. 2*, 1997, 1689.

152. H. Chandra and M.C.R. Symons, *J. Chem. Soc., Chem. Commun.*, 1986, 1301.

153. M.J. Davies, B.C. Gilbert, J.K. Stell and A.C. Whitwood, *J. Chem. Soc., Perkin Trans. 2*, 1992, 333.

154. E. Finkelstein, G.M. Rosen and E.J. Rauckman, *Mol. Pharmacol.*, 1981, **21**, 262.

155. G.R. Beuttner, *Free Rad. Res. Comm..*, 1993, **19**, 579.

156. J.W. Hilborn and J. A. Pincock, *J. Am. Chem. Soc.*, 1991, **113**, 2683.

157. W.A. Pryor, C.K. Govindan and D.F. Church, *J. Am. Chem. Soc.*, 1982, **104**, 7563.

158. G.R. Beuttner, *Free Rad. Biol. Med.*, 1987, **3**, 159.

159. B.C. Gilbert and M. Jeff in 'Free Radicals: Chemistry, Pathology and Medicine', (eds. C.A. Rice-Evans and T. Dormandy), Richlieu Press, London, 1988, vol 3, 25.

160. P. Jones, M.L. Haggett, D. Holden, P.J. Robinson, J.O. Edwards, S.J. Bachofer and Y.T.Hayden, *J. Chem. Soc., Perkin Trans. 2*, 1989. 443.

161. E.G. Janzen and J.P. Liu, *J. Magn.. Reson.*, 1973, **9**, 510.

162. J. Chateauneuf, J. Lusztyk and K.U. Ingold, *J. Am. Chem. Soc.*, 1988, **110**, 2866.

163. B.C. Gilbert, R.O.C. Norman and R.C. Sealy, *J. Chem. Soc., Perkin Trans. 2*, 1975, 303.

164. J.K. Thomas, *Trans. Faraday Soc.*, 1965, **61**, 702.

165. P. Jones and D.N. Middlemiss, *Biochem. J.*, 1972, **130**, 411.

166. H. Kaur, K.H.W. Leung and M.J. Perkins, *J. Chem. Soc., Chem. Commun.*, 1981, 142.

167. H. Kaur, *Free Rad. Res.*, 1996, **24**, 409.

168. T. Ozawa and A. Hanaki, *Bull. Chem. Soc. Jpn.*, 1987, **60**, 2304.

169. P. Smith and J.S. Robertson, *Can. J. Chem.*, 1988, **66**, 1153.

170. M.J. Davies and T.L. Greenley, *Biochim. Biophys. Acta*, 1993, **1157**, 23.

171. M.J. Davies and T.L. Greenley, *Biochim. Biophys. Acta*, 1994, **1226**, 56.

172. C. Frejaville, H. Karoui, B. Tuccio, F. le Moigne, M. Culcasi, S. Pietri, R. Lauricella and P. Tordo, *J. Chem. Soc., Chem. Commun.*, 1994, 1793.

173. B. Tuccio, R. Lauricella, C. Frejaville, J.C. Bouteiller and P. Tordo, *J. Chem. Soc., Perkin Trans. 2*, 1995, 295.

174. S. Barbati, *PhD Thesis, University of Marseille*, 1997.

175. S. Silvester, *DPhil Thesis, University of York*, 1998.

176. G. Harrington, *DPhil. Thesis, University of York*, 1995.

177. G.P. Laroff, R.W. Fessenden and R.H. Schuler, *J. Am. Chem. Soc.*, 1972, 94, 9062.

178. G.S. Timmins, Personal Communication.

179. J-L. Clément, B.C. Gilbert, W.F. Ho, N.D. Jackson, M.S. Newton, S. Silvester, G.S. Timmins, P. Tordo and A.C. Whitwood, *J. Chem. Soc., Perkin Trans. 2*, 1998, 1715.

180. P. Tordo, Personal Communication.

181. W.A. Seddon and R.O. Allen, *J. Phys. Chem.*, 1967, **71**, 1914.

182. G. Czapski, *J. Phys. Chem.*, 1971, **75**, 2957.

183. B.C. Gilbert, R.O.C. Norman and R.C. Sealy, *J. Chem. Soc., Perkin Trans. 2*, 1973, 2174.

184. B.C. Gilbert, J.K.Stell and M. Jeff, *J. Chem. Soc., Perkin Trans. 2.*, 1988, 1867.

185. R.T. Dean, S. Fu, R. Stocker and M.J. Davies, *Biochem. J.*, 1997, **324**, 1.

186. D.C. Carter and J.X. Ho, *Advances in Protein Chemistry*, 1994, **45**, 153.

187. T. Peters, *Advances in Protein Chemistry*, 1985, **37**, 161.

188. M.J. Davies, B.C. Gilbert and R.M. Haywood, *Free Rad. Res. Comms.*, 1991, **15**, 111.

189. M.J. Davies and C.L. Hawkins, *J. Chem. Soc., Perkin Trans. 2*, 1998, 2617.

190. R.M. Haywood, *D. Phil. Thesis, University of York*, 1993.

191. W.A. Prutz in, "Sulfur-Centred Reactive Intermediates in Chemistry and Biology", (eds. C. Chatgilialoglu and K-D. Asmus), Plenum Press, New York, 389.

192. W.A. Prutz in "Radiation Research", (eds. E.M. Fielden, J.F. Fowler, J.H. Hendry

and D. Scott), Taylor and Francis, London, 1987, vol 2, 134.

193. M.J. Davies, J.A. Silvester G.S. Timmins and X.D. Wei, *Redox Report*, 1997, **3**, 225.

194. H. Schuessler and A. Herget, *Int, J. Radiat. Biol.*, 1980, **37**, 71.

195. G, Hajos and H. Delcinee, *Int. J. Radiat. Biol.*, 1983, **44**, 333.

196. H. Schuessler and K. Schilling, *Int. J. Radiat. Biol.*, 1984, **45**, 267.

197. G.R. Means and R.E. Feeney, "Chemical Modification of Proteins", Holden-Day Inc., San Francisco, 1971.

198. M.J. Davies, R.M. Haywood and B.C. Gilbert, *Free Rad. Res. Comms.*, 1993, **18**, 353.

199. R.L. Levine, C.N. Oliver, R.M. Fulks and E.R. Stadtman, *Proc. Natl. Acad. Sci. USA*, 1981, **78**, 2120.

200. R.L. Levine and C.N. Oliver, *J. Biol. Chem.*, 1991, **266**, 2005.

201. R.L. Levine, *J. Biol. Chem.*, 1983, **258**, 11821.

202. A. Amici, R.L. Levine, L. Tsai and E.R. Stadtman, *J. Biol. Chem.*, 1989, **264**, 3341.

203. R.L. Levine, D. Garland, C.N. Oliver, A. Amici, I. Climent, A-G. Lenz, B-W. Ahn, S. Shaltiel and E.R. Stadtman, *Methods in Enzymology*, 1990, **186**, 464.

204. R.L. Levine, J.A. Williams, E.R. Stadtman and E. Shacter, *Methods in Enzymology*, 1994, **233**, 346.

205. A. Reznick and L. Packer, *Methods in Enzymology*, 1994, **233**, 357.

206. P.K. Smith, R.I. Krohn, G.T. Hermanson, A.K. Mallia, F.H. Gartner, M.D. Provenzano, E.K. Fujimoto, N.M. Goeke, B.J. Olson and D.C. Klenk, *Anal. Biochem.*, 1985, **150**, 76.

207. D.M. Bollag and S.J. Edelstein, "Protein Methods", Wiley-Liss, New York, 1991.

208. G.L. Ellman, *Arch. Biochem. Biophys.*, 1959, **82**, 70.

209. P.W. Riddles, R.L. Blakely and B. Zerner, *Methods in Enzymology*, 1983, **91**, 49.

210. S. Gebicki and J.M. Gebicki, *Biochem. J.*, 1993, **289**, 743.

211. R.E. Pacifici and K.J.A. Davies, *Methods in Enzymology*, 1990, **186**, 485.

212. M.J. Davies, *Biochim. Bipohys. Acta*, 1988, **964**, 28.

213. S.P. Barr and R.P. Mason, *J. Biol. Chem.*, 1995, **270**, 12709.

214. B. Kalyanaraman, C. Motley and R.P. Mason, *J. Biol. Chem.*, 1985, **258**, 3855.

215. R. Radi, L. Thomson, H. Rubbo and E. Prodanov, *Arch. Biochem. Biophys.*, 1991, **288**, 112.

216. M.L. McCormick, G.R. Beuttner and B.E. Brittigan, *J. Biol. Chem.*, 1995, **270**, 29265.

217. J.M.C. Gutteridge, *FEBS Letters*, 1986, **201**, 291.

218. R.C. Bruch and W.S. Thayer, *Biochim. Biophys. Acta*, 1983, **733**, 216.

219. G.E. Dorbetsov, T.A. Borschevskaya, V.A. Petrov and Y.A. Vladimirov, *FEBS Letters*, 1977, **84**, 125.

220. H.W. Gardner, *Free Rad. Biol. Med.*, 1989, **7**, 65.

221. M.F. Moghaddam, K. Motoba, B. Borhan, F. Pinot and B.D. Hammock, *Biochim. Biophys. Acta*, 1996, **1290**, 327.

222. R.L. Melnick and M.C. Kohn, *Carcinogenesis*, 1995, **16**, 157.

223. J. Heritage, E.G.V. Evans and R.A. Killington, "Introductory Microbiology", Cambridge Univeersity Press, Cambridge, 1996.

224. I.A. Siddiqi, S.M. Osman, M.R. Subbaram and K.T. Achaya, *J. Indian Chem.*, 1971, **9**, 211.

225. J.F. Glockner, S-W. Norby and H.M. Swartz, *Am. J. Physiol.*, 1992, **259**, 12.

226. A. Keith, G. Bulfield and W. Snipes, *Biophys. J.*, 1970, **10**, 618.

227. T.J. Stone, T. Buckman, P.L. Nordio and H.M. McConnell, *Proc. Natl. Acad. Sci. USA*, 1965, **54**, 1010.

228. B.J. Gaffney, *Proc. Natl. Acad. Sci. USA*, 1975, **72**, 664.

229. B.L. Bales, E.S. Lesin and S.B. Oppenheimer, *Biochim. Biophys. Acta*, 1977, **465**, 400.

230. F. Morno, A. Wisniewska and R. Stevanato, *Biochim. Biophys. Acta*, 1995, **1240**, 89.

231. G. Haerig, P.L. Luisi and H. Hauser, *J. Phys. Chem.*, 1988, **92**, 3574.

232. A. Caragheorgheopol, H. Caldararu, I. Dragutan, H. Jeola and W. Brown, *Langmuir*, 1997, **13**, 6912.

233. V.V. Khramstov, D. Marsh, L. Weiner and V.A. Reznikov, *Biochim. Biophys. Acta*, 1992, **1104**, 317.

234. B.J. Gaffney in "Spin Labelling 1 - Theory and Apllications," (ed. L.J. Berliner), Academic Press, New York, San Francisco and London, 1976, 373.

235. B.J. Gaffney and H.M. McConnell, *J. Magn. Reson.*, 1974, **16**, 1.

236. G. Minotti and S.D. Aust, *J. Biol. Chem.*, 1987, **262**, 1098.

237. G. Minotti and S.D. Aust, *Chemistry and Physics of Lipids*, 1987, **44**, 191.

238. J.M.C. Gutteridge, *Free Rad. Res. Comms.*, 1986, **1**, 173.

239. H.H. Draper and M. Hadley, *Methods in Enzymology*, 1990, **186**, 421.

240. S. Chirico, *Methods in Enzymology*, 1994, **233**, 314.

241. Y. Yamamoto, B. Frei and B.N. Ames, *Methods in Enzymology*, 1990, **186**, 371.

242. F.J.G.M. van Kuuk, D.W. Thomas, R.J. Stephens and E.A. Dratz, *Methods in Enzymology*,1990, **186**, 388.

243. K. Hasegawa and L.K. Patterson, *Photochem. Photobiol.*, 1978, **28**, 817.

244. M.S. Stark, *J. Phys. Chem. A*, 1997, **101**, 8296.

245. J. Fuchs, W.H. Nitschmann, L. Packer, O.H. Hankovszky and K. Hideg, *Free Rad. Res. Comms.*, 1990, **10**, 315.

246. Y. Miura, H. Utsumi and A. Hamada, *Arch. Biochem. Biophys.*, 1993, **300**, 148.

247. Solvay-Interox Test Method for Bactericdal Activity.

248. G.P. Snowdon, *PhD. Thesis, University of Sunderland*, 1993.

249. A. Samuni, A. Samuni and H.M. Swartz, *Free Rad. Biol. Med.*, 1989, **6**, 179.

250. A. Samuni, A.J. Carmichael, A. Russo, J.B. Mitchell and P. Riesz, *Proc. Natl. Acad. Sci. USA*, 1986, **83**, 7593.

251. H.M. Swartz, *Free Rad. Res. Comms.*, 1990, **9**, 399.

252. J.A. Howard and J.C. Scaiano, in "Landolt-Bornstein, Numerical Data and Functional Relationships in Science and Technology, New Series, Group II: Atomic and Molecular Physics, Volume 13: Radical Reaction Rates in Liquids, Subvolume d: Oxyl-, Peroxyl- and Related Radicals," (ed. H. Fischer), Springer-Verlag, Berlin and Heidelburg, 1984.

253. D.A. Avilla, C.E. Brown, K.U. Ingold and J. Lusztyk, *J. Am. Chem. Soc.*, 1993,

115, 466.